Biogeochemical cycling of trace elements in a tropical coastal lagoon system (Chilika, India)

A Thesis

Submitted in Partial Fulfilment of the Requirements

for the Degree of

Doctor of Philosophy

By

Mohd Danish

ID: 20163435

Research Supervisor: **Dr. Gyana Ranjan Tripathy**

IISER PUNE

Indian Institute of Science Education and Research

Dr. Homi Bhabha Road, Pune-411008, India

Dedicated to

Abbu and Ammi

भारतीय विज्ञान शिक्षा एवं अनुसंधान संस्थान पुणे
INDIAN INSTITUTE OF SCIENCE EDUCATION AND RESEARCH PUNE
(An Autonomous Institution under Ministry of HRD, Govt. of India)
Dr. Homi Bhabha Road, Pune -411008

IISER PUNE

Dr. Gyana Ranjan Tripathy
(Associate professor)
Department of Earth and Climate Science
Indian Institute of Science Education and Research
Dr. Homi Bhabha Road
Pune-411008, India

Certificate

Certified that the work incorporated in the thesis entitled "Biogeochemical cycling of trace elements in a tropical coastal lagoon system (Chilika, India)" submitted by **Mr. Mohd Danish** was carried out by the candidate, under my supervision. The work presented here or any part of it has not been included in any other thesis submitted previously for the award of any degree or diploma from any other university or institution.

Tripathy 27/12/20

Date: 27th December 2020
Place: Pune

Dr. Gyana Ranjan Tripathy
(Research Advisor)

भारतीय विज्ञान शिक्षा एवं अनुसंधान संस्थान पुणे

INDIAN INSTITUTE OF SCIENCE EDUCATION AND RESEARCH PUNE

(An Autonomous Institution under Ministry of HRD, Govt. of India)

Dr. Homi Bhabha Road, Pune -411008

IISER PUNE

Declaration

I declare that this written submission represents my ideas in my own words and where other's ideas have been included; I have adequately cited and referenced the original sources. I also declare that I have adhered to all principles of academic honesty and integrity and have not misinterpreted or fabricated any idea/data/fact/source in my submission. I understand that violation of above will cause for disciplinary action by the Institute and can also evoke the penal action from the sources which have thus not been properly cited or from whom proper permission has not been taken when needed.

Mohd Danish

Date: 27th December 2020

Place: Pune

Mr. Mohd Danish

ID: 20163435

Acknowledgements

Every page of this thesis work hides the effort and support of my PhD supervisor, Dr. Gyana Ranjan Tripathy. Thank you so much for allowing me to work in your GRASP lab and providing me with exciting projects. I never overlook the kind of motivations and inspirations that he has presented during the hard-hitting moments of my journey in the GRASP lab. As this lab was newly established, he taught me experimental work from beaker cleaning to generate reliable and accurate data using the newly installed Q-ICP MS facility. His trust on me while I went for sample collection from different parts of India is worth to remember. During every discussion on research planning and execution, he has enhanced my research interest on low-temperature aquatic geochemistry and for pursuing quality research in future. In addition to academic support, he always stood and guided me during hard times of my life. His qualities as a supervisor can't be stated in words, I can simply say that this thesis would not have been possible without his guidance and persistent support.

I would also like to thank and express my deep sense of gratitude to Dr. Rajani Panchang Dhumal for her encouragement, guidance and support throughout this thesis work. She taught me the geological and sedimentological details about coastal lagoon system during our first field trip. I am highly grateful to Prof. Shyam Rai, whose suggestions were always fruitful which improved my scientific knowledge. I thank him for his constant encouragement, concern, advice, teaching and care. I am thankful to Dr. Ankush (Ankush Bhaiyya) for his immense support and concern to my work. I benefited a lot by discussing and sharing my ideas and knowledge with him.

I am very grateful for the help and support of my research advisor committee members (Dr. R. Bhushan and Dr. S. Chakraborty). I thank all the academic committee members for reviewing my research work from time to time. I sincerely thank all the faculty members of ECS department (particularly, Dr. Shreyas and Dr. Argha) whose suggestion during the departmental seminar helped me a lot for successful execution of the project and also developing the manuscript. I would like to thank my collaborators Dr. Waliur Rahaman, NCPOR, Goa; Dr. Satya Praksh, INCOIS, Hyderabad; Dr. Naveen Gandhi, IITM, Pune, and Dr. Sirsha Mitra and Ms. Shubhangi Raskar, SPPU, Pune. Their suggestions and feedback helped me a lot in writing the manuscripts. I am also grateful to Dr. Shaikh Abdul Rashid of AMU who encouraged and suggested me for doing the PhD under the supervision of Dr. Tripathy. Furthermore, I am highly thankful to Anirban Mondal (Anirban Bhaiyya) for his help during field trips and experiments in lab. I also thank my colleagues Preeti, Jimmy, Anupam, Rakesh, and Achyuth for their help and support during the thesis work. I am also thankful to summer trainee students in GRASP lab (Shubhangi, Smurti, and Sanjay) for their help during this period. I am thankful to the Das family from Berhampur (especially, Sitansu Das) for their support during the field work carried out in and around Chilika lagoon, especially. Mrs. Sarla Das has generously helped us in collecting rain water samples. I thank Mrs. Sharada Das for making one of the figure about rhenium cycle in coastal lagoon. I sincerely acknowledge the local support received from Ramachandra, Avinash and Madhu, Sanjay during the field trips for collecting the samples from Chilika. I sincerely express thanks to Vibhas and Vikrant for their help during this thesis work. I spend joyful moments at IISER hostel with my friends (Anees bhai, Nayeem bhai, Abad Bhai, Javid, Muttalib, Manzoor, Zahid, Javed, Saleem, Saddam, Akram, Firdousi, Shabnam, Tarique and player of furious XI), who made my stay at IISER pleasant and enjoyable. Thanks to Ruby for her help in administration-related works. Thanks are also due to the administrative, academic and library staffs of IISER, Pune for their cooperation and support. I am also oblighed to Danish aftab, Qausim, Syed Arif, Shruti Chauhan, Sadia Khan, Tauheed and Iftikhar bhai for their motivation and encouragements during my tough time. I am thankful to Mohammed Nuruzzama and Mohd Tarique for their help during my stay at NCPOAR, Goa for the analysis of Sr isotopes.

I am deeply grateful to my parents and family members for their continuous support, wishes and encouragement. They have always stood by my side during tough times and supported me to complete my thesis. I am also thankful to Rabia Fatima for her support during my tough time. I am thankful to the IISER for providing the PhD fellowship and also DST-SERB for providing the fund to the GRT for this project. I sincerely acknowledge the editorial board of Marine chemistry Journal for providing the copy rights for including the two published papers (Danish et al., 2019 and Danish et al., 2020) in thesis. Lastly, I offer my regards and extend my sincere thanks to all of those who supported me in any respect during the completion of my PhD thesis.

Abstract

This thesis work was designed to assess biogeochemical cycling of selected trace elemental (B, Sr, Ba and Re) and isotopic ($^{87}Sr/^{86}Sr$ and $\delta^{13}C$) compositions along the salinity gradient of a large tropical coastal lagoon (Chilika lagoon, India) system during four different seasons, *viz*. pre-monsoon (May, 2017), monsoon (August, 2017), post-monsoon (January 2018) and onset of monsoon (June, 2016). These analyses were carried out appropriately in lagoon water, their sources, (bed and suspended) sediments and macrophytes samples. The dataset was used to quantify influence of coastal processes (submarine groundwater discharge (SGD), ion-exchange and biological uptake) in regulating trace elemental inventory.

Dissolved Sr concentrations in the Chilika co-vary linearly with water salinity, indicating conservative mixing between river and seawater. Unlike Sr concentrations, the $^{87}Sr/^{86}Sr$ ratios show non-conservative behavior during the monsoon and pre-monsoon seasons. This non-conservative behavior during monsoon has largely been restricted to low salinity (< ~2) regime, and is attributable to ion-exchange process. The non-conservative nature during the pre-monsoon period, however, is linked to additional ^{87}Sr supply *via* SGD to the lagoon. Inverse modeling of the dataset estimate that the SGD contributes ~20% of total water during lean flow stages, which corresponds to a flux of 1.51×10^6 m^3/d to the lagoon. Data from this and earlier studies indicate that the $^{87}Sr/^{86}Sr$ ratios of the SGD to the western Bay of Bengal are relatively higher (~0.715) than the seawater value (0.7092) and therefore, would not contribute in reducing the oceanic imbalance which requires a less-radiogenic source.

Distributions of boron and barium concentrations in the lagoon show impact of ion-exchange processes on trace elemental inventory. Dissolved barium along the salinity gradient of the Chilika shows non-conservative release with a mid-salinity peak during all the seasons. About three-fourth of the total Ba fluxes from the Chilika to the Bay of Bengal during monsoon season is released through ion-exchange processes. Sedimentary Ba concentrations in bulk and exchangeable fractions show that the barium production in the Chilika is mainly linked with Ba desorption from clay particles through cation (Mg and Al) replacement. In contrast to Ba, the boron concentration shows conservative behavior during onset of the monsoon and monsoon seasons. The pre-monsoon samples, however, point to non-conservative removal of boron at low-saline regime through adsorption. These boron losses are mainly linked to higher residence

time during pre-monsoon season, which allows efficient particulate-water interaction for adsorptive removal. This proof-of-process of boron removal from coastal regimes indicates that exchangeable boron in clay-rich sediments is authigenic in nature and hence, may serve as a proxy for past oceanic conditions.

Non-conservative elemental mixing has also been observed for Re in the Chilika during three seasons, which is in clear contrast to existing a few studies. The observed rhenium removal is linked to both adsorption and biological uptake. Significant correlations of sedimentary Re with Mg and Al concentrations point to adsorptive rhenium removal onto Mg-Al rich clay (montmorillonite and chlorite) surfaces. Further, huge occurrence of biomass in the lagoon, appreciable Re concentrations in macrophytes (~428 pg/gm) and a significant Re-TN (total nitrogen) correlation indicate possible biological uptake of Re by amino acids during cellular membrane formation. Mass balance calculations show that about 60 % of sedimentary Re is accumulated through clay adsorption, whereas the remaining 40 % is scavenged through biological activities. The burial rate for these rhenium removals from the Chilika (5.95×10^{-3} $ng/cm^2/yr$) is ~4 times higher than its accumulation onto oxic marine sediments (1.6×10^{-3} $ng/cm^2/yr$) globally. Outcomes of this study, therefore, identify this new and significant coastal sink for rhenium and warrant the need to revisit the oceanic Re budget. Impact of biological activities on coastal water chemistry is also evident from the distribution of dissolved inorganic carbon (DIC) and $\delta^{13}C_{DIC}$ compositions in the Chilika lagoon, which indicates degradation of organic matter and calcite precipitation in regulating the coastal carbon cycle.

Table of contents

Chapter 1 Introduction **1**

1.1. Introduction 2

1.2. Objectives of this thesis 9

1.3. Outline of the thesis 10

Chapter 2 Materials and Methods 11

2.1. Study area 12

2.1.1. Climatic condition 12

2.1.2. Hydrology of the lagoon 14

2.1.3. Geology of the lagoon 18

2.1.4. Flora and fauna 19

2.2.1. Sampling 19

2.3. Methods 22

2.3.1. Elemental analyses 22

2.3.1.1. Geochemical analyses of water samples 22

2.3.1.1.1. Dissolved Strontium 22

2.3.1.1.2. Dissolved Boron 23

2.3.1.1.3. Dissolved Barium 23

2.3.1.1.4. Dissolved Rhenium 26

2.3.1.2. Geochemical analyses of sediment samples 27

2.3.1.2.1. Major and trace elemental analyses 27

2.3.1.2.2. Rhenium analyses in particulate phases 30

2.3.2. Isotopic analyses 30

2.3.2.1. Sr isotopic analysis 30

2.3.2.2. Dissolved inorganic ($\delta^{13}C_{DIC}$) and sedimentary organic ($\delta^{13}C_{org}$) carbon isotopes 31

2.3.2.3. Oxygen isotope 32

Chapter 3 Submarine groundwater discharge to the Chilika lagoon: An estimation using Sr isotopes 34

3.1. Introduction 35

3.2. Results 36
3.2.1. Compositions of possible sources 36
3.2.2. Sr and $^{87}Sr/^{86}Sr$ ratios of the Chilika 37
3.2.2.1 Diurnal variations 41
3.3. Discussion 45
3.3.1. Behavior of Sr and $^{87}Sr/^{86}Sr$ along the salinity gradient 45
3.3.2. Estimation of SGD to the Chilika during the pre-monsoon season 47
3.3.2.1. Inversion approach 48
3.3.2.2. "Variable SGD end-member" approach 50
3.3.3. SGD and related Sr fluxes to the Chilika lagoon 52
3.4. Conclusion 56
Chapter 4 Impact of ion-exchange process on Trace elements (B and Ba) in coastal lagoon system 57
4.1. Dissolved boron in Chilika water and its possible sources 58
4.1.1. Introduction 58
4.1.2. Results 60
4.1.2.1. Composition of source waters 60
4.1.2.2. Composition of the Chilika Lagoon 64
4.1.2.3. Chemical composition of Chilika sediments 65
4.1.2.4. $\delta^{18}O$ values of the Chilika system 65
4.1.3. Discussion 66
4.1.3.1. Hydrology of the lagoon: Evaporative loss estimates 67
4.1.3.2. Variation of boron with salinity 69
4.1.3.3. Possible causes for removal of dissolved boron 72
4.1.3.4. Impact of tides on the boron distribution 76
4.1.3.5. Boron budget of the Chilika lagoon 79
4.2. Dissolved barium in the Chilika lagoon 82
4.2.1. Introduction 82
4.2.2. Results 83
4.2.2.1. Ba in the source waters 83
4.2.2.2. Dissolved barium in lagoon water 83

4.2.2.3. Impact of (semi-diurnal and fortnight) tides on Ba composition.......................... 86
4.2.2.4. Sedimentary composition.. 86
4.2.3. Discussion.. 88
4.3. Evidence of ion-exchange process from sediment chemistry data 94
4.4. Conclusion.. 95
Chapter 5 Distribution of δ^{13}C and Re concentrations in the Chilika lagoon: Role of biological processes in regulating water chemistry.. 96
5.1. Dissolved Re in the Chilika lagoon system.. 97
5.1.1. Introduction 97
5.1.2. Results 99
5.1.2.1. Source water compositions 99
5.1.2.3. Sedimentary Re variations in the Chilika System 103
5.1.3. Discussion.. 105
5.1.4. Re burial rate and its significance... 109
5.2. Stable carbon isotopic systematics of the Chilika lagoon system.................................. 113
5.2.1. $\delta^{13}C_{DIC}$ of dissolved inorganic carbon (DIC) 113
5.2.1.1. Source composition.. 113
5.2.2.2. Chilika composition.. 113
5.4. Conclusion.. 120
Chapter 6 Conclusion and future perspectives 121
6.1.1. Estimation of submarine groundwater discharge (SGD) to the Chilika using Sr isotopic approach 122
6.1.2. Coastal behavior of dissolved B and Ba in the Chilika lagoon.................................. 123
6.1.3. Re concentrations and stable carbon isotopic study of the Chilika lagoon.................. 124
6.2. Future directions.. 124
References.. 126
Annexure... 149
List of Publications 184

List of Tables

Table 1.1. Typical composition of key parameters of elements of interest for the ocean system **7**

Table 2.1. Water residence time estimated spatially and temporally in the Chilika Lagoon (Mahanty et al., 2016). **18**

Table 2.2. Results of analyses for elements in water reference material. **23**

Table 2.3. Data on Re concentration analysed in blank samples. **27**

Table 2.4. Results on repeat analysis of Re measurement in water samples (n = 9). **27**

Table 2.5. Result (in µg/g) of repeat dissolution of Chilika bed sediments and clay fractions. **28**

Table 2.6. Results of elemental analyses in USGS reference materials. **29**

Table 2.7. Results of duplicate analyses for CN measurement. **29**

Table 2.8. Replicate analyses of $^{87}Sr/^{86}Sr$ of water samples from the Bay of Bengal and the Chilika lagoon. **31**

Table 2.9. Repeat analysis of the $\delta^{13}C_{DIC}$ in the Chilika water samples. **32**

Table 2.10. Repeat analysis of the $\delta^{13}C_{org}$ in the Chilika sediments samples. **33**

Table 3.1. Average chemical (salinity and Sr concentrations) and Sr isotopic data for the Chilika lagoon system. **38**

Table 3.2. A-priori salinity, Sr and $^{87}Sr/^{86}Sr$ data used in the inverse model for different end-members. These compositions are constrained based on measured data from this study. **49**

Table 3.3. Contributions (in %) of hydrological input from three end-members (river, seawater and SGD) to the Chilika lagoon during the pre-monsoon season. These contributions estimated using both the inversion and variable-SGD approaches are provided below. **52**

Table 4.1.1. Dissolved boron and salinity data for the Chilika lagoon samples collected during three field trips (*viz*. May, 2017; Aug, 2017; June, 2016). **61**

Table 4.1.2. Data on elemental boron, oxygen isotopes and salinity for possible source waters to the Chilika lagoon. **63**

Table 4.1.3. Results comparison of statistical analyses using various approaches of spatial and seasonal distribution of B, salinity and B/salinity values of the Chilika lagoon. **66**

Table 5.1.1. Average and range of rhenium and salinity data for the Chilika lagoon samples collected during monsoon, pre-monsoon and post-monsoon seasons. This table also includes average and range data of possible sources (river, groundwater and Bay of Bengal). **100**

Table 5.2.1. Average data and ranges of DIC, $\delta^{13}C_{DIC}$ and other parameters investigated in the waters of Chilika for all seasons. The details data of these parameters are provided in the supplementary material. **114**

Table A1. Data on pH, temperature, salinity, dissolved oxygen (DO), dissolved boron, dissolved barium and geographical coordinates of Chilika lagoon water samples collected during four filed campaigns (January-2018, May-2017, June-2016, August-2017). **150**

Table A2. Data on salinity, Sr, B, Ba, Re, DIC, $^{87}Sr/^{86}Sr$, and $\delta^{13}C_{DIC}$ of Chilika lagoon samples collected during three filed campaigns (January-2018, May-2017, August-2017). **160**

Table A3. Two-hourly data for pH, temperature, salinity, DIC, elemental (B, Ba, Re, Sr) and isotopic composition ($^{87}Sr/^{86}Sr$, $\delta^{13}C_{DIC}$) at two locations (Outer (Satapada) and southern (Barkul) sectors) of the Chilika lagoon during pre-monsoon, monsoon and post-monsoon seasons. **163**

Table A4. Data on pH, temperature, salinity, DIC, geographical coordinates and elemental (B, Sr, Re, Ba) and isotopic composition ($^{87}Sr/^{86}Sr$ and $\delta^{13}C_{DIC}$) of source (river/rivulets, rain, groundwater, coastal and western Bay of Bengal, Palur canal) water samples collected during all filed campaigns. **166**

Table A5. Data on elements (Major and trace elements), clay abundances, TOC, TN, P, and $\delta^{13}C_{org}$ isotopic data for bed sediments from the Chilika lagoon and bed sediments from the rivers. **174**

Table A6. Data on Re content in the bulk bed sediments and clay fractions are listed in this table. This tables also includes data on the exchangeable fraction of bed sediments and clay. **177**

Table A7. Elemental and Sr isotopic data for suspended sediments and exchangeable fractions from the Chilika lagoon. **179**

Table A8. Stable oxygen isotopic data for the Chilika lagoon water collected during June, 2016. The $\delta^{18}O$ values for the source water (river, rain and ground water) samples are also included. **180**

Table A9. Sequences of the primer pairs used for amplification of genomic DNA from different plant accessions. **182**

Table A10. Blast result of the DNA sequences showing similarity with different plant species. DNA sequences obtained from the amplified product of the respective plant samples collected from the Chilika lagoon were subjected to BLAST. BLAST result showing the percentage query cover, percent identity, E-value and identity of the plant samples. **183**

List of Figures

Figure 1.1. Schematic diagram showing major sources, sinks and internal cycling of trace metals in coastal systems (Figure modified after Stumm and Morgan, 2012). **4**

Figure 2.1. Map of the Chilika Lagoon including its drainage basin (A) and surrounding geology (B). The spatial distribution of rainfall (A) in the Chilika drainage basin during the sampling period (2016 to 2018) is also shown (data source: https://giovanni-.gsfc.nasa.gov/). **13**

Figure 2.2. Monthly average variation of rainfall and temperature near to the Chilika basin during three consecutive years of sampling i.e. 2016, 2017 and 2018. Rainfall data has been taken from the CRIS ((http://hydro.imd.gov.in) and temperature data were taken from the Wunderground (https://www.wunderground.com). **15**

Figure 2.3. (A) Shows the monthly distribution of freshwater discharge to the Chilika Lagoon from the Mahanadi distributaries (Data from Muduli et al., 2013) and (B) Plot shows the distribution of suspended sediments in the north sector of Chilika lagoon (Data from Kumar et al., 2016). **17**

Figure 2.4. Map of sampling collections in the Chilika lagoon during the four field campaigns (Jan-2018, May-2017, June-2016, and August-2017). Additionally, locations of groundwater, river and seawater samples from the coastal and western Bay of Bengal (BoB) also presented. The symbol of red stars represents the two locations (Barkul and Satapada) where the diurnal sampling of 2-hr resolution were carried out. The wetland area in the north-east part of the lagoon is also highlighted. **21**

Figure 2.5. (A) Showing the relationship of two times Sr measurement which produces a precision of ~4% and (B) Comparison of Sr concentration data measured with and without internal standards (Indium). **24**

Figure 2.6. Plots show the relationship between the two times measurements of same samples during the analysis (B and Ba). These repeat analyses produced the reproducibility of 3 % (n = 28) and 5% (n = 40) for B and Ba, respectively. **25**

Figure 3.1. Spatial distribution of dissolved Sr concentrations and $^{87}Sr/^{86}Sr$ ratios of the Chilika lagoon during monsoon period. For reference, these data for possible source waters (groundwater, river, and sea (Bay of Bengal) water; Table 3.1) are also shown. **39**

Figure 3.2. Significant correlation between water salinity and Sr concentrations confirm conservative behavior of Sr during (i) pre-monsoon, (ii) monsoon and (iii) post-monsoon seasons. The slopes of linear regression lines during the three seasons overlap with that expected (~2.6) for conservative mixing of river and seawater. **40**

Figure 3.3. Mixing diagram between dissolved Sr concentrations and $^{87}Sr/^{86}Sr$ ratios during different seasons. The Sr isotopes behave conservatively during post- monsoon, but non-conservatively during monsoon and pre-monsoon seasons. **42**

Figure 3.4. Two-hourly resolution water salinity, Sr, and $^{87}Sr/^{86}Sr$ data at the Chilika outflow during the monsoon. Variations in salinity show effect of tides and ebb on the lagoon chemistry. The observed variations are due to seawater exchange during semi-diurnal tidal cycles. **43**

Figure 3.5. Variations in (A) Sr/Al and (B) $^{87}Sr/^{86}Sr$ ratios of the suspended sediments (in both bulk and exchangeable fractions) with their corresponding water salinity. These ratios broadly show a declining trend with salinity, indicating release of Sr through ion-exchange (desorptive) processes and/or dissolution of Sr-rich minerals to the Chilika. **44**

Figure 3.6. Co-variation between (A) Sr and salinity, and (B) Sr and $^{87}Sr/^{86}Sr$ ratios of groundwater samples from the Chilika basin. For reference, the conservative mixing line for river and seawater is shown in (A). These plots show variable SGD compostion **54**

Figure 3.7. Mixing plot between Sr concentration and $^{87}Sr/^{86}Sr$ for the Chilika lagoon during pre-monsoon season. For reference, theoretical river-sea water mixing trend and also, variable SGD composition has also been shown. The SGD compositions show an increasing Sr concentrations with salinity (Fig. 3.6) with a near constant $^{87}Sr/^{86}Sr$ ratio (~0.715 for pre-monsoon season; Table 3.1). The SGD contribution has been estimated assuming a conservative behavior for Sr element in this lagoon system. **55**

Figure 4.1.1. Contour map showing the salinity and boron distributions of the Chilika lagoon during different seasons: pre-monsoon (May-2017; inset A-B), onset of monsoon (June-2016; inset C-D) and monsoon (August-2017; inset E-F). The dotted lines in each figure inset represent the sector (i.e. southern, central and northern) boundaries. Spatial distribution of boron concentration follows that of the salinity pattern. **70**

Figure 4.1. 2. (A) Frequency distribution of the boron/salinity ratio (in µmol/kg/salinity) during different seasons. The frequency in this histogram stands for the count of the samples within

the given bin of B/salinity ratio. The boron/salinity ratios of most of the samples fall between of the Bay of Bengal (12.8 ± 0.4 μmol/kg/salinity) and riverine (11.6 ± 6 μmol/kg/salinity) input. Several pre-monsoon (May) samples show relatively lower B/salinity ratios than that of its possible sources. This observation indicates removal of dissolved boron from the lagoon which we interpret as ion-exchange (i.e. adsorption) processes. (B) Box plot showing the B/salinity distribution for three different months. The pre-monsoon (May) samples with relatively lower B/salinity ratios are mostly from the northern sector of the lagoon. This B/salinity decline has been attributed to adsorptive removal of boron from the Chilika. **71**

Figure 4.1.3. Co-variation between salinity and boron concentrations of the lagoon during (A) monsoon (Aug), (B) onset of monsoon (June) and (C) pre-monsoon (May) seasons. Error bars here represent the uncertainty associated with the boron measurements. The end-member compositions for the river (gray squares) and Bay of Bengal (open squares) waters are shown here. The dotted (red) line reflects the theoretical river-sea water mixing line. Average groundwater composition (red triangle) is also shown for comparison. The linear regression line of the dataset (bold black) and the corresponding 95% confidence level (blue dotted line) are also shown. (D) B-salinity trend of low-saline samples with salinity<15 from the pre-monsoon (May) season. Most of these data fall below the theoretical mixing line for river and sea water. **74**

Figure 4.1.4. Estimated dissolved boron removal (in %) with respect to salinity of the lagoon during the pre-monsoon (May) period. The removal process is restricted mostly to the low saline regime of the Chilika. **75**

Figure 4.1.5. Correlation between boron concentration (in bulk fraction of sediments) and clay abundance of the bed sediments from the Chilika lagoon. **76**

Figure 4.1.6. (A) Two-hourly data for salinity and relative contribution from seawater to the lagoon at Satapada (outer channel) during the monsoon season. Variation in these datasets points to fluctuation of Bay of Bengal water influx into the Chilika due to tidal cycle. (B) Combined salinity and boron data on 2-h basis sampling at two different locations (Barkul and Satapada) for two seasons (monsoon and non-monsoon) show a conservative behavior. Analytical uncertainties associated with these two parameters are smaller than the symbol size. **78**

Figure 4.1.7. Spatial correlation of boron data between monsoon samples for two different spatial sampling (1-day sampling versus spatial sampling over ~3 weeks' time). We compare here salinity-weighted boron data for each grid (7 km × 7 km) shown in Fig. 1 for the two sampling trips in the same season. The boron concentrations for the 1-day sampling are different than those collected by spatial sampling in about 3 weeks duration, attributable to tidal effect on water chemistry. **80**

Figure 4.1.8. Boron budget of the Chilika lagoon for the monsoon season. The boron and salinity data shown here from this study, whereas the hydrological data are from Gupta et al. (2008). Please note that the arrow size does not reflect the water volume of the sources to the lagoon. **81**

Figure 4.2.1. Spatial distribution of (A) water salinity and (B) dissolved barium concentrations of the Chilika lagoon during the monsoon seasons. **84**

Figure 4.2.2. Co-variation between salinity and barium concentrations of the lagoon during (a) post monsoon (Jan), (b) pre-monsoon (May) and (c) monsoon (Aug) seasons. Most of the data either fall above, or below the theoretical mixing line, suggesting non-conservative behavior of Ba in the lagoon. **85**

Figure 4.2.3. Two-hourly data for salinity and dissolved barium concentration at Satapada (outer channel) during the monsoon season. This observed variation in Ba and salinity points to fluctuation of Bay of Bengal water influx into the Chilika due to tidal cycle. **87**

Figure 4.2.4. Estimated gain/loss of dissolved barium from the Chilika lagoon during different seasons. **89**

Figure 4.2.5. Plot shows the strong negative and positive correlation between sedimentary barium and clay abundances (A), suggesting the involvement of clay fraction in ion exchange process. Plot B, between Ba/Al and Mg/Al ratio of suspended sediments, indicating that the adsorption of Mg in response to the desorption of Ba. **91**

Figure 4.2.6. Barium budget of the Chilika lagoon with its major sources and internal cycling pathways. **93**

Figure 5.1.1. Spatial distribution of dissolved Re concentrations of the Chilika lagoon during the monsoon season. Representative compositions for major sources (river, groundwater and Bay of Bengal) are also shown. **101**

Figure 5.1.2. Two-hourly variations in salinity and Re concentrations show impact of seawater exchange with the lagoon during semi-diurnal tidal cycles. **102**

Figure 5.1.3. Co-variation between salinity and Re concentrations of the lagoon for all seasons (monsoon, pre-monsoon post-monsoon). The solid (black) line reflects the theoretical line for conservative river-sea water mixing. For reference, average groundwater and Bay of Bengal compositions are also shown. **103**

Figure 5.1.4. Distribution of Re concentrations in the bulk, clay and exchangeable fractions of the bed sediments and coastal macrophytes from the Chilika lagoon system. For reference, the Re concentrations for the riverine sources (this study) and upper continental crust (UCC; Miller et al., 2011) have also been shown. **104**

Figure 5.1.5. Estimated addition/removal of rhenium (in %) with respect to salinity of the Chilika lagoon during all seasons investigated herein. **106**

Figure 5.1.6. Correlation of sedimentary Re with (a) Mg, (b) Al and (c) TN (total nitrogen) concentrations for the Chilika lagoon. The river samples consistently show lower concentrations for all the parameters. The significant positive correlation with Mg and Al point to accumulation of rhenium via clay adsorption, whereas the Re-TN covariation hints at biological uptake by amino acids during cellular membrane formations. **110**

Figure 5.1.7. Sources and cycling of rhenium in the Chilika lagoon, India. The figure depicts all possible pathways (e.g. clay adsorption and biological uptake) and rates of Re removal from this coastal system. **112**

Figure 5.2.1. Comparison of DIC and $\delta^{13}C_{DIC}$ values of Chilika Lagoon with other rivers/estuaries and carbonate-silicate sources. The compiled data and their references are given in the supplementary material. **115**

Figure 5.2.2. Two-hourly variations in salinity, DIC and $\delta^{13}C_{DIC}$ concentrations (selected samples 5 out of 12) show impact of seawater exchange with the lagoon during semi-diurnal tidal cycles. **116**

Figure 5.2.3. DIC distribution along the salinity gradient in the Chilika lagoon is shown in the left panel and $\delta^{13}C_{DIC}$ signatures along the salinity gradient is present in right panel. The dotted line presents the conservative mixing between river and seawater, data which is used to construct this line is provided in Table A4. **117**

Figure 5.2.4. Plot shows the deviations from conservative mixing lines of $\delta^{13}C_{DIC}$ ($\Delta\delta^{13}C_{DIC}$) as a function of DIC (ΔDIC) for the Chilika lagoon. Different colors represent the sampling campaigns. The origin represents the conservative mixing between fresh-seawater end-members. The four quadrants indicate biogeochemical processes which are responsible for affecting the DIC and $\delta^{13}C_{DIC}$ values. The quadrant of primary production/ CO_2 degassing is indicative of decrease of DIC concentration and increase of $\delta^{13}C_{DIC}$ values. The quadrant of calcite dissolution represents the enrichment of DIC concentrations and $\delta^{13}C_{DIC}$ values. The quadrant of calcite precipitation is representative of depletion of DIC concentrations and $\delta^{13}C_{DIC}$ values. The quadrant of the degradation of organic carbon indicates the enrichment of DIC concentration and depletion of $\delta^{13}C_{DIC}$ values. **118**

Figure 5.3.1. Frequency distribution of sedimentary organic carbon isotopic composition of the Chilika lagoon. For references, the average isotopic values for river sediments (this study). C3 and C4 plans (Tipple and Pagani, 2007), typical marine organic matter (Ramaswamy et al., 2008) and macrophytes (Amir et al., 2019) from the Chilika lagoon is also shown. **119**

Chapter 1
Introduction

1.1. Introduction

Trace elements play key role in ocean biogeochemical cycle, mainly due to their bio-essential properties, redox-sensitive nature and multiple oxidation states. These elements and their isotopes also serve as reliable proxies for various oceanic processes, which include reconstruction of paleo-redox conditions, paleo-alkalinity, water circulation and productivity pattern (Calvert and Pedersen, 1993; Dean et al., 1997; Tribovillard et al., 2006; Nameroff et al., 2002; Dehairs et al., 1980; McManus et al., 1999; Paytan et al., 1996; Lea and Boyle, 1989; Jeandel et al., 1996; Rubin et al., 2003; Costa et al., 2018; Horner et al., 2020). Distribution of these elements in the modern ocean is largely regulated by the balance between their sources (continental input, atmospheric deposition, hydrothermal activities and sea-floor alteration) and sinks (authigenic and biogenic mineral formations) (Murray, 1987; SCOR Working Group, 2007; GEOTRACES, 2006, Anderson and Henderson, 2005). In coastal oceans, inventory of these elements, however, is complicatedly governed by their additional release (*via* desorption, mineral re-dissolution, submarine groundwater discharge (SGD)) and/or removal (*via* adsorption, biological uptake) due to physical (tidal cycles, suspended sediment loads and clay content), chemical (pH and ionic strength) and biological changes at the freshwater-seawater interfaces (Charette et al., 2005; Charette et al., 2016; Flegal et al., 1991; Samanta and Dalai, 2016). Quantification of this internal elemental cycling is a challenging task due to its indirect and non-point nature. Consequently, imprecise estimation of these coastal processes contributes to the existing oceanic imbalances of several elements, which in turn limits their application as paleo-oceanographic proxies.

The coastal oceans are biologically active aquatic systems with strong exchange of matter and energy between land and oceans. These coastal regimes support intense productivity and efficient organic carbon burial within the lagoon, regulating both the regional and global carbon cycles. For instance, although these shallow systems cover only 7% of the surface area and 0.5% volume of the global ocean, it is characterized with disproportionally higher amount of total oceanic primary production (~25%), organic carbon burial (~80%) and $CaCO_3$ deposition (~50%) (Berner, 1982; Smith and Hollibaugh, 1993; Gattuso et al., 1998). Furthermore, these regions are of large societal relevance as one fourth of the world population resides in the low laying regions (Nicholls et al., 2007). Anthropogenic supplies through various manmade activities from these regions also contribute to the eutrophication of the coastal ocean and degradation of several environmental factors (e.g. water quality, changes in the acidity, alteration of the marine food web and community structure) at a global scale (Rabouille et al., 2001; Cai et al., 2011; Regnier et al., 2013).

Chemistry of the coastal waters is complicatedly regulated by its sources, sinks and internal cycling within the aquatic and/or sediment-water interfaces. The major pathways which regulate the abundance and distribution of trace metals include fresh-sea water mixing, submarine groundwater discharge (SGD), sediment-water interactions (e.g. adsorption, desorption), co-precipitation and re-dissolution of minerals, and biological uptake (Fig. 1.1.) (Flegal et al., 1991; Charette and Sholkovitz, 2006; Moore, 1996; Charette et al., 2016; Samanta and Dalai, 2016). The freshwater and seawater mixing with varying ionic strength, pH, redox potential and water chemistry (Bowden, 1963; Dyer, 1974; Duinker and Nolting, 1978; Griffin and LeBlond, 1990; Nepf and Geyer, 1996; Feely et al., 2010) dominant the coastal water chemistry. Covariation between salinity and trace elements (TEs) has often been used to constrain solute contribution from these two source waters. The "conservative" elements follow a linear salinity-TEs trend as expected for river and seawater mixing, confirming their supply only from these two sources. In contrast, non-conservative elements do not follow the theoretical mixing line and their deviation from the line serve as a measure to estimate relative contribution of TEs from the additional sources/sinks.

The amount of TEs supplied by surface runoff to coastal system depends on flow stage of rivers with higher amount of TEs being supplied during high flow stages. The seawater-driven TE fluxes to these shallow systems mainly depend on the tidal cycles. In addition to river and seawater, the submarine groundwater discharge (SGD) is also an important supplier of TEs to the coastal system (Knee and Paytan, 2011). The SGD, which is inclusive of both fresh and brackish groundwater, have been recognized to supply high amount of nutrients (N, Si), alkali-earth metals (Ba and Ra) and other trace metals (e.g. U) to the ocean (Moore, 1997; Swarzenski and Baskaran, 2007; Santos et al., 2011; Cho et al., 2018)). Interestingly, the SGD-derived elemental fluxes are also found to be higher than that supplied by rivers in selected basins, underscoring significance of this subsurface source in regulating the trace elemental inventory in near-shore environments (Cho et al., 2018). The amount of SGD supplied to any coastal system vary significantly at semi-diurnal, diurnal, fortnightly and seasonal timescales (Taniguchi, 2002; Knee and Paytan, 2011). The semi-diurnal to diurnal variations in the SGD flux is mainly linked to hydraulic gradient between the land and sea during tidal cycles, whereas this flux during the fortnightly scale is regulated by tidal pumping. The seasonal-scale SGD variation is associated with water table elevation changes due to rainfall and evapotranspiration effects. At spatial scale, the SGD vary as a factor of offshore distance and aquifer heterogeneity.

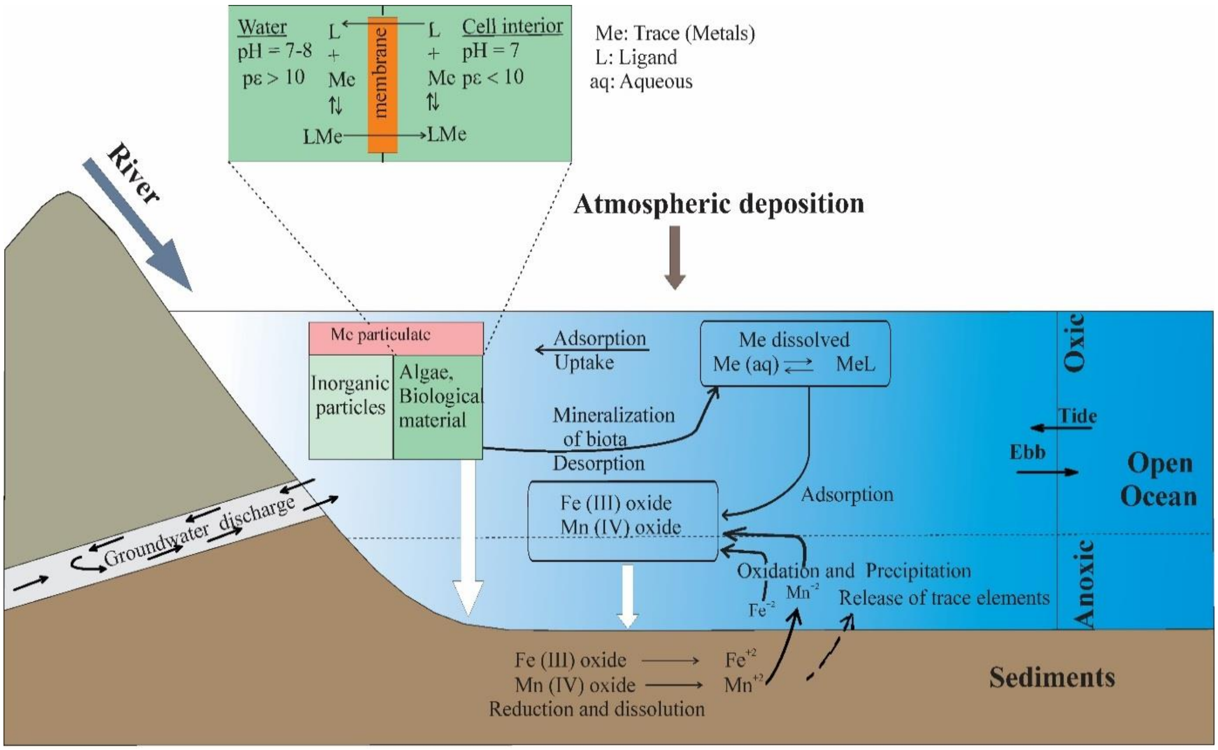

Figure 1.1. Schematic diagram showing major sources, sinks and internal cycling of trace metals in coastal systems (Figure modified after Stumm and Morgan, 2012).

In addition to source waters, trace element inventory of the coastal waters is also regulated by ion-exchange processes, such as desorption and adsorption (Boyle et al., 1974; Coeffy et al., 1997). Both inorganic (oxyhydroxides, clay, organic debris) and organic (algae) particles participate as substrates in this particulate-water interaction. Intensity of this process is mainly regulated by affinity of metals ions to get adsorbed and surface reactivity of substrates. The affinity of metals to get adsorbed can be assessed by their partition coefficient, K_d, which is defined as: $K_d = C_s/C_w$, where C_s and C_w stand for metal concentrations for solid and water phases, respectively (Stumm and Morgan, 2012). The Fe-Mn oxides serve as an important substrate for the metal adsorption in oceanic systems. The manganese oxides in aquatic systems generally form as poorly-crystalized birnessite (δ-MnO_2) which contains less oxygen (in the range of $MnO_{1.6}$ to $MnO_{1.95}$) than the ideal MnO_2 phase (Drever, 1997). These fine-grained oxides are negatively charged at high pH and thier cation-exchange capacity (CEC) increases with increase in pH. Considering high (alkaline) pH of natural waters (typically, 7-8.5), adsorption of TEs to these oxyhydroxides is most favorable. In contrast to pH, the adsorption affinity of elements from water to particulate (K_d) decrease with high salinity. This inverse relation is due to metal desorption because of competition from major cations (Mg, Ca) and anions present in seawater for active sites. The K_d also show an inverse relation with the suspended particulate matter (SPM) load (Stumm and Morgan, 2012). This trend is mainly linked with abundance and type of suspended clay particles. The negatively charged clay particles adsorb the dissolved free cations (TEs) present in water column to get neutralized. The intensity of TEs-adsorption on the clay substrate depends on the clay type. The CEC for Smectite (80-150 mEq/100 g) is more than Kaolinite (1-10 mEq/100 g), illite (10-40 mEq/100 g) and chlorite (<10 mEq/100 g) and hence, has higher potential to participate in adsorption (Drever, 1998). Additionally, TEs may also interact with organic matter and form chelate-type complexes, which may contribute to high TEs concentrations in some of the coastal regions with high dissolved organic carbon.

Biological processes also influence the trace metals concentrations in coastal regimes. Several bio-essential elements serve as cofactors of metalloenzymes and proteins in metabolic processes of marine organisms (Luome, 1983; Stumm and Morgan, 2012; Morel and Price, 2003). Surface concentrations of these elements are often found to be low due to uptake by biota, whereas their high deep-water concentrations are linked to re-dissolution of organic matter. A few bio-essential elements, such as Mn, also show high surface concentration, which resulted from photochemical reductive dissolution of its oxides. The biological uptake of trace metals occurs at and across the interface between non-polar aqueous medium and polar medium in the organisms (membrane and cellular interior). Figure 1.1. depicts the mechanism of trace metal uptake which involves complex formation by the metal ions with appropriate organic ligands (e.g. EDTA or, NTA) and their subsequent transport into the cell interior by molecular "porter". The rate of these biological processes, therefore, mainly depends on total concentrations of free metal ions and/or the organic ligands. Diffusion also play a part in metal transportation from extracellular part to the cell interior. Metal uptakes from solutes for selected metals (Cd, Cu, Fe, Mn and Zn) also occur through bioaccumulation by eukaryotic and prokaryotic algae, invertebrate and fishes. Interestingly, the uptake of Zn and Cu in marine organisms often happens in fixed ratios, similar to the Redfield ratios for major nutrients. These bioinorganic properties of elements are still an active field of research to constrain their uptake mechanisms via biological processes.

Understanding the coastal behavior of trace metals and quantifying related processes are crucial to assess their impact on coastal ecosystem and also, to evaluate their potential as a proxy for paleo-oceanographic processes. Available studies on coastal behavior of trace elements have mostly been restricted to estuarine regions and there have been insignificant efforts to assess these properties in coastal lagoons. These shallow and semi-restricted aquatic systems with rigorous matter and energy exchange with the ocean and high sediment suspension due to tidal forces influence the coastal chemistry and also, ultimate fate and delivery of nutrients to the open ocean. The Chilika lagoon, Asia's largest brackish-water lagoon system, provides a natural environment with estuarine features, intense productivity patterns, heterotrophic nature and higher carbon burial efficiency. Many of these processes are intimately linked with abundance of chemical elements in the lagoon. Despite its significances, the biogeochemical cycling of major and trace elements in the Chilika lagoon has not yet been studied in detail. Prior to this thesis work, available studies on chemistry of the Chilika system has mainly focused on its water quality (Nayak et al., 2004; Panigrahi et al., 2007, 2009; Barik et al., 2017), productivity pattern and sources and type of inorganic and organic carbon (Nazneen et al., 2017; Amir et al., 2020; Patra et al. 2017; Kanuri et al., 2018; Amir et al., 2019). Earlier studies on dissolved inorganic (DIC) and organic (DOC) carbon (Gupta et al., 2008; Muduli et al., 2012; 2013) indicates that the Chilika lagoon is heterotrophic in nature and its 92 % of net ecological production is by the pelagic community with minor role of the benthic community (Gupta et al., 2008). The phytoplankton productivity in the lagoon has been reported to be limited by the nitrogen availability (Panigrahi et al., 2007). The nitrogen and organic carbon isotopic studies of the Chilika sediments indicate that the sedimentary organic matter are mainly supplied through terrestrial sources and macrophytes, with minor contributions from phytoplankton and cyanobacteria (Amir et al., 2019; Mukherjee et al., 2019). The CO_2 fluxes from the lagoon were observed to be higher during the high flow stages, compared to lean flow stages, and are attributable to high riverine supply of organic matter and its subsequent degradation. The DIC/DOC ratio in the lagoon is mainly regulated by source water mixing and intense respiration

(Gupta et al., 2008). Further, the seagrass and macrophytes of the Chilika also play a key role in the carbon cycling within the lagoon (Banerjee et al., 2018). Sequential extraction analyses of sedimentary phosphorus in the Chilika lagoon indicate dominancy of calcium bound P (~55%) with subordinate contribution from Fe-bound P (~15 %) in regulating the nutrient abundance (Barik et al., 2016). These data also hint at impact of manmade activities (rapid developments of industry, agriculture, and urbanization) in regulating the P content. In contrast to these studies, the distribution of trace metals in the Chilika lagoon and factor regulating their spatio-temporal variation has received little attention.

Table 1.1. Typical composition of key parameters of elements of interest for the ocean system

Element	Major minerals	UCC	River water	Surface seawater	Residence time	Ref.
Boron	Phyllosilicates (micas) and clay minerals	17 μg/g	0.94 μmol/kg	433 ± 2 μmol/kg	14 Myr	[1-3]
Strontium	Carbonates, gypsum and Ca-plagioclase	320 μg/g	1.22 μmol/kg	87.4 μmol/kg	~4 Myr	[3-7]
$^{87}Sr/^{86}Sr$		0.716	0.7111	0.70916		
Barium		624 μg/g	153 nmol/kg	30-40 nmol/kg	~8 kyr	[3, 8-10]
Rhenium	Sulphides, black shales	198 pg/g	11.2 pmol/kg	41 ± 2 pmol/kg	130 kyr	[11-13]

[1]Gaillardet and Lemarchand 2018; [2]Lemarchand et al., 2002; [3]Rudinick and Gao, 2003; [4]Richter et al., 1992; [5]Peucker-Ehrenbrink et al., 2010; [6]Goldstein and Jacobson, 1998; [7]Tripathy et al., 2012; [8]Hsieh and Henderson, 2017; [9]Carter et al., 2020; [10]Das and Krishnaswami, 2006; [11]Pecucker-Ehrenbrink and Jahn, 2001; [12]Miller et al., 2011; [13]Goswami et al., 2012

This thesis work attempts to investigate distribution and coastal behavior of selected elements (B, Sr, Ba, Re and $^{87}Sr/^{86}Sr$) in the Chilika lagoon. The strategy behind selecting these elements was their existing oceanic imbalance, complex coastal nature and their potential as a proxy for various biogeochemical processes (*e.g.* oceanic pH, redox state, continental weathering, water circulation and productivity patterns). The typical seawater compositions and related parameters for these elements and Sr isotope are summarized in Table 1.1. Existing studies on coastal properties of these elements document diverging views and report both conservative and non-conservative nature along the salinity gradient of estuaries. For instance, the distribution of boron, which is an essential micronutrient for phytoplankton and algae (Red algae; Bangia and Porphyra; Henkel 1952) and a paleo-pH proxy, shows both conservative behavior in estuaries connected to several major systems (Tamar, Zaire, Magdalena, Elbe, Changjiang, Gaoping, Narmada and Tapi estuaries; Fanning and Maynard, 1978; Liddicoat et al., 1983; Barth, 1998; Xiao et al., 2007; Wang et al., 2009; Singh et al., 2013) and also, non-conservative behavior for Alde, Purna, Auranga, Gulf of Papua (Liss and Pointon, 1973; Narvekar and Zingde, 1987; Brunskill et al., 2003; Russak et al., 2016). Although the exact cause for this difference is not well understood, non-conservative behavior of boron is mainly attributed to the removal of B onto the clay surfaces via adsorption processes. The suggested process draws support also from high B content of the clay-rich shales (Leeman and Sisson, 1996). This coastal sink involving ion-exchange process may explain the existing imbalance between sources (4.47 – 5.91 Tg B/yr) and sink (0.86 – 2.87 Tg B/yr) in oceanic boron cycle (Park and Schlesinger, 2002).

Unlike boron, dissolved Sr concentrations in the estuaries exhibit a conservative mixing between fresh and sea water in coastal regions. However, Sr isotopes mostly show a non-conservative trend along the salinity gradient of estuaries. Different coastal properties for Sr concentration and Sr isotopes are intriguing and have been attributed to isotopic exchange of Sr in subsurface aquifers (Rahaman and Singh, 2012). The deviation of $^{87}Sr/^{86}Sr$ is largely due to additional supply of ^{87}Sr via SGD and hence, has been used to estimate the SGD contribution by following a flux-by-difference approach. Beck et al. (2013), using the non-conservativeness of $^{87}Sr/^{86}Sr$, estimated that the SGD-derived Sr can account for 13‑30% of the present-day seawater $^{87}Sr/^{86}Sr$ budget, which is currently in imbalance with a missing sink with less radiogenic values. This source of Sr is relatively less radiogenic (~0.7089) compared to seawater $^{87}Sr/^{86}Sr$ (0.7092), which may be the potential missing sink required for the oceanic Sr isotopic budget (Beck et al., 2013). More coastal studies on SGD-Sr flux and their isotopic composition can help in refining this proposition at a global scale. Although both Sr and Ba are alkaline-earth metals with similar chemistry, their coastal behavior is distinctly different. Available large number of coastal studies on barium shows a non-conservative behavior with mid-salinity release of barium to the dissolved phases (Hanor and Chan, 1977; Edmond et al., 1978; Li and Chan, 1979; Carroll et al., 1993; Coffey et al., 1997; Moore, 1997; Joung and Shiller, 2014; Samanta and Dalai, 2016). This additional supply of Ba is mainly linked to the desorptive release from suspended sediments and/or submarine groundwater discharge. Although the non-conservativeness of Ba has been well-constrained, its intensity at different regimes are found to be variable and the Ba production via desorption in global estuaries vary significantly between 23-70% of its total inventory

(Samanta and Dalai, 2016). These large spatial variations are by and large regulated by particulate matter flux/water flux in a given estuary (Coffey et al., 1997; Samanta and Dalai, 2016).

The other element of interest for this thesis is rheniums, which is redox-sensitive in nature and serve as a reliable paleo-redox proxy. Despite of its oceanographic significance, there exists only a few studies focusing on coastal behavior of Re. These studies mostly show conservative behavior of Re in estuaries of large river system. A few studies also hint at removal/addition of Re via ion-exchange processes or, biological pathways. Rahaman and Singh (2010) also document impact of anthropogenic sources in regulating the Re abundance of eastern coast of the Arabian Sea. Recent studies have carried out detailed investigation on Re distribution in coastal macro-algae and show Re uptake by these organisms, mostly by green and brown algae (Rooney et al., 2016; Sproson et al., 2018, 2020). These biological pathways in Re scavenging are similar to that reported for several elements (e.g., Mn, Mo, Co, Cu) onto coastal algae and macrophytes (Sánchez-Quiles et al., 2017). Impact of these processes although have been established in lab-controlled experiments, this non-conservative sink for rhenium has yet been explored in coastal systems.

1.2. Objectives of this thesis

The major objectives identified for this thesis work are listed below:

- To quantify the fractional contribution from the major possible sources (e.g., river, seawater and submarine groundwater discharge (SGD)) to the water chemistry of the Chilika lagoon, India using Sr isotopes.
- To assess the impact of ion-exchange process on coastal water chemistry of the lagoon by investigating distribution of dissolved boron and barium concentrations along the salinity gradient of the lagoon for different seasons.
- To evaluate the role of biological processes in regulating dissolved rhenium (Re) and stable carbon isotopic (for dissolved inorganic ($\delta^{13}C_{DIC}$) and sedimentary organic carbon ($\delta^{13}C_{org}$) phases) compositions of the Chilika lagoon.

1.3. Outline of the thesis

The **chapter 1** introduces the biogeochemical cycling of trace elements in coastal regions and reviews the existing literature on various sources, sinks and internal cycling of trace elements. This chapter, based on the current research gaps, also identifies the objectives of this thesis work.

The **chapter 2** provides details about spatial and seasonal collection of samples from the Chilika lagoon and its source waters. The analytical details regarding chemical and isotopic measurements of these samples are also part of this chapter.

The **chapter 3** of the thesis focuses on estimating the submarine groundwater discharge (SGD) to the Chilika lagoon using dissolved Sr concentrations and $^{86}Sr/^{86}Sr$ ratios. These estimations were done using both forward and inverse modeling of Sr elemental and isotopic datasets; details on these mass balance calculations are also included of this chapter.

The **chapter 4** discusses the impact of ion-exchange processes on the chemical inventory of coastal lagoon system. For this, we have investigated the spatial and seasonal distributions of boron and barium along the salinity gradient of the Chilika lagoon. Impact of adsorption (for B), or desorption (for Ba) on the coastal behavior of these elements have been discussed. Additional insight on particulate-solute interaction, based on sediment chemistry data for the lagoon, is also presented in this chapter.

The **chapter 5** presents distribution of rhenium concentrations and stable carbon (both in dissolved inorganic and sedimentary organic phases) isotopic data for the Chilika lagoon system. These data are used to evaluate impact of biological activities on the coastal cycling of chemical constituents.

The **chapter 6** summarizes the major conclusions drawn from this thesis work. This chapter also highlights the future directions for these researches on coastal cycling of trace metals and its impact on global (oceanic) chemical budgets.

Chapter 2
Materials and Methods

The main objective of this thesis work, as mentioned in chapter 1, was to evaluate the role of coastal processes (SGD, ion-exchange process, biological activities) in regulating inventory of selected TEs and carbon in a tropical coastal lagoon (Chilika, India). To achieve this objective, geochemical (B, Ba, Sr, and Re) and isotopic ($\delta^{18}O$, $\delta^{13}C_{org}$, $\delta^{13}C_{DIC}$, and $^{87}Sr/^{86}Sr$) analyses was carried out in water and sediments samples collected from the Chilika and its possible sources (rain, river, groundwater, coastal and western Bay of Bengal) during four different seasons. However, proper understanding of these spatial and seasonal dataset would require information about climate, hydrology and geology of the basin. Though these details have already been presented in several early works and have been briefly presented here based on available literature. Further, details about samples collection, and their chemical analyses have also presented in this chapter.

2.1. Study area

The Chilika lagoon, a polymictic and shallow (mean water depth ~2 m) brackish water lagoon, is situated parallel to the east coast of India between the Eastern Ghat and the Bay of Bengal (Fig. 2.1). This lagoon system is a Ramsar wetland site of international importance, and known for its rich biodiversity, migratory waterfowls in winter, and fishery resources. This highly productive ecosystem houses several fish species and varieties of aquatic and non-aquatic plants (Rath and Adhikary, 2005; Madhusmita, 2012). The lagoon was formed about 3750 years ago as a consequence of sea level rises and subsequent land emergence due to minor tectonic uplift (Venkatarathnam, 1970). The coastal lagoon is about 65 km in length with a variable width reaching up to 20 km (Fig. 2.1; Sarkar et al., 2012). The water depth of the lagoon varies from 0.9 to 2.6 m during dry season and from 1.8 to 3.7 m during the rainy season (Kumar and Pattnaik, 2012). It contains about 2.06×10^{12} L volume of water. The drainage basin of Chilika Lagoon covers a total area of almost 4300 km^2. Out of which, the size of the lagoon has a maximum area of 1165 km^2 during the monsoon which decreases to 950 km^2 during the non-monsoon period (Siddiqui and Rao, 1995). Additionally, the drainage basin also includes 2325 km^2 of agricultural land, 525 km^2 of forests, 190 km^2 of permanent vegetation, 70 km^2 of swamps and wetlands, and 90 $km^2$of grassy mud flats (Kumar and Pattnaik, 2012).

2.1.1. Climatic condition

The Chilika basin mainly experiences tropical climate with strong seasonal variation

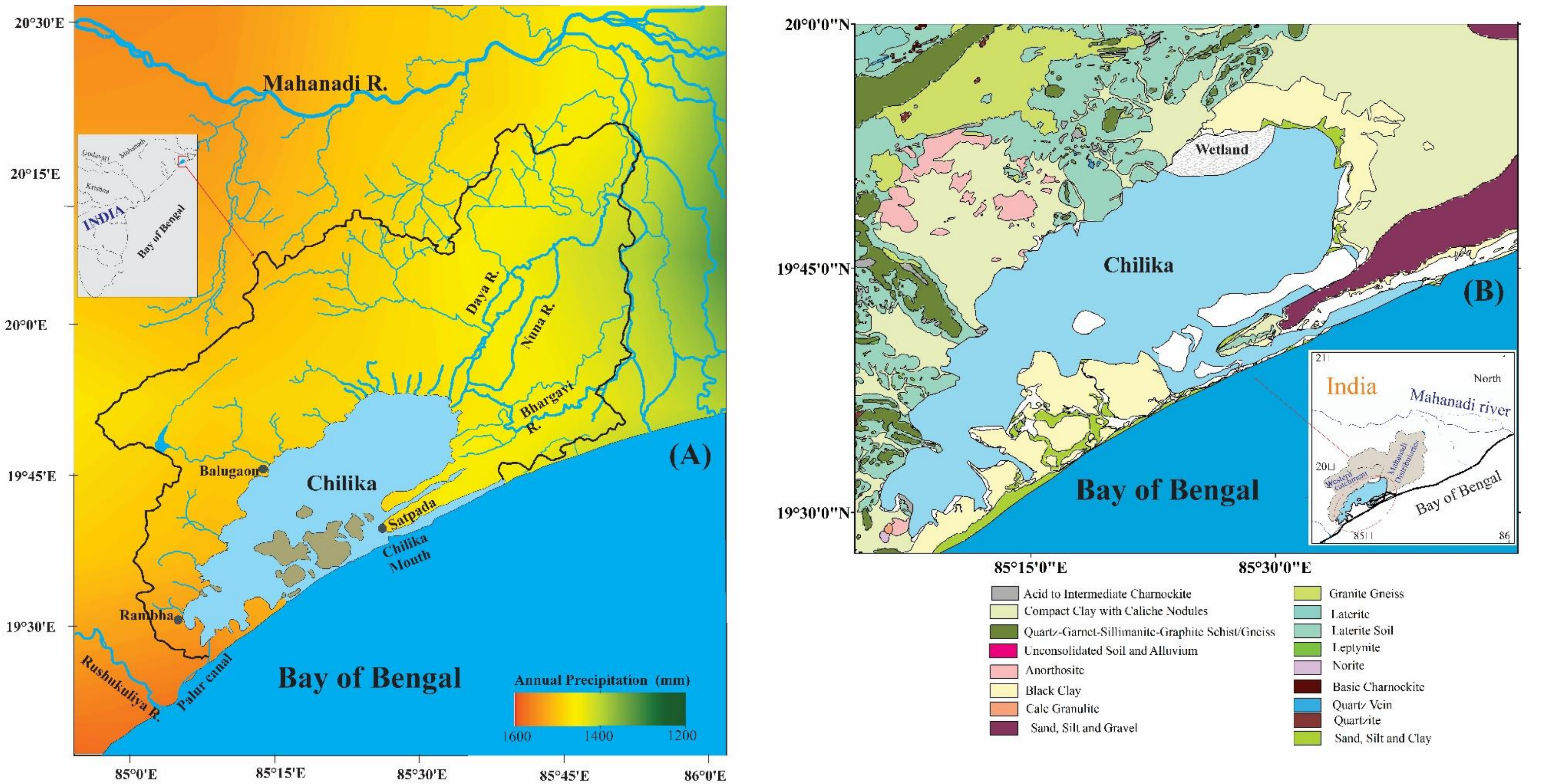

Figure 2.1. Map of the Chilika Lagoon including its drainage basin (A) and surrounding geology (B). The spatial distribution of rainfall (A) in the Chilika drainage basin during the sampling period (2016 to 2018) is also shown (data source: https://giovanni-.gsfc.nasa.gov/).

in temperature and rainfall. The air temperature of the Chilika varies from ~20 °C to ~32°C with the maximum temperature being observed during the summer season (~32°C) whereas the lowest temperature being observed during the winter season (~20 °C) (Fig. 2.2B). The annual rainfall for this region is 1240 mm and its month variation has been depicted in Fig. 2.2A. The monthly rainfall intensity varies from ~0 to ~653 mm (http://hydro.imd.gov.in). About 75 % of the annual rainfall occurs during the summer season, due to the impact of southwest monsoon (www.Chilika.com). The lagoon also experiences significant seasonal and diurnal variation of the wind speed and direction (Tripathy, 1995). The wind speed is high during the month of March to July as compared to winter season. The wind speed ranges between 4.5 and 18.3 kmph (Panigrahi et al., 2007). The wind direction is mostly north-easterly during the winter season, whereas it is southwesterly directed during the summer season. Variation in these wind speed and direction often lead to many cyclonic events of high magnitude in the east coast of India, which also influence the Chilika hydrology. Consistent with the wind pattern, the Chilika lagoon experiences a clockwise circulation due to the influence of south-west wind during monsoon period whereas north-west wind creates a counterclockwise circulation in the lagoon during the winter season (Panigrahi et al., 2007). In addition to wind, the water circulation in the Chilika is also influenced by bathymetry, wind stress, tides and freshwater influx from the rivers.

2.1.2. Hydrology of the lagoon

The Chilika lagoon exhibits estuarine characteristics with water supply from both fresh and seawater sources. Based on hydrology, lagoon has divided into four sectors viz. northern sector, central sector, southern sector and outer channel. The lagoon receives about 75 % of riverine input from its northern catchments, whereas about 25 % of riverine input comes from the western catchments (Kumar and Pattnaik, 2012). The northern sector mainly receives freshwater via Mahanadi distributaries, such as Daya and Bhargavi (Kumar and Pattnaik, 2012). These two streams are small streams of the Mahanadi river system and account only 31% of water discharge of this large river system. The annual discharge to the lagoon from these streams is 5.1 $\times 10^{12}$ L/yr (Muduli et al., 2012). This riverine influx varies significantly seasonally, with about 60 - 80% of water being supplied during the monsoon period (Fig. 2.3A). Freshwater discharge during the monsoon season (~170 $\times$ 10^6 m^3d^{-1}) is higher by about two order of magnitude compared to that during the pre-monsoon period (4 $\times 10^6$ m^3d^{-1}; Fig. 2.3A; Muduli et al., 2012).

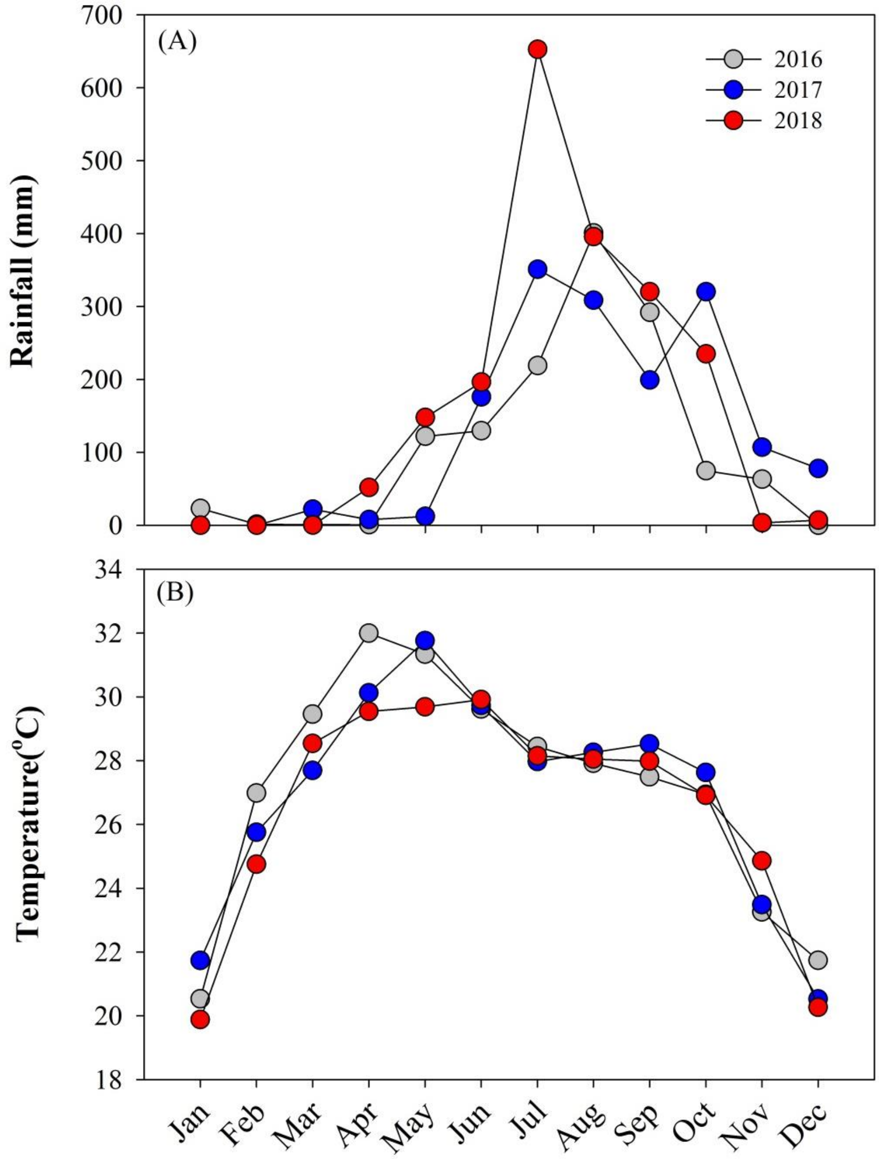

Figure 2.2. Monthly average variation of rainfall and temperature near to the Chilika basin during three consecutive years of sampling i.e. 2016, 2017 and 2018. Rainfall data has been taken from the CRIS ((http://hydro.imd.gov.in) and temperature data were taken from the Wunderground (https://www.wunderground.com).

The seawater from the Bay of Bengal to the lagoon is mostly supplied to the central sector through an opening of ~32 km. Additionally, the southern sector of the Chilika is also connected with the Bay through a small channel, Palur canal. The amount of water exchange between the Chilika and Bay of Bengal is different during the flood (88×10^6 m^3d^{-1}) and ebb (205×10^6 m^3d^{-1}) phases of the tidal cycle (Gupta et al., 2008). These efficient exchange lead to low residence time of water in the Chilika Lagoon (Table 2.1). The residence time (RT) of lagoon water varies both spatially and seasonally (Gupta et al., 2008; Mahanty et al., 2016). The

RT is lowest (4-5 days) in the outer channel due to efficient water exchange between the lagoon and the sea. In the northern sector, this varies widely from 132 days during the dry periods (November-June) to 8 days during the monsoon (July-October; Mahanty et al., 2016). These residence times are also influenced by the tidal cycle of the lagoon. Tides in the Chilika are predominantly semi-diurnal (12.4 hours) and fortnightly (12 days periodicity) in nature (Mahanty et al., 2015). The water level of the lagoon at its inlet (near Satapada) varies by ~1 m (between 0.84 and 1.92 m) during the non-monsoon and by ~1.5 m (between 1.07 and 2.53 m) during the monsoon season (Mahanty et al., 2016). These tidal cycling introduce temporal changes in the seawater incursion into the lagoon and hence, can influence the lagoon chemistry.

In addition to river and seawater, groundwater, both fresh and brackish-water, can serve as an important source of water to the lagoon. There exists no data on groundwater influx to the lagoon. Additionally, anthropogenic activities often influence the chemistry and water quality of lagoon water that interferes in the ecosystem functioning (Campesan et al. 1981; Sorokin et al. 1996; Collavini et al. 2001). Chilika lagoon also influence by different types of contaminants, it receives several types of inputs, viz., urban, industrial and agricultural wastes, which results in significant alteration in the water quality and ecology (Pal and Mohanty 2002; Panigrahi 2006). The lagoon also receives significant anthropogenic supplies (~550 million L/day) from agriculture, aqua-culture and domestic practices (Panigrahi et al., 2009). Depending on the seasonal agricultural practices, these supplies to the Chilika are expected to show large monthly variations.

The abundance of suspended sediments and their resuspension, like in any aquatic system, regulate the photic property (transparency) of the Chilika lagoon. The average sedimentation rate for the lagoon is higher in the northern (7.6 mm/yr) and central (8.0 mm/yr) sectors, compared to that of the southern sector (2.8 mm/yr; Sarakar et al., 2012). The lagoon receives about 3.65×10^6 tons silt during the monsoon season, out of which about 75% of silt (2.75×10^6 tons) is delivered by the Mahanadi distributaries from the northern catchment and remaining 25% (0.90×10^6 tons) of sediment is derived from the western catchments (Mishra et al., 2013). The average concentrations of suspended sediments show significant spatial variation with their concentrations being higher in the northern (89 ± 58 mg/L), than that of the southern (45 ± 36 mg/L) and central (31 ± 25 mg/L) sectors. The suspended sediment concentrations also show significant seasonal changes, with high sediment load being observed for the monsoon seasons

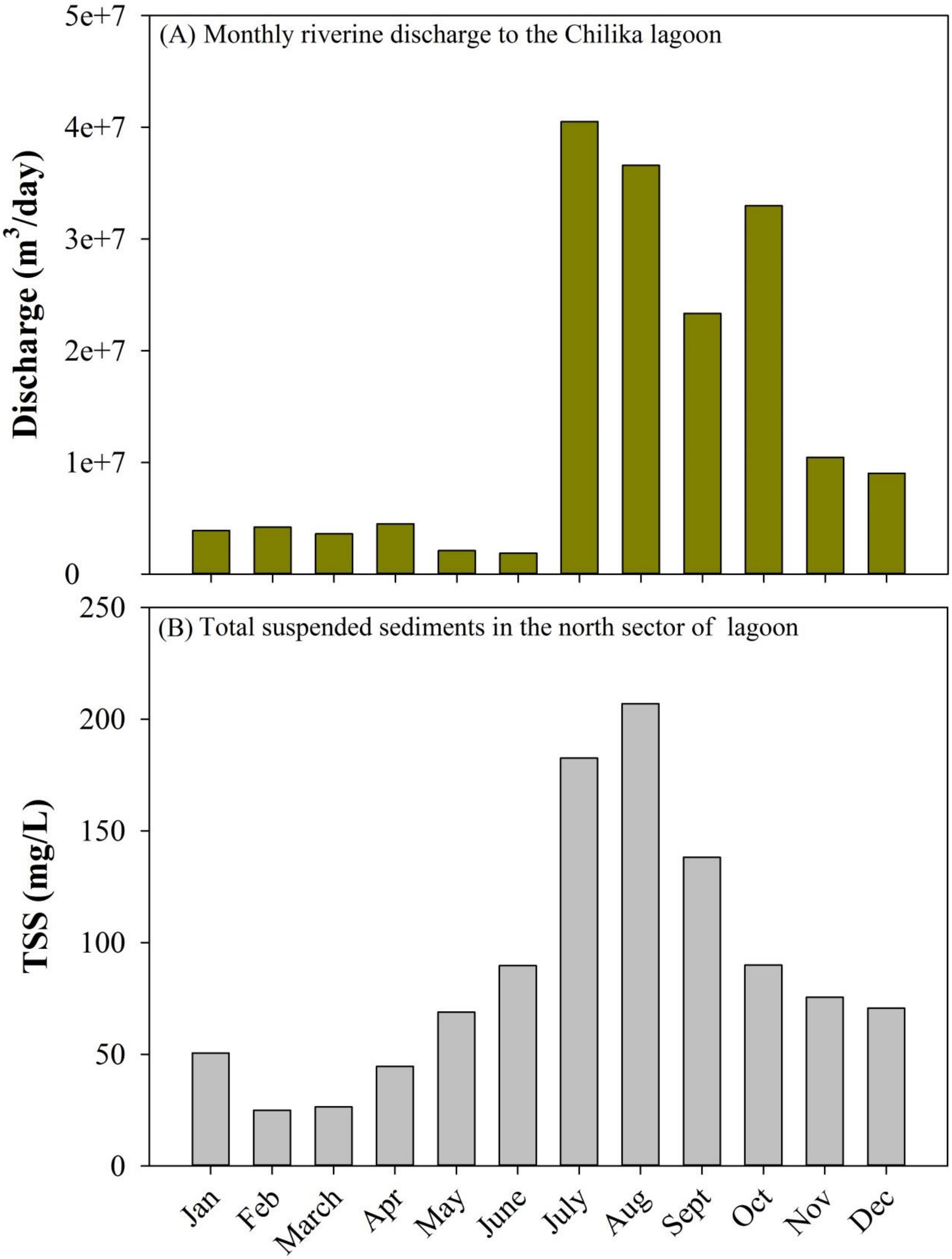

Figure 2.3. (A) Shows the monthly distribution of freshwater discharge to the Chilika Lagoon from the Mahanadi distributaries (Data from Muduli et al., 2013) and (B) Plot shows the distribution of suspended sediments in the north sector of Chilika lagoon (Data from Kumar et al., 2016).

(Fig. 2.3B). The total sediments supply to the Bay of Bengal from the lagoon is 0.3 million metric tonnes (Kumar and Pattnaik, 2012). The littoral drift carries ~ 1.5×10^6 m^3 yr^{-1} of sand, mostly between March and October months, from south to the north along the coast, which is responsible for choking and northward shifting of the inlet mouth (Chandramohan et al., 1993; Chandramohan and Nayak 1994). Further, long shore drifts carry about 0.1 million metric tons sand annually which is responsible for the shifting and closing and opening of inlet (Sarkar et al, 2012).

Table 2.1. Water residence time estimated spatially and temporally in the Chilika Lagoon (Mahanty et al., 2016).

Location	**Dry period**	**Wet period**
	RT (day)	**RT (day)**
Outer channel	4.9	5.6
North sector	132.2	7.6
Central sector	28.6	16.3
South sector	123.2	34.9

2.1.3. Geology of the lagoon

The drainage basin of the Chilika lagoon, both in its northern and western catchments, is mainly composed of crystalline rocks of the Eastern Ghat mobile belts. These major rock types are khondalites, granites, charnockites, anorthosites, granulites, laterites and alluvium plain (Kumar and Pattnaik, 2012). These rocks are mainly composed of quartz and feldspar minerals. Although the exact spatial extent of these bedrocks in the basin is unknown, the areal exposure of granite (34%), khondalite (7%), charnockites (15%) and Gondwana rocks (34 %) are found to be significant in the Mahanadi river basin (Chakrapani, 1990). The weathered and fractured zones of the crystalline rocks and the porous alluvial and coastal deposits form the groundwater aquifer of this region. Depending on the water yielding properties of various formations, the area can be broadly grouped into three distinct hydrogeological units i.e. consolidated formations, semi-consolidated formations, and un-consolidated formations (http://cgwb.gov.in). Consolidated formations include granites and granite gneisses, khondalites and charnockites. The semi-consolidated formations constitute laterites which are highly porous in nature and formed as capping over the older crystalline. Alluvium of recent ages (in Kyr timescale) constitutes the unconsolidated formations.

2.1.4. Flora and fauna

The phytoplankton community of the Chilika Lagoon is composed of about 128 species (Panigrahi et al., 2009), which include diatoms (~54 %), blue-green algae (~44.7 %), dinoflagellates (~0.8 %) and green algae (~0.6%; Sarkar et al, 2012). The diatoms are found in all part of the lagoon, except in the northern sector. The blue-green algae occur in the northern and central sectors. The density of zooplanktons in the lagoon varies between 1740 and 10370 individuals/m^3 with a biomass value of 1.72 - 3.3 g/m^3 (Sarkar et al., 2002). Additionally, the Chilika is also comprised of three vegetation types, *viz*. aquatic, littoral scrub and vegetation on sand dunes (Pandey et al., 2013). Their distribution depends on marine incursion, inundation frequency, salinity and nature of substratum. The northern and central sectors of the lagoon house several macrophytes (Rath and Adhikary, 2005; Madhusmita, 2012). Growth and decomposition of these macrophytes influence the dissolved oxygen content of the Chilika greatly. The Chilika houses several species of fish (323 types), mammals (24 types) and reptiles and amphibians (37 types; Sarkar et al., 2002). It is also responsible for huge (10,000 Mt per annum) fishery production.

2.2. Materials

2.2.1. Sampling

Detailed spatial and seasonal collection of water and sediment samples from the Chilika lagoon system have been conducted for this thesis work. These samples were collected from the Chilika lagoon and its possible sources (e.g. Bay of Bengal, rivers, rain and groundwater). The spatial sampling of water samples from the Chilika lagoon were carried out during four field campaigns (June, 2016; May, 2017; August, 2017 and January, 2018) (Fig. 2.4; Table A1 – A5). The samples collected during August, 2017 represents the monsoon season, whereas those from May, 2017 and January, 2018 represent pre-monsoon and post-monsoon seasons, respectively.

The post-monsoon samples were collected after two heavy rainfall events [during mid-November (BOB-06 cyclone) and early-December (BOB-08 cyclone); http://www.imd.-gov.in] due to low depression developed over the Bay of Bengal. The field trip during June, 2016 was conducted to collect samples during the onset of monsoon. Typically, the lagoon receives about 21% of its annual riverine discharge during August (monsoon), about 1 % during both May (pre-monsoon) and June months and about 2 % in January (Fig. 2.3A; Muduli et al., 2013). Spatial collection of surface water samples throughout this lagoon using a boat took around 3-4 weeks during each campaign. The fortnightly tidal cycle may influence the water chemistry within the total sampling period of 3-4 weeks. Realizing this, we have also sampled the whole lagoon (with limited spatial resolution) within 1 day during the monsoon and post-monsoon seasons for comparison. A total of thirty-one water samples throughout the Chilika lagoon were collected on 16th August, 2017, whereas 23 samples were collected on 10th January, 2018. Further, water samples at two different locations (Satapada (outer sector), Barkul (southern sector); Fig. 2.4) were also collected at 2-hours interval for a duration of 24 hours during the monsoon (August) pre-monsoon (May) and post-monsoon (January) seasons.

The Chilika receives freshwater from its northern (Mahanadi distributaries) and western (small rivers /rivulets) catchments. Water samples from these rivers/rivulets were collected from mid channel of the stream during different seasons. The groundwater samples (n = 78) either from open wells or hand pumps from the basin have also been collected during the four field trips. The rain water samples (n = 31) at three near-by locations (Berhampur, Barkul and Rambha) were also collected during the southwest monsoon period of 2017. Sampling of rain water was collected at ~ 5 m above the ground using a pre-cleaned plastic container. The seawater samples have also collected from the coastal Bay of Bengal (n = 9) during the January, 2018 using a motorized boat. Additionally, samples from the western Bay of Bengal collected during the RR1317 cruise (Nov-Dec, 2013) have also been used to constrain the seawater composition.

Sampling of water samples were conducted following the approach adopted by Rahaman and Singh (2010). Surface water samples were collected in 10 L plastic containers, after rinsing them with the ambient water. Water temperature, pH, salinity and dissolved oxygen (DO) of the samples were measured on-board using portable multi-parameter probes. In addition, the total water depth of the lagoon at the sampling sites was also measured manually using a graduated wooden pole. Salinities and DO of reference solutions and pH of buffer solutions were constantly monitored for the data accuracy. The collected samples were filtered on the same day (or, within 24 hours for few samples) through 0.45 µm nylon filters using vacuum filtration system. We have used HDPE bottles for sample storage and prior to sampling, these bottles were soaked with 1 N HCl at room temperature for 2-3 days and rinsed thoroughly using MilliQ water. About 500 ml of filtered water were acidified to pH~2 using nitric acid and stored in the pre-cleaned bottles. Additionally, 30 ml filtered samples also stored in amber bottles which was poisoned by adding saturated $HgCl_2$ (100 µl in 30ml sample) for the $\delta^{13}C_{DIC}$ analysis.

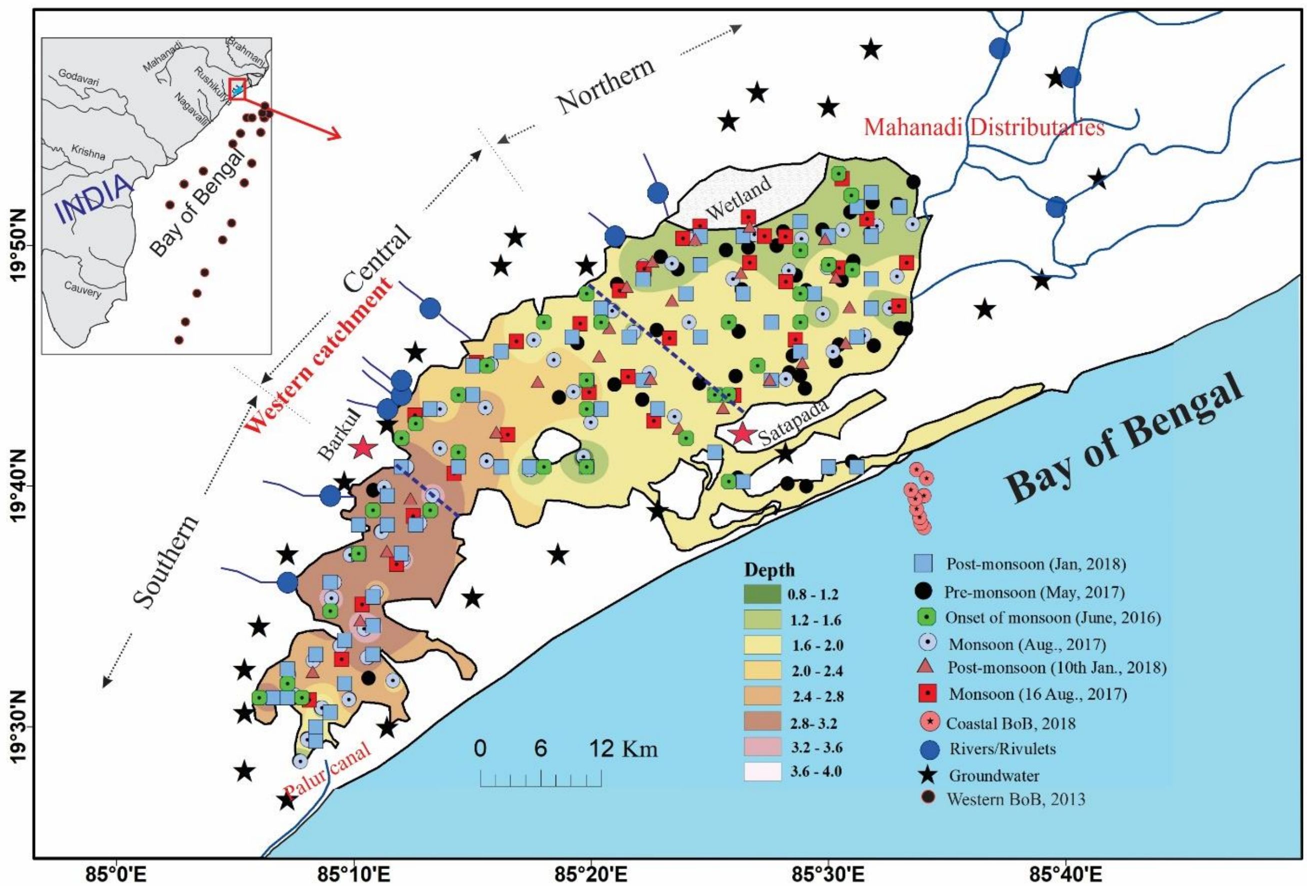

Figure 2.4. Map of sampling collections in the Chilika lagoon during the four field campaigns (Jan-2018, May-2017, June-2016, and August-2017). Additionally, locations of groundwater, river and seawater samples from the coastal and western Bay of Bengal (BoB) also presented. The symbol of red stars represents the two locations (Barkul and Satapada) where the diurnal sampling of 2-hr resolution were carried out. The wetland area in the north-east part of the lagoon is also highlighted.

In addition to water samples, several bed sediments from the Chilika (n = 33) and Mahanadi distributaries (n = 4) were also collected during the onset of monsoon seasons (June, 2016). These samples beneath the water column were collected using a plastic scoop. About 100 gm of water-washed and dried aliquots of these sediments, after removing roots and litter particles, were powdered (up to 100 mesh size) using agate mortar and pestle. Further, ten suspended sediments from the northern sector of the Chilika lagoon were also collected during the monsoon season. For this, approximately twenty liters of water was collected and kept undisturbed for 3-4 days. This water sample was decanted and the residue of about 500 ml was dried to collect the suspended sediments. These suspended sediments, after washing with water, were powdered without any metal contamination. In this study, eleven macrophyte samples from the Chilika lagoon were also collected during pre-monsoon period. These macrophytes were mostly floating on the water surface. These samples were collected manually and stored in zip lock bags at -20°C till further analyses.

2.3. Methods

2.3.1. Elemental analyses

2.3.1.1. Geochemical analyses of water samples

2.3.1.1.1. Dissolved strontium

The Sr concentrations in the dissolved phases were measured using Quadrupole-inductively coupled plasma mass spectrometer (Q-ICP MS facility at IISER, Pune) in its kinetic energy discrimination mode (Table A2 –A4). For this, filtered and acidified water samples were diluted to a salinity of ~1 to minimize matrix effect and these aliquots were measured. The ^{88}Sr isotopic signals of the samples were quantified using a standard calibration method to compute their Sr concentrations. Average ^{88}Sr counts of the samples (~200, 000 cps) were about four orders of magnitude higher than the background counts (~100 cps) and hence, no background corrections were done. Sr concentrations of fourteen water samples were measured in replicates to constrain the measurement precision (~4 %; Fig. 2.5A). Further, a few replicate samples (n = 23) were also measured using internal (indium) standards. The Sr concentrations data yielded from the internal standard approach compare well (± 5 %) with that measured using the standard calibration method (Fig. 2.5B). The accuracy of Sr measurement was constrained by analyzing international natural water (NIST-1640a) reference materials. The measured Sr concentrations for NIST-1640a (123 ± 7 µg/kg; (n = 7)) are consistent with its reported values (125.03 ± 0.86 µg/kg) (Table 2.2).

2.3.1.1.2. Dissolved Boron

Dissolved boron concentrations of all samples, after their appropriately dilution to minimize the matrix effect, were analyzed using a standard calibration method (Table A1, A3 and A4). Each sample was measured 10 times and the average is reported here. The relative standard deviation for these 10 analyses is about ± 2 %. The background counts were always insignificant compared to signal observed for the samples. Several samples were measured in replicate and the average precision of these measurements is ± 3% (n = 28) (Fig. 2.6A). International seawater (NASS-7) and natural (NIST 1640a) water reference materials were measured to check the accuracy for boron measurements. The measured boron concentrations of NASS-7 (3877 ± 307 µg/kg; n = 4) and NIST 1640a (293 ± 20 µg/kg; n = 3) were found consistent with its reported values (3670 ± 120 µg/kg and 301 ± 3 µg/kg, respectively) (Table 2.2).

Table 2.2. Results of analyses for elements in water reference material.

	NIST 1640a		NASS-7	
Elements	**Reported**	**Measured**	**Reported**	**Measured**
		µg/kg		
B	301 ± 3	293 ± 20 (n=4)	3670 ± 120	3877 ± 307 (n=)
Sr	125.03 ± 0.86	123 ± 7 (n = 7)	-	-
Ba	151 ± 0.3	154 ± 12 (n = 6)	-	-

2.3.1.1.3. Dissolved Barium

The Ba concentrations of the water samples were measured by adding an internal (In) standard of known concentration (1ppb) to monitor the nebulization effects during the analysis (Samanta and Dalai, 2016) (Table A1, A3 and A4). Isotopic abundances of ^{135}Ba and ^{137}Ba were measured along with the ^{117}In. Counts of ^{137}Ba isotope was used to estimate the barium concentration through the standard calibration approach. Measured barium concentration of

NIST 1640a (154 ± 12 μg/kg; n = 6) was found consistent with its reported values 151 ± 0.3 μg/kg (Table 2.2), ensuring data accuracy. Replicate Ba analyses of forty water samples found to match each other and yield a precision of 5 % for these measurements (Fig. 2.6B).

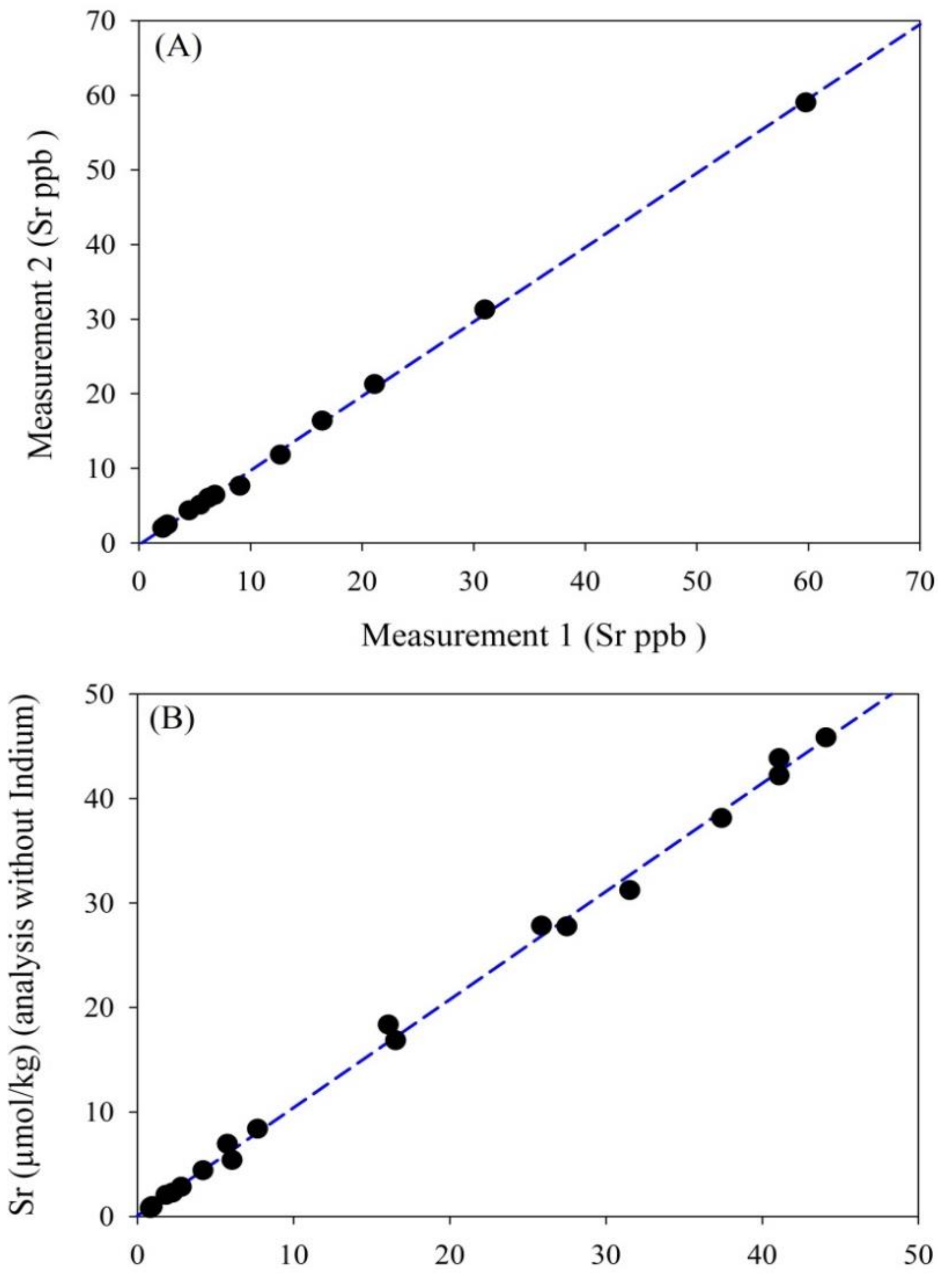

Figure 2.5. (A) Showing the relationship of two times Sr measurement which produces a precision of ~4% and (B) Comparison of Sr concentration data measured with and without internal standards (Indium).

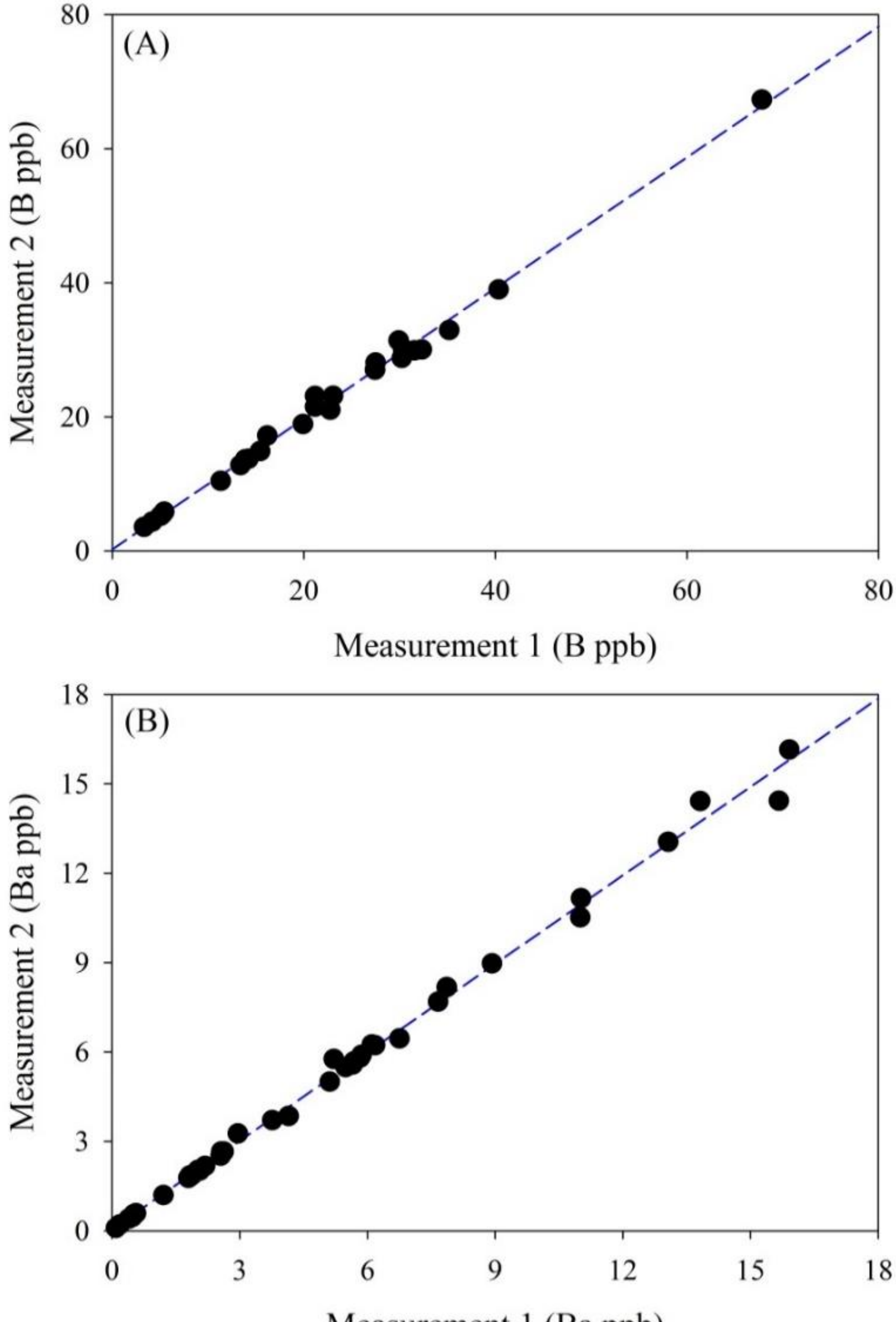

Figure 2.6. Plots show the relationship between the two times measurements of same samples during the analysis (B and Ba). These repeat analyses produced the reproducibility of 3 % (n = 28) and 5% (n = 40) for B and Ba, respectively.

2.3.1.1.4. Dissolved Rhenium

Dissolved Re concentrations of the Chilika lagoon samples were measured using isotope dilution approach (Rahaman and Singh, 2010) (Table A2 –A4). For this, we have used a 185-Re enriched pure rhenium metal powder (assay 96.740%) obtained from the Oak Ridge National Laboratory, USA. This isotopic abundance of ^{185}Re and ^{187}Re are 96.74% and 3.26%, respectively. About ~2 mg of this Re metal was dissolved using ultra-pure nitric acid. This solution was diluted further to prepare two spikes (Re-GT-A and Re-GT-B; in 1 N HNO_3 medium) of different concentration levels. Rhenium concentrations of these spike solutions were calibrated using a Re certified reference material (CRM) of 1001 ± 5 mg/l (lot no: BCBT5013; traceable to NIST SRM; isotopic abundance ^{185}Re (37.4%), ^{187}Re (62.6%); Sigma-Aldrich®). The estimated concentrations for Re-GT-A were found to be 5.26 ± 0.07 μg/g, whereas that of Re-GT-B is 4.96 ± 0.04 ng/g. The Re-GT-B spike solution was used in this study for rhenium analyses.

For dissolved Re measurement, about 50-100 gm of filtered and acidified sample was spiked with a known amount of ^{185}Re tracer. This mixture was kept at room temperature for 24 hrs to achieve sample-spike equilibration. The solution was processed through conventional anion exchange (Bio-Rad AG 1-X8 resin) chromatography to extract pure Re. This Re aliquot was finally brought to 0.32 N HNO_3 medium and their isotopic analyses were conducted using a Quadrupole inductively coupled plasma mass spectrometer (Q-ICPMS). The ^{185}Re/^{187}Re ratio of a rhenium standard solution was regularly measured to correct for instrumental mass fractionation. The mass-corrected isotopic ratios were used to compute their Re concentrations using isotope dilution approach. Typically, the signal/background ratios for these measurements were of the order of 1,000-10,000. We have processed seven water samples from the Southern Ocean which yielded an average Re concentration of 40 ± 1 pmol/kg (n = 7), which is consistent with earlier reported open seawater value (Colodner et al., 1993; Goswami et al., 2012). The average procedural blank for the Re analyses was 3.6 ± 0.8 pg (n = 6; Table 2.3), which is two orders of magnitude lower than the average Re processed (~500 pg) and hence, no blank corrections were made. Precision of the Re measurements (3 ± 1 %) were established by analyzing nine samples in replicates (Table 2.4).

Table 2.3. Data on Re concentration analysed in blank samples.

Sample id	Re (pg)
Blank-1	4.2
Blank-2	3.2
Blank-3	2.6
Blank-4	3.5
Blank-5	3.3
Blank-6	4.9

Table 2.4. Results on repeat analysis of Re measurement in water samples (n = 9).

Sample id	Re (pmol/kg)	Re (pmol/kg) repeat
CLK17-M14	19.3	20.0
CLK17-M17	17.2	18.1
CLK17-M32	14.8	15.0
CLK17-M33	9.3	9.1
CLK17-M34	7.1	7.3
CLK17-M35	7.4	7.2
CLK17-M36	12.4	12.0
CLK17-M71	4.5	4.6
CLK17-M76	7.6	7.3

2.3.1.2. Geochemical analyses of sediment samples

2.3.1.2.1. Major and trace elemental analyses

Major and trace elemental analyses of sediments were measured in their bulk, clay and exchangeable fractions in this study (Table A5, A6 and A7). The size fraction of the bed sediments from the Chilika were quantified using a gravimetric approach (Panchang and Nigam, 2012) and the corresponding clay fractions were separated for geochemical analyses of the clays. For exchangeable fraction, about 0.5 gm of sediments were treated with 1 N ammonium acetate for 16 hours at room temperature and the supernatant was used for measuring the elemental composition of exchangeable fraction in sediments. For bulk and clay fraction, about ~0.1 gm of water-washed and powdered samples were completely digested using HF-HNO_3-HCl acids. The digested solution in 0.32 N HNO3 medium was used for elemental analyses. These solutions, representing bulk, clay and exchangeable fractions of sediments, were analyzed in a Q-ICP MS to measure their major (Na, K, Ca, Mg, Al, Fe, Mn and Ti) and trace (B, Cr, Cu, Ni, Zn, V, Sr, Mo, Ba, and U) elemental concentrations using a standard calibration approach. Concentration of phosphorus was measured by quantifying absorbance of molybdenum blue complexes (Strickland and Parsons, 1968) of the dissolved solutions in a spectrophotometer. Accuracy for the major and trace elemental analyses were established by analyzing three USGS sediment standards (BCR-2, BHVO-2 and W-2a). The measured chemical data for these sediment standards are compared with their reported values in Table 2.6. Several samples were processed in replicates and their measured concentration data are compared for measurement precision (Table 2.5). Average precision for these measurements are found to be ~10 %. The measured counts in procedural blank samples were always few orders of magnitude lower than the sample signal and hence, no blank corrections were made.

Table 2.5. Result (in µg/g) of repeat dissolution of Chilika bed sediments and clay fractions.

	Sediments						**Clay**			
Element	**CLK16-27**		**CLK16-29**		**CLK16-35**		**CLK16-18**		**CLK16-31**	
	(i)	(ii)	(i)	(ii)	(i)	(ii)	(i)	(ii)	(i)	(ii)
Na	12,010	12,575	10,574	10,144	11,706	12,034	15,162	12,435	32,009	32,736
Mg	16,183	14,818	20,404	19,038	14,895	17,075	16,379	15,899	13,449	12,375
Al	133,016	121,874	170,480	158,844	121,075	136,759	138,174	133,852	122,331	109,908
K	21,803	20,300	26,608	25,555	19,427	22,126	19,313	18,077	14,810	14,951
Ca	3,218	3,129	7,954	7,381	4,849	5,676	5,470	5,124	3,995	3,783
Ti	5,414	4,890	6,669	6,183	4,763	5,198	619	4,396	1,564	685
Fe	70,886	64,303	89,069	82,743	63,618	71,527	62,436	62,782	62,263	56,593
U	2.8	2.6	3.4	3.2	2.4	2.7	2.4	2.5	2.4	2.2
V	137	132	135	113	127	133	117	124	128	115
Mn	772	761	1090	948	784	1021	647	666	1392	1345
Co	23	22	22	19	21	22	20	21	22	20
Zn	89	86	91	76	86	84	120	108	115	96
Sr	72	72	82	69	68	79	69	71	59	60
Mo	1	1	1.1	0.7	0.8	0.9	1.1	1	2.1	2
Ba	332	327	345	287	288	340	247	261	224	240

Total carbon and nitrogen abundances in the sediment samples were measured using a CN analyser (Thermo Scientific *flash smart*) (Table A5). About 10 mg of powdered samples were combusted at 1080°C and the liberated gases were quantified using a standard calibration approach to measure the C and N concentrations. Measurement of a sediment standard (SGR-1) constrained the accuracy for carbon (~1 %) and nitrogen (8 %) measurement. The inorganic carbon content for the samples was measured in a CO_2-Coulometer. About 10-30 mg of sediments was treated with phosphoric acid and the amount of CO_2 liberated was quantified for the carbonate concentration measurement. Difference between total and inorganic carbon concentration was used to compute the organic carbon concentration of sediments. Replicate analyses of four samples yielded a measurement precision of 9% for carbon analyses (Table 2.7).

Table 2.6. Results of elemental analyses in USGS reference materials.

	BCR-2		W-2		BHVO-2	
Elements	**Reported**	**Measured**	**Reported**	**Measured**	**Reported**	**Measured**
			µg/gm			
Na	23400	25561 ± 643	16322	17414 ± 381	16400	17025 ± 849
Mg	21600	24543 ± 621	38475	42173 ± 929	43600	45169 ± 928
Al	71400	82594 ± 1978	81777	85399 ± 2895	71600	68781 ± 2419
K	14900	16360 ± 434	5196	4771 ± 307	4300	3097 ± 451
Ca	50900	55953 ± 1449	77616	78336 ± 1602	81700	77783 ± 4853
Ti	13500	14809 ± 437	6354	6393 ± 181	16300	15326 ± 415
Fe	96500	103871 ± 2911	75745	73998 ± 2367	86300	77349 ± 1970
B	-	-	12	10.5 ± 1.5	-	-
Ba	683	702 ± 22	170	182 ± 8	130	-
Sr	346	390 ± 21	190	206 ± 5	389	421
V	416	435 ± 18	260	248 ± 7	317	296
Mn	1520	1650 ± 55	1293	1253 ± 27	1290	1245
Co	37	41 ± 2	43	39 ± 1	45	39
Mo	248	266 ± 13	-	-	-	-
Zn	127	121 ± 16	80	-	103	125
U	1.69	1.8 ± 0.02	1	0.41 ± 0.04		0.29 ± 0.05

Table 2.7. Results of duplicate analyses for CN measurement.

Sample id	**C %**		**N %**	
	(i)	**(ii)**	**(i)**	**(ii)**
CLK16-17	0.39	0.44	0.03	0.03
CLK16-20	2.78	2.50	0.27	0.24
CLK16-29	1.04	1.14	0.12	0.11
CLK16-45	0.53	0.63	0.03	0.02

2.3.1.2.2. Rhenium analyses in particulate phases

Rhenium concentrations of bed sediments (in the bulk, clay and exchangeable fractions) and macrophytes (seagrass samples) of the Chilika were measured using isotope dilution approach (Table A6). As mentioned earlier for exchangeable fraction extraction, about 0.1 gm of water-washed powder was leached with 10 ml of 1 M ammonium acetate in a shaker for 24 hours (Gupta and Chen, 1975). After shaking, the slurry was centrifuged and the supernatant was decanted. The powdered and water-washed aliquots of bulk and clay fractions of the sediments were completely digested using HF-HNO_3-HCl acids and the digested solutions, equilibrated with known amount of ^{185}Re tracer, were passed through an anion-exchange column for Re purification. For macrophytes, the samples were washed with Milli-Q water 3-4 times, dried at 80°C and ashed at 450°C for 6 hours. After ashing, approximately ~0.1 gm of powdered samples was dissolved by using the HF-HNO_3-HCl acids. The pure Re fractions from the solutions of digested sediments, macrophytes and exchangeable fractions were measured following the above-mentioned isotope dilution approach (cf. section 2.3.1.1) using the Q-ICPMS instrument. Precision of sedimentary Re measurements (~10 %) were constrained through replicate analyses of three samples.

2.3.2. Isotopic analyses

2.3.2.1. Sr isotopic analysis

The Sr isotopic compositions of water (Rahaman and Singh, 2012), and bulk and exchangeable fractions of sediment (Singh et al., 2008; Anand et al., 2019) samples were carried out following established protocols (Table A2-A4 and A7). For water (filtered and acidified) samples, about 10-50 gm of the aliquot were dried at 80°C and re-dissolved in 3N HNO_3 medium. This solution was passed through Eichrom® Sr-Spec resin (50-100 µm) to extract the pure Sr. In case of sediment samples, the acid-digested solutions of the water-washed sediments were passed through a cation-exchange column to collect pure Sr. Exchangeable fraction of sedimentary Sr was extracted after treating the water-washed sediments with 1 M ammonium acetate and the supernatant was used for isotopic analyses. Isotopic analyses of the pure Sr fractions were carried out using the multi-collector ICP MS (Neptune Plus, Thermo® Scientific) at NCPOR, Goa. We have constantly monitored the signal at mass 85 amu to monitor any ^{87}Rb interference. The isotopic data were corrected for any instrumental fractionation by normalizing the measured $^{86}Sr/^{88}Sr$ ratio to its natural value of 0.1194, and subsequently normalized with the reported value of NIST NBS-987 (0.71025; Weis et al., 2006). The $^{87}Sr/^{86}Sr$ ratio of NBS-987 standard solution was monitored after five analyses to establish the measurement accuracy. The measured $^{87}Sr/^{86}Sr$ ratio (0.710268 ± 0.000016; 2σ, n = 36) of the NBS-987 is consistent with its reported values. Three Bay of Bengal samples were analyzed for their Sr isotopic ratios (Table 4); the average $^{87}Sr/^{86}Sr$ values for these samples (0.70919 ± 0.00001; n = 3) were found consistent with the average seawater $^{87}Sr/^{86}Sr$ ratio for open ocean (~ 0.70918; Peucker-Ehrenbrink and Fiske, 2019). A few replicate samples were also investigated (Table 2.8) and these results yield a measurement precision of ~7 ppm. The procedural Sr blank for the isotopic analyses was ~500 pg, which is lower by few orders of magnitude than the total amount of Sr processed (~1 µg) for samples and hence, no blank corrections were made.

Table 2.8. Replicate analyses of $^{87}Sr/^{86}Sr$ of water samples from the Bay of Bengal and the Chilika lagoon.

Sample id	$^{87}Sr/^{86}Sr$
Leg-2-5	0.709189 ± 0.000006
Leg-2-5 (Repeat)	0.709186 ± 0.000005
Leg-2-20	0.709189 ± 0.000007
Leg-2-13	0.709189 ± 0.000008
CLK17 - 119	0.709198 ± 0.000005
CLK17 - 119 (Repeat)	0.709200 ± 0.000005
CLK18 - Ja72	0.709874 ± 0.000004
CLK18 - Ja72 (Repeat)	0.709792 ± 0.000004

2.3.2.2. Dissolved inorganic ($\delta^{13}C_{DIC}$) and sedimentary organic ($\delta^{13}C_{org}$) carbon isotopes

Stable isotopic analyses of dissolved inorganic carbon ($\delta^{13}C_{DIC}$) were carried out in water samples using $HgCl_2$-poisoned samples stored in amber bottles (Table A2-A4 and A5). These analyses were carried out at Wadia Institute of Himalayan Geology, Dehradun using established analytical protocols (Samanta et al., 2015; Tiwari et al. 2016). For this, these water samples were treated with pure phosphoric acid and liberated CO_2 gas, after isotopic equilibration, was used for isotopic analyses using a Continuous Flow Isotope Ratio Mass Spectrometer (CF-IRMS; Thermo-Finnigan Delta V Plus). The carbon isotopic data were corrected for isobaric interferences and normalized with respect to that of V-PDB standard. For accuracy check, NBS-(IAEA standard) and Merck® $CaCO_3$ (internal standard) were measured during the analyses.

Accuracy of these analyses was better than ±0.2 ‰. Replicate analyses of samples and standard solutions yielded a measurement precision of ~ ±0.2% (Table 2.9).

Table 2.9. Repeat analysis of the $\delta^{13}C_{DIC}$ in the Chilika water samples.

Sample id	$\delta^{13}C_{DIC}$ (‰)	
	(i)	(ii)
CLK17-79	-12.18	-12.31
CLK17-86	-3.89	-3.80
CLK17-117	-3.07	-3.07
CLK18-Ja73	-5.22	-5.17
CLK17- M106	-3.46	-3.52
CLK17-SM2	-6.59	-6.50
CLK17-SM16	-1.65	-1.64

The stable organic carbon isotopes ($\delta^{13}C_{org}$) of bed sediments from the Chilika lagoon were measured following established analytical protocols (Agrawal et al., 2015). Briefly, about ~0.5 to 2 mg of decarbonated sediment samples were combusted at ~1020°C using an elemental analyzer (Flash EA 2000) in an oxygenated environment to efficiently convert the sedimentary organic carbon into CO_2 gas. This CO_2 gas was introduced into the Delta V plus Continuous Flow Isotope Ratio Mass Spectrometer (CFIRMS) coupled with ConFlow IV interface for their isotopic analyzes. Isotopic signals corresponding to masses 44, 45 and 46 were measured for the samples and a reference gas. The carbon isotopic compositions were calculated after correcting for isobaric interferences. The measured $\delta^{13}C_{org}$ data (in ‰ units) for the samples are reported here with reference to V-PDB. The accuracy and precision of these analyses were constrained using the ε-Amino-n-Caproic Acid or ACA and IAEA-CH3 standards. The measured $\delta^{13}C_{org}$ for these standards ((−24.81 ± 0.15 ‰ for IAEA-CH3, n = 4) and (−25.18 ± 0.03 ‰ for ACA, n = 4) were found consistent with their reported values (−24.72 ± 0. 04 ‰; ~-25.3 ‰; Agrawal et al., 2015), respectively. Isotopic analyses of four replicate samples and nine standards yielded a measurement precision of ~3 ‰.

2.3.2.3. Oxygen isotope

Stable oxygen isotopic compositions of the Chilika lagoon and its possible source waters collected during June, 2016 were investigated using the methodology adopted in Sengupta et al. (2013) (Table A8). Briefly, the filtered water samples, after equilibration with CO_2, were analyzed for their oxygen isotopic composition using a Thermo Delta V Plus isotope ratio mass spectrometer. The accuracy and precision of these analyses was monitored using in-house NARM and IITM-B standards. The measured $\delta^{18}O$ for these standards (-4.43 ± 0.12 ‰ (NARM); -1.79 ± 0.11 ‰ (IITM-B), n = 4) were consistent with its reported values (-4.52 ± 0.09 ‰; -1.90 ± 0.13 ‰; Sengupta et al., 2013). The measured oxygen isotopic data are reported here in ‰ units with reference to V-SMOW. The precision of these $\delta^{18}O$ measurements is better than 0.13 ‰ (Table 2.10).

Table 2.10. Repeat analysis of the $\delta^{13}C_{org}$ in the Chilika sediments samples.

Sample id	$\delta^{13}C_{org}$ (‰)	
	(i)	(ii)
CLK16-03	-21.600	-21.803
CLK16-06	-21.421	-21.478
CLK16-14	-25.203	-25.188
CLK16-20	-21.210	-21.116

Chapter 3

Submarine groundwater discharge to the Chilika lagoon: An estimation using Sr isotopes

3.1. Introduction

Submarine groundwater discharge (SGD) is comprised of subsurface seepage of fresh groundwater and wave/tide-induced recycled seawater through porous terrestrial rocks or sediment aquifers to the coastal ocean (Burnett et al., 2003; Moore, 2010; Knee and Paytan, 2011). This source has been recognized as an important source of nutrients and trace metals (e.g. carbon, nitrogen, alkaline earth metals and rare earth elements) to the coastal ecosystem (Charette et al., 2001; Street et al., 2008; Rodellas et al., 2015). Precise estimation of the SGD and associated chemical fluxes is often complicated due to its non-point and spatio-temporal behavior (Taniguchi et al., 2002; Charette et al., 2008). In this context, source-mixing calculations for chemical tracers (e.g. Ra, Rn and Sr isotopes) and associated "flux-by-difference" approaches have been successful in quantifying the SGD to different coastal regimes (Moore, 1996; Charette et al., 2008). Available global estimates on meteoric (2.4×10^{15} L/y) and brackish ($2 - 5 \times 10^{16}$ L/y) SGD are found comparable with the global river discharge (3.89×10^{16} L/y; Beck et al., 2013 and references therein). Furthermore, a recent continental-scale study based on Ra isotopic data from the Atlantic and the Indo-Pacific oceans estimate that the SGD flux (12×10^{16} L/yr) is higher than the riverine flux (3×10^{16} L/yr; Kwon et al., 2014) to these oceans and hence, warrants detailed investigation to assess importance of SGD in global chemical budgets for different elements.

The SGD serves as an important source in regulating past and contemporary oceanic Sr budgets (Chaudhuri and Clauer, 1986; Basu et al., 2001; Beck et al., 2013). The oceanic Sr isotopic budget is currently in an imbalance with missing flux from less radiogenic Sr sources (Vance et al., 2009; Allègre et al., 2010; Tripathy et al., 2012; Peucker-Ehrenbrink and Fiske, 2019). The global lithology-weighted average $^{87}Sr/^{86}Sr$ ratio for SGD (0.7089) is lower compared to the present-day seawater ratio (0.7092) and hence, may account for a part of the missing less radiogenic component (Beck et al., 2013). Recent estimates indicate that the range of SGD-derived Sr flux is $7 - 28 \times 10^9$ mol/yr, which is about one-third of the riverine flux (47.6×10^9 mol/yr; Peucker-Ehrenbrink and Fiske, 2019) and can account for 13 - 30% of the present-day seawater $^{87}Sr/^{86}Sr$ budget (Beck et al., 2013). Available SGD estimates based on Sr isotopes are mainly based on the non-conservativeness of $^{87}Sr/^{86}Sr$ in estuaries/coastal oceans (Huang et al., 2011; Rahaman and Singh, 2012; Beck et al., 2013; Trezzi et al., 2017; Chakrabarti et al., 2018). These non-conservative behaviors of Sr isotopes are mostly attributed to isotope exchange from aquifer solids to groundwater without changing the Sr content (Rahaman and Singh, 2012). Existing Sr isotopic studies in global estuaries report both conservative (Ingram and Sloan, 1992; Andersson et al., 1994; Sharma et al., 2007) and non-conservative (Wang et al., 2001; Rahaman and Singh, 2012; Beck et al., 2013) behavior in the coastal regions. Although the exact cause is not clear, these contrasting behaviors could be attributed to variable efficiency of particulate-water interaction in these river basins and their estuaries (Barth, 1998).

Earlier studies on $^{87}Sr/^{86}Sr$ have largely been restricted to estuaries but not extended to coastal lagoons, whose areal extent account for ~13% of total coastline area globally (Barnes, 1980). Considering this, the objectives for this study are identified as (i) to assess the coastal behavior of Sr and $^{87}Sr/^{86}Sr$ in a large tropical coastal lagoon system and (ii) to estimate SGD-derived Sr fluxes to the coastal ocean. Spatial distributions of dissolved Sr and $^{87}Sr/^{86}Sr$ ratios of the Chilika lagoon (the largest brackish water lagoon in Asia; Herdendorf, 1982) have been investigated in this study for three seasons (pre-monsoon (April–May 2017); monsoon (July-Aug., 2017); post-monsoon (Jan., 2018)). Further, possible source waters (river, groundwater and seawater) to the lagoon were also measured for their Sr concentration and isotopic compositions. The SGD flux were estimated using two approaches, (i) an inverse model approach assuming fixed groundwater composition (Rahaman and Singh, 2012) and (ii) source-mixing approach using variable groundwater compositions across salinity gradient. Although variable SGD compositions within a coastal system have already been reported elsewhere (Charette et al., 2008; Debnath et al., 2019), its impact on SGD estimations have not yet been assessed thoroughly.

3.2. Results

3.2.1. Compositions of possible sources

Elemental analyses of three surface water samples from the Bay of Bengal have constrained the average salinity (33 ± 1) and Sr concentrations (85 ± 2 μmol/kg) for the seawater input to the lagoon (Table 3.1). The average $^{87}Sr/^{86}Sr$ ratio for these Bay samples (0.70919 ± 0.00001; n = 3) is similar to that reported for open ocean (~0.70918; Peucker-Ehrenbrink and Fiske, 2019) globally. Average Sr concentration and $^{87}Sr/^{86}Sr$ ratios of four riverine samples from monsoon season were 957 ± 156 nmol/kg and 0.719 ± 0.001, respectively (Table 3.1). The average Sr concentrations of the less saline (salinity ≤0.3) samples from the Chilika show seasonal variations with lower values during the monsoon (938 ± 265 nmol/kg; n = 15) compared to other seasons (1311 ± 27 nmol/kg; n = 2). However, the $^{87}Sr/^{86}Sr$ ratios of these samples show no significant difference between the monsoon (0.716 ± 0.002) and lean-flow seasons (0.7170 ± 0.0001). The Sr concentration of the groundwater samples (with salinity range of 0.12 to 8.18) vary between 0.35 and 35 μmol/kg with an average value of 7 ± 7 μmol/kg (n = 70; Table A4). We have analyzed thirty-two groundwater samples for Sr isotopic analyses. The $^{87}Sr/^{86}Sr$ ratios of groundwater samples vary between 0.70993 and 0.86605, with an average value of 0.72 ± 0.03 (n = 32; Table 3.1 and A4).

3.2.2. Sr and $^{87}Sr/^{86}Sr$ ratios of the Chilika

Average salinity and Sr concentrations of the lagoon during the monsoon season are 4 ± 6 (range: 0.1–20.1; n = 18) and 12 ± 17 μmol/kg (range: 0.8 - 54 μmol/kg; n = 18), respectively. The northern sector receives dominant amount of the riverine influx to the lagoon and exhibits an estuarine characteristics. Consistent with this, the average Sr concentration of the northern sector samples (3 ± 2 μmol/kg) is lower than that for the other sectors (37 ± 15 μmol/kg) during the monsoon (Fig. 3.1). The Sr concentrations of the pre-monsoon (1.3 - 93 μmol/kg; n = 20) and post-monsoon (1.3 - 20 μmol/kg; n = 10) samples also show significant spatial distributions (Table 3.1). Further, the spatial distribution of $^{87}Sr/^{86}Sr$ ratios (Fig. 3.1) also depicts dominancy of freshwater influxes in the northern sector and seawater fluxes to the central and southern sectors. The $^{87}Sr/^{86}Sr$ ratios of the lagoon during the monsoon vary from 0.70936 to 0.71790, with an average value of 0.712 ± 0.003 (n = 18). This average isotopic value for the spatial sampling over three-weeks' period is similar to that observed for the whole lagoon sampled within 24 h (0.712 ± 0.003; n = 30). The $^{87}Sr/^{86}Sr$ ratios for the pre-monsoon (0.70918 - 0.71706; n = 20) and post-monsoon (0.70968 - 0.71697; n = 10) seasons also show similar spatial distributions with high radiogenic values in the northern sectors.

Fig. 3.2 depicts correlation between dissolved Sr concentrations and salinity of the Chilika lagoon during three seasons. The correlation factors for the Sr-salinity linear relationship for the pre-monsoon (r = 0.999 (n = 20); p < .01), monsoon (r = 0.999 (n = 48); p < .01) and post-monsoon (r = 0.999 (n = 10); p < .01) seasons are statistically significant at a confidence level of 99%. Further, the slopes of the regression lines between these two param--eters for pre-monsoon

(2.6 ± 0.2), monsoon (2.7 ± 0.2) and post-monsoon (2.5 ± 0.3) seasons overlap with that expected (~2.56) for river seawater mixing line. These observations confirm conservative

Table 3.1. Average chemical (salinity and Sr concentrations) and Sr isotopic data for the Chilika lagoon system.

		Counts	Salinity	Sr (µmol/kg)	$^{87}Sr/^{86}Sr$
Chilika (Spatial Sampling)					
Pre-monsoon (Apr.-May, 2017)	*Range*	20	0.2 - 35.8	1.3 - 93	0.7092 - 0.7171
	Average		13 ± 10	34 ± 25	0.711 ± 0.002
Monsoon (Jul.-Aug., 2017)	*Range*	18	0.1 - 20.1	0.8 - 54	0.7094 - 0.7179
	Average		4 ± 6	12 ± 17	0.712 ± 0.003
Monsoon (16th Aug. 2017)	*Range*	30	0.1 - 17.2	0.8 - 46	0.7094 - 0.7183
	Average		5 ± 6	13 ± 16	0.712 ± 0.003
Post-monsoon (Jan., 2018)	*Range*	10	0.3 - 7.7	1.3 - 20	0.7097 - 0.7170
	Average		4 ± 3	10 ± 7	0.712 ± 0.002
Chilika (2-h resolution sampling)					
Barkul (monsoon)	Range	9	15.9 - 16.6	44 - 47	0.70939 - 0.70941
	Average		16.2 ± 0.3	46 ± 1	0.70940 ± 0.00001
Barkul (pre-monsoon)	Range	11	13.5 - 15.6	35 - 40	0.70954 - 0.70958
	Average		14.2 ± 0.6	37 ± 1	0.70956 ± 0.00001
Satapada (Monsoon)	Range	12	6.4 - 9.2	18 - 24	0.70949 - 0.70963
	Average		8 ± 1	21 ± 2	0.70957 ± 0.00005
Satapada (pre-monsoon)	Range	12	35.1 - 36.6	89 - 95	0.70918 - 0.70920
	Average		35.6 ± 0.5	91 ± 2	0.70919 ± 0.00001
Possible major sources					
River water	Range	4	0.12 - 0.26	0.8 - 1.1	0.7178 - 0.7194
	Average		0.17 ± 0.06	1.0 ± 0.2	0.719 ± 0.001
Groundwater (Pre-monsoon)	Range	20	0.15 – 8.18	1 - 35	0.7099 - 0.8660
	Average		1.4 ± 1.7	9 ± 9	0.723 ± 0.034
Groundwater (Monsoon)	Range	12	0.27 – 3.02	2 - 34	0.7107 - 0.7334
	Average		1.0 ± 0.8	10 ± 9	0.716 ± 0.006
Seawater (Bay of Bengal)	Range	3	31.5 - 33.6	82 - 87	0.70918 - 0.70920
	Average		33 ± 1	85 ± 2	0.70919 ± 0.00001
Suspended Sediments (Bulk)	Range	10	-	83 - 109	0.7207 - 0.7374
	Average		-	95 ± 8*	0.731 ± 0.005
Suspended Sediments (Exchangeable)	Range	10	-	28 - 44	0.7110 - 0.7180
	Average		-	34 ± 4*	0.714 ± 0.002

**Units for particulate Sr are µg/g; Salinity data are from Danish et al. (2019)*

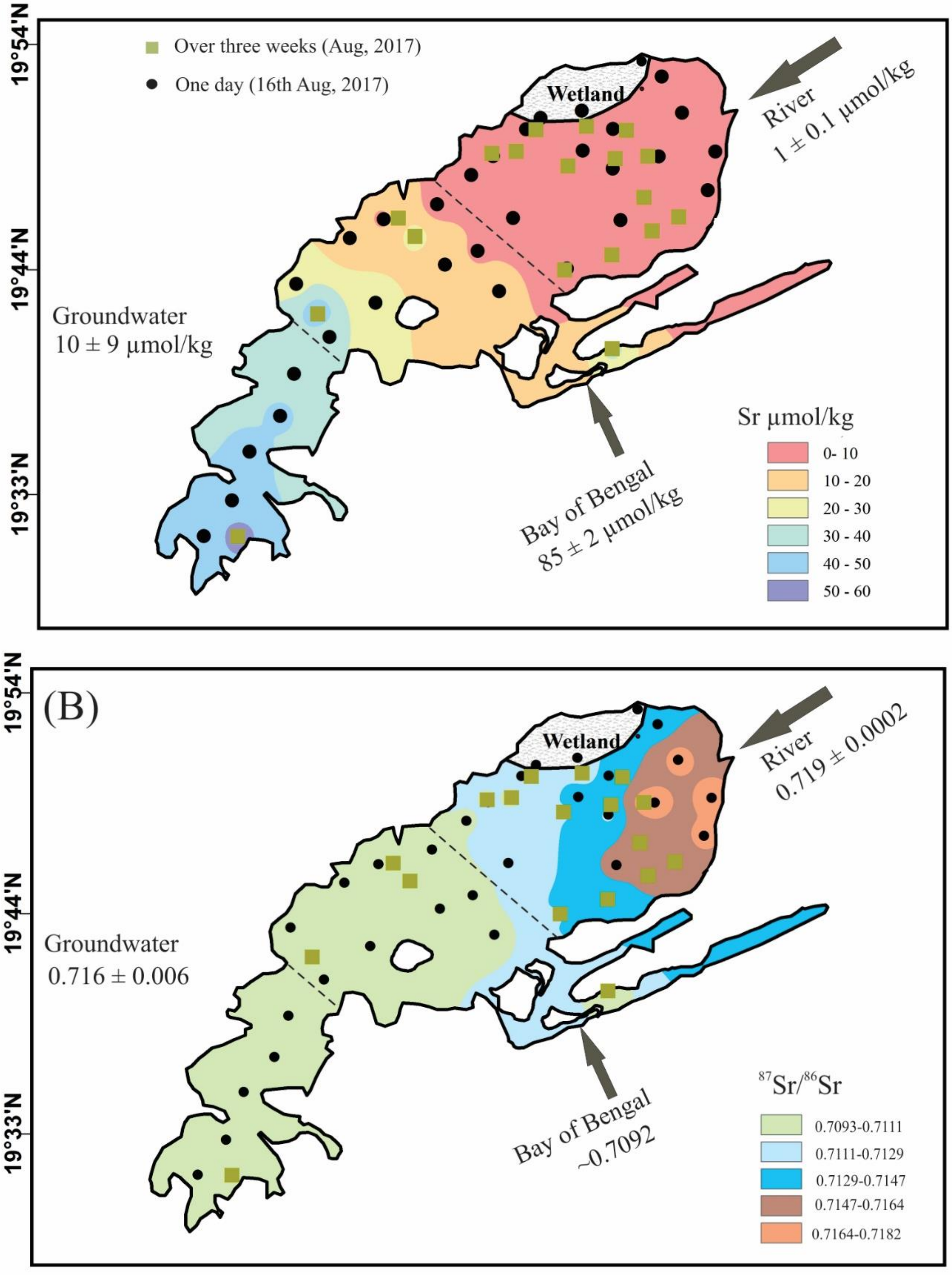

Figure 3.1. Spatial distribution of dissolved Sr concentrations and $^{87}Sr/^{86}Sr$ ratios of the Chilika lagoon during monsoon period. For reference, these data for possible source waters (groundwater, river, and sea (Bay of Bengal) water; Table 3.1) are also shown.

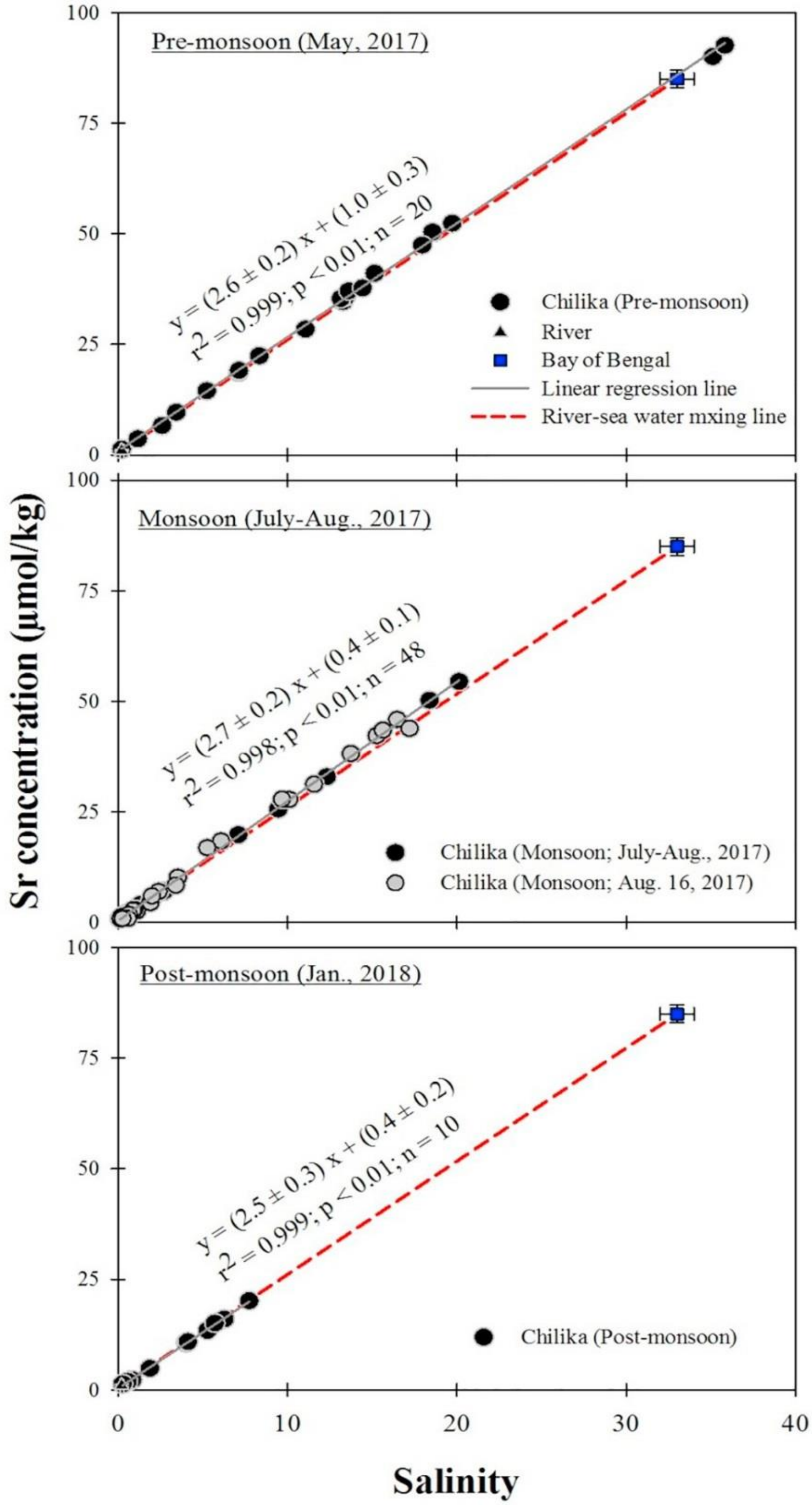

Figure 3.2. Significant correlation between water salinity and Sr concentrations confirm conservative behavior of Sr during (i) pre-monsoon, (ii) monsoon and (iii) post-monsoon seasons. The slopes of linear regression lines during the three seasons overlap with that expected (~2.6) for conservative mixing of river and seawater.

behavior of Sr concentration in the Chilika lagoon. Two samples from the pre-monsoon season are characterized with relatively higher salinity and Sr concentrations than the Bay of Bengal samples. Although these outliers follow the conservative trend, their higher values are attributable to evaporation effects (Danish et al., 2019). In contrast to Sr concentrations, the $^{87}Sr/^{86}Sr$ ratios show seasonal changes in its coastal behavior (Fig. 3.3). The post-monsoon samples from the Chilika follow a near linear trend in 1/Sr-versus-$^{87}Sr/^{86}Sr$ ratio plot (Fig. 3.3), which is consistent with conservative river-seawater mixing line. However, these data for monsoon and pre-monsoon samples deviate from the conservative mixing line (Fig. 3.3). During the monsoon season, selected samples (mainly from the low-saline region) show non-conservative behavior and fall below the expected binary mixing line. The monsoon samples with relatively higher salinities mostly follow the conservative mixing trend (Fig. 3.3). These trends are consistent during two different set of monsoon sampling, viz. detailed (over three-week period) spatial (Aug., 2017) and 1-day (16^{th} Aug., 2017) sampling of the lagoon. For the pre-monsoon period, most of the lagoon samples fall above the expected river-seawater mixing line and hence, confirm their non-conservative behavior.

3.2.2.1. Diurnal variations

The water levels of the lagoon at its outflow are higher during the monsoon (1.07 to 2.53 m) compared to that during the non-monsoon (0.84 to 1.95 m) seasons (Mahanty et al., 2015). These water levels increase during the flood tides by ~1.5 m during the monsoon and ~1 m during the non-monsoon seasons with a periodicity of 12.4 h (Mahanty et al., 2015, 2016). We investigated the Sr and $^{87}Sr/^{86}Sr$ ratio of the Chilika at its outflow (Satapada) and in its southern sector (Barkul; Fig. 2.4) at 2 h interval to assess variation in water chemistry due to tide-ebb related depth fluctuations. At the outflow, the Sr concentrations during the monsoon vary by about 10 % with an average value of 21 ± 2 μmol/kg (Fig. 3.4, Table A3). The highest Sr concentration was observed for the samples with highest salinity (Fig. 3.4, Table A3), confirming seawater incursion into the lagoon during the flood tides. The $^{87}Sr/^{86}Sr$ ratios at Satapada ranged from 0.70949 to 0.70963 (0.70957 ± 0.00005) within 24 h during the monsoon, with the lowest ratio being observed for the highest saline (9.2) sample (Table A3). In contrast to the monsoon, the Sr concentrations only show minimal change (~2%) during the pre-monsoon season. The semi-diurnal tidal impact at the southern sector (Barkul) on lagoon salinity and Sr concentrations is weak (2 - 4%) during both monsoon and pre-monsoon seasons. The average

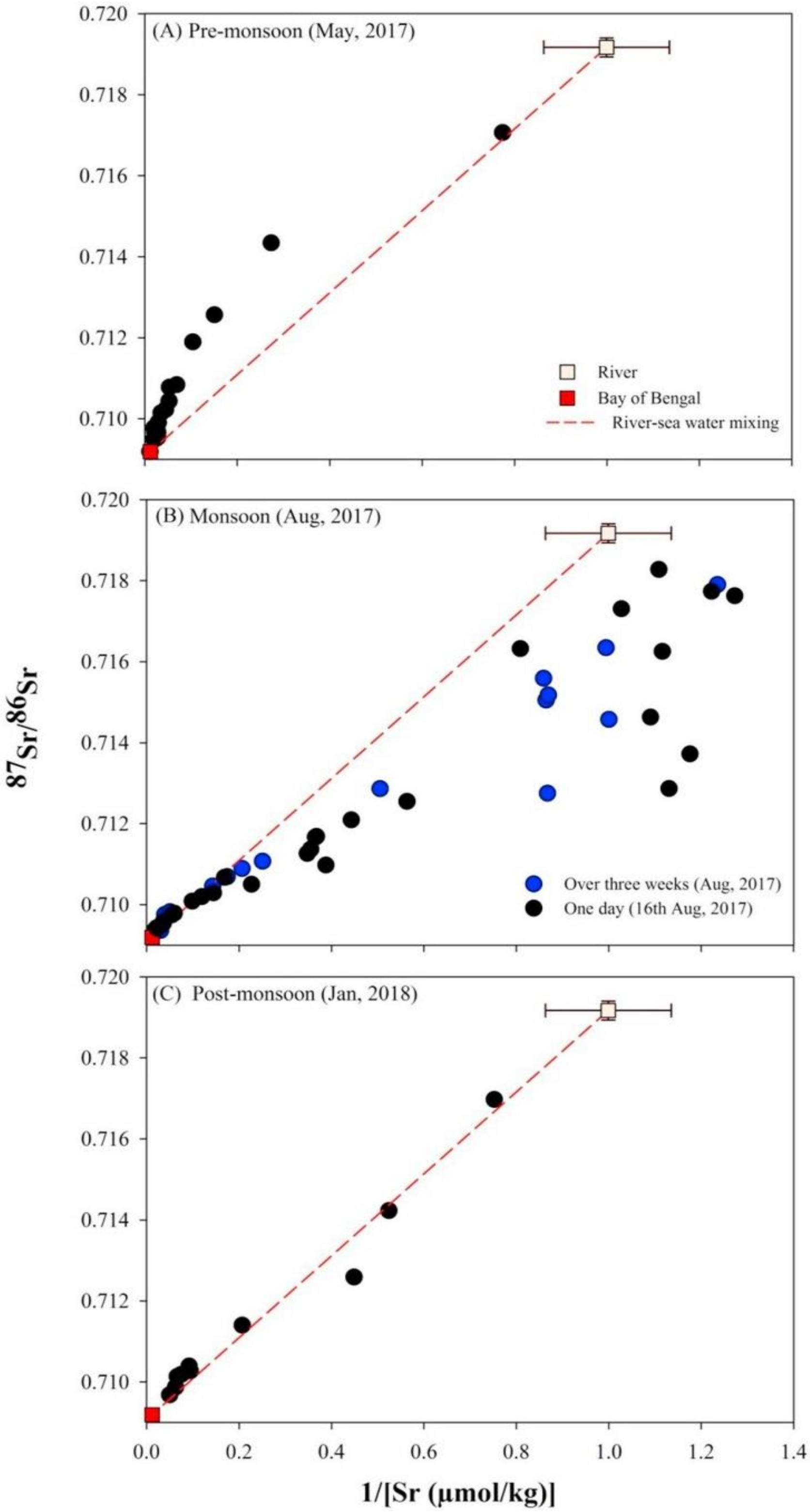

Figure 3.3. Mixing diagram between dissolved Sr concentrations and $^{87}Sr/^{86}Sr$ ratios during different seasons. The Sr isotopes behave conservatively during post- monsoon, but non-conservatively during monsoon and pre-monsoon seasons.

Sr concentration at Barkul during the monsoon (46 ± 1 μmol/ kg) is higher than that during the pre-monsoon (37 ± 1 μmol/kg). The $^{87}Sr/^{86}Sr$ ratios at this location show minimal change during the monsoon (0.70940 ± 0.00001; n = 9) and pre-monsoon (0.70956 ± 0.00001; n = 11) seasons.

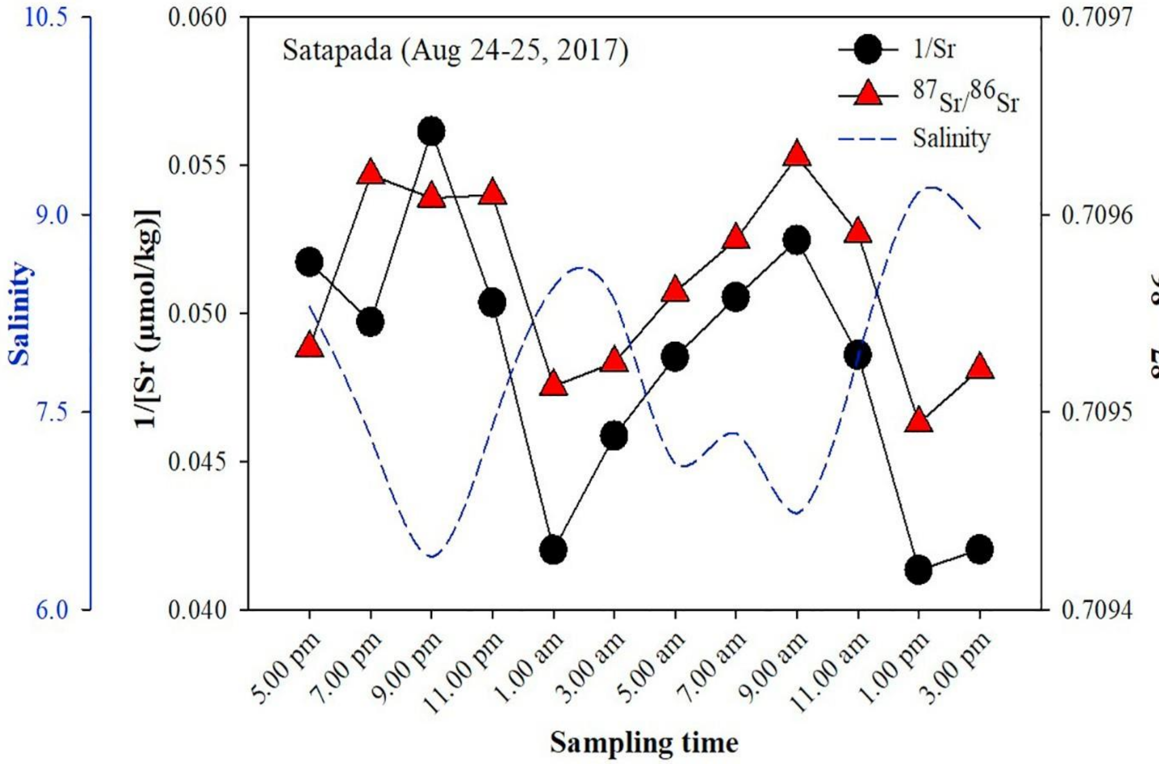

Figure 3.4. Two-hourly resolution water salinity, Sr, and $^{87}Sr/^{86}Sr$ data at the Chilika outflow during the monsoon. Variations in salinity show effect of tides and ebb on the lagoon chemistry. The observed variations are due to seawater exchange during semi-diurnal tidal cycles.

3.2.2.2. Sediment compositions

The Al concentrations of the suspended sediments from the Chilika lagoon (13.2–14.9 wt%; n = 10) are about two times higher than that of the bed sediments of the Mahanadi distributaries (6.1 ± 0.7 wt%; n = 4; Table A5 and A7). In contrast, the Sr concentrations for the suspended sediments (95 ± 8 μg/g; n = 10) and the river sediments (102 ± 16 μg/g; n = 4) are found to be comparable. The Sr/Al ($\times 10^{-4}$) ratios for the suspended sediments (6.8 ± 0.5) are lower than the bed sediments (17 ± 4); this may be attributed to release of Sr to the dissolved phases. The Sr content of the exchangeable fraction of sediments vary between 28 and 44 μg/g, with an average value of 34 ± 4 μg/g (n = 11; Table A7). This exchangeable Sr content, on average, accounts for ~30% of the bulk Sr concentrations of the suspended sediments. The $^{87}Sr/^{86}Sr$ ratios of the suspended sediments from the Chilika vary between 0.72070 and 0.73739,

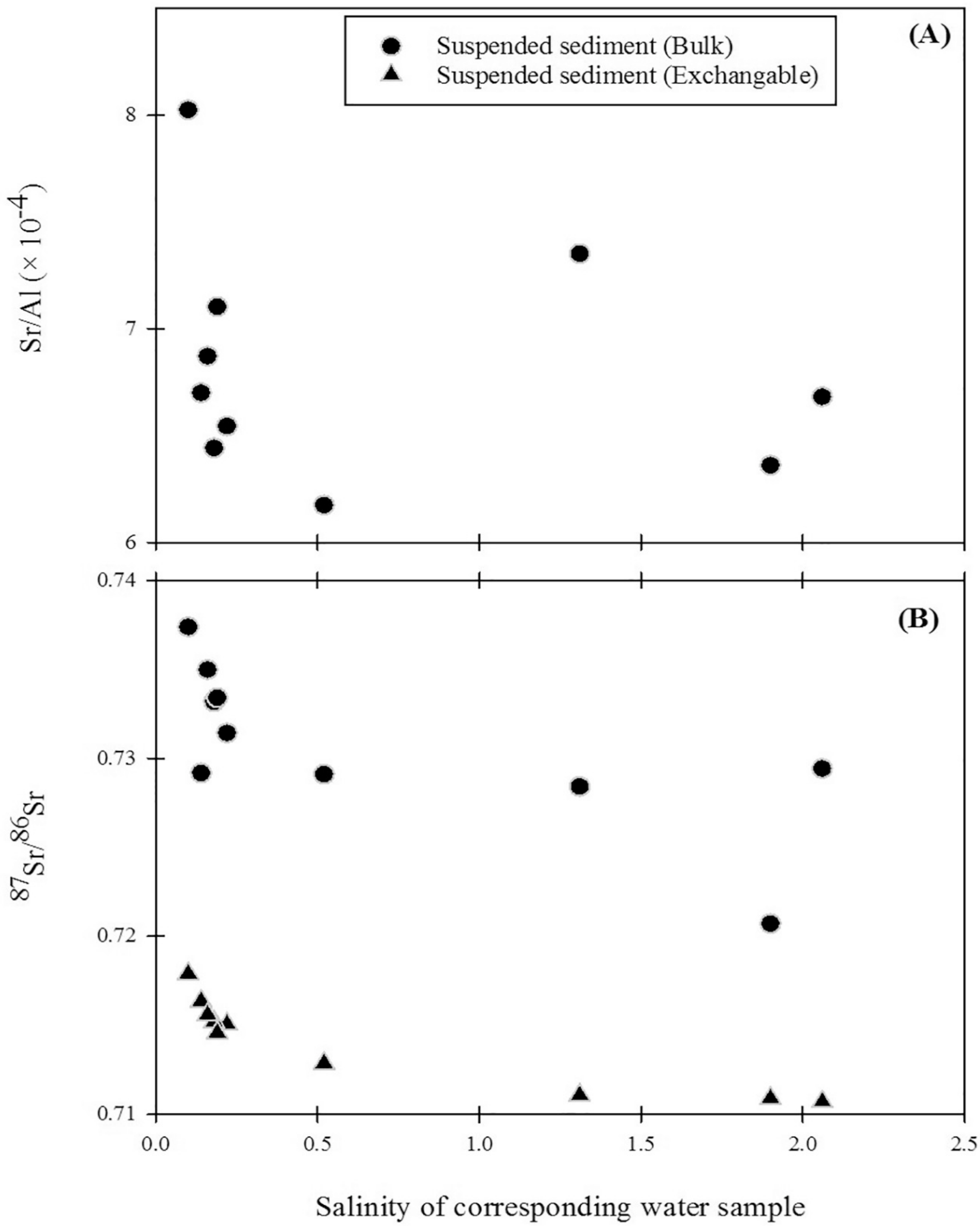

Figure 3.5. Variations in (A) Sr/Al and (B) $^{87}Sr/^{86}Sr$ ratios of the suspended sediments (in both bulk and exchangeable fractions) with their corresponding water salinity. These ratios broadly show a declining trend with salinity, indicating release of Sr through ion-exchange (desorptive) processes and/or dissolution of Sr-rich minerals to the Chilika.

with an average value of 0.731 ± 0.005. The Sr isotopic values of the exchangeable fractions are less radiogenic (compared to that of the bulk sediments) with their values ranging between 0.71097 and 0.71801. The Sr/Al and $^{87}Sr/^{86}Sr$ ratios of the suspended sediments show a broadly decreasing trend with their corresponding water salinities (Fig. 3.5). Similar to the Sr/Al ratios, their corresponding Ca/Al and Fe/Al ratios (figure not shown) also show decreasing trends, indicating possible release of Sr through re-dissolution of Ca-rich minerals and Fe-Mn hydroxides to the dissolved phase of the lagoon.

3.3. Discussion

3.3.1. Behavior of Sr and $^{87}Sr/^{86}Sr$ along the salinity gradient

Co-variation between salinity and dissolved elemental concentrations in coastal systems serves as a measure for constraining the solute sources (river, seawater, and SGD) and/or internal cycling of elements [such as, ion-exchange, association with biological activities, and re-dissolution of minerals (Fe-Mn oxyhydroxides, carbonates)] (Coffey et al., 1997; Moore, 1999; Samanta and Dalai, 2016; Rahaman et al., 2011; Danish et al., 2019). Linear trend between these two parameters confirms that the elemental distribution along the salinity gradient is regulated only by its supply through river and seawater, whereas deviation of data from the linearity points to either removal or addition of the element through additional sources/sinks. As discussed in the result section, dissolved strontium concentrations of the Chilika samples exhibit significant correlation ($r^2 = 0.999$, $p < .01$; Fig. 3.2) with salinity during all the three seasons. This linear relationship confirms efficient mixing of river and seawater in regulating the dissolved Sr concentrations within the Chilika. This observation on conservative behavior of strontium along the salinity gradient is consistent with that reported earlier for various estuaries worldwide (Andersson et al., 1994; Wang et al., 2001; Sharma et al., 2007; Rahaman and Singh, 2012; Beck et al., 2013; Wang and You, 2013). Unlike Sr concentrations, Sr isotopic ratios in the Chilika lagoon exhibit non-conservative behavior during monsoon and pre-monsoon seasons (Fig. 3.3). Although the observed non-conservative behavior of Sr isotopes (and conservative behavior for Sr) is consistent with few earlier reports (Rahaman and Singh, 2012; Beck et al., 2013), these results, however, are not in accordance with conservative $^{87}Sr/^{86}Sr$ behavior reported for other global estuaries (Ingram and Sloan, 1992; Andersson et al., 1994; Sharma et al., 2007). Available literature differences on behavior of Sr isotopes along salinity gradient indicate the controlling factors for dissolved $^{87}Sr/^{86}Sr$ vary at regional scales depending on their biogeochemical properties and aquifer conditions.

The non-conservative behavior of $^{87}Sr/^{86}Sr$ ratios during monsoon and pre-monsoon seasons (Fig. 3.3) could be attributed to various possible mechanisms, which includes (i) removal of dissolved Sr through its incorporation onto Fe-Mn oxyhydroxides (Andersson et al., 1994; Xu and Marcantonio, 2007) and/or calcite precipitation, (ii) desorptive release of Sr from Fe-Mn oxides and/or clay surfaces (Huang and You, 2007; Huang et al., 2011), (iii) re-dissolution of minerals in the coastal regime and/or (iv) Sr supply through SGD to the lagoon (Rahaman and Singh, 2012; Beck et al., 2013; Trezzi et al., 2017). The Sr/Al (and, Ca/ Al and Fe/Al) ratio of suspended sediments from the Chilika show a steady decline up to 2 salinity (Fig. 3.5), and the non-conservative behavior of $^{87}Sr/^{86}Sr$ during monsoon is mostly restricted to these low salinity regimes. The observed decrease in Sr/Al points to possible release of Sr through re-dissolution of Ca-rich minerals and/or Fe-Mn hydroxides to the dissolved phase of the lagoon. Possible supply of dissolved Sr to the Chilika through re-dissolution of Ca-rich minerals is not supported by the observed decreasing $^{87}Sr/^{86}Sr$ trends for the Chilika sediments (Fig. 3.5B). The Sr isotopic ratios decrease from 0.73739 to 0.72070 along the salinity gradient of corresponding water samples. Decrease in sedimentary $^{87}Sr/^{86}Sr$ ratios can be attributed to preferential dissolution of minerals with higher Sr isotopic ratios than that of the bulk sediments, which is in clear contrast with less radiogenic Ca-rich minerals. The most likely explanation for the observed non-conservative behavior of $^{87}Sr/^{86}Sr$ during monsoon could be desorptive Sr release from the sediments. This proposition is strongly supported by $^{87}Sr/^{86}Sr$ ratios of exchangeable Sr fraction which steadily decreased from 0.71802 to 0.71097 along the salinity gradient (Fig. 3.5B). This declining $^{87}Sr/^{86}Sr$ trend is in accordance with the observed lower Sr isotopic ratios (compared to the river-sea water mixing line) during the monsoon period (Fig. 3.3). Further, the suspended sediments from the Chilika contains appreciable amount of exchangeable Sr (~30%) to promote release of Sr during cation-exchange processes (Table A7). These observations, which support non-conservative behavior of Sr isotopes, are not in agreement with the conservative behavior of Sr concentrations. One possible explanation for this disagreement could be lack of appreciable impact of these processes in the low-saline regime. The Sr concentrations of low-saline regimes of the Chilika are lower by about two orders of magnitude than the seawater. These large concentration differences among the sources may subdue any difference in slope (Sr/salinity ratio) between regression (~2.7 for monsoon) and conservative (2.56) mixing lines (Fig. 3.2).

Earlier studies (Rahaman and Singh, 2012; Beck et al., 2013) on non-conservative behavior of $^{87}Sr/^{86}Sr$ in estuaries have invoked possible SGD supply to coastal ocean. These studies have suggested a mechanism involving isotopic exchange between subsurface water and aquifer lithology to explain non-conservative $^{87}Sr/^{86}Sr$ behavior with conservative Sr trends in estuaries (Rahaman and Singh, 2012). The SGD can also serve as a potential source of Sr to the Chilika lagoon. However, the riverine discharge to the Chilika (~167 × 10^6 m^3/d; Gupta et al., 2008) during monsoon is higher by two orders of magnitude than the SGD flux reported for the Gautami estuary (1.34–5.60 × 10^6 m^3/d) (Rengarajan and Sarma, 2015) from the east coast of India. The impact of SGD on Sr behavior during the monsoon season, therefore, is not resolvable within the analytical uncertainty on Sr measurements. However, the SGD can serve as an important source during pre-monsoon season when the riverine discharge (4 × 10^6 m^3/d) is limited. The possible SGD impact on lagoon chemistry during pre-monsoon is evident from non-conservative $^{87}Sr/^{86}Sr$ trends with higher Sr isotopic values compared to conservative mixing line (Fig. 3.3). This isotopic mixing trend with high $^{87}Sr/^{86}Sr$ ratios (Fig. 3.3) during pre-monsoon season can not be attributed to cation-exchange processes, which supplies low Sr isotopic values with decreasing trends along the salinity gradient (Fig. 3.5B).

3.3.2. Estimation of SGD to the Chilika during the pre-monsoon season

Two different approaches have been adopted in this study to estimate SGD flux to the Chilika during the pre-monsoon season. The first approach involves an inversion modeling of chemical mass balance equations (Rahaman and Singh, 2012), and assumes that the SGD is characterized with a fixed end-member composition throughout the lagoon. Several studies suggest that the SGD chemistry may vary within a coastal system depending on subsurface ion exchange processes and/ or relative contribution from seawater (e.g. Charette et al., 2008; Debnath et al., 2019). There has been limited effort in addressing this aspect of variable composition and its impact on SGD estimation. We, therefore, have also adopted a second approach based on mixing of major source waters to estimate the SGD flux by assuming a variable SGD composition. Details of these approaches and related results have been discussed below.

3.3.2.1. Inversion approach

Inverse modeling of geochemical datasets have been found successful in apportioning solute source contributions to various aquatic reservoirs (Nègrel et al., 1993; Tripathy and Singh, 2010; Goswami et al., 2014). Rahaman and Singh (2012) have used this approach involving mass balance equations for Sr elemental and isotopic compositions in the Narmada estuary to estimate the SGD flux to the west coast of India. We have adopted a similar method in this study for the SGD estimation to the Chilika. As mentioned earlier, two samples are characterized with higher salinity and Sr concentrations than the seawater and have not been used in this model calculation. The inverse method assumes a fixed SGD composition for the whole lagoon. Details about the inverse model and the computational code are provided in Tripathy and Das (2014). Briefly, the model uses a non-linear Quasi-Newton optimization algorithm to find a best-fit between the observed and model parameters. The observed data for this model are the measured salinity, Sr concentration and $^{87}Sr/^{86}Sr$ ratios for the lagoon samples, whereas the model data are those for their possible source waters. A set of mass balance equations relates the observed and model parameters, which are provided below.

$$Sal = \sum_{i=1}^{3}(Sal_i \times f_i) \qquad (1)$$

$$Sr = \sum_{i=1}^{3}(Sr_i \times f_i) \qquad (2)$$

$$\frac{^{87}Sr}{^{86}Sr} \times Sr = \sum_{i=1}^{3}(\left(\frac{^{87}Sr}{^{86}Sr}\right)_i \times Sr_i \times f_i) \qquad (3)$$

$$1 = \sum_{i=1}^{3}(f_i) \qquad (4)$$

where, Sal, Sr and $^{87}Sr/^{86}Sr$ refer to the water salinity, Sr concentration and isotopic composition of the lagoon samples. The subscript, i (=1, 2, 3) stands for three possible sources, viz. river, seawater and SGD, respectively. The f_i stands for the fractional water contribution from the source, i. The Eqs. (1) - (4) are in the form of d = g(p) where, d and p are the matrices of observed and model parameters respectively. The inverse model iterates to minimize the d-g(p) (Tarantola, 2005; Tripathy and Singh, 2010). The iteration algorithm starts from the a-priori data for the model parameters and converge to their *a-posteriori* values, which can best fit the mass balance equations with least residual.

The a-priori data and associated uncertainties used for the model parameters are provided in Table 3.2, whereas the source-apportionment results obtained from the inversion method are included in Table 3.3. These results show steady decline in riverine contribution from 96 to 5% with increase in lagoon salinity (range: 0.2–19.7). The SGD contribution to the Chilika varies between 1 and 42% (average: 19 ± 11% (n = 18)), with the maximum contribution at salinity of 18.6. We have used this dataset and the following equation to estimate the absolute SGD flux.

$$Q_{SGD} = \frac{\sum_{j=1}^{18}(f_{SGD})_j}{\sum_{j=1}^{18}(f_{riv})_j} \times Q_{riv} \qquad (5)$$

where, the subscript, j (= 1,.., 18) stand for samples collected from the Chilika during the pre-monsoon season. The Q_{riv} and Q_{SGD} refer to the water discharge from the rivers and submarine groundwater discharge to the lagoon during this period, respectively. The lagoon receives water of about 4×10^6 m^3/d during the pre-monsoon (Feb-May) seasons (Muduli et al., 2013) and this value has been used as Q_{riv} for this calculation. The Eq. (5), which is formulated based on cumulative supply of SGD throughout the lagoon, calculates the SGD contribution by comparing riverine discharge and its fractional water contributions at every location. The inversion results and Eq. (5) estimate a SGD contribution of 1.5×10^6 m^3/d to the Chilika lagoon. This estimate is comparable with that reported earlier based on Ra isotopic investigation for few other estuaries linked to the Bay of Bengal (Godavari (1.34 - 43.02 × 10^6 m^3/d; Rengarajan and Sarma, 2015), Ganga (6.3 - 63 × 10^6 m^3/d; Moore, 1997)). Implications of these SGD estimations in terms of regional SGD-Sr fluxes and impact of these fluxes in global oceanic budget have been discussed in a subsequent section (cf. section 3.3.3.)

Table 3.2. A-priori salinity, Sr and $^{87}Sr/^{86}Sr$ data used in the inverse model for different end-members. These compositions are constrained based on measured data from this study.

Source	**Salinity**	**Sr (µmol/kg)**	**$^{87}Sr/^{86}Sr$**
River water	0.2 ± 0.1	1.0 ± 0.2	0.716 ± 0.002
Seawater	33 ± 1	85 ± 2	0.70919 ± 0.00001
SGD[a]	0.8 ± 0.5	4 ± 3	0.715 ± 0.002

[a]*After excluding outliers based on Turkey's univariate method.*

3.3.2.2. "Variable SGD end-member" approach

Efforts were also made in this study to estimate SGD flux to the Chilika by assuming a variable composition for this end-member. We have used Sr concentrations of seventy groundwater samples collected over three seasons from the Chilika basin to evaluate variability of groundwater with their salinity (Table A4). The salinity of these samples varies significantly (0.1 - 8.2), out of which only eight samples were similar to that of the freshwater ($\leq$ 0.3). Average Sr concentration of the fresh groundwater samples (0.9 ± 0.2 μmol/kg; n = 8) is similar to that of the river water samples (Table A4). The samples with higher salinities may provide a first-order clue for the SGD composition. Fig. 3.6A confirms that the Sr concentration for the groundwater samples changes with salinity and the Sr concentration of the SGD is highly variable within this coastal lagoon. Most of the groundwater samples from the Chilika basin seem to have higher Sr concentrations (with respect to their salinity) when compared to the river-sea water mixing line (Fig. 3.6A). Tukey univariate analyses of these 70 samples confirms that samples with high salinities ($\geq$ 3) and with high Sr concentrations ($\geq$ 13 μmol/kg) can be considered as outliers and may be excluded to constrain a general trend. A linear regression between salinity and Sr data for groundwater samples, after excluding outliers in terms of their salinity concentrations, yielded a statistically significant ($r = 0.71$; $p < .01$; $n = 64$) line with a slope of 6.3 ± 0.8. The slope of the regression line ($r = 0.54$; $p < .01$; $n = 59$) changes to 3.5 ± 0.7, if outlier samples in terms of both salinity and Sr concentrations are excluded during regression analyses. These regression slopes are systematically higher than that expected (~2.6) for river-sea water mixing line. Consistent with this observation, higher Sr/salinity slopes for coastal groundwater have also been documented in earlier studies (Vengosh et al., 1999; Trezzi et al., 2017) and has been attributed to several processes, with includes supply of Sr to the groundwater through its release from bedrocks, clay particles, leakage of deeper groundwater or anthropogenic sources. In contrast to Sr concentrations, the Sr isotopes of the groundwater samples show limited variation (Fig. 3.6B). The Sr isotopic composition of these samples, after excluding three outliers based on Tukey's method ($\geq$ 0.7215), vary between 0.70993 and 0.70918 with an average value of 0.715 ± 0.002 (n = 29). This average value matches well with the riverine $^{87}Sr/^{86}Sr$ ratio for this basin (~0.716; Table 3.1). The exact cause for anomalously higher $^{87}Sr/^{86}Sr$ ratio observed for three outlier samples is not clear. Possible explanations for these high radiogenic values could be (i) supply of Sr from fertilizers and other agricultural practices, and/or (ii) subsurface leaching of radiogenic Sr from K-rich minerals with faster dissolution kinetics. We recognize here that more studies are required to constrain the exact source(s) of Sr to the coastal groundwater. However, this information on source of groundwater Sr will have limited impact on the SGD estimation.

We have adopted a source-mixing approach with variable SGD composition to estimate the SGD fluxes to the Chilika (Fig. 3.7). The Sr concentrations and $^{87}Sr/^{86}Sr$ of the Chilika samples were accounted by mixing of (i) a combined river-seawater mixture source, and (ii) the SGD with varying chemistry along the salinity gradient. As discussed earlier, the Sr concentrations of the groundwater from the basin show a steady increase with salinity with limited changes in $^{87}Sr/^{86}Sr$ ratios (Fig. 3.6B). We have used a constant $^{87}Sr/^{86}Sr$ ratio (0.715 ± 0.002) with varying Sr concentrations for the SGD end member composition. The expected $^{87}Sr/^{86}Sr$ ratios for the combined RW-SW sources ($R_{RW\text{-}SW}$) and SGD (R_{SGD}) sources were computed for the measured Sr concentration of sample using relevant mixing equations (Eqs. (1) - (3)). The $R_{RW\text{-}SW}$ was calculated from the river-seawater mixing line, whereas the R_{SGD} was calculated using the variable-SGD equation for the given salinity and Sr concentration (Fig. 3.7). Considering conservative behavior of Sr concentration, the SGD flux for each sample can be estimated using the following equations:

$$R = [R_{RW-SW} \times Sr_{RW-SW} \times (f_{RW} + (1 - f_{RW}))] + [R_{SGD} \times Sr_{SGD} \times p] \qquad (6)$$

For conservative behavior, the Sr concentrations at a given salinity are expected to be same for RW-SW and SGD sources. For same Sr, the equation (6) reduces to:

$$R = [R_{RW-SW} \times (f_{RW} + (1 - f_{RW}))] + [R_{SGD} \times p] \qquad (7)$$

$$Sal = Sal_{RW} \times f_{RW} + Sal_{SW} \times (1 - f_{RW}) \qquad (8)$$

where, the subscripts *RW*, *SGD* and *RW-SW* stand for river, SGD and combined river-sea water sources. R represents the $^{87}Sr/^{86}Sr$ ratio. The term, p refers to relative water supply from the SGD. The computed f_{SGD} and f_{RW} (after normalizing to unity for all three sources) values were used in Eq. (7) to estimate the absolute SGD to the Chilika. The relative SGD contribution to the Chilika lagoon estimated using this approach varies between 4 and 84% (Table 3.3, with a steady decline with salinity values. These contributions account for a SGD flux of 1.51 × 10^6 m^3/day to the Chilika lagoon during the pre-monsoon season.

Table 3.3. Contributions (in %) of hydrological input from three end-members (river, seawater and SGD) to the Chilika lagoon during the pre-monsoon season. These contributions estimated using both the inversion and variable-SGD approaches are provided below.

Sample ID	Salinity	Inverse model approach			Variable-SGD composition approach		
		River	Seawater	SGD	River	Seawater	SGD
		(%)			(%)		
CLK17-06	13.3	43	38	18	54	36	11
CLK17-25	13.4	37	39	24	56	40	4
CLK17-28	18.6	5	53	42	37	53	9
CLK17-34	13.1	36	38	27	55	38	6
CLK17-38	15.1	23	43	34	50	46	4
CLK17-79	13.6	30	39	31	54	40	6
CLK17-80	14.4	37	41	21	52	40	8
CLK17-82	11.1	57	32	12	58	28	14
CLK17-84	3.4	82	10	9	54	6	40
CLK17-87	0.2	96	0	4	100	0	0
CLK17-88	1.2	92	3	5	16	1	84
CLK17-91	7.1	69	20	11	60	16	24
CLK17-94	19.7	8	57	35	37	58	4
CLK17-118	18	18	52	30	41	51	7
CLK17-132	7.1	67	20	13	65	18	17
CLK17-133	2.6	92	7	1	47	3	50
CLK17-134	5.2	73	15	13	64	12	23
CLK17-136	8.3	60	24	16	64	22	14

3.3.3. SGD and related Sr fluxes to the Chilika lagoon

Our estimates using both fixed and variable groundwater compositions show that the Chilika lagoon, on average, receives about 20% of SGD during the pre-monsoon season (Table

3.3). These estimates can be considered as a lower limit, as desorptive Sr supply with lower $^{87}Sr/^{86}Sr$ ratio (Fig. 3.5B) may also contribute to the non-conservativeness in Sr isotope mixing. Appreciable SGD signature in the water chemistry during pre-monsoon season could be attributed to intense seawater incursion into the seepage head due to limited freshwater discharge/ stream-power during the lean-flow stage (Debnath et al., 2019). The variable SGD approach estimates an absolute SGD flux of 1.51 × 106 m3/d for the pre-monsoon season to the Chilika, which is comparable to that computed (1.5 × 106 m3/d) using a fixed-SGD inverse modeling approach. Although both the approaches yield comparable estimates, we propose that the variable-SGD approach is more robust for better constraining SGD fluxes and in explaining the non-conservative $^{87}Sr/^{86}Sr$ behavior with limited changes in elemental concentrations. The groundwater samples from the Chilika basin depict significant concentration changes with salinity (Fig. 3.6) and hence, the variable-SGD approach is possibly more appropriate for this kind of aquifer system. We, however, recognize that the better understanding on variability of $^{87}Sr/^{86}Sr$ and Sr concentration in submarine groundwater fluxes is indeed essential for more accurate estimation.

The estimated SGD flux of 1.51×10^6 m^3/day for the Chilika lagoon is consistent with that reported earlier for estuaries from the eastern coast of India (Godavari ($1.34 - 43.02 \times 10^6$ m^3/d; Rengarajan and Sarma, 2015); Ganga ($6.3 - 63 \times 10^6$ m^3/d; Moore, 1997);) and other lagoons (e.g., Vanice Lagoon (1 to 6×10^6 m^3/d; Garcia-Solsona et al., 2008); Mar Menor (1 to 5×10^6 m^3/d; Baudron et al., 2015); Laoye Lagoon (4.11×10^6 m^3/d; Ji et al., 2013)) using Ra isotopes. The a-posteriori Sr (13.8 μM) and $^{87}Sr/^{86}Sr$ (0.7155) values of the SGD to the Chilika correspond to an annual Sr flux of 6.9×10^6 mol/yr. These SGD fluxes account for ~0.1% of total SGD-Sr fluxes (7.1×10^9 mol/yr; Beck et al., 2013) to the global coastal ocean. Considering the SGD flux to the Chilika lagoon is only 0.02% of global SGD flux, the computed Sr fluxes through SGD to the Chilika lagoon is disproportionally higher by an order of magnitude than the global Sr fluxes via SGD. Again, the $^{87}Sr/^{86}Sr$ ratio of the SGD to the eastern coast of India (~0.715; This study; Basu et al., 2001) is significantly higher than reported for the global average SGD value (~0.7089; Beck et al., 2013) and the present- day seawater value of 0.7092. Considering the drainage lithology of Archean rocks, this study indicates that the SGD fluxes from the granitic shield regions are expected to supply relatively higher radiogenic Sr (than the global-average SGD) to the coastal region. Further, the earlier reported Sr isotopic composition of the SGD to the eastern coast of India is always found higher than the global oceanic $^{87}Sr/^{86}Sr$ ratio.

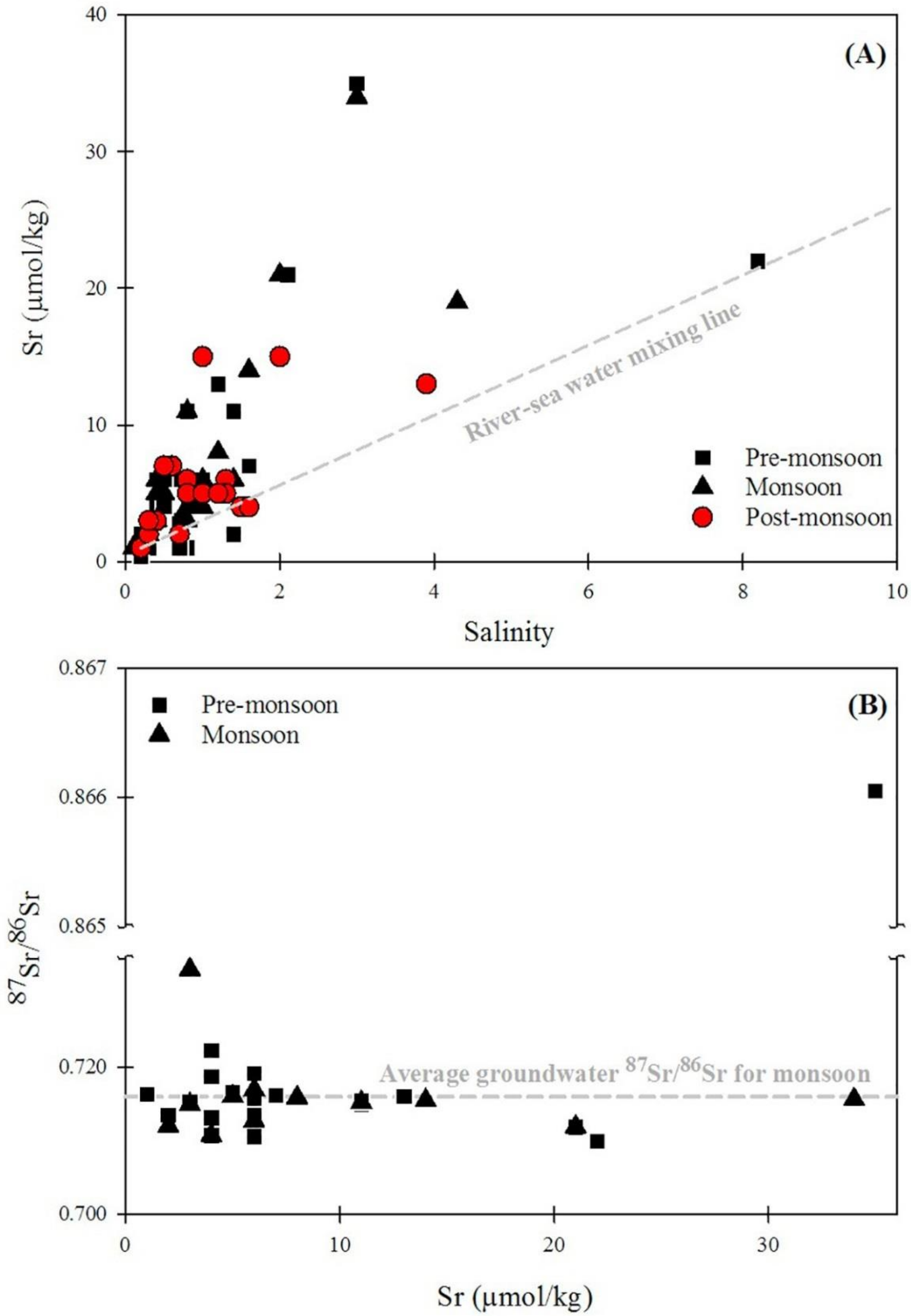

Figure 3.6. Co-variation between (A) Sr and salinity, and (B) Sr and $^{87}Sr/^{86}Sr$ ratios of groundwater samples from the Chilika basin. For reference, the conservative mixing line for river and seawater is shown in (A). These plots show variable SGD compostion

It has been well documented that the ^{87}Sr supply via rivers from these regions plays a dominant role in regulating the oceanic Sr isotopes in a global scale (Tripathy et al., 2012 and references therein). The SGD supplies from these basins, however, are relatively highly radiogenic (~0.715) compared to present-day seawater (~0.7092) and will have minimal (and, may also have opposite) impact on reducing the marine imbalance, which requires a missing source with lower $^{87}Sr/^{86}Sr$ ratios than the seawater.

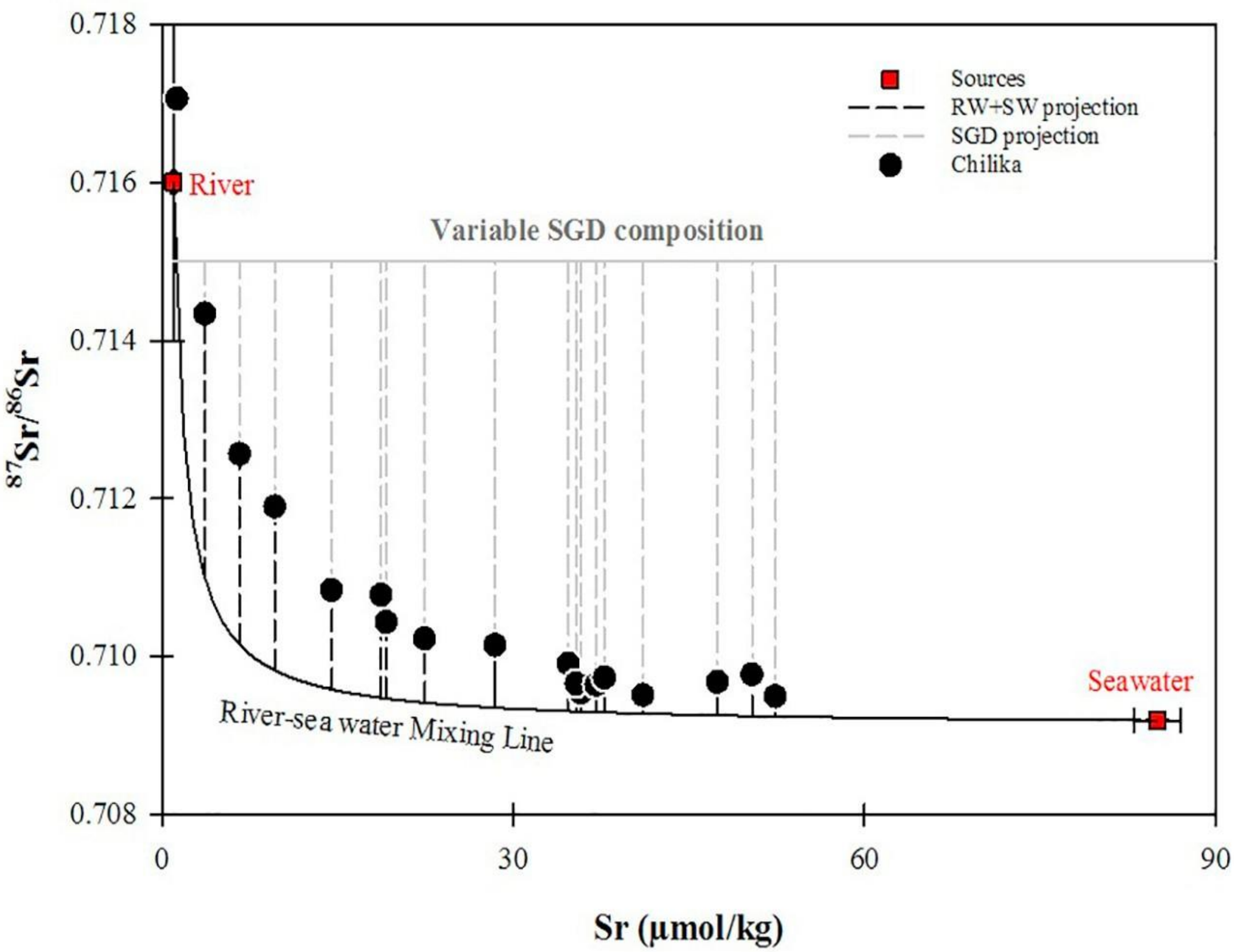

Figure 3.7. Mixing plot between Sr concentration and $^{87}Sr/^{86}Sr$ for the Chilika lagoon during pre-monsoon season. For reference, theoretical river-sea water mixing trend and also, variable SGD composition has also been shown. The SGD compositions show an increasing Sr concentrations with salinity (Fig. 3.6) with a near constant $^{87}Sr/^{86}Sr$ ratio (~0.715 for pre-monsoon season; Table 3.1). The SGD contribution has been estimated assuming a conservative behavior for Sr element in this lagoon system.

3.4. Conclusion

Distribution of Sr concentrations in the Chilika lagoon co-varies with the water salinity during three different seasons (pre-monsoon, monsoon and post-monsoon). These linear trends confirm conservative Sr mixing between fresh and sea water. Unlike Sr concentrations, the $^{87}Sr/^{86}Sr$ does not follow a conservative trend during the pre-monsoon and monsoon seasons. The non-conservative Sr isotopic behavior during the monsoon period is restricted only to low saline region and is attributable to additional ^{87}Sr supply via ion-exchange processes. In contrast, the non-conservative $^{87}Sr/^{86}Sr$ trend during the pre-monsoon season is attributable to additional supply of ^{87}Sr via submarine groundwater discharge to the Chilika. We computed the SGD flux during this season using two mass balance caclulations involving inversion and variable end member approaches. The inversion approach used fixed end member values for the SGD, whereas the second approach involves the variable end member composition of SGD. The estimated SGD, during pre-monsoon, from both variable end member (1.51×10^6 m^3/d) and inversion (1.5×10^6 m^3/d) approaches yielded comparable results. The fractional contribution obtained from the inversion approach indicates that the SGD supplies ~20 % of total hydrological inputs to the lagoon during lean flow stages. The Sr isotopic value of SGD to the lagoon during pre-monsoon season (0.715) is higher than the present day seawater ratio (~0.7092), hence may not minimize the exisiting oceanic imbalance which requires less radiogenic sources.

Chapter 4

Impact of ion-exchange process on Trace elements (B and Ba) in coastal lagoon system

The freshwater-seawater interface, a biogeochemically active aquatic regime, regulates the ultimate delivery of dissolved solutes from rivers to the ocean. Conservative elements supplied by rivers mix with the ocean without any discernible loss/gain in this zone. Several chemical elements, however, behave non-conservatively and their dissolved concentrations either increase or decrease in the salinity gradient due to contributions from additional sources (i.e. submarine groundwater discharge (SGD) (Moore, 1999; Rahaman and Singh, 2012; Beck et al., 2013), desorption and anthropogenic supplies (Coffey et al., 1997; Vengosh et al., 1999; Petelet-Giraud et al., 2009; Samanta and Dalai, 2016) and/or removal through particulate-water interactions (e.g. adsorption, biological activities) (Boyle et al., 1977; Edmond et al., 1985; Bourg, 1987; Charette et al., 2005). Relative contributions from these sources/sinks to the coastal hydrochemistry vary both at spatial and seasonal scales. These variations are complicatedly regulated by various parameters, which include water pH (Bourg, 1987), hydraulic gradient and salinity (Flegal et al., 1991; Gonnea et al., 2014), abundance and composition of suspended sediments (Samanta and Dalai, 2016), and turbidity, redox state, and biological activities (Du Liang et al., 2009). Proper quantification of these coastal processes and their spatial and seasonal variations are crucial for balance in marine chemical budgets. In this chapter, we investigate the spatial and seasonal distributions of boron (B) and barium (Ba) conentrations of Chilika lagoon and its possible sources to assess the effect of ion exchange process in regulating coastal inventories of these two elements.

4.1. Dissolved boron in Chilika water and its possible sources

4.1.1. Introduction

Boron is a bio-essential metalloid and its concentrations as well as isotopic compositions are useful tracers for various environmental processes; however, its oceanic budget is not yet well-constrained. For instance, the boron isotopic composition of marine biogenic carbonates serves as a reliable paleo-pH proxy (Lemarchand et al., 2000; Park and Schlesinger, 2002; Carrano et al., 2009; Gaillardet and Lemarchand, 2018; Saldi et al., 2018). The present-day seawater boron concentration is nearly uniform globally (433 ± 2 μmol/kg; Lee et al., 2010), consistent with its higher residence time (~10 Myr; Gaillardet and Lemarchand, 2018) compared to the average ocean mixing time (~1500 years; Broecker and Peng, 1982). In contrast to open ocean, existing studies on the behavior of boron in coastal realm report both conservative

(Fanning and Maynard, 1978; Liddicoat et al., 1983; Barth, 1998; Xiao et al., 2007; Wang et al., 2009; Singh et al., 2013) and non-conservative (Liss and Pointon, 1973; Pelletier and Lebel, 1978; Narvekar et al., 1981, 1983; Narvekar and Zingde, 1987; Rajagopal et al., 1981; Shirodkar and Anand, 1985; Ghosh and Jana, 1993; Zingde et al., 1995; Padmavathi and Satyanarayana, 1999; Brunskill et al., 2003; Russak et al., 2016) nature. The exact cause(s) for these diverging results is unclear. The non-conservative behavior has often been linked to the removal of dissolved boron through its adsorption onto clay minerals, hydrous oxides of Fe and Al, and organic matters (Liss and Pointon, 1973; Keren and Mezuman, 1981; Goldberg, 1997). The amount of boron removal is typically 10-30% in most of these estuaries. Contrary to this behavior, boron has been reported to be conservative in several estuaries, including those of certain large rivers (*e.g.*, Zaire, Changjiang, Magdalena, Narmada, Tapi and Tamar). Prolonged river water-suspended load interaction in these large river basins may reduce the adsorptive capacity of sediments, which in turn may lead to conservative mixing of boron in large estuaries (Barth, 1998). The above discussion indicates that our understanding on boron behavior in coastal oceans is elusive and has mainly been limited to estuarine zones.

Coastal lagoons are another important component of coastal systems and occupy ~13% of world’s coastline (Barnes, 1980). The behavior of boron in these shallow and highly productive regions has not yet been studied. In this contribution, the sources and behavior of boron have been investigated along the salinity gradient of the Chilika lagoon (India), the largest brackish-water lagoon in Asia (Herdendorf, 1982). Towards this, about 200 surface water samples from three different months (June-2016, May-2017, and August-2017) were measured for their boron abundances. These three sampling periods (May (Pre-monsoon), June (Onset of monsoon) and August (Monsoon)) represent different seasons. Surface water samples (n = 47) were also collected at 2-hours’ time interval for one day at two locations during both monsoon (August) and pre-monsoon (May) seasons to assess tidal impact on lagoon chemistry. Additionally, several water samples (n = 152) from possible sources (rain, river, ground and sea water) were also analyzed during this study. Outcomes of this detailed geochemical research show seasonality in behavior of boron in the Chilika lagoon with conservative behavior during the monsoon season and non-conservative removal of boron during pre-monsoon period through ion-exchange processes.

4.1.2. Results

Chemical Data on dissolved boron and other relevant parameters for the Chilika lagoon, its source waters and sediments are provided in Annexure (Table A1- A3 and Table A5). Table 4.1.1 summarizes the spatial and seasonal distribution of boron in the Chilika lagoon system. Average chemical compositions of possible major source waters to the lagoon are provided in Table 4.1.2. The river water samples with salinities ≤ 0.5 have been used to constrain the average riverine composition. The samples with higher (>0.5) salinities are expected to have appreciable seawater influence and hence, are excluded in finding the average value for this end-member. We have conducted various statistical analyses (e.g. t-test, F-test, ANOVA and Kolmogorov-Smirnov (K-S) test) of the boron and salinity datasets; results from these analyses are listed in Table 4.1.3.

4.1.2.1. Composition of source waters

Boron concentrations of seawater samples from the coastal and western Bay of Bengal vary between 338 and 439 µmol/kg (average: 387 ± 31 µmol/kg (n = 28)), whereas their corresponding salinity ranges from 26.4 to 33.6 (Table A4). Average salinity and boron concentration of these samples are 30 ± 3 and 387 ± 31 µmol/kg respectively. Considering these average values, the B value for the Bay of Bengal samples when extrapolated to a salinity of 35 is found to be 448 ± 13 µmol/kg, which is consistent (within 3 %) with that reported earlier for the open ocean (433 ± 2 µmol/kg; Lee et al., 2010). Boron concentrations of rain water samples (n = 31) collected near the Chilika coast varied from 0.2 µmol/kg to 2.9 µmol/kg (Table A4). Most (27 out of 31) of these samples have concentrations less than 1 µmol/kg, with an average value of 0.5 ± 0.2 µmol/kg. This average boron value is consistent with that reported earlier for global marine sites (~0.6 µmol/kg; Schlesinger and Vengosh, 2016). The lagoon is connected with the Mahanadi distributaries and also, several small rivulets which are often anthropogenic-influenced. The dissolved boron concentrations of these streams (samples with salinity < 0.5) range between 0.5 µmol/kg and 3.0 µmol/kg (Table A4); their average value (1.7 ± 0.7 µmol/kg; n = 18) is marginally lower than that reported earlier for Indian rivers (~2.4 µmol/kg; Singh et al., 2013). These samples do not show any systematic seasonal variation. The salinities of the groundwater (GW) samples vary widely from 0.12 to 8.2. The average salinity and boron concentration of low-saline (with salinity < 0.5) GW samples were 0.28 ± 0.12 and 6 ± 4 µmol/kg (n = 18), respectively. Higher salinity (0.50 - 8.18) and boron concentrations

Table 4.1.1. Dissolved boron and salinity data for the Chilika lagoon samples collected during three field trips (*viz*. May, 2017; Aug, 2017; June, 2016).

Lagoon Sector		**Depth (m)**	**Temp (°C)**	**pH**	**Salinity**	**B (µmol/kg)**	**B/Salinity (µmol/kg/Salinity)**	**DO (mg/l)**
Monsoon (July-August, 2017)								
Southern (n = 22)	Min	1.14	29.9	7.89	18.3	203	10.3	5.06
	Max	3.86	32.1	8.14	20.1	246	12.5	6.8
	Average	*2.8 ± 0.7*	*31 ± 0.5*	*8.1 ± 0.1*	*19.5 ± 0.4*	*231 ± 11*	*11.8 ± 0.5*	*6 ± 0.5*
Central (n = 11)	Min	0.97	29.8	7.85	7.1	93	12.1	5.14
	Max	2.84	31.4	8.22	18.8	231	13.1	8.06
	Average	*2.1 ± 0.6*	*30.5 ± 0.5*	*8.1 ± 0.1*	*15 ± 5*	*184 ± 55*	*12.3 ± 0.3*	*7 ± 1*
Northern (n = 25)	Min	1.32	30	7.7	0.1	2	11	5.61
	Max	1.85	32	8.7	16.6	203	22.2	8.06
	Average	*1.6 ± 0.1*	*30.9 ± 0.7*	*8.2 ± 0.3*	*7 ± 7*	*83 ± 83*	*14 ± 3*	*7 ± 0.8*
Monsoon (16th July, 2017)								
Southern (n = 6)	Min	-	30.4	8.23	11.6	132	10.8	-
	Max	-	31.9	8.29	17.2	187	11.8	-
	Average	-	*31.2 ± 0.6*	*8.28 ± 0.02*	*15 ± 2*	*171 ± 21*	*11 ± 0*	-
Central (n = 7)	Min	-	29.8	8.2	2.4	36	11.8	-
	Max	-	33	8.46	10.1	119	15.1	-
	Average	-	*32 ± 1*	*8.4 ± 0.1*	*6 ± 3*	*72 ± 34*	*13 ± 1*	-
Northern (n = 18)	Min	-	28	6.96	0.1	2	3.2	-
	Max	-	33	9.14	2	28	20	-
	Average	-	*31 ± 1*	*7.9 ± 0.7*	*1 ± 1*	*8 ± 8*	*13 ± 5*	-
Pre-monsoon (April-May, 2017)								

Southern (n = 22)	Min	0.61	29.6	8.13	13.1	144	11	2.31
	Max	3.05	31.7	8.74	29.7	364	12.7	11.0
	Average	*1.9 ± 0.6*	*30.1 ± 0.5*	*8.3 ± 0.1*	*15 ± 5*	*179 ± 56*	*12.1 ± 0.4*	*7 ± 2*
Central (n = 14)	Min	1.22	26.6	8.1	12.9	148	11.3	2.64
	Max	4.57	32.1	9.73	36.8	463	12.8	7.11
	Average	*2 ± 1*	*29 ± 2*	*8.5 ± 0.4*	*21 ± 9*	*255 ± 119*	*12 ± 0.5*	*5 ± 2*
Northern (n = 37)	Min	0.91	26.8	7.37	0.2	3	4.3	2.31
	Max	1.52	35.9	9.41	39.9	477	15	10.21
	Average	*1.2 ± 0.2*	*30 ± 2*	*8.1 ± 0.5*	*17 ± 14*	*198 ± 180*	*10 ± 3*	*6 ± 2*
Onset of Monsoon (June, 2016)								
Southern (n = 11)	Min	1.78	30.1	7.64	18.5	246	11.4	5.67
	Max	2.92	31	7.85	24.15	301	13.3	6.74
	Average	*2.3 ± 0.4*	*30.6 ± 0.2*	*7.8 ± 0.1*	*21 ± 2*	*264 ± 19*	*12 ± 1*	*6 ± 0.3*
Central (n = 11)	Min	0.8	31.1	7.53	21.7	281	12.2	5.22
	Max	2.09	32.2	8.06	32.1	418	14.2	7.03
	Average	*1.7 ± 0.4*	*31.7 ± 0.3*	*7.8 ± 0.1*	*26 ± 4*	*338 ± 48*	*13 ± 1*	*6.3 ± 0.5*
Northern (n = 12)	Min	1	32.2	6.89	7.49	92	12.3	2.4
	Max	2	33.6	8.08	31.7	416	14.1	5.89
	Average	*1.6 ± 0.3*	*32.7 ± 0.4*	*7.7 ± 0.4*	*19 ± 10*	*253 ± 130*	*13 ± 0.5*	*5 ± 1*

Table 4.1.2. Data on elemental boron, oxygen isotopes and salinity for possible source waters to the Chilika lagoon.

	Salinity	**Boron (μmol/kg)**	**B/salinity (μmol/kg/salinity)**	**$\delta^{18}O$ (‰)**
Bay of Bengal	32 ± 1 (n = 19)	406 ± 13 (n = 19)	12.8 ± 0.4 (n =19)	-0.3 ± 0.1[a]
Open ocean	35	433 ± 2[b]	12.36 ± 0.03	0
Ground water	1 ± 1 (n = 54)	25 ± 38 (n = 54)	22 ± 16 (n = 54)	-4.2 ± 0.8 (n = 5)
River/Rivulets[c]	0.17 ± 0.08 (n = 18)	1.73 ± 0.75 (n = 18)	12 ± 6 (n = 18)	1.3 ± 2.4 (n = 4)
Nearby river basins[c]	0.34 ± 0.01 (n = 2)	1.56 ± 0.9 (n = 12)	7 ± 6 (n = 2)	-3.8 ± 0.9 (n = 5)
Rain water	-	0.6 ± 0.5 (n = 31)	-	0.1 ± 0.1 (n = 1)

River samples with higher salinities (> 0.5) are expected to have seawater influence and hence, not included in constraining the average riverine composition.
a Singh et al. (2010).
b Lee et al. (2010).
c Samples with salinity≤0.5 .

(2.0-239.0 µmol/kg; n = 36) were observed for several GW samples, attributable to anthropogenic seepage and/or seawater incursion into the coastal aquifer through tidal pumping. It is worth mentioning here that two GW samples with higher salinities (4.32 and 8.18) are characterized with disproportionally higher B concentration (123 and 239 µmol/kg) than that expected for river-seawater mixing (55 and 104 µmol/kg), indicating supply of B from additional sources. These additional sources could be possible seepage of anthropogenic supplies into the aquifer (Vengosh et al., 1994, 1999; Petelet-Giraud et al., 2009) and/or groundwater interaction with the aquifer lithology.

4.1.2.2. Composition of the Chilika Lagoon

The pH of the lagoon samples varies from 6.9 to 9.7, with an average value of 8.1 ± 0.4 (n = 250). The lowest pH value is observed for the sample collected near the wetland area, whereas the sample with the highest value is sampled close to the river (Mahanadi distributaries) mouth during the pre-monsoon season. Large variations in the salinity of the lagoon (August (11.5 ± 8; n = 62), May (17.2 ± 11; n = 73) and June (22 ± 7; n = 34)) are observed during the three field campaigns (Fig. 4.1.1). The northern sector of the lagoon receives large riverine influx and exhibits estuarine characteristics. The salinities of the northern sector samples were, therefore, lower than that observed for the other sectors (Fig. 4.1.1). The salinity of the northern Chilika vary between 0.1 and 12.6 (3 ± 4; n = 25) during the monsoon season, systematically lower than that observed for the pre-monsoon season (14 ± 12; n = 31). The lagoon salinities in the southern sector show limited spread during August (~2% (19.5 ± 0.4; n = 22)) and June (~11% (21 ± 2; n = 11)) months, compared to the pre-monsoon (May) samples (~30% (15 ± 5; n = 22)). The spatial distribution of the boron concentrations by and large follows the salinity trend (Fig. 4.1.1) and the B-salinity relationships are statistically significant for $p < 0.05$ (c.f. Fig. 4.1.3 for Pearson's correlation values). The boron concentrations of the Chilika lagoon vary widely from 1.0 to 477 µmol/kg. Few non-monsoon samples (n = 9) with higher boron concentrations than that of the Bay of Bengal are also characterized with higher salinity values (36 ± 1), attributable to evaporation effect. The average boron content for the Chilika was 139 ± 99 µmol/kg (n = 62) during the monsoon and 203 ± 143 µmol/kg (n = 73) for the pre-monsoon season. Similar to salinity trend, systematically lower boron concentrations were observed for samples from the northern sector (Fig. 4.1.1). Figure 4.1.2 depicts the spatial and seasonal variations in boron/salinity ratios for the Chilika lagoon. These variations are statistically significant both at seasonal and spatial scale (c.f. Table 4.1.3 for statistical analysis details). Average boron/salinity ratios for the pre-monsoon (11 ± 2 μmol/kg/salinity (May, 2017); n = 73), onset-of-monsoon (12.8 ± 0.6 μmol/kg/salinity (June, 2016); n = 34) and monsoon (12 ± 2 μmol/kg/salinity (August, 2017); n = 62) samples were comparable with that of the Bay of Bengal (12.8 ± 0.4 μmol/kg/salinity; Table A4) and open ocean (12.36 ± 0.03 μmol/kg/salinity; Lee et al., 2010). Few samples, particularly from the pre-monsoon (May) season, are also characterized with lower boron/salinity ratio compared to their source waters (Fig. 4.1.2; 4.1.3D).

4.1.2.3. Chemical composition of Chilika sediments

The size fraction of bed sediments from the Chilika lagoon is dominated by clay (64 ± 26 wt%; n = 33) fractions. Aluminum concentrations of the river sediments from the Chilika drainage basin vary between 5.3 and 6.8 wt% (average: 6.1 ± 0.7 wt%; n = 4; Table A5). These values are consistent with that reported earlier for sediments from the Mahanadi river (6.22 wt%; Chakrapani and Subramanian, 1990). The Al concentrations of river sediments are found systematically lower than that of the bed sediments from the Chilika lagoon (12 ± 4 wt%; n = 33) and their clay fractions (12 ± 1 wt%; n =19). Boron concentrations of riverine (bed) sediments vary between 3.5 and 5.3 μg/g (mean: 4 ± 1 μg/g; Table A5). This average B concentration is lower than that reported for upper continental crust (17 μg/g; Rudnick and Gao, 2004), but consistent with average B content for igneous rocks (<10 μg/g; Mao et al., 2019). Similar to Al, the boron concentrations of the Chilika bed sediments (10 ± 4 μg/g; n = 33) and their clay fractions (10 ± 2 μg/g; n = 19) are also higher than that of the river sediments (4 ± 1 μg/g; Table A5)

4.1.2.4. $\delta^{18}O$ values of the Chilika system

The $\delta^{18}O$ value of the rain water sample from this coastal location is found to be 0.09 ± 0.06 ‰ (Table A8). The average $\delta^{18}O$ values of the groundwater (-4.2 ± 0.8 ‰) samples are found similar to that of the river samples from the drainage basin of the Chilika (-3.8 ± 0.9 ‰; n = 5) (Table 4.1.2). The $\delta^{18}O$ values of the lagoon samples collected varies from 0.6 to 3.3 ‰, with an average value of 2.2 ± 0.7 ‰ (n = 34). These isotopic compositions are highly enriched compared to its source waters (Table 4.1.2). The $\delta^{18}O$ values were found to be least for the northern sector (1.8 ± 0.6 ‰; n = 11) and highest for the southern sector samples (2.7 ± 0.3 ‰; n

= 12). A few river samples collected near the lagoon are found to have enriched $\delta^{18}O$ values (1.3 ± 2.4 ‰; n = 4), indicating incursion of lagoon water during tidal periods.

Table 4.1.3. Results comparison of statistical analyses using various approaches of spatial and seasonal distribution of B, salinity and B/salinity values of the Chilika lagoon.

	ANOVA	**t-test**	**F-test**	**K-S test**
Salinity data comparison				
Within the sectors (Pre-monsoon; May)	**2.9**	-	-	-
Within the sectors (Onset-monsoon; June)	124.7	-	-	-
Within the sectors (Monsoon; August)	173.5	-	-	-
Within May, June and Aug sampling	15.5	-	-	-
May vs June	5.9	2.4	2.7	0.5
May vs Aug	11.4	3.4	1.7	0.3
June vs Aug	41.7	6.5	**1.6**	0.7
Aug vs 16th Aug	17.6	4.2	2.0	0.4
Boron data comparison				
Within the sectors (Pre-monsoon; May)	4.2	-	-	-
Within the sectors (Onset-monsoon; June)	3.5	-	-	-
Within the sectors (Monsoon; August)	184.7	-	-	-
Within May, June and Aug sampling	16.7	-	-	-
May vs June	9.2	3	2.6	0.6
May vs Aug	8.9	3	2.1	0.3
June vs Aug	50.4	7.1	**1.2**	0.8
Aug vs 16th Aug	18.6	4.3	2.2	0.5
B/salinity ratio comparison				
Within the sectors (Pre-monsoon; May)	21.7	-	-	-
Within the sectors (Onset-monsoon; June)	102	-	-	-
Within the sectors (Monsoon; August)	**1.54**	-	-	-
Within May, June and Aug sampling	12.9	-	-	-
May vs June	20.9	4.6	12.8	0.5
May vs Aug	15.4	3.9	**1.2**	0.2
June vs Aug	**0.24**	**0.5**	15.1	0.5
Aug vs 16th Aug	**0.004**	**0.07**	2.0	**0.3**

Bold numbers show significant similarity within the sample groups for p<0.05.The t, F and K-S tests were carried out using the PAST software, whereas ANOVA analysis were done using MS-Office.

4.1.3. Discussion

4.1.3.1. Hydrology of the lagoon: Evaporative loss estimates

The hydrology of the Chilika is mainly regulated by mixing of source waters (*e.g.* river, rain, groundwater and seawater) and/or evaporation process. The relative contributions from river and sea water to the lagoon are by and large reflected in the spatial distribution of salinities (Fig. 4.1.1). Interestingly, salinities of few (13 out of 73) samples from the pre-monsoon season (May, 2017) were higher than those reported for the Bay of Bengal (~32 salinity; Table A1), attributable to evaporative loss of the lagoon water. We have analyzed $\delta^{18}O$ values of samples collected only during June, 2016 to assess the impact of evaporation on the Chilika hydrology. Average $\delta^{18}O$ values of these samples (2.2 ± 0.7 ‰; Table A8) is found enriched compared to that reported for the Bay of Bengal (-0.3 ± 0.1 ‰; Singh et al., 2010), indicating evaporative loss of water from the lagoon. Efforts were made in this study to estimate the evaporative water loss using salinity and $\delta^{18}O$ values of the water samples. Towards this, we employed an iterative approach involving mass balance (Eq. 1-2) and Rayleigh fractionation (Eq. 3) equations.

$$S_{Chilika} = S_{river} \times f_{river} + S_{BoB} \times (1 - f_{river}) \qquad (1)$$

$$\delta^{18}O_{calc} = \delta^{18}O_{river} \times f_{river} + \delta^{18}O_{BoB} \times (1 - f_{river}) \qquad (2)$$

$$\delta^{18}O_{meas} = (\delta^{18}O_{calc} + 1000) \times f_{Ev}{}^{(\alpha-1)} - 1000 \qquad (3)$$

where, $S_{Chilika,}$ S_{river} and S_{BoB} stand for salinities of the Chilika, riverine supply and the Bay of Bengal respectively. $\delta^{18}O_{river}$ and $\delta^{18}O_{BoB}$ represent the oxygen isotopic compositions of the river and sea water respectively. The $\delta^{18}O_{calc}$ and $\delta^{18}O_{meas}$ are the calculated (*i.e.* expected value before evaporation) and measured oxygen isotopic value for the sample respectively. The f_{river} is the fraction of water supplied by the rivers, whereas f_{Ev} reflects the fraction of water remained in the lagoon after evaporation. A value of 0.9908 is used for the fractionation factor, α (at 25 °C; Gat and Gonfiantini, 1981). The mass balance calculation (Eq (1-3)) considers that the Chilika receives waters from rivers and Bay of Bengal, and assumes insignificant supply of groundwater (GW) to the lagoon. The assumption on negligible GW supply may not be strictly valid. Although there is lack of GW flux data for the Chilika, radium isotopic investigations have computed a submarine groundwater discharge of (1.55 - 7.44) × 10^6 m^3/d for a nearby river (Guatami) estuaries (Rangarajan and Sarma, 2015). These SGD fluxes are of similar order when compared with the riverine discharge (3.1× 10^6 m^3/d; Gupta et al., 2008) to the Chilika during the non-monsoon periods. We, therefore, recognize that omission of GW flux from the mass balance calculation based on two end-member mixing equations (Eq. (1-3)) may overestimate the riverine contribution to the Chilika. However, this approach will have minimal influence on the estimation of evaporation rates. This is mainly due to similar $\delta^{18}O$ composition of the river (-3.8 ± 0.9 ‰; n = 5 (collected in June)) and groundwater samples (-4.2 ± 0.8 ‰; n = 5) from the basin and our evaporation rate estimation largely depends Rayleigh isotopic fractionation of oxygen isotopes.

Table 4.1.2 lists the salinity and $\delta^{18}O$ values for source waters used for the estimating the evaporation rates. The average salinity and $\delta^{18}O$ values for the sea water were constrained using the data reported for the Bay of Bengal (Singh et al., 2010). The mass balance equations for salinity (Eq. 1) and $\delta^{18}O$ (Eq. 2) values were used for estimating the expected pre-evaporation $\delta^{18}O$ (*i.e.* $\delta^{18}O_{calc}$) values for the lagoon water samples. The measured $\delta^{18}O$ value represents the post-evaporation value of the sample and hence, a Rayleigh fractionation calculation using the $\delta^{18}O_{calc}$ and $\delta^{18}O_{meas}$ values (Eq. 3) was carried out to find the fraction of water lost during evaporation. However, the measured salinity is already influenced by evaporation and hence, the pre-evaporation salinity (S_{calc}) value is computed (Eq. 4). The estimated S_{calc} is iteratively used in Eq. 1-3 to estimate the fraction of water lost from the lagoon during the month of June.

$$S_{calc} = \frac{S_{Chilika}}{(1-f_{Ev})} \tag{4}$$

The amount of surface water lost from the lagoon during June month varies from 14 % to 48 %, with an average value of 38 ± 9 % (n = 34). The evaporative loss was highest for the southern sector (43 ± 3 %; n = 11) compare to the central (36 ± 10 %; n = 11) and northern (35 ± 11 %; n = 12) sectors. Relatively higher evaporation in the southern sector is consistent with limited water exchange from fresh and sea water sources. There is lack of estimates on evaporative loss of water for coastal lagoons in India for comparison with the present results. The present estimates, however, are of similar order (up to 70%) that reported earlier for coastal lagoons from along the Mediterranean coast (Lécuyer et al., 2012). The estimated evaporative loss of ~40% from the Chilika is higher compared to insignificant evaporation (0.31 %; Gupta et al., 2008) water loss from the Chilika during the monsoon season and lower as compared to annual evapotranspiration loss (~57 %) reported for a nearby river (Subernarekha) basin (Jain et al., 2007). Our estimate is based on oxygen isotopic composition of the surface water and hence, precise estimation of the evaporative loss will also require $\delta^{18}O$ data for the benthic water of the lagoon.

4.1.3.2. Variation of boron with salinity

We have investigated the co-variations between boron and salinity of the lagoon samples collected during three different seasons to infer sources and behavior of dissolved boron in this tropical coastal lagoon (Fig. 4.1.3). Towards this, data on average compositions for river and sea water were required to constrain the theoretical mixing line. Average salinity (0.2 ± 0.1) and boron (1.7 ± 0.8 µmol/kg) concentrations of the rivers draining into the Chilika were used as the riverine end-member composition (Table 4.1.2). The average salinity (32 ± 1) and boron concentration (406 ± 13 µmol/kg) of the Bay of Bengal samples analyzed during this study is used as the seawater end-member composition (Table 4.1.2). As mentioned earlier, the average boron concentration of the Bay of Bengal samples (448 ± 13 µmol/kg (normalized to salinity of 35)) matches well with the reported boron data for global ocean (433 ± 2 µmol/kg; Lee et al., 2010). Considering these B and salinity concentrations, the mixing between river and Bay of Bengal waters should yield a B/salinity ratio of 12.7 (Fig. 4.1.2). In addition, salinity (1 ±1) and B (25 ± 38 µmol/kg) composition of the groundwater fluxes can also contribute to the B-salinity trend of the Chilika. Figure 4.1.3 depicts the salinity-boron relationship for the Chilika lagoon during the three seasons sampled. The figure also shows the characterized values for river, ground and sea water for reference. Samples from all the seasons show strong linearity ($r^2 \geq 0.97$; $p < 0.05$) between the two parameters, pointing to dominant contributions from river and seawater to the lagoon chemistry. The slope of the regression lines for the pre-monsoon (May; 13.0 ± 0.2), onset of monsoon (June; 13.2 ± 0.4) and monsoon (August; 12.0 ± 0.2) seasons are found comparable with that expected (12.7) for river-sea water mixing line (Fig. 4.1.2). This indicates a conservative behavior of boron in the coastal lagoon system and hence, the supply of boron is delivered to the Chilika mainly through river and sea water. The conservative B-salinity mixing trends, further, corroborates that the boron supply from any other (groundwater and anthropogenic) sources is only minimal. This behavior of boron is consistent with an earlier reported study for large estuary systems from the western India (Singh et al., 2013).

The pre-monsoon samples although show a linear trend between boron and salinity,

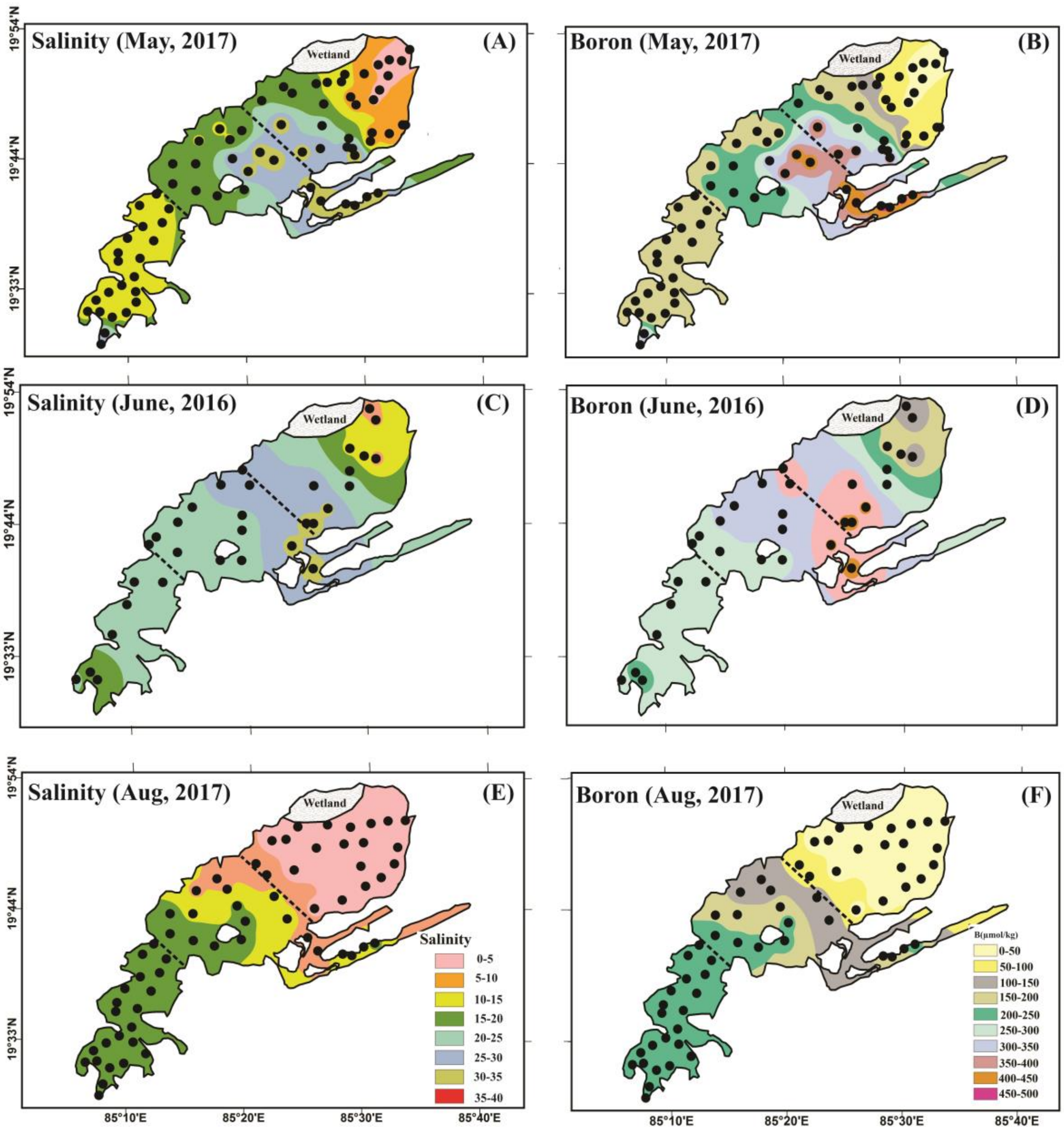

Figure 4.1.1. Contour map showing the salinity and boron distributions of the Chilika lagoon during different seasons: pre-monsoon (May-2017; inset A-B), onset of monsoon (June-2016; inset C-D) and monsoon (August-2017; inset E-F). The dotted lines in each figure inset represent the sector (i.e. southern, central and northern) boundaries. Spatial distribution of boron concentration follows that of the salinity pattern.

several data systematically fall below the theoretical mixing line (Fig. 4.1.3D).Fig. 4.1.3D presents the B-salinity trend for low-saline (< 15) samples collected during the pre-monsoon (May) period. All these samples fall systematically below the river-seawater mixing line. The B/salinity for most (40 out of 42; Fig. 4.1.3D) of these samples vary between 4.3 and 12.5, which is lower compared to the ratio expected (12.7; Fig. 4.1.2) for river and seawater mixing. These systematically lower ratios demand an additional source/sink to explain their boron distribution. These additional sources/sinks for the Chilika could be influx from SGD and/or removal of boron through ion-exchange (adsorption) mechanisms. The B and salinity data for the ground-

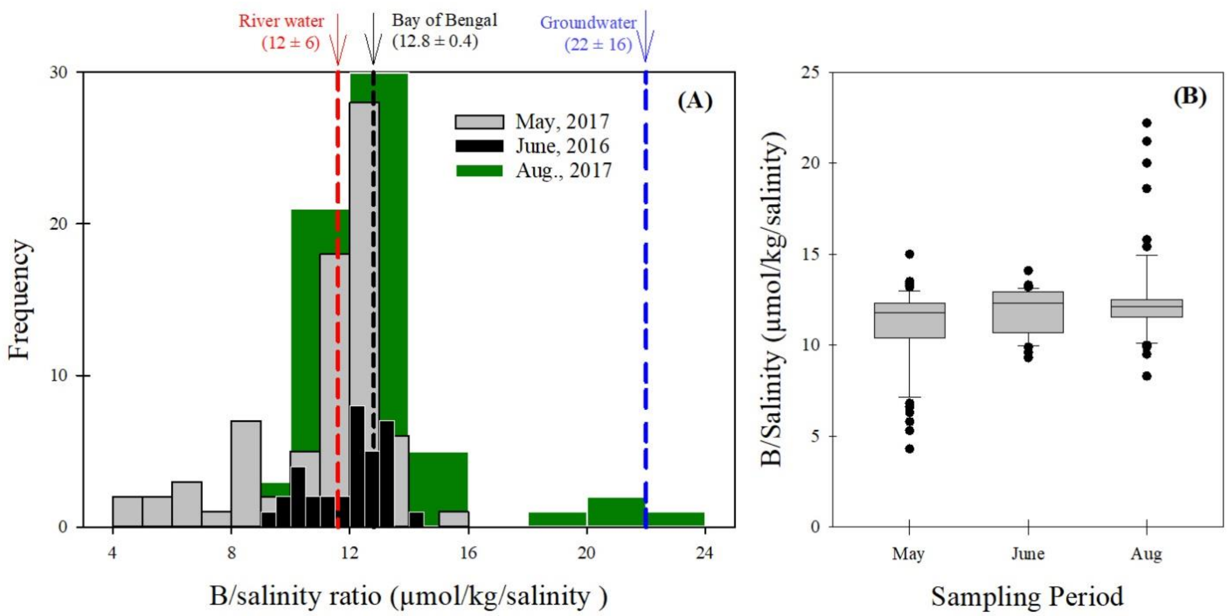

Figure 4.1.2. (A) Frequency distribution of the boron/salinity ratio (in µmol/kg/salinity) during different seasons. The frequency in this histogram stands for the count of the samples within the given bin of B/salinity ratio. The boron/salinity ratios of most of the samples fall between of the Bay of Bengal (12.8 ± 0.4 µmol/kg/salinity) and riverine (11.6 ± 6 µmol/kg/salinity) input. Several pre-monsoon (May) samples show relatively lower B/salinity ratios than that of its possible sources. This observation indicates removal of dissolved boron from the lagoon which we interpret as ion-exchange (i.e. adsorption) processes. (B) Box plot showing the B/salinity distribution for three different months. The pre-monsoon (May) samples with relatively lower B/salinity ratios are mostly from the northern sector of the lagoon. This B/salinity decline has been attributed to adsorptive removal of boron from the Chilika.

water influx falls above the river-seawater mixing line (Fig. 4.1.3D), which is consistent with its higher B/salinity ratio (Fig. 4.1.2). Any solute supply through this pathway, therefore, is expected to elevate the B/salinity ratio of the lagoon, which is clearly in contrast with the observed lower values for the low-saline samples from May. These observations point to non-conservative behavior of boron in the coastal regime with appreciable amount of boron removal from the lagoon during the pre-monsoon period. The boron-salinity trends of the Chilika, therefore, indicate seasonality in the behavior of boron in the coastal system with conservative nature during the monsoon and non-conservative nature during the pre-monsoon period.

Efforts are made to quantify the amount of boron lost from the low-saline regions during May, 2017. Towards this, the expected boron for the given salinity of a sample was computed from the river-sea water mixing equation. The difference between measured and expected boron is used as a measure of loss of boron in the lagoon. This estimation of boron loss, however, will be an underestimation, in case of appreciable water supply from any additional (groundwater/anthropogenic) sources to the lagoon. The estimated boron removal from the Chilika for the May samples is presented in Fig. 4.1.4. Consistent with our earlier observation, strong removal of boron from the low-saline samples (<15) was observed. The amount of boron removal (in %) show a decreasing trend from ~60% to zero in the 0-15 salinity zone. This decreasing trend is consistent with earlier reported trend of adsorptive removal of elements from estuaries with salinity (Salomons, 1980; Bourg, 1987). Samples from the higher saline zone do not show any B loss (Fig. 4.1.4), indicating dominance of river and sea water mixing in this zone. As the lesser-saline samples are more restricted to the northern sector (strongly influenced by freshwater influx), the non-conservativeness is more pronounced in this river-dominated part of the lagoon. In concurrence with this, the amount of loss of boron (in %) in the southern (1 ± 3 %; n =22) and central (2 ±4 %; n =14) sectors are found statistically similar ($F = 1.34$; $t = 0.68$) for $p < 0.05$. However, the boron loss in the northern sector (25 ± 21 %; n =31) is found statistically different when compared with that from the central ($F = 26.8$; $t = 4.05$) and southern ($F = 35.9$; $t = 5.27$) sectors. Possible mechanisms contributing to the boron removal from the Chilika are discussed below.

4.1.3.3. Possible causes for removal of dissolved boron

Removal of dissolved boron from coastal lagoon can be regulated by several factors, which includes volatilization of boron complexes (Chetelat et al., 2005; Gaillardet and Lemarchand, 2018), biological activities (Harriss, 1969; Park and Schlesinger, 2002) and adsorption on to the surface of clays (Liss and Pointon, 1973; Salomons, 1980), and/or organic matter (Goldberg, 1997) and. Earlier studies have shown that boric acid, which constitutes about 90% of seawater B, is highly volatile in nature and it contributes significant fraction of the B present in the atmosphere (Gaillardet et al., 2001; Xiao et al., 2007; Gaillardet and Lemarchand, 2018). This removal mechanism involving evaporative loss of boron is expected to be uniform across different salinity gradient, which is in clear contrast to observed preferential removal of boron only from the low-saline (<15) regimes of the Chilika (Fig. 4.1.3D). Minimal impact of B volatilization from the Chilika is also evident from the observed conservative mixing of boron (Fig. 4.1.3B) during the month of June, when significant evaporation impact on the lagoonal hydrology has already been established (cf. section 4.1.3.1). Although available dataset from this study does not allow proper evaluation of impact of biological matter on removal of boron from the Chilika, co-variation of boron with dissolved oxygen (a possible proxy for biological activities) was assessed for this purpose. The boron concentrations of the Chilika samples from the month of May show insignificant correlation with their dissolved oxygen concentrations ($r = 0.05$; $n = 73$; $p > 0.05$, pointing to limited role of biological activities in the boron loss. However, more rigorous data analysis of boron distribution with other key biological proxies (*e.g.* suspended organic matter, organic carbon isotopes) can provide more insight on the removal of boron through biological pathways.

Particulate-water interaction has been recognized to be the primary process that removes boron from aquatic systems (Schwarcz et al., 1969; Liss and Pointon, 1973; Salomons, 1980). The observed boron removal from the Chilika during the month of May, therefore, can be attributed to adsorptive processes. Earlier studies have shown removal of boron from water column through its adsorption onto clay minerals (more readily to illites) and/or oxides of Fe and Al (Liss and Pointon, 1973). Consistent with this removal process, boron concentration in clay minerals (up to 1000 μg/g) are always higher than that of the continental crust (10 μg/g) (Gaillardet and Lemarchand, 2018). Average B concentrations in the Chilika bed sediments (10 ± 4 μg/g; n = 33) and their clay fractions (10 ± 2 μg/g; n = 19) are higher than their riverine source value (4 ± 1 μg/g; n = 4; Table A5). We estimated the enrichment factors (EF) for the bulk and clay fractions of the bed sediments with respect to their riverine input using the following equation. The EF values are calculated based on Al-normalized ratios to take care of size-sorting chemical changes and hence, provides a good measure of elemental enrichment in sedimentary basins (Tripathy et al., 2018).

$$EF = \frac{\left({}^{B}/_{Al}\right)_{Chilika}}{\left({}^{B}/_{Al}\right)_{river}} \qquad (5)$$

By the definition (Eq. (5)), the average EF for the river sediment is 1. Average EF of boron in the bulk (1.3 ± 0.4 (n =33)) and clay (1.7 ± 0.5 (n =19)) fractions of the Chilika bed sediments are about 30 % and 70% higher than the riverine EF value (~1), respectively. This boron enrichment hints at possible removal of this element through their adsorption onto clay particles. To evaluate

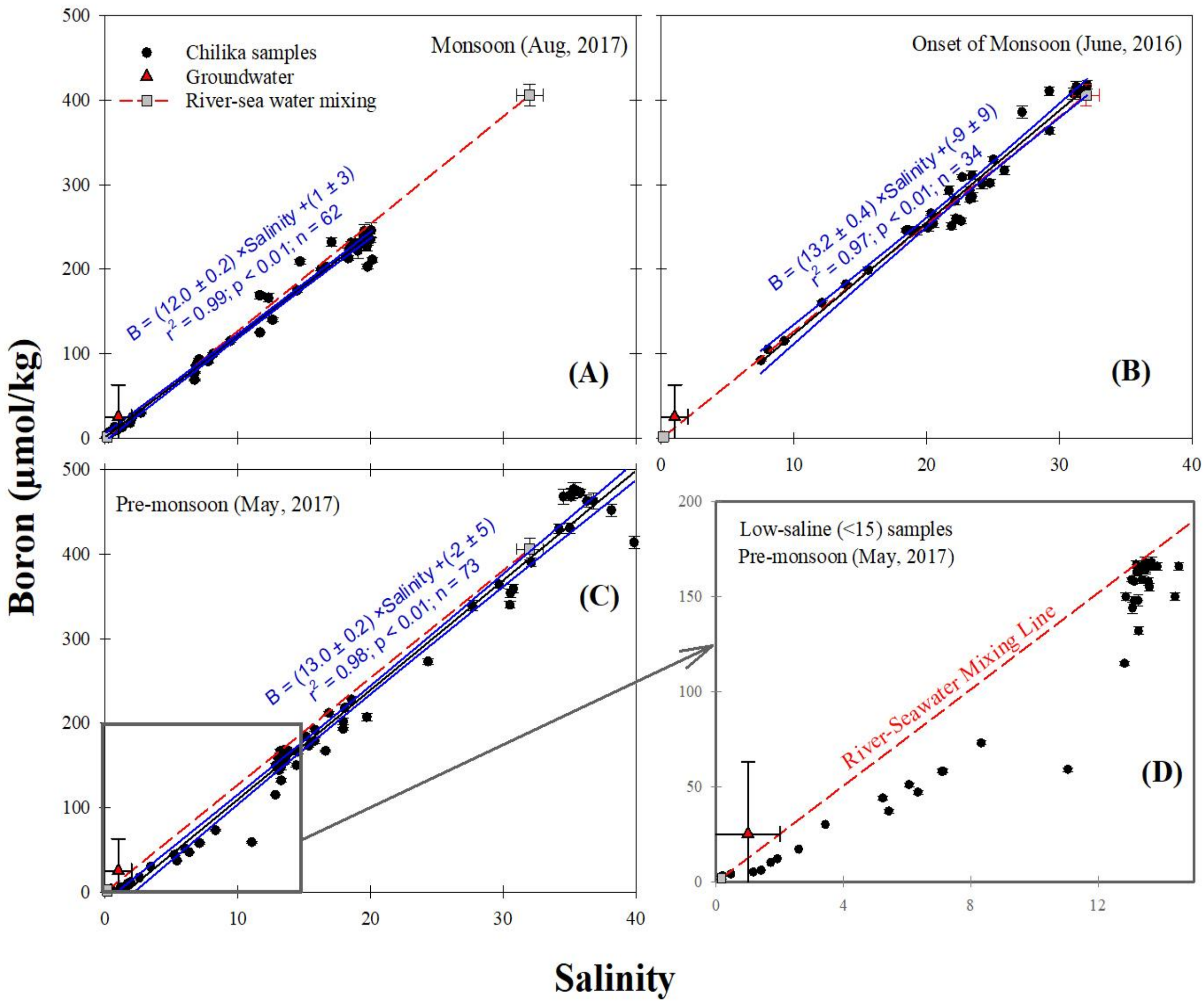

Figure 4.1.3. Co-variation between salinity and boron concentrations of the lagoon during (A) monsoon (Aug), (B) onset of monsoon (June) and (C) pre-monsoon (May) seasons. Error bars here represent the uncertainty associated with the boron measurements. The end-member compositions for the river (gray squares) and Bay of Bengal (open squares) waters are shown here. The dotted (red) line reflects the theoretical river-sea water mixing line. Average groundwater composition (red triangle) is also shown for comparison. The linear regression line of the dataset (bold black) and the corresponding 95% confidence level (blue dotted line) are also shown. (D) B-salinity trend of low-saline samples with salinity<15 from the pre-monsoon (May) season. Most of these data fall below the theoretical mixing line for river and sea water.

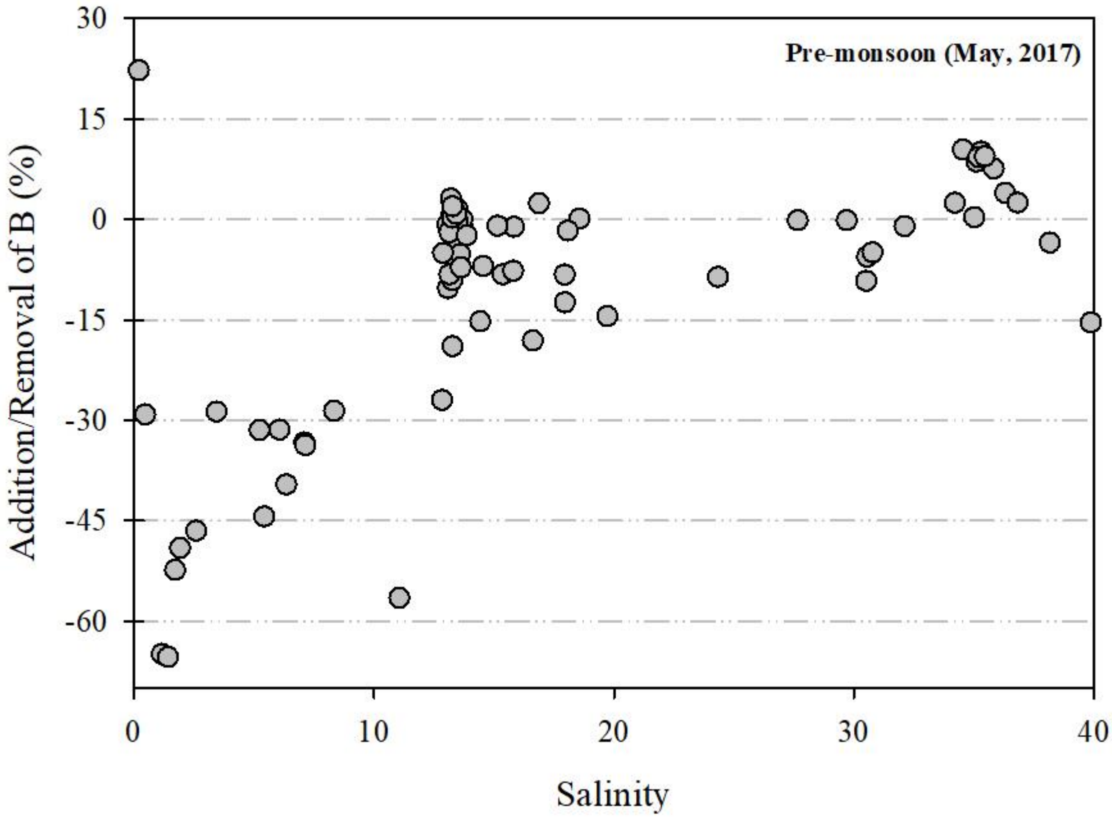

Figure 4.1.4. Estimated dissolved boron removal (in %) with respect to salinity of the lagoon during the pre-monsoon (May) period. The removal process is restricted mostly to the low saline regime of the Chilika.

this proposition, co-variation between the clay and boron abundances of the Chilika bed sediments were evaluated (Fig. 4.1.5). The clay content of these sediments vary from 5 and 100 wt%, with a median value of 76 wt%. Despite of this large variation, the clay abundance of these samples show significant correlation with their boron concentrations, corroborating again the possibility of boron removal from the Chilika lagoon through their adsorption onto clay surfaces.

Various factors can control the adsorptive removal of elements in the coastal regions, which include salinity, pH, turbulence and sediment abundances (Bourg, 1987). No significant correlation between pH and dissolved boron is observed, pointing to minimal role of pH in regulating the ion-exchange process. The intensity of elemental removal through adsorption generally shows an inverse relation with salinity (Bourg, 1987). Further, turbulence and sediment abundances are other possible controlling factors for adsorptive removal. These parameters (salinity, turbulence and sediment load) are expected to be more influential during the monsoon

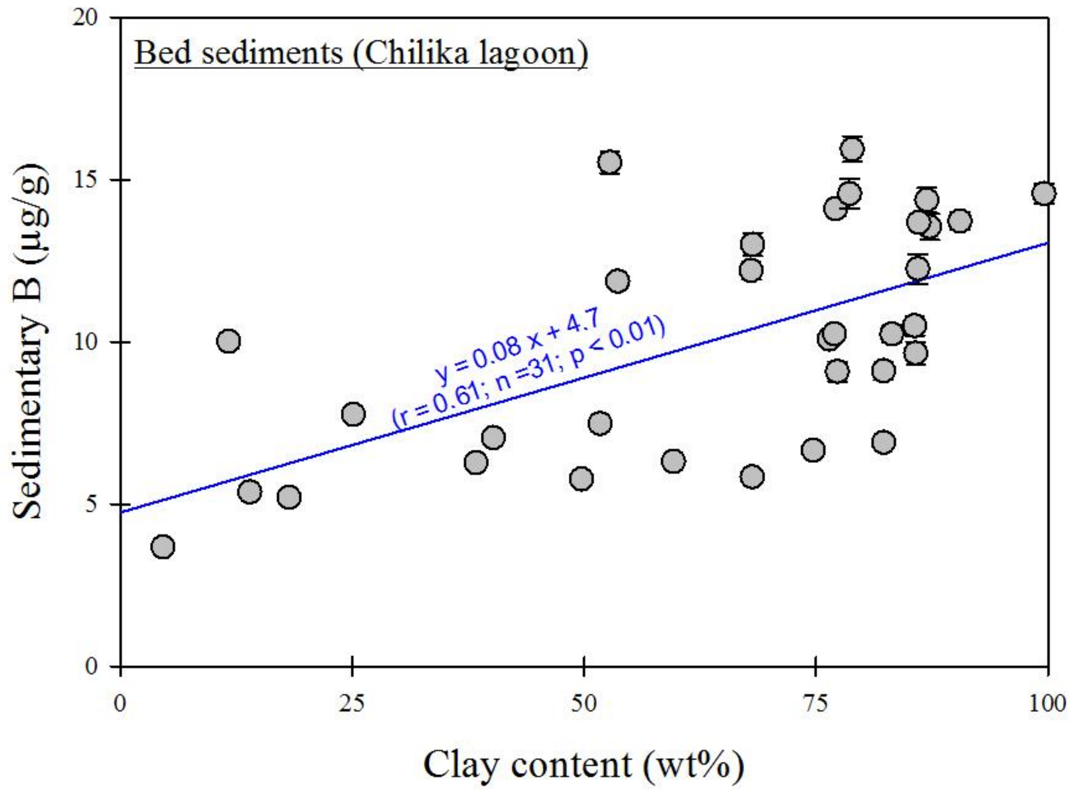

Figure 4.1.5. Correlation between boron concentration (in bulk fraction of sediments) and clay abundance of the bed sediments from the Chilika lagoon.

seasons. This is not consistent with the conservative behavior of boron during monsoon with no significant removal. This observation points to minimal role of these parameters in controlling removal of boron from the Chilika. Higher removal of boron during the pre-monsoon seasons can be due to higher residence time of the water during this period. The water residence time of the lagoon is significantly higher during the pre-monsoon season than that during the monsoon period. Higher residence time would increase the particulate-water interaction time, which in turn can increase the adsorption removal of boron from the Chilika. Intensity of this adsorptive process is also supported by re-suspension of fine sediments due to low depth of the lagoon and churning of the water column by winds (Kumar et al., 2016).

4.1.3.4. Impact of tides on the boron distribution

Tides in the Chilika are pre-dominantly semi-diurnal (12.4 hours) and fortnightly (12 days periodicity) in nature (Mahanty et al., 2015). The water level of the lagoon at its inlet (near Satapada) varies by ~1 m (between 0.84 and 1.92 m) during the non-monsoon and by ~1.5 m (between 1.07 and 2.53 m) during the monsoon season (Mahanty et al., 2016). These tidal cycling introduce temporal changes in the seawater incursion into the lagoon and hence, can influence the lagoon chemistry. In particular, collection of water samples throughout this large lagoon generally took 2-3 weeks' time during each field trip and hence, some of the observed boron variations can be attributed to variation in the tide/ebb intensity within the lagoon. In order to assess tidal influence at semi-diurnal timescale, water samples at two locations (*i.e.* Barkul and Satapada; Fig. 2.4 in chapter 2) were collected on 2-hourly interval basis for a duration of 1-day during monsoon and pre-monsoon seasons. The salinity at Barkul (from southern sector) within 1 day varies by about 6 % (mean: 16 ± 1) during the monsoon season. Considering average salinity of river and seawater (Table 4.1.2), this salinity change accounts for variation in seawater contribution from 41 % to 52% to the lagoon (estimated using equation 1). A similar degree (~5%) of salinity change at Barkul was also observed for the pre-monsoon season. However, the salinity changes at Satapada (near the Chilika inlet) during the pre-monsoon season were only limited (1.4 %). On the contrary, the salinity at Satapada varies from 6.4 to 9.2 over duration of 1-day during the monsoon season (Fig. 4.1.6A). These changes in salinity indicate variation in seawater water supply from 19.6 to 28.6% (Fig. 4.1.6A). These changes in seawater influx to the lagoon are linked with the tide and ebb cycle of the lagoon system. Similar to salinity, the boron concentrations of these samples also show significant diurnal variation due to tidal changes. Despite these variations, Boron concentrations of these samples co-vary with their corresponding salinity and show conservative behavior (Fig. 4.1.6B). The boron-salinity regression equation yields a boron concentration of 440 µmol/kg for a salinity of 35, consistent (within 1.6 %) with that of the global ocean value (433 ± 2 µmol/kg; Lee et al., 2010). These observations confirm conservative behavior of boron during different tidal conditions of the lagoon. This evidence of conservative river-seawater mixing, further, points to minimal impact of groundwater influx to the lagoon during tidal pumping.

To assess the tidal impact on lagoon chemistry at fortnightly timescales, the spatial sampling of the whole lagoon during the monsoon season has been carried out two times. In addition to high-resolution (n = 62) spatial sampling over a period of 2-3 weeks' time (Table A1), the whole lagoon with limited spatial resolution (n = 31) was also collected within 1 day on a waning crescent moon phase day (16^{th} August, 2017; 9^{th} day after full moon). The boron concentrations of the 1-day sampling varies widely between 2 and 187 µmol/kg with a salinity-

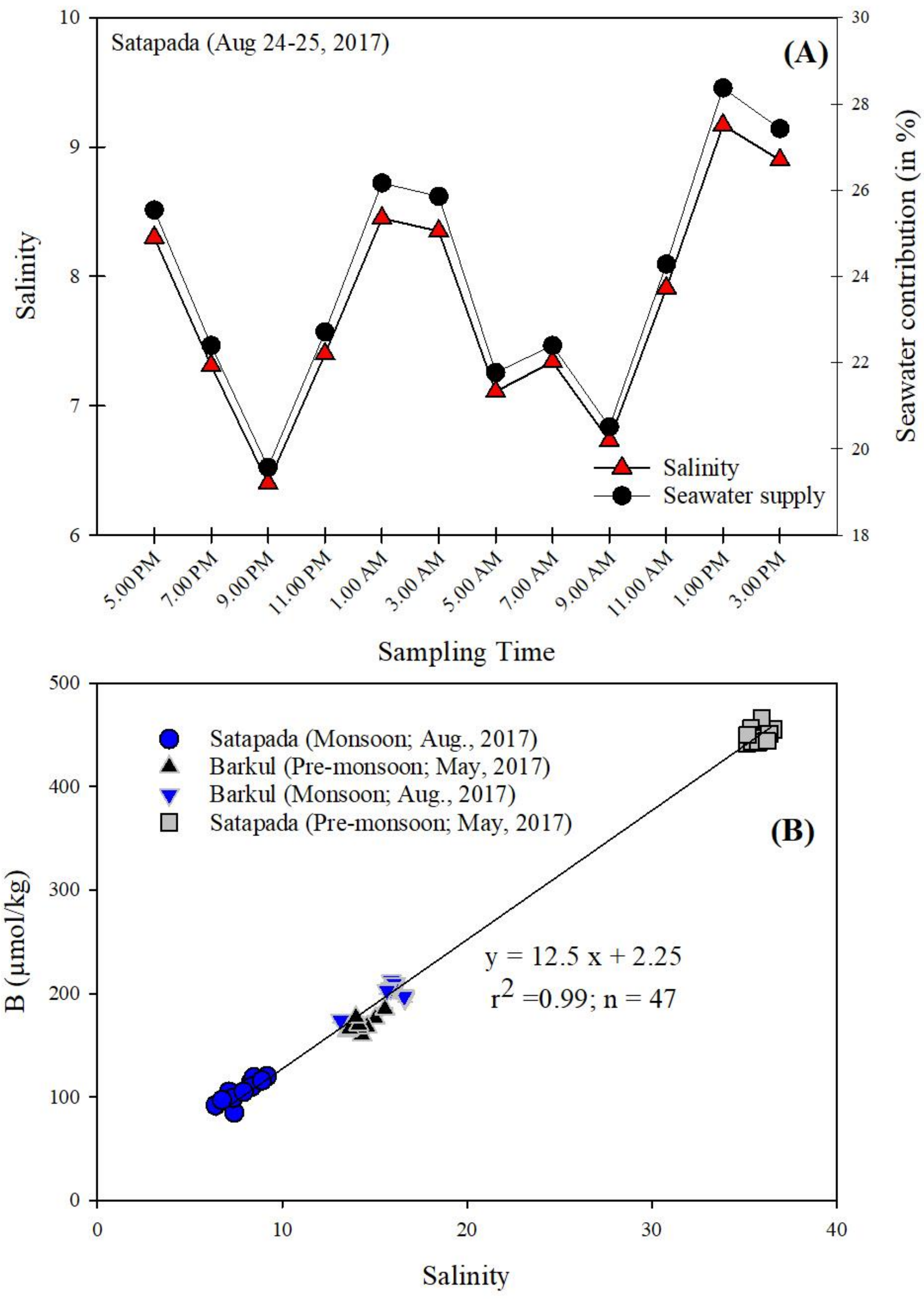

Figure 4.1.6. (A) Two-hourly data for salinity and relative contribution from seawater to the lagoon at Satapada (outer channel) during the monsoon season. Variation in these datasets points to fluctuation of Bay of Bengal water influx into the Chilika due to tidal cycle. (B) Combined salinity and boron data on 2-h basis sampling at two different locations (Barkul and Satapada) for two seasons (monsoon and non-monsoon) show a conservative behavior. Analytical uncertainties associated with these two parameters are smaller than the symbol size.

weighted average value of 74 µmol/kg, which is about 63 % lower than that of the high-resolution spatial sampling of the lagoon (203 µmol/kg) during the same season. Further, attempts were made to compare the spatial boron data during the two sampling trips for the monsoon. For this, we identified grids at 7 km × 7 km areal resolution for the Chilika lagoon. The salinity-weighted average boron concentrations of all the points within a given grid during both of the sampling trips are compared in Fig. 4.1.7. The boron abundance of the one-day sampling data is found consistently lower (by ~ 34 %; Fig. 4.1.7) than that of the high-resolution spatial sampling of the lagoon. This difference in boron abundance is mainly due to the degree of seawater exchange into the lagoon during the different tidal stages. Despite these differences in boron concentrations, the linearity between boron and salinity and hence, conservative nature of boron during monsoon period persists for both the sampling durations. This observation indicates that boron concentration of the Chilika and its spatial distribution depends on the tidal/ebb cycle and related seawater exchange. However, the coastal behavior of boron remains invariant during different tidal phases.

4.1.3.5. Boron budget of the Chilika lagoon

The salinity and boron budgets of the Chilika lagoon for the monsoon (August) period are presented in Figure 4.1.8. For this, the hydrological data are taken from Gupta et al. (2008), whereas the salinity and boron data are from this study. There exists no literature data for SGD flux to the Chilika. Assuming the SGD value for the Chilika is similar to that (1.55-7.44 × 10^6 m^3/d; Rangarajan and Sarma, 2015) reported for a nearby river (Guatami) estuary, the submarine groundwater discharge to this lagoon is found ~1.5-7.0 % of the river water supply (167 × 10^6 m^3/d; Fig. 4.1.8) during the monsoon. Further, the conservative B-salinity trend ensures minimal impact of SGD on the Chilika boron budget. We, however, recognize here that precise SGD flux estimation for the lagoon can provide better constrains on the chemical budget. The salinity and boron compositions for the tide and ebb are computed from the diurnal data (Fig. 4.1.6) obtained at the Chilika outflow (Satapada). Area-weighted salinity and boron concentrations for the lagoon presented in Fig. 4.1.8 were estimated by considering surface area, average salinity and boron of all of the identified grids in Fig. 4.1A (chapter 2). The average salinity of the lagoon is found to be 10.5, which corresponds to about 30% of seawater influx to the Chilika. Average boron content of the Chilika lagoon (128 µmol/kg) corresponds to a total B inventory of 2.85 × 10^6 kg. Similar to salinity, mass balance calculation show about 70% of boron in the Chilika is supplied through the freshwater sources. In addition to these sources, the samples from the month of May also show removal of dissolved boron from low-saline (<15) regions of the

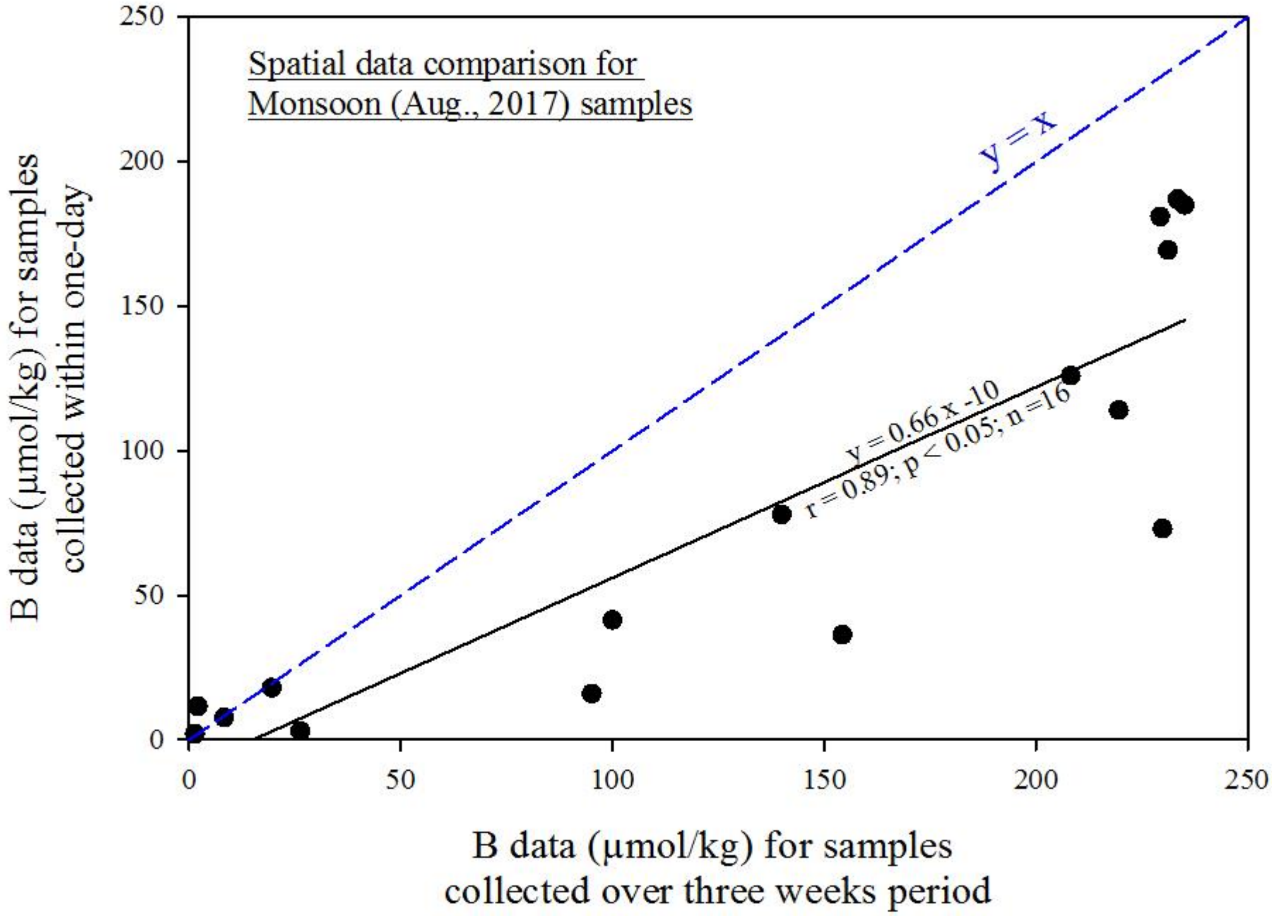

Figure 4.1.7. Spatial correlation of boron data between monsoon samples for two different spatial sampling (1-day sampling versus spatial sampling over ~3 weeks' time). We compare here salinity-weighted boron data for each grid (7 km × 7 km) shown in Fig. 1 for the two sampling trips in the same season. The boron concentrations for the 1-day sampling are different than those collected by spatial sampling in about 3 weeks duration, attributable to tidal effect on water chemistry.

Chilika through adsorptive processes (cf. section 4.1.3.2.). Gridded data analysis of these samples provides an area-weighted average boron concentration of 239 µmol/kg for the lagoon, whereas the low-saline (<15) regions yield a B content of 123 µmol/kg. This analysis also provides an estimation of adsorptive B removal of 13 µmol/kg from the low-saline regions, which is only 3% of the open seawater boron value. Although extrapolating these regional data at global scales is likely to yield large uncertainties, we used the present data to compute total boron removal from the coastal lagoons worldwide. Available global database for total area

(700,000 km^2) and volume (104,000 km^3) of saline lakes (Herdendorf, 1982) were used for this estimation. These data yield a total boron loss of 1.5×10^{10} kg from coastal lagoons globally,

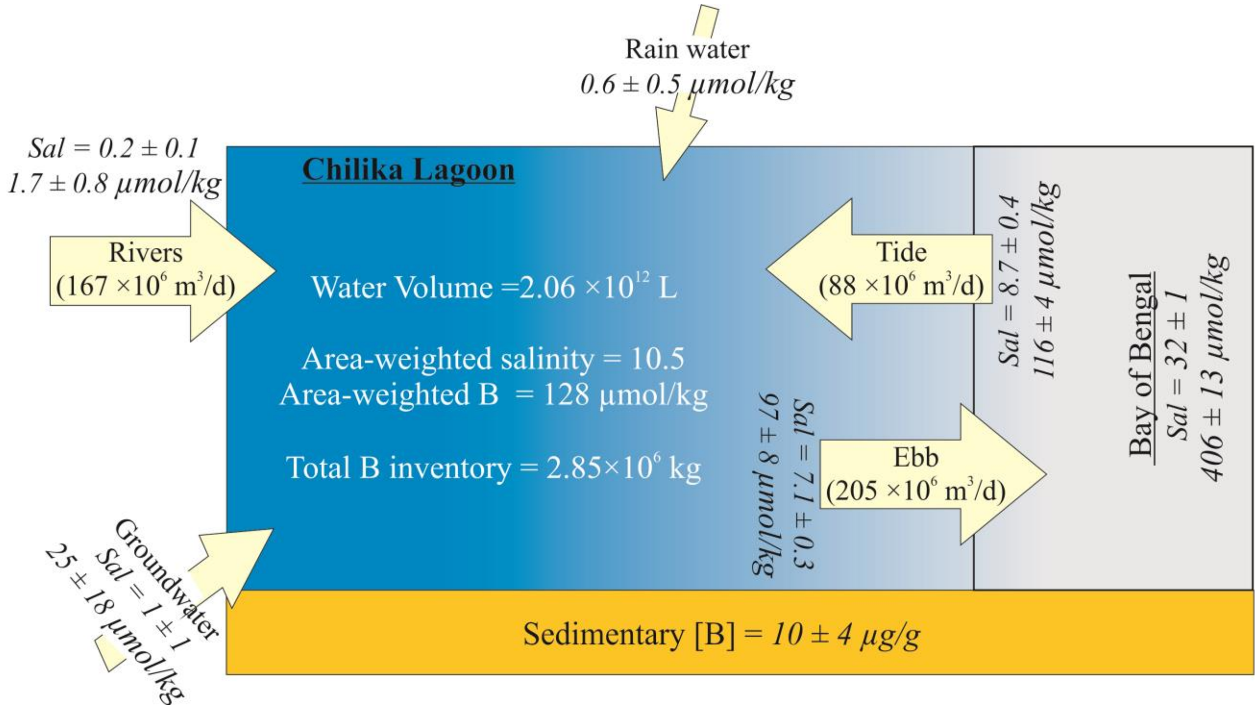

Figure 4.1.8. Boron budget of the Chilika lagoon for the monsoon season. The boron and salinity data shown here from this study, whereas the hydrological data are from Gupta et al. (2008). Please note that the arrow size does not reflect the water volume of the sources to the lagoon.

which is lower by few orders of magnitude than the total boron inventory in seawater (6.32 × 10^{15} kg). The adsorptive removal of boron from coastal lagoons, therefore, seems to have insignificant impact on global oceanic boron budget. This minimal impact is mainly due to lower concentration of boron in the low-saline regions by 1-2 orders of magnitude when compared with open ocean values. Outcomes of this study, however, provide "proof of a chemical process" involving removal of dissolved boron through ion-exchange mechanism. This observation can find implications in understanding authigenic boron distribution in clay-rich sedimentary archives and its applications to paleo-fluvial processes in continental/near-shore settings.

4.2. Dissolved barium in the Chilika lagoon

4.2.1. Introduction

Barium (Ba) is a bio-intermediate element and an important tracer for several biogeochemical processes (export production, biological productivity, seawater alkalinity and water circulation), whose oceanic cycle is poorly constrained (Dymond et al., 1992; Francois et al., 1995; Paytan and Kastner, 1996; Gonneea and Paytan, 2006; Lea and Boyle, 1989; Bahr et al., 2013; Guay and Falkner, 1998, Cooper et al., 2008). This alkaline-earth metal actively participates in biological activities by marine bacteria and coastal plankton *via* either binding onto phosphate complexes or, by bio-accumulating onto extracellular organic matter/cytoplasm of living organisms (Carter et al., 2020). Seawater Ba mostly follows a nutrient-like distribution with relatively uniform concentrations (30-45 nmol/kg) in the near-surface water of the global ocean, excluding few regions with high riverine input or, oceanic upwelling (Hsieh and Henderson, 2017). Dissolved barium in oceans are mainly abundant in the finer fractions (<0.02 µm) than other colloidal phases (size ~0.02-0.45 µm; Joung and Shiller, 2014). In coastal systems, available studies on dissolved barium have documented its non-conservative behavior along the salinity gradient (Hanor and Chan, 1977; Edmond et al., 1978; Li and Chan, 1979; Carroll et al., 1993; Coffey et al., 1997; Moore, 1997; Joung and Shiller, 2014; Samanta and Dalai, 2016). This non-conservativeness is mainly linked to its removal *via* Fe-Mn hydroxides in low salinity zone (salinity ≤ ~2) and/or, its release in low to mid salinity region (salinity ~2 to 20) *via* desorptive release from sediments. In addition to cation-exchange processes, submarine groundwater discharge (Moore, 1997, Isaac et al., 2011), carbonate dissolution (Samanta and Dalai, 2016) and redox-dependent release from minerals (Charette and Shilkovitz, 2006; Joung and Shiller, 2014) can also supply barium to the coastal ocean. The barium removal/release fluxes are found to be variable in different coastal regimes depending on their hydrodynamics, sediment load and its type, and water composition.

In this study, spatial and seasonal distribution of dissolved barium in the Chilika lagoon (Asia's largest brackish-water lagoon) and its possible source waters (Bay of Bengal, river and groundwater) have been investigated to evaluate the sources and cycling of Ba in this coastal system. Additionally, particulate Ba concentrations in (bulk and clay fractions of) bed and suspended (in their bulk and exchangeable fractions) sediments have also been analyzed. These data have been used to assess the non-conservative processes and related mechanism in regulating coastal barium cycle.

4.2.2. Results

4.2.2.1. Ba in the source waters*:* Average Ba concentration for the western Bay of Bengal (BoB) samples (salinity ~ 32 ± 1) is 38 ± 7 nmol/kg (n = 15), which is consistent with that reported earlier for the BoB surface waters (Ba: 40 ± 3 nmol/kg for salinity of 33 ± 1; Singh et al., 2013) (Table A4). The average Ba content for the coastal Bay of Bengal is found to be 106 ± 30 nmol/kg (n = 9) for a salinity of 27 ± 1(Table A4). The Ba concentration of the riverine supply (the Mahanadi distributaries) to the Chilika during the pre-monsoon seasons (398 ± 161 nol/kg; n = 3) is found to be comparable or, marginally higher than that observed for the monsoon (287 ± 32 nmol/kg; n = 3) and post-monsoon (338 ± 91 nmol/kg; n = 3) seasons (Table A4). These seasonally-varying riverine Ba values are systematically higher than those reported for the Deccan basalt draining rivers (8-105 nmol/kg; Das et al., 2006), attributable to high Ba abundance of the source rock (charnockites and khondalites) for the Chilika basin (Tripathy et al., 2019). The mean Ba concentration for the groundwater samples from three seasons (784 ± 954 nmol/kg; n = 67) is about 2-3 times higher than riverine composition (Table A4). These groundwater Ba abundances are consistent with that reported earlier for the groundwater from the Hooghly estuary (782 ± 877 nmol/kg; n = 15; Samanta and Dalai, 2016).

4.2.2.2. Dissolved barium in lagoon water*:* Dissolved barium concentration varies spatially and seasonally along the salinity gradient of the Chilika Lagoon (Fig. 4.2.1; Table A1). The average barium concentration is found higher for the northern sector samples, as compared to that for the central and southern sectors (Fig. 4.2.1). The Ba concentrations for the monsoon vary from 72 to 921 nmol/kg, with a salinity-weighted Ba value of 642 nmol/kg. This average value is lower than that observed for the pre-monsoon (852 nmol/kg), but higher than that observed for the post-monsoon (345 nmol/kg) samples. Figure 4.2.2 depicts the covariation between salinity and Ba concentrations of the Chilika lagoon during different seasons. These samples from three seasons show a non-conservative behavior with most of the data either fall above (for higher salinity), or below (in the low salinity region) the theoretical river-seawater mixing line. The Ba release/removal trend is found to be distinctly different for different sectors. The Ba removal has been observed mostly for low saline region (salinity < 2) of the northern sector, which receives most of the freshwater supply to the lagoon. Further, the post-monsoon samples, mostly from the northern sector, show Ba removal upto a salinity of ~10. The Ba release is mostly restricted to the high salinity (>2) region of the lagoon.

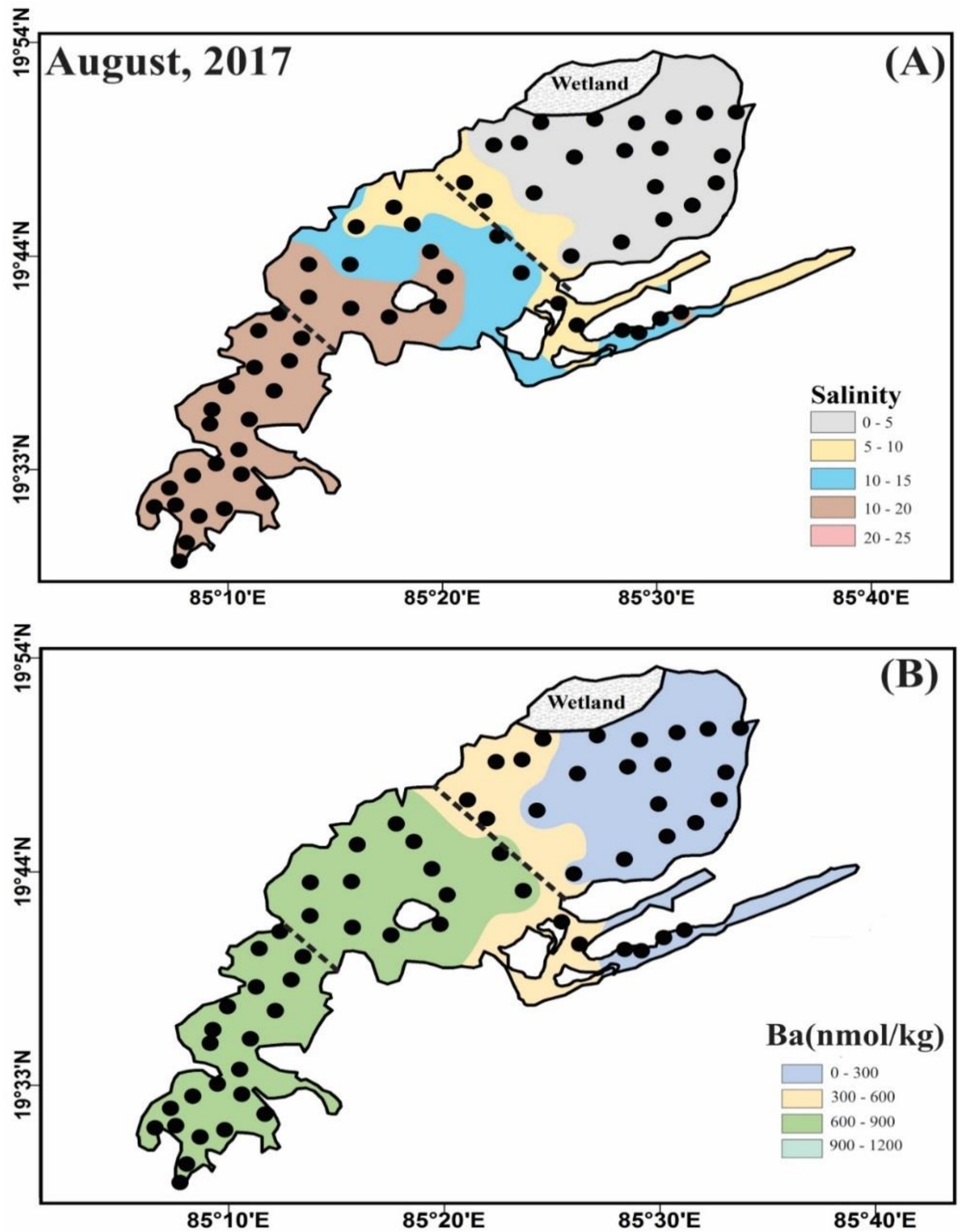

Figure 4.2.1. Spatial distribution of (A) water salinity and (B) dissolved barium concentrations of the Chilika lagoon during the monsoon seasons.

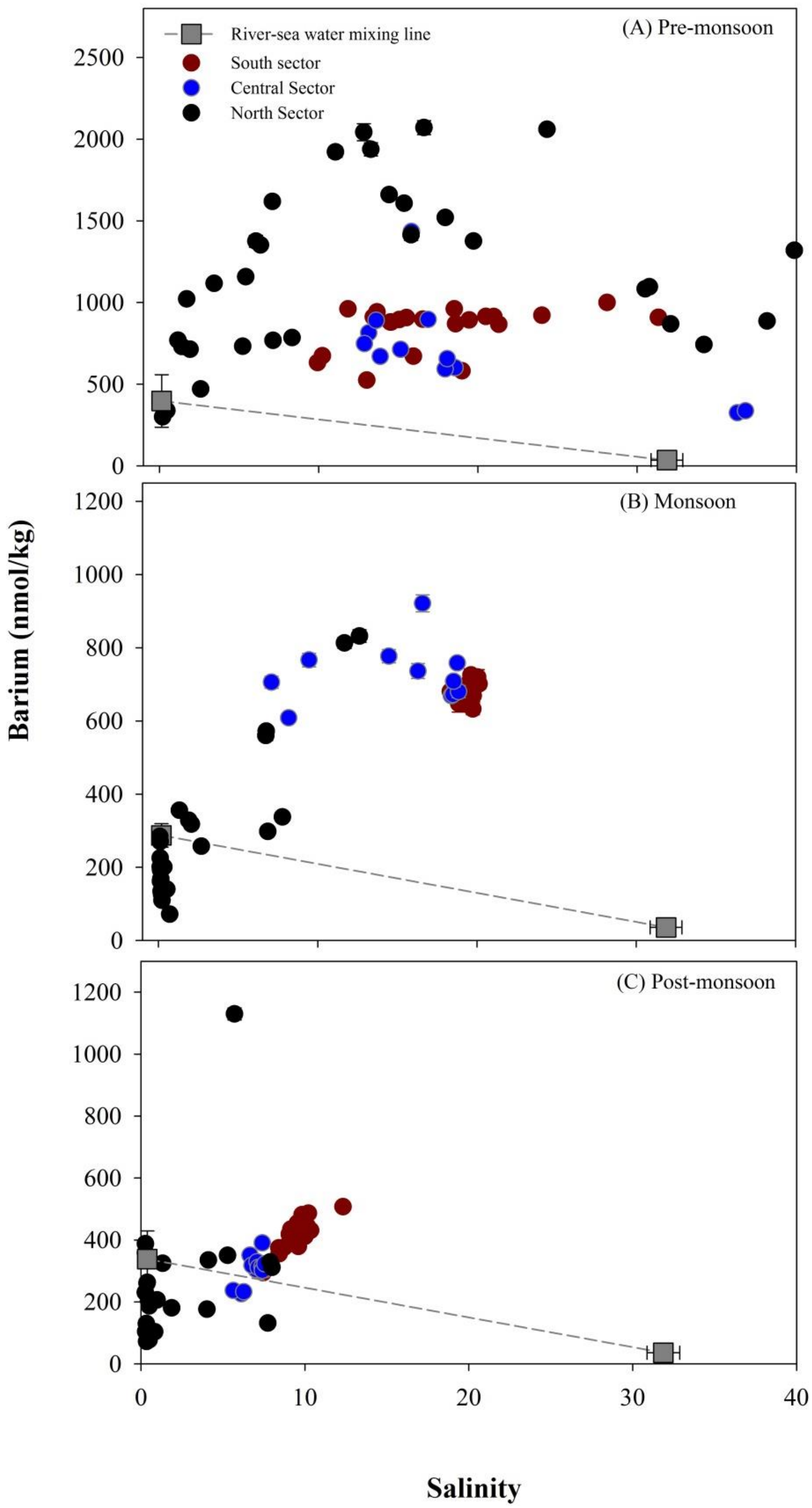

Figure 4.2.2. Co-variation between salinity and barium concentrations of the lagoon during (a) post monsoon (Jan), (b) pre-monsoon (May) and (c) monsoon (Aug) seasons. Most of the data either fall above, or below the theoretical mixing line, suggesting non-conservative behavior of Ba in the lagoon.

The northern sector samples show a peak of Ba release at a salinity of about 12 for pre-monsoon and monsoon seasons (Fig. 4.2.2). In contrast, the Ba release to the lagoon in the central and southern sectors although has been observed for high saline region, these data show increase in Ba concentration with salinity for all three seasons (Fig. 4.2.2).

4.2.2.3. Impact of (semi-diurnal and fortnight) tides on Ba composition*:* The Chilika lagoon, as mentioned earlier, get influenced by tidal cycles with periodicities at fortnight (12.4 days) and semi-diurnal (12 hrs) timescales. We compared the salinity-weighted Ba concentrations of the Chilika for two different sampling (spatial sampling with 3-4 week duration and one-day sampling with limited spatial-resolution) for monsoon and post-monsoon seasons to assess impact of fortnight tides on lagoon Ba composition (Table A1). During the monsoon, the salinity-weighted average Ba concentration for the lagoon was 642 nmol/kg for the spatial sampling, whereas that for the one-day sampling was found to be 702 nmol/kg (Table A1). For the post-monsoon seasons, the salinity weighted average content of Barium for the one day samples (288 nmol/kg) is 17 % lower than samples collected for the spatial sampling carried out over 3-4 weeks duration (345 nmol/kg). These observations suggested that the measured barium abundances may vary by about 10-15% due to fortnight tidal cycles. However, the seasonal trends of Ba distribution donot change significantly during both sampling trips and hence, the coastal behavior of Ba along the salinity gradient show minimal change.

Two-hourly sampling at the Chilika outflow (Satapada) for a period of one day shows limited variation in Ba distribution for monsoon (284 ± 25 nmol/kg; Fig. 4.2.3) and post-monsoon (602 ± 97 nmol/kg) (Table A3). In contrast, the pre-monsoon samples show a variation of ~50 % in the Ba concentration (209 ± 109 nmol/kg) within duration of 24 hrs. At southern sector (Barkul), the two-hourly variations were only 2-4% during the monsoon and pre-monsoon seasons. The Ba concentrations changes at Barkul, however, are significantly higher during the post-monsoon samples (579 ± 260 nmol/kg).

4.2.2.4. Sedimentary composition*:* The Ba concentrations of bed sediments from the Chilika vary between 247 and 611 μg/g with an average value of 373 ± 103 μg/g (n = 33). The average Ba value for the clay fraction of these sediments is found to be 261 ± 38 μg/g (n = 18). The average Ba values for bulk and clay fraction of Chilika sediments are about two times lower than that of river bed sediments (665 ± 64 μg/g) and the upper continental crust (~630 μg/g, Rudnick

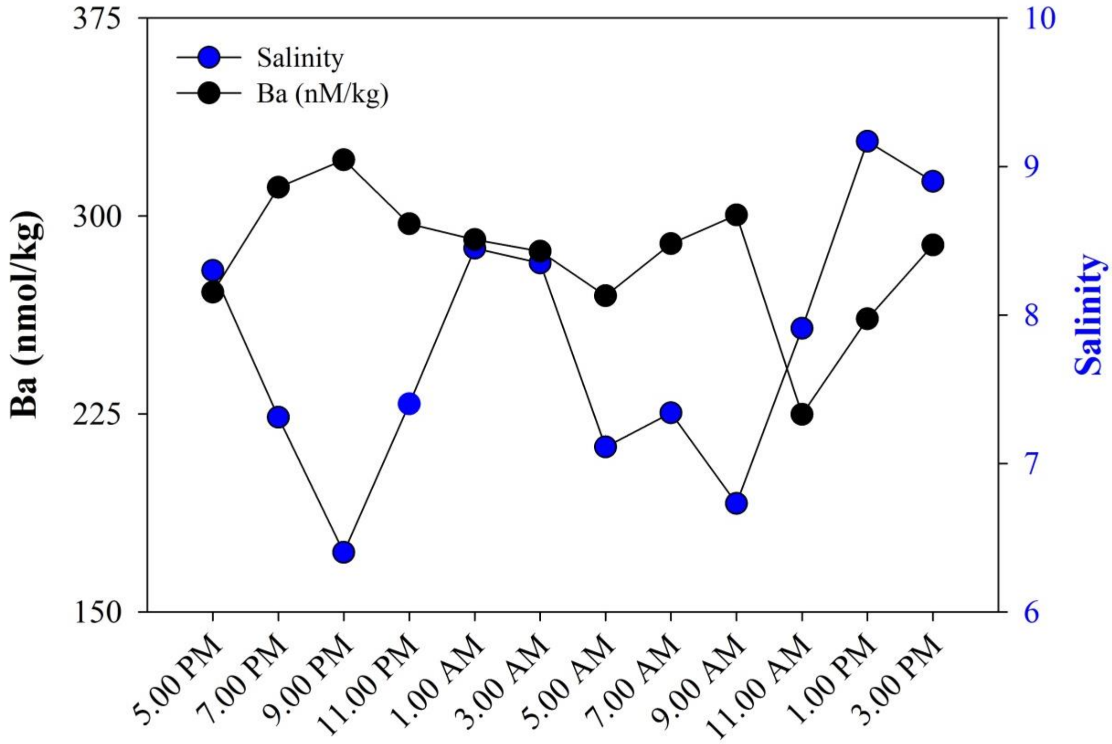

Figure 4.2.3. Two-hourly data for salinity and dissolved barium concentration at Satapada (outer channel) during the monsoon season. This observed variation in Ba and salinity points to fluctuation of Bay of Bengal water influx into the Chilika due to tidal cycle.

and Gao, 2003). The Ba concentrations of the bulk and exchangeable fraction of suspended sediments show that the elemental concentrations are significantly higher in the bulk fractions (245 ± 56 µg/g; n = 10) than the exchangeable fraction (38 ± 18 µg/g; n = 10) of sediments. We have computed the distribution coefficient (K_d^{Ba}) values using the dissolved and exchangeable Ba concentrations for the Chilika (Samanta and Dalai, 2016). These K_d^{Ba} values range from 409 to 2567, with an average value of 1699 ± 955 mL/g (n = 10). This average K_d^{Ba} value is higher than that observed for the Hooghly estuary (945 ± 1000 mL/g; Samanta and Dalai, 2016).

Average aluminium content of the Chilika samples is 12 ± 4 wt. % (n = 33), whereas river bed sediments is 6.1 ± 0.7 wt. % (n = 4). The Mg and Fe content in the Chilika samples vary from 0.2 to 2.6 wt.% and 1.5 to 9.4 wt. %, respectively, and their average value of river bed sediments (n = 4) is 0.3 ± 0.1 wt. % for Mg and 4 ± 3 wt. % for Fe. Al content of the clay fractions (n = 18) is varies from 7.9 to 13.8 wt. % with Mg and Fe content from 1.2 to 1.9 wt. % and 4.6 to 7.5 wt. %, respectively. Average content of Al, Fe and Mg for suspended sediments (n = 10) are 14 ± 0.5 wt. %, 6.8 ± 0.4 wt. % and 1.6 ± 0.2 wt. %, respectively. The exchangeable fractions of suspended sediments (n = 10) has Al, Fe and Mg content of 13 ± 10 μg/g, 26 ± 21 μg/g and 3604 ± 1622 μg/g, respectively. The average Mn content of the suspended sediments and their exchangeable fractions are 2072 ± 916 μg/g and 140 ± 86 μg/g, respectively.

4.2.3. Discussion

Non-conservative behavior of dissolved barium for the Chilika lagoon has been observed during three different seasons (Fig. 4.2.2). This observation is consistent with earlier studies in the Hudson (Li and Chan, 1979), Amazon (Boyle, 1976), Zaire (Edmond et al., 1978), Ganga-Brahmaputra (Moore, 1997), and Hooghly (Samanta and Dalai, 2016) estuaries. Similar to the Chilika, available studies also show both Ba removal in low saline regions and its release in high-saline regions. Although the coastal behavior for different estuaries is similar, the intensity and location (in terms of salinity) are different for these coastal regions. We have estimated the barium gain/loss in the Chilika lagoon from the deviation of Ba data for given salinity from the theoretical river-seawater mixing line. The Ba removal from the Chilika, which is mostly restricted to low-saline regions, varies between 4 and 211 nmol/kg during the monsoon season. The average Ba removal (-112 ± 60 nmol/kg; 30) during the monsoon values account for ~40 % of Ba loss compared to the expected "conservative" concentrations. The salinity-weighted Ba removal from the Chilika for the monsoon (~102 nmol/kg), pre-monsoon (~68 nmol/kg) and post-monsoon (~65 nmol/kg) seasons shows limited seasonal variations. The estimated Ba gain for the pre-monsoon samples range from 101 to 1938 nmol/kg with an average value of 773 ± 428 nmol/kg (n = 59), which account for ~405 % of Ba gain when compared to expected Ba value for conservative mixing (Fig. 4.2.4). The excess Ba for the monsoon (477 ± 275 nmol/kg; n = 58) and post-monsoon (155 ± 161 nmol/kg; n = 48) samples account for ~329 % and 75 % gain in barium, respectively. The salinity-weighted excess barium for the pre-monsoon (~768 nmol/kg), which is higher than that reported for the Hooghly estuary during pre-monsoon season (~436 nmol/kg; Samanta and Dalai, 2016). The salinity-weighted excess barium for the monsoon (~541 nmol/kg) and post-monsoon (~163 nmol/kg) samples are lower compared to the pre-monsoon season, indicated seasonal variation in Ba supply to the Chilika.

The observed barium removal in the low-saline regions of the Chilika lagoon is consistent with few earlier reported studies from estuaries (Coffey et al., 1997; Samanta and Dalai 2016).

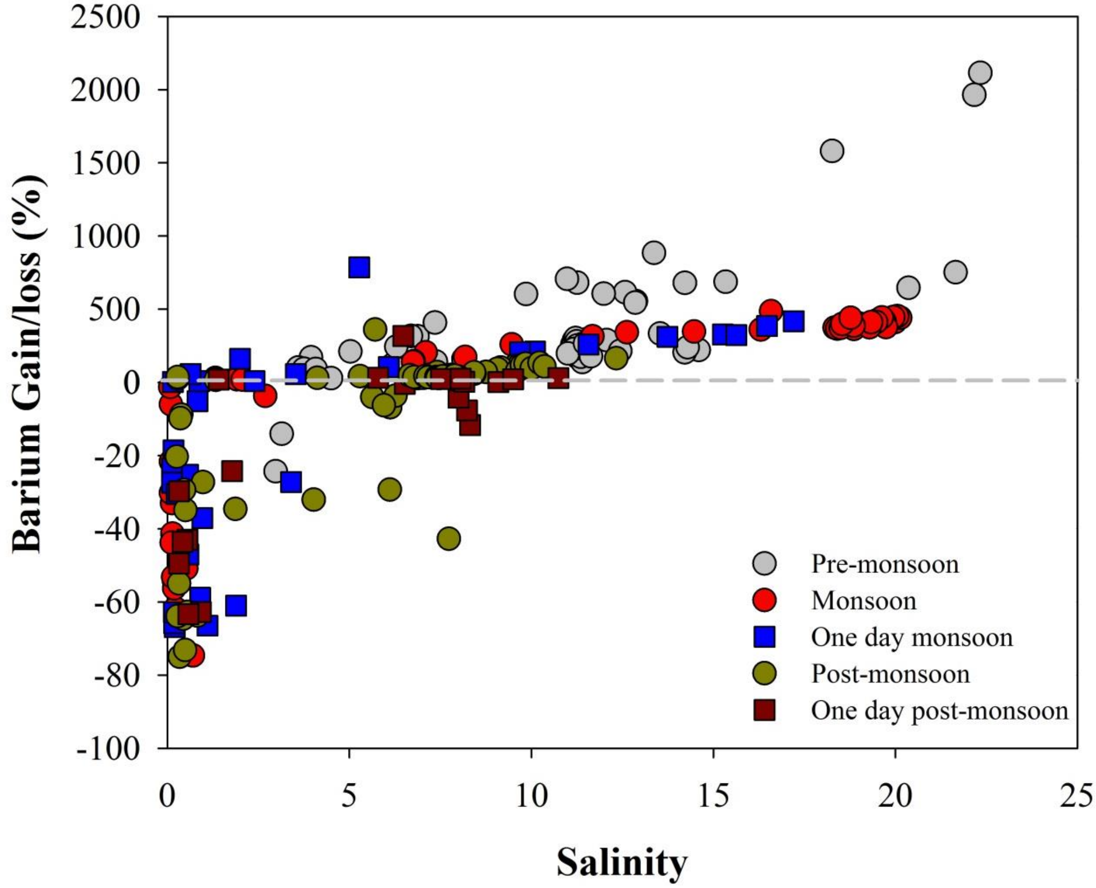

Figure 4.2.4. Estimated gain/loss of dissolved barium from the Chilika lagoon during different seasons.

These studies have attributed coastal barium removal to the variations of water pH and ionic strength, adsorption/co-prcipitation onto Fe-Mn oxyhydroxides (Falkner et al., 1993; Coffey et al., 1997; Ingri and Widerlund, 1994), the flocculation of organic colloids (Pokrovsky and Schott, 2002) and biological uptakes (Guay and Falkner, 1998; Nozaki et al., 2001; Stecher and Kogut, 1999). The barium removal is mainly restricted in the north sector during monsoon season and post-monsoon season. The observed pH in this region varies from the 6.96 to 9.14 with weak relationship (r = -0.36; n = 30) with the estimated amount of Ba removal during monsoon. Further, the Ba removal show no discernable correlation (r = -0.1; n = 30) with the dissolved oxygen, pointing to minimal role of biological productivity in barium scavenging. The Fe-Mn hydroxide may serve as a potential substrate for Ba removal from the low-saline regions. This proposition is consistent with significant correlation between Fe and K_d^{Ba}(r = 0.40; n = 10) for the Chilika suspended sediments, pointing to enhanced Ba adsorption with increase in sedimentary Fe concentrations. However, inverse correlation between Mn and K_d^{Ba} (r = -0.58; n =10) challenges the dominancy of Ba adsorption onto the Fe-Mn hydroxides. Further, scavenging of barium from the Chilika onto clay particles are less likely as evidence from lower Ba concentrations of clay fractions compared to the bulk sediments. These observations suggest that the Ba removal in the Chilika is less associated with Fe-Mn oxides/clay particles, which is in contrast with earlier studies. Sedimentary organic matter is likely to play an important role in barium removal from this biologically-active lagoon system. This possibility, however, could not be evaluated due to lack of organic carbon data for suspended sediments to assess its correlation with exchangeable Ba fraction.

In addition to low-salinity Ba removal, the salinity-barium covariation plot also shows additional barium supply to the high-salinity region of the lagoon. The major sources which may supply dissolved barium, in addition to river and seawater, to the Chilika are desorption of Ba from the suspended sediments (Hanor and Chan, 1977; Li and Chan, 1979; Li et al., 1984; Carroll et al., 1993; Coffey et al., 1997; Samanta and Dalai, 2016) and submarine groundwater discharge (Moore et al., 1997; Gonneea et al., 2013). Further, carbonate dissolution and anthropogenic contribution may also contribute to the excess barium in the Chilika lagoon. However, previous investigations in nearby estuary (Hooghly) have shown minimal supply of barium from these sources to coastal system (Samanta and Dalai, 2016). The low $CaCO_3$ concentration (< 0.1 %) of Chilika sediments also rule out the possibility of carbonate dissolution in supplying Ba to the dissolved phases. Cation-exchange processes involving clay particles have been suggested to be one of the primary pathways for desorptive release of Ba to coastal systems (Hanor and Chan, 1977; Li and Chan, 1979; Li et al., 1984; Carroll et al., 1993; Coffey et al., 1997; Samanta and Dalai, 2016). In case of the Chilika, the Ba concentrations of the clay fractions (261 ± 38 μg/g) of bed sediments are found to be significantly lower than that observed for bulk sediments (373 ± 103 μg/g) and river sediments (665 ± 64 μg/g), supporting Ba release from clay particles. This proposition also draws support from significant correlation between clay abundance and Ba/Al ratios (Fig. 4.2.5A), pointing to steady decline in Ba content due to ionic exchange/release of Ba with major cations (such as, Mg) from the clay structure. The strong correlation between Ba/Al and Mg/Al ratios points to involvement of Mg-rich clay particles (e.g. montmorillonite) in this process (Fig. 4.2.5B). Earlier studies have shown that the clay particles present in the Chilika are mostly montmorillonite (~9 %), Kaolinite and chlorite together (~45%) (Barik et al., 2020). It is worth mentioning here that the montmorillonite, which

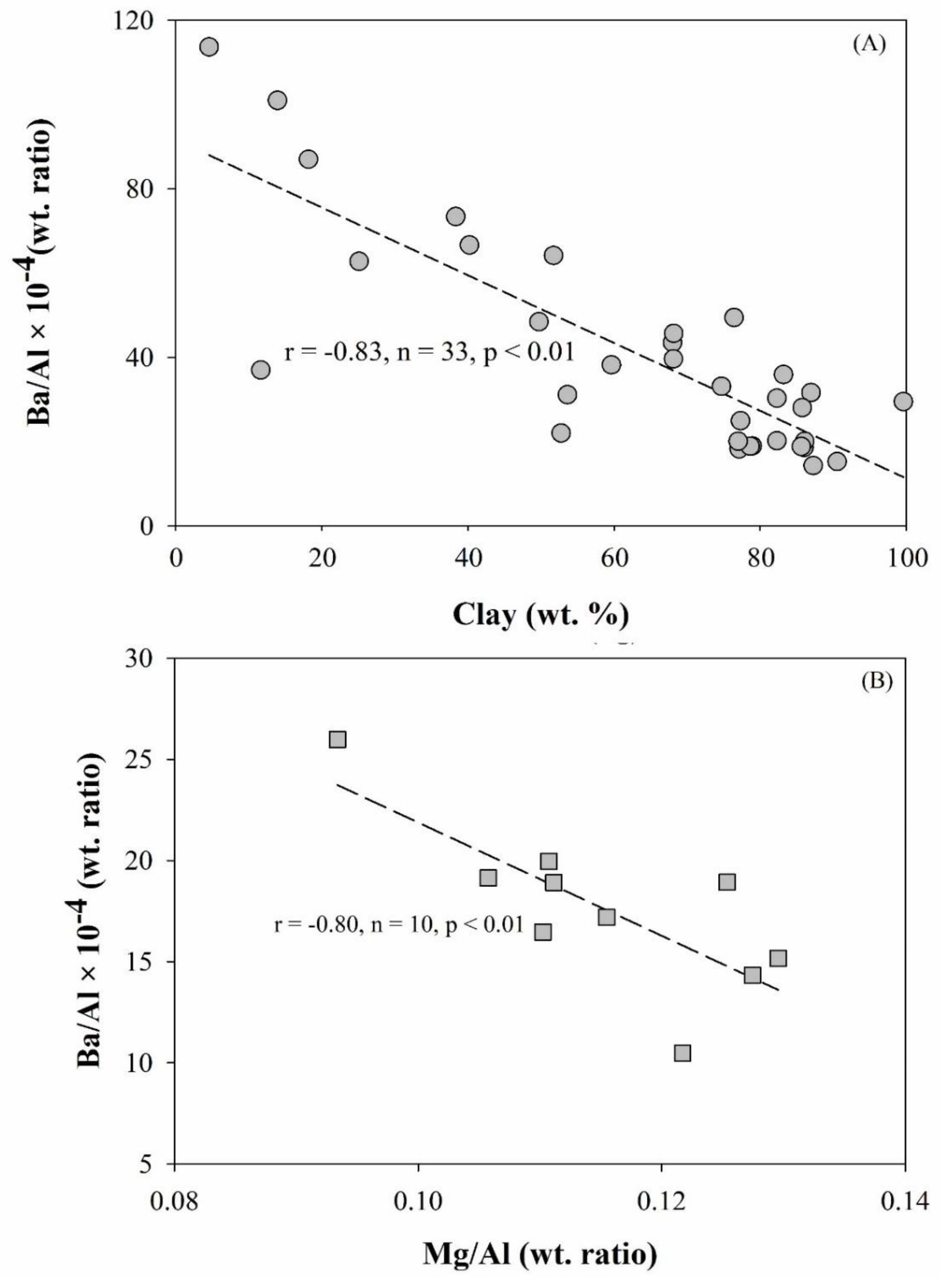

Figure 4.2.5. Plot shows the strong negative and positive correlation between sedimentary barium and clay abundances (A), suggesting the involvement of clay fraction in ion exchange process. Plot B, between Ba/Al and Mg/Al ratio of suspended sediments, indicating that the adsorption of Mg in response to the desorption of Ba.

is the abundant clay mineral in the Chilika, is characterize with high cation-exchange capacities (80-150 meq/100g; Drever, 1997) and hence, likely to promote cation-exchange process for releasing Ba to the Chilika. Additional to the desorption, SGD may also play a sub-ordinate role in supplying Ba to the lagoon. To assess this proposition, we have estimated the SGD-derived Ba flux for the Chilika. In absence of seasonal SGD estimation, the SGD fluxes to the lagoon of the pre-monsoon season have been used for all season. The average Ba concentrations for the groundwater samples during the pre-monsoon (salinity~1.3 ± 1.7; n = 21), monsoon (salinity~0.9 ± 1.0; n = 24) and post-monsoon (salinity~1.3 ± 1.4; n = 21) are 1113 ± 1438, 620 ± 591, and 662 ± 604 respectively. These data show that the SGD-driven Ba flux for the monsoon (930 mol/d) is <1% of the riverine Ba flux (~4.8×10^4 mol/d). This SGD fluxes for pre-monsoon (~1.7×10^3 mol/d), however, is found to be comparable to that from the riverine flux during this season (~1.4×10^3 mol/d). These flux comparison indicates that the SGD supply of Ba is negligible for peak-flow (monsoon) stages, but may be significant for the Chilika lagoon during the lean-flow stages.

Figure 4.2.6 depicts the barium budget of the Chilika lagoon for the monsoon season. The average salinity for the lagoon is 12 ± 8 with a salinity-weighted average Ba value of ~642 nmol/kg. Considering water volume of the Chilika (2.06×10^{12} L), the total inventory of the Ba is found to be 1.3×10^6 moles. This Ba inventory is regulated by several sources (river, Bay of Bengal, tide, desorption) and sinks (adsorption and ebb phases). Average composition for these sources and the salinity-weighted Ba gain for high-saline samples and Ba loss for low-saline (salinity ~0-2) are shown in the figure 4.2.6. The representative Ba value for the tide and ebb phases are constrained based on semi-diurnal dataset for high and low saline samples respectively (Fig. 4.2.3). Additionally, efforts were also made to estimate the desorbable barium for the samples of monsoon season. Towards this, the desorbable barium content was calculated from the difference of Ba concentrations of suspended sediments and their exchangeable fractions. This approach yields a desorbable-Ba concentration of 497 nmol/kg for the monsoon season. This value is marginally lower than with effective riverine "end-member" value (~779 nmol/kg) estimated from the salinity-Ba linear trend for high-saline samples (salinity ~10-20). We have used average of these two estimates (638 nmol/kg) as a representative desorbable-Ba value for the Chilika. Using the riverine water flux for the monsoon (167×10^6 m^3/day), the Ba

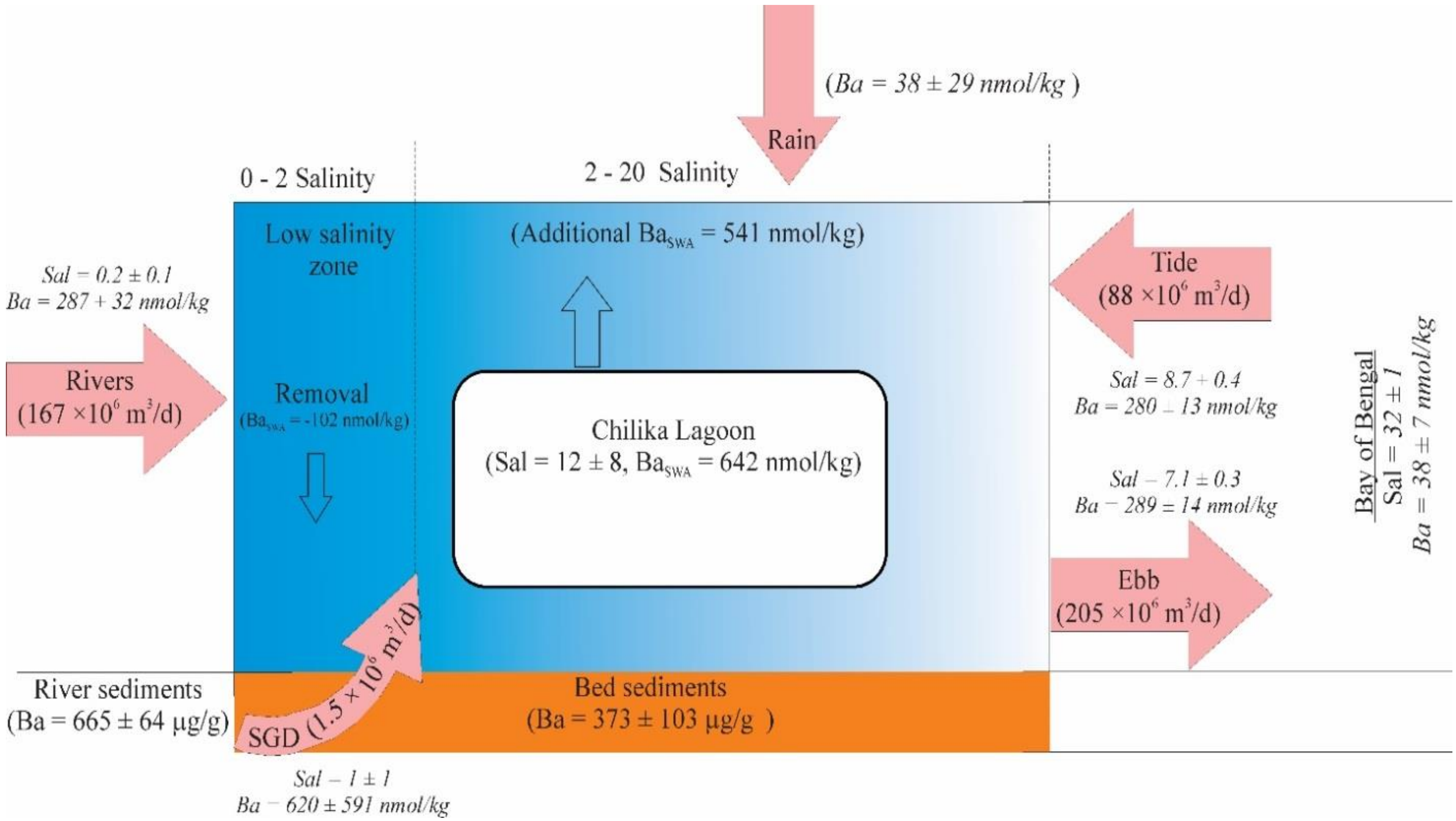

Figure 4.2.6. Barium budget of the Chilika lagoon with its major sources and internal cycling pathways.

fluxes from the riverine input (~4.8×10^4 mol/d) are found about 2 times lower than that supplied through desorption (~10.6×10^4 mol/d). The annual desorptive-Ba supply to the Bay of Bengal from the Chilika is close (~3.9×10^7 mol/year) to that supplied by Hooghly estuary (~4.3×10^7 mol/year). As the riverine water flux to the Chilika is only 0.6 % compared to that of the Hooghly, the desorptive release of barium in this coastal lagoon is found disproportionally higher. This high-Ba supply in this shallow lagoon system is attributable to high sediment suspension activity due to rigorous tidal forcing and efficient water exchange between its water sources.

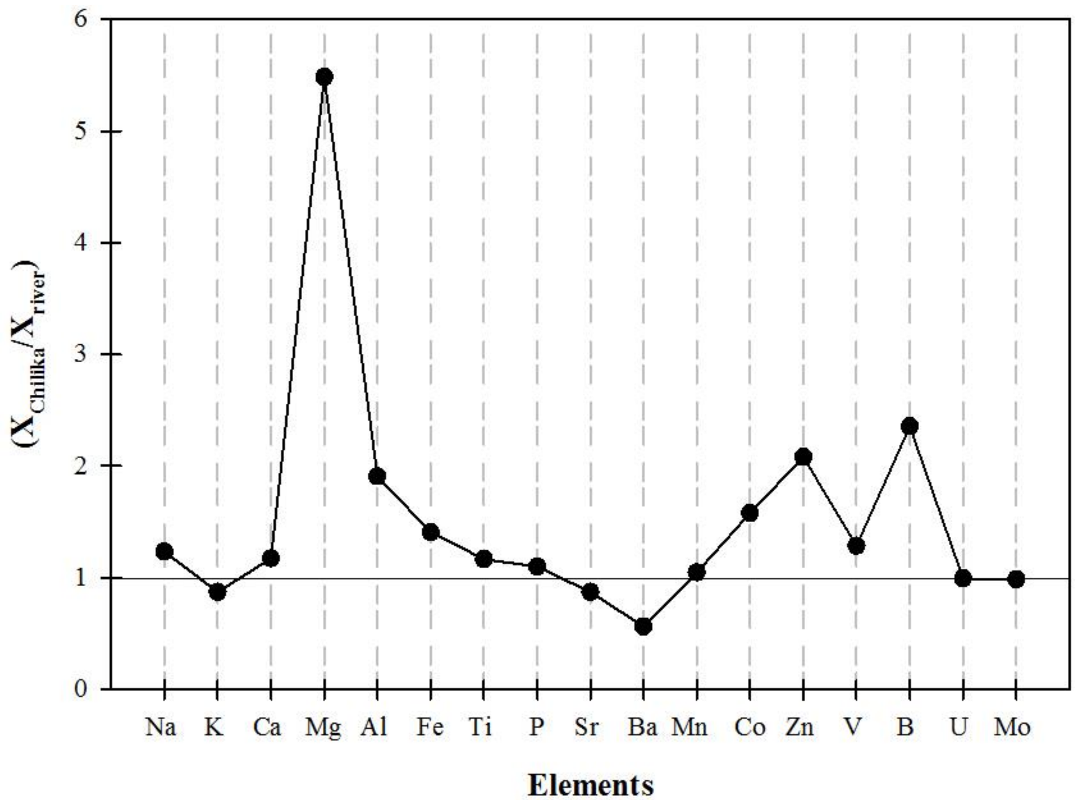

Figure 4.3.1: Distribution of enrichment factors (X_{sample}/X_{river}) for different elements for the Chilika sediments. High enrichment factor for Mg points to possible removal of dissolved Mg from the lagoon.

4.3. Evidence of ion-exchange process from sediment chemistry data

Depletion/enrichment of elements in the Chilika bed sediment (Table A5) relative to that in rivers can provide clues for additional elemental release/removal through ion-exchange process. For this, we computed the enrichment factors (Xsample/Xriver)), for selected elements and their average values are shown in Fig. 4.3.1. This data comparison show that most of the major and trace metals are close to unity. In exception, the sedimentary Mg is found to be very high. Considering substitution of Mg during ion-exchange processes, these Mg anomalies hint at significant removal of dissolved Mg onto the particulate phases. This indicates that ion-exchange Mg sink for coastal system. This can be best assessed further by investigating dissolved Mg distribution along the salinity gradient, which may show depleted Mg trends with respect to mixing line.

4.4. Conclusion

Detailed spatial and seasonal distributions of dissolved boron and barium have been investigated to assess the role of coastal processes (particularly, ion-exchange processes) in regulating their distribution. Co-variations between boron and salinity of the Chilika waters during monsoon and post-monsoon seasons confirm its conservative mixing. In contrast, the pre-monsoon samples exhibit non-conservative behavior of boron with its significant removal in the low-saline regime (with salinity < 15). This boron removal is attributed to its adsorption onto particulate phases (clay and/or oxyhydroxides). High water residence time during pre-monsoon season is expected to increase the particulate-water interaction time, which in turn regulate the intensity of adsorptive boron removal from the Chilika. In contrast to boron, dissolved barium shows non-conservative release with a mid-salinity peak during all the seasons. This Ba addition attributable to its desorption from clay minerals through cationic (Mg) replacement. This Ba production through ion-exchange processes is significantly higher than the riverine supply of Ba to the lagoon. Outcomes of this research work, therefore, highlight the dominance of ion-exchange process in controlling the coastal inventory of these two bio-essential elements and their ultimate flux to the open ocean.

Chapter 5

Distribution of Re concentrations and $\delta^{13}C$ in the Chilika lagoon: Role of biological processes in regulating water chemistry

This chapter discusses the coastal behavior of rhenium and $\delta^{13}C$ in dissolved inorganic and sedimentary organic carbon phases in the Chilika lagoon. These data have been used to assess impact of biological activities in regulating elemental and isotopic compositions at the freshwater-seawater interfaces. Earlier studies have established strong association of rhenium with organic carbon in organic-rich sediments and have been linked to Re scavenging in regions (reducing conditions) with high productivity. This geochemical property of rhenium makes it a reliable proxy for past oceanic conditions. However, there have been limited efforts to understand the incorpotation of Re via biological uptake. In this study, we aim to investigate the spatial and seasonal distribution of rhenium along the salinity gradient of the Chilika to assess the impact of biological activities, if any, to regulate Re inventory in coastal regions. Furthermore, we have also investigated the dissolved inorganic and sedimentary organic carbon isotopes to understand the regional carbon cycle in this biogeochemically active lagoon system.

5.1. Dissolved Re in the Chilika lagoon system

5.1.1. Introduction

Rhenium (Re) serves as a reliable proxy for past oceanic redox state and terrestrial organic carbon cycling (Crusius et al., 1996; Dalai et al., 2002; Morford et al., 2005; Kendall et al., 2009; Planavsky et al., 2018). Its radioactive and stable isotopes have also found frequent applications in constraining depositional age and environment of organic-rich marine sedimentary rocks (Ravizza and Turekian, 1989; Kendall et al., 2009; Miller et al., 2015; Tripathy et al., 2018). These applications are mainly motivated by redox-sensitive nature of rhenium and its strong association with organic matter and sulphides (Yamashita et al., 2007; Sheen et al., 2018). In modern-day ocean, the Re concentration behave conservatively in open ocean and is mostly homogenous (~40 pmol/g) globally (Anbar et al., 1992; Colodner et al., 1993; Goswami et al., 2012). It forms stable perrhenate (ReO_4^-) ions in oxygenated water and gets scavenged in reducing conditions to underlying sediments through abiotic redox reactions (Colodner et al., 1993; Yamashita et al., 2007). The supply of rhenium to the ocean is dominated by riverine fluxes with insignificant supply from hydrothermal sources (Sheen et al., 2018). The discharge-weighted (pre-anthropogenic) rhenium concentration of rivers is 11.2 pmol/kg, which accounts for an annual flux of about 4.29×10^5 mol/yr to the oceans (Miller et al., 2011). The major sink of seawater rhenium is sub-oxic sediments which scavenges about 3.75×10^5 mol of Re annually. In addition, the anoxic (2.80×10^4 mol/yr) and oxic (2.61×10^4 mol/yr) sediments also serve as minor marine Re sinks (Sheen et al., 2018 and references therein). The residence time of rhenium in oceans is about 1.3×10^5 yr (Miller et al., 2011), which is higher compared to the ocean mixing time (~1.5×10^3 yr; Broecker and Peng, 1982). Although the oceanic budget of rhenium is well-constrained, there have been only a few studies on coastal behavior of Re and related chemical changes (Colodner et al., 1993; Rahaman and Singh, 2010; Sproson et al., 2018).

The coastal regimes, owing to its complex physical, chemical and biological processes, can influence the elemental abundances and hence, the ultimate delivery of elements from land to the ocean (Samanta and Dalai, 2016; Danish et al., 2019). Available a few studies on Re in estuaries show both conservative and non-conservative nature, and the exact cause for this difference is not clear. Rahaman and Singh (2010) have reported a conservative behavior of rhenium in selected estuaries from India (Ganga and Mandovi), which is consistent with earlier reported trends for the Amazon estuary (Colodner et al., 1993). In contrast, the samples from Amazon estuaries also hint at desorptive release of Re in the low-saline regime (Colodner et al., 1993). Similar to this, additional supply of Re have also been observed for the Hudson river (Walker and Peucker-Ehrenbrink, 2004), pointing to non-conservative behavior of Re. In addition to the natural sources, impact of anthropogenic fluxes on the Re abundances have also been observed for two estuarine systems (Narmada and Tapi) from the western part of India (Rahaman and Singh, 2010). Further, recent studies have documented uptake of dissolved rhenium onto coastal macroalgae (Yang, 1991; Rooney et al., 2016; Racionero-Gomez et al., 2017; Sproson et al., 2018, 2020). Removal of dissolved rhenium from aquatic systems via its adsorption on to clay surfaces have also been reported (Olafsson and Riley, 1972; Wakoff and Nagy, 2004; Tanaka et al., 2019). These studies, therefore, point to diverging mixing trends of rhenium in coastal regions. In particular, impact of biological uptake and ion-exchange processes on coastal biogeochemistry of rhenium have received limited attention.

The present study investigates spatial and seasonal changes in dissolved Re concentrations along the salinity gradient of the Chilika lagoon (Asia’s largest brackish-water lagoon), India, and its possible source waters. Additionally, rhenium concentrations in macrophytes and bed sediments, in their bulk, clay and exchangeable fractions, of the Chilika have also been analysed.

These data were employed to constrain sources and behavior of Re in coastal oceans. Outcomes of this study, in contrast to existing literature, show non-conservative removal of dissolved rhenium in this coastal regime. Intensity of these removals and its significance in oceanic rhenium cycle have been assessed.

5.1.2. Results

Water salinity and dissolved rhenium concentrations data for the Chilika lagoon samples and source waters are summarized in Table 5.1.1. The Re concentration data for Chilika water, its source waters, coastal macrophytes and bed sediments (in their bulk, clay and exchangeable fractions) are provided in the annexure (Table A2 – A4, and Table A6).

5.1.2.1. Source water compositions

Salinities of the fresh water samples from the Mahanadi distributaries vary between 0.12 and 0.26 with a mean value of 0.2 ± 0.1 (n = 6). The Re concentrations of these samples vary from 3.5 to 6.5 pmol/kg (average: 5 ± 1 pmol/kg; n = 6), which is consistent with those reported earlier for the Indian rivers (Dalai et al., 2002; Rahaman et al., 2012), but lower than the global (pre-anthropogenic) riverine Re value (11.2 pmol/kg; Miller et al., 2011). The riverine samples show a seasonal trend with relatively lower Re values during the monsoon (4.0 ± 0.6 pmol/kg; n = 3) than the pre-monsoon (6.1 ± 0.4 pmol/kg; n = 3) seasons. The salinities of the groundwater samples vary from 0.19 to 3.02, with their corresponding Re contents varying between 0.28 and 38 pmol/kg (mean: 12 ± 14 pmol/kg; n = 11). We have analysed five coastal Bay of Bengal (BoB) and six western BoB samples to constrain the seawater end-member value (Table 5.1.1 and A4). The average Re concentration of the coastal samples (salinity: 26.4 to 27.2) is 31 ± 1 pmol/kg (n = 5), which corresponds to 41 pmol/kg when normalized to open ocean salinity (~35). The Re concentrations of the western BoB samples (salinity: 31.8 ± 0.4) vary between 38 and 41 pmol/kg, with an average value of 40 ± 1 pmol/kg (n = 6). This average value when normalized to 35 salinity corresponds to 43.5 pmol/kg, which is marginally higher than the oceanic Re value (~40 pmol/kg). This higher Re abundance is consistent with that reported earlier for the western BoB, and has been attributed to influence of the Godavari river which is characterized with significantly high Re content (Singh et al., 2011).

5.1.2.2. Spatial and seasonal distributions of Re in the Chilika

The salinities of the Chilika lagoon show significant spatial variations during pre-monsoon (0.2-19.7; n = 17), monsoon (0.1-20.1; n = 34) and post-monsoon (0.3-7.7; n = 10) seasons (Table 5.1.1). Consistently, the spatial distributions of rhenium concentrations also show

Table 5.1.1. Average and range of rhenium and salinity data for the Chilika lagoon samples collected during monsoon, pre-monsoon and post-monsoon seasons. This table also includes average and range data of possible sources (river, groundwater and Bay of Bengal).

		Counts	Salinity	Re (pmol/kg)
Chilika (Spatial Sampling)				
Pre-monsoon (Apr.-May, 2017)	*Range*	17	0.2 - 19.7	6.1 - 20.9
	Average		11 ± 6	14 ± 4
Monsoon (Jul.-Aug., 2017)	*Range*	17	0.1 - 20.1	3.8 - 20.0
	Average		8 ± 7	10 ± 5
Monsoon (16^{th} Aug. 2017)	*Range*	17	0.1 - 17.2	2.1 - 16.6
	Average		7 ± 6	8 ± 4
Post-monsoon (Jan., 2018)	*Range*	10	0.3 - 7.7	2.5 - 8.4
	Average		4 ± 3	5 ± 2
Possible major sources				
River (Pre-monsoon)	Range	3	0.12 - 0.16	5.7 - 6.5
	Average		0.14 ± 0.02	6 ± 0.4
River (monsoon)	Range	3	0.12 - 0.26	3.5 - 4.6
	Average		0.18 ± 0.07	4 ± 1
Groundwater (Pre-monsoon)	Range	5	0.19 – 2.06	0.2 - 38.0
	Average		1 ± 0.7	13 ± 16
Groundwater (Monsoon)	Range	6	0.27 – 3.02	0.3 - 35.0
	Average		1 ± 1	12 ± 13
Seawater (Coastal Bay of Bengal)	Range	5	26.4 - 27.2	30.4 - 33.0
	Average		26.7 ± 0.3	31.4 ± 1.0
Seawater (Western Bay of Bengal)	Range	6	31.2 - 32.3	38.5 - 41.4
	Average		31.8 ± 0.4	39.6 ± 1.2

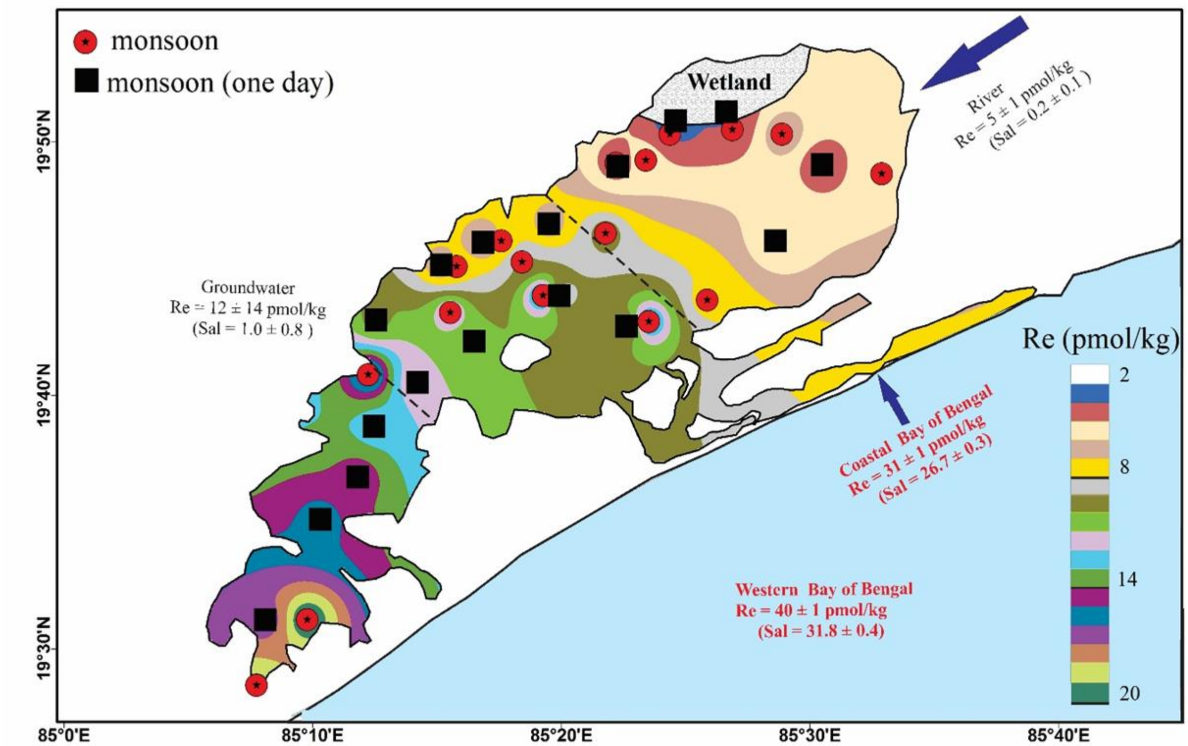

Figure 5.1.1. Spatial distribution of dissolved Re concentrations of the Chilika lagoon during the monsoon season. Representative compositions for major sources (river, groundwater and Bay of Bengal) are also shown.

wide variations (Fig. 5.1.1). The Re concentrations during the monsoon seasons vary from 2.1 to 20.0 pmol/kg (n = 34). The salinity-weighted Re concentrations for the pre-monsoon (15.5 pmol/kg), monsoon (14.1 pmol/kg) and post-monsoon (6.4 pmol/kg) seasons are found to be intermediate to average river (5 ± 1 pmol/kg), sea (40 ± 1 pmol/kg) and groundwater (12 ± 14 pmol/kg) concentrations. This spatial Re trend shows systematically lower concentrations in the northern sector (which receives most of the freshwater) when compared to that in the other sectors (Fig. 5.1.1). Additional to seasonal and spatial distributions, the dissolved rhenium at the Chilika mouth (Satapada) also shows significant variation (9.5-11.6 pmol/kg; n = 12) within 24 hours due to semi-diurnal tidal effects (Fig. 5.1.2). The salinity for these samples vary between 6.4 and 9.2, with the highest value representing seawater incursion during the tide period (Fig. 5.1.2). Although the broad changes in salinity and Re are similar, the relative changes in salinity (~11 %) during 1-day duration were marginally higher than that of the Re variations (~7 %; Table A2).

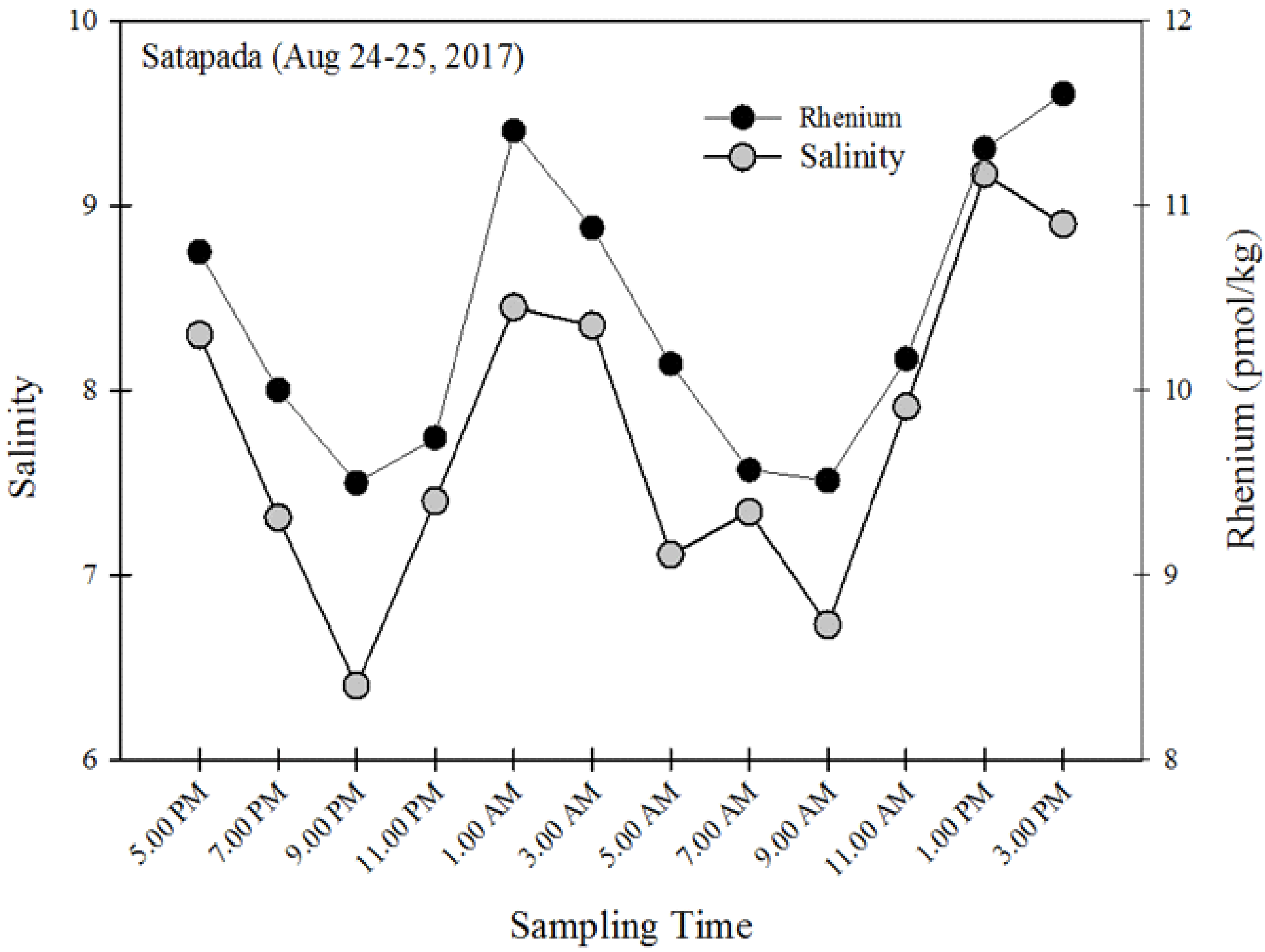

Figure 5.1.2. Two-hourly variations in salinity and Re concentrations show impact of seawater exchange with the lagoon during semi-diurnal tidal cycles.

Figure 5.1.3 depicts the salinity-Re plot for the Chilika water samples and their possible sources. The major water sources to the Chilika lagoon, as mentioned earlier, are river (Mahanadi distributaries), western BoB and groundwater. We have constrained the end-member (salinity and Re) compositions based on measured datasets for these sources [river (0.2 ± 0.1; 5 ± 1 pmol/kg), western BoB (31.8 ± 0.4; 40 ± 1 pmol/kg) and groundwater (1.0 ± 0.8; 12 ± 14 pmol/kg)] (Fig. 5.1.1). The salinity-Re data for the Chilika lagoon show deviation from its expected conservative (river-sea water) mixing line (Fig. 5.1.3). The lagoon samples from the three different seasons mostly fall below the linear trend, confirming non-conservative behavior of Re in this coastal lagoon. In addition to Re removal, the pre-monsoon samples with lower salinities (<10) fall above the conservative mixing trend (Fig. 5.1.1), indicating additional supply of rhenium during lean flow stages.

5.1.2.3. Sedimentary Re variations in the Chilika System

Distribution of particulate rhenium concentrations in bulk, clay and exchangeable fractions of sediments show large variations (Fig. 5.1.4). The Re concentrations of the bulk

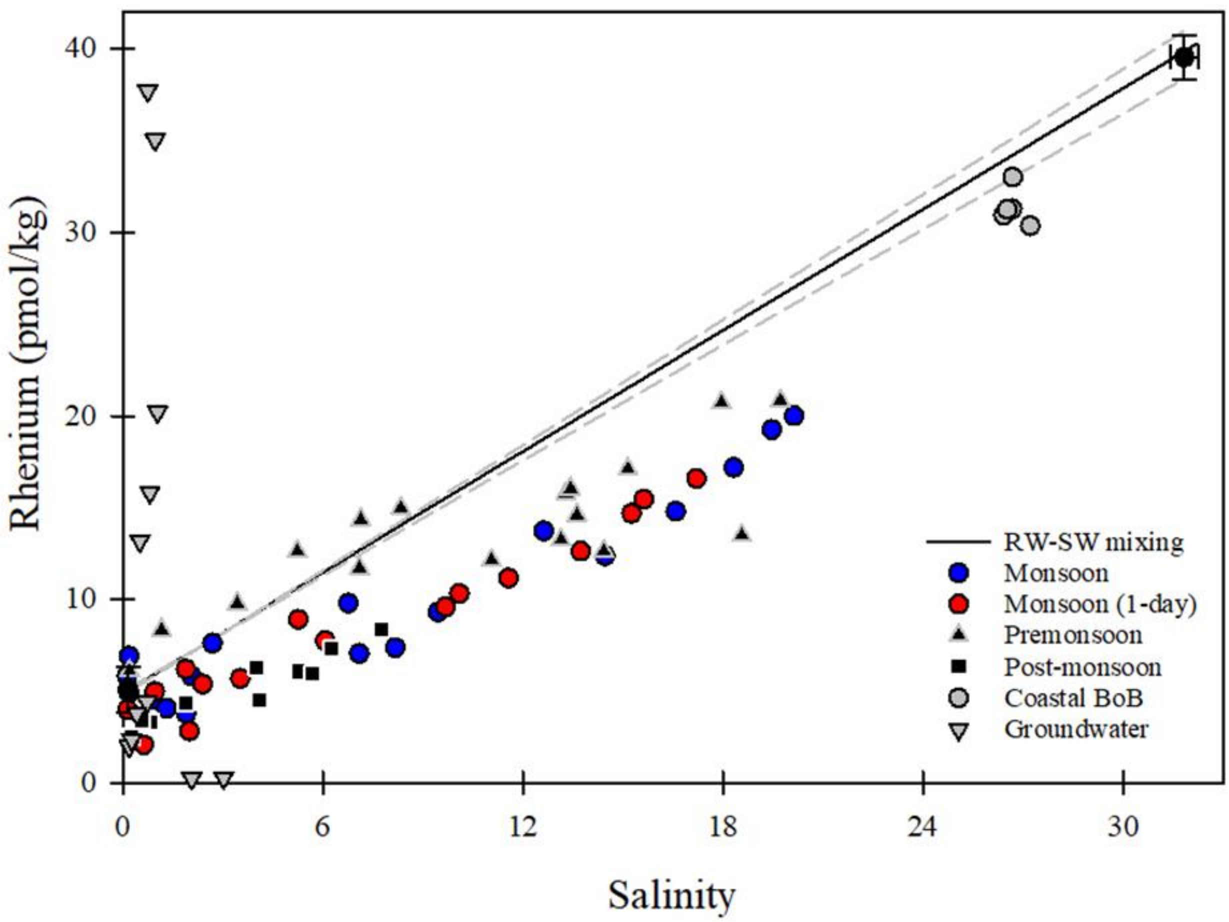

Figure 5.1.3. Co-variation between salinity and Re concentrations of the lagoon for all seasons (monsoon, pre-monsoon post-monsoon). The solid (black) line reflects the theoretical line for conservative river-sea water mixing. For reference, average groundwater and Bay of Bengal compositions are also shown.

sediments from the Chilika vary from 130 to 652 pg/gm with an average value of 354 ± 129 pg/gm (n = 33; Table A6). In comparison, the Re concentrations in the clay fractions of sediments range from 298 to 927 pg/gm with an average of 501 ± 166 pg/gm (n = 18; Table A6). The average concentrations for bulk and clay fractions of the Chilika sediments are higher than those reported for the upper continental crust (198 pg/gm; Peucker-Ehrenbrink and Jahn, 2001). Exchangeable fractions of the bulk and clay sediments have the average Re contents of 141 ± 94 pg/gm (n = 5) and 303 ± 148 pg/gm (n = 11), respectively. On average, the exchangeable Re fraction, therefore, accounts for ~35 % of total rhenium in bulk sediments, and ~60% of total Re in clay fractions (Fig. 5.1.4).

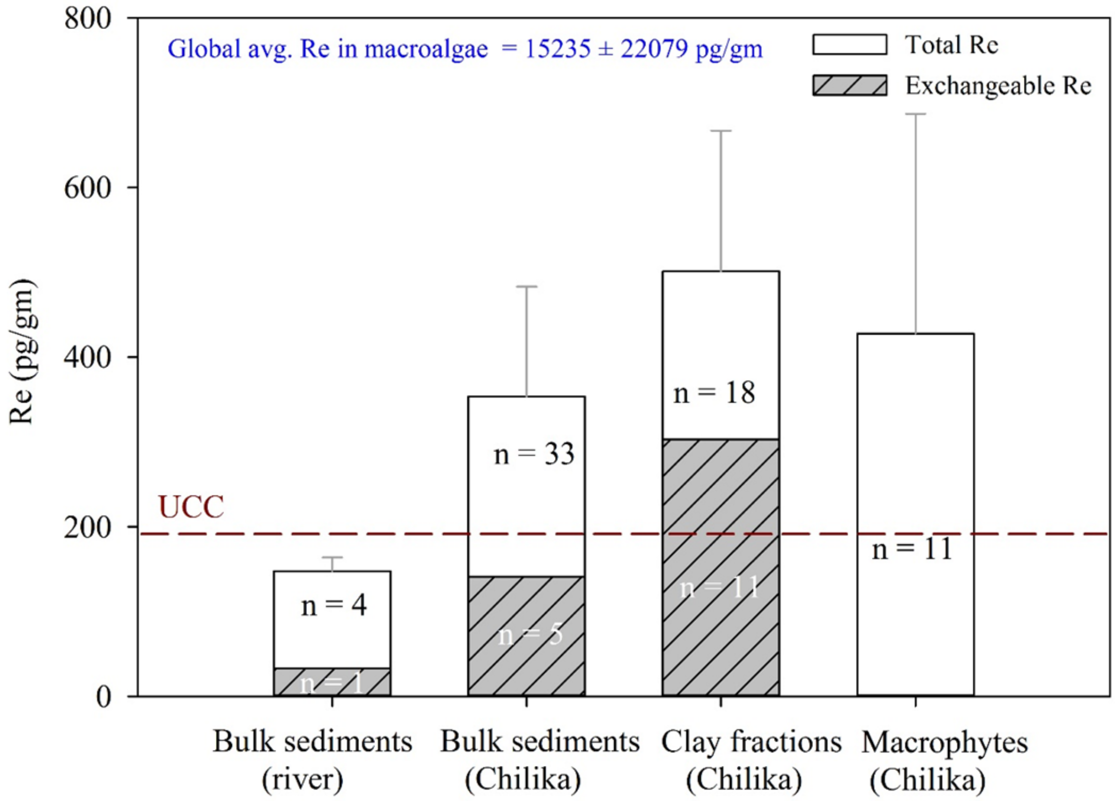

Figure 5.1.4. Distribution of Re concentrations in the bulk, clay and exchangeable fractions of the bed sediments and coastal macrophytes from the Chilika lagoon system. For reference, the Re concentrations for the riverine sources (this study) and upper continental crust (UCC; Miller et al., 2011) have also been shown.

The molecular identification of eleven plant samples reveal that these samples are mainly monocotyledonous. Five of them show identity with *Stukenia Pectinata* (L.) Börner (Potamogetonaceae), whereas two with *Panicum hallii* Vasey (Poaceae). Other samples are found to be of *Polygala alba* Nutt. (Polygalaceae), *Phyllostachys heteroclada* Oliv (Poaceae) and *Enteromorpha intestinalis* (L.) Link (Ulvaceae) (Table A10). The average Re content of these plant samples was 428 ± 259 pg/gm (n = 11; Fig. 5.1.4), which is higher than that observed for the Chilika sediments and UCC (Fig. 5.1.4). Among these, the highest Re abundance (838 pg/gm) is found for the *P. heteroclada*, whereas the lowest Re concentration (168 pg/gm) is obtained for *S. pectinata*.

5.1.3. Discussion

Distribution of dissolved rhenium along the salinity gradient of the Chilika lagoon confirms non-conservative behavior in this coastal system (Fig. 5.1.3). This observation is not consistent with available a few studies which shows near-conservative behavior of rhenium in estuarine settings (Coldner et al., 1993; Rahaman and Singh, 2010). However, the studies of Colodner et al. (1993) have not excluded the possibility of Re gain in the Amazon estuaries through ion-exchange processes in the low saline regimes (Walker and Peucker-Ehrenbrink 2004). Further, impact of anthropogenic sources has also been invoked in the Gulf of Cambay region to explain higher Re concentrations in coastal regions of the Arabian sea (Rahaman and Singh, 2010). Our study also shows a gain in Re concentrations in the low saline (<10) region during pre-monsoon season (Fig. 5.1.3). The Re gain in these samples with respect to the conservative mixing line varies from 1 to 2.3 pmol/kg with the maximum gain being observed for a salinity of ~1.2 (Fig. 5.1.5). These Re enrichments account for 7 to 38 % increase compared to their expected value for conservative mixing. These additional supply of Re can be linked to desorptive release, anthropogenic supply and/or submarine groundwater discharge during lean-flow stages. The intensity of ion-exchange processes (such as, desorption) are often found to have strong dependence on suspended sediment load, in addition to pH and ionic strength of the water column. Considering that the Re gain has only been observed for the pre-monsoon season with relatively lower sediment load than the monsoon season, the desorptive release may not be the dominant Re source for the Chilika. Further, our continental Re composition was constrained based on human-influenced river samples, and hence, additional anthropogenic supply of rhenium is less likely. Also, the maximum Re gain for the Chilika has been observed at a salinity of 1.2 (Fig. 5.1.3), which rules out the possibility of any direct supply of Re *via* anthropogenic sources during pre-monsoon period. The most likely source of rhenium to the Chilika during pre-monsoon, therefore, is submarine groundwater discharge (SGD). The SGD may comprise of fresh and brackish (recycled seawater) groundwater and infiltrated anthropogenic sewages, if any, to the coastal aquifer. Higher salinity and Re concentrations of the groundwater samples compared to the conservative mixing line also support influence of SGD to the Re inventory (Fig. 5.1.3). Further, the hydraulic pressure for the SGD during this lean flow is likely to be higher due to low riverine discharge during pre-monsoon compared to monsoon seasons. The salinity-Re regression line for the pre-monsoon samples ($Re = 0.53 \times Sal + 8.1$) yields an "effective" riverine composition of 8.1 pmol/kg, which is about 2 pmol/kg higher than the measured riverine value (6.1 pmol/kg) for this season. This additional Re supply of 2 pmol/kg to the lagoon would require an additional water supply of about 33 % of riverine flux (4×10^6 m^3/d; Muduli et al., 2012) during this season, which corresponds to 1.33×10^6 m^3/d. This value matches well with the SGD flux estimated earlier based on Sr isotopic data for the lagoon during pre-monsoon period (1.5×10^6 m^3/d; Danish et al., 2020). This consistency in flux estimates, further, corroborates the impact of SGD in supplying rhenium to low-saline regions of the Chilika during pre-monsoon season.

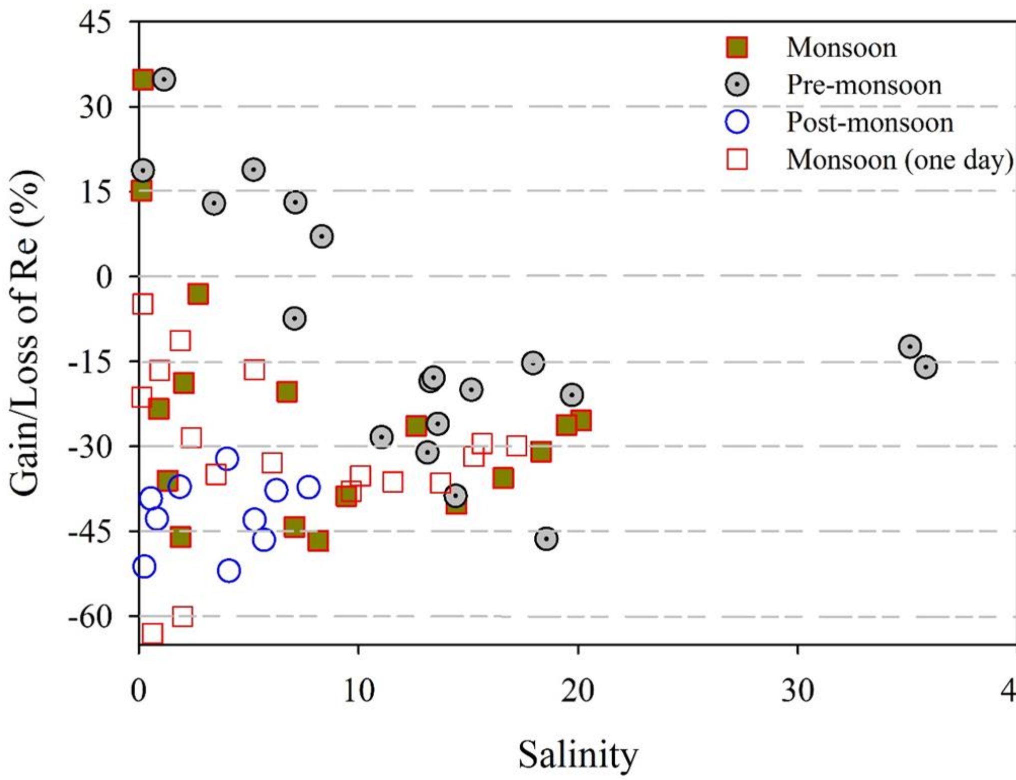

Figure 5.1.5. Estimated addition/removal of rhenium (in %) with respect to salinity of the Chilika lagoon during all seasons investigated herein.

The salinity-Re concentration plot also shows rhenium removal from the Chilika during all the three seasons and across all the salinity range during monsoon and post-monsoon seasons. The Re removal during the monsoon varies from 0.1 to 8.3 pmol/kg, whereas these values vary between 2 and 5 pmol/kg during post-monsoon seasons. The Re loss (in %) shows a declining trend with salinity and the removal is found to be minimum at higher salinity regimes (Fig. 5.1.5). The observed Re removal in the coastal lagoon system is in contrast with the observed conservative trends for estuarine systems. Although the exact cause for this difference is not known, the coastal lagoons, unlike the estuaries, are characterized with intense biological activities and high sediment suspension due to tidal activity in these shallow basins. These physical and biological properties may cause dynamic chemical reactions involving rhenium in the lagoons. Several mechanisms may act as a Re sink for the Chilika lagoon, which includes (i) its removal under reducing conditions (Morford et al., 2005) (ii) incorporation onto Fe-Mn hydroxides (Colodner et al., 1993) (iii) ion-exchange processes (adsorption onto clay/organic matter) and/or (iv) biological uptake (Yang, 1991; Racionero-Gomez et al. 2016). Among these, redox changes in water column can influence removal of dissolved rhenium to the sediment phases. For instance, the dissolved Re forms a stable perrhenate (ReO_4^-) ions under oxygenated conditions, which gets transformed to particulate-reactive ReO_2 and/or Re-S phases in reducing conditions (Yamashita et al., 2007; Helz and Dolor, 2012; Morford et al., 2012). We have assessed covariation between dissolved oxygen and rhenium concentrations of the Chilika lagoon to evaluate the impact of reductive change on the rhenium accumulation onto the sediments. Although the DO concentrations vary significantly (2-14 mg/L), the rhenium concentrations of the Chilika show no statistically significant correlation with the DO content ($r = -0.17$; $n = 17$). This observation indicates that the redox state of the water column has limited effect on the observed Re removal from the Chilika waters (Fig. 5.1.3). Consistent with this, Goswami et al. (2012) have also shown insignificant redox-sensitive removal of dissolved Re from the Arabian sea water column, despite of prevalence of oxygen minimum zones in the basin. Another possible, but less likely mechanism for Re removal from the Chilika lagoon is its scavenging via Fe-Mn hydroxides. Fe-Mn hydroxides serve as an efficient pathway for removing dissolved trace elements through ion-exchange processes to particulate phases in oxygenated conditions (Colodner et al., 1993 and references therein). To assess this, the correlation of sedimentary Re with the Mn concentrations was evaluated for the Chilika lagoon. No significant correlation ($r = -0.14$; $n = 33$) between these two parameters was observed. Further, the Mn/Al ($\times 10^{-4}$) ratios of the Chilika sediments (80 ± 57; $n = 33$) show insignificant enrichment with respect to that of its riverine input (141 ± 87; $n = 4$). These observations of minimal impact of Fe-Mn hydroxides in accumulating sedimentary rhenium are consistent with low Re concentrations in Mn nodules and sediments with high Fe-Mn oxide phases (Morford et al., 2005).

Adsorptive interaction between water and particulates can be a possible mechanism for scavenging rhenium from the Chilika lagoon (Olafsson and Riley, 1972; Wakoff and Nagy, 2004; Tanaka et al., 2019). Laboratory experiments have shown that the perrhenate ions may get adsorbed onto Mg-Al rich layered double hydroxides to remove Re from solutions (Tanaka et al., 2019). The Chilika sediments are composed of ~64 % of clay particles, which contains appreciable amount of Mg-Al rich clay minerals, such as illite, chlorite and montmorillonite (Barik et al., 2020). Considering high ionic exchange capacity of montmorillonite and illite, these sheet-structured phyllosilicates minerals may serve as important substrates for rhenium adsorption. Strong correlation between sedimentary Re with Mg and Al concentrations also support possible adsorptive removal of Re onto clay surfaces (Fig. 5.1.6A, 5.1.6B). Further, the adsorptive removal of Re from the Chilika seems evident from higher Re concentrations of clay fractions (501 ± 106 pg/gm, n = 18) of the sediments than their corresponding bulk aliquots (354 ± 129 pg/gm, n = 331). Further, the amount of exchangeable-Re in Chilika sediments, both in bulk and clay fractions, are also found to be significantly higher than that in river sediments (Fig. 5.1.4). The excess exchangeable-Re in the lagoon sediments with respect to detrital supply confirms ~200 pg/gm of Re in the Chilika sediments are authigenic in nature. Based on these data comparisons and clay composition of Chilika sediment, we hypothesize that the observed loss of dissolved Re is linked with adsorption of ReO_4^- onto clay particles, mainly montmorillonite and illite, through anionic replacement. The Re accumulation rate onto clay particles have been quantified in a subsequent section (cf. section 5.1.4.).

Another possible mechanism that can explain the observed non-conservative rhenium removal from the Chilika lagoon can be uptake of Re during biological activities of coastal macroalgae/macrophytes. The laboratory culture experiments have shown strong enrichment of Re in brown algae (up to ng/gm level) during their seawater interaction (Racionero-Gomez et al., 2016). Compilation of available Re data for macroalgae from different locations yield an average Re concentration of 15.2 ng/gm (n = 70; Yang, 1991; Prouty et al., 2014; Rooney et al., 2016; Sporson et al., 2018, 2020 and references therein), which is about five orders of magnitude higher than the Re concentration for the upper continental crust (~198 pg/gm; Peucker-Ehrenbrink and Jahn, 2001). Available studies have shown that Re uptake monotonically increase with Re concentration of the ambient water and hence, macroalgae-Re abundances and their ratios have found successful applications to reconstruct past coastal processes (Rooney et al., 2016). The Chilika lagoon is a biologically active system and estimated to house ~30,000 tonnes of macro-algae biomass within only ~8% of its area (Rath and Adhikary, 2005). It also houses around 726 flowering plant species (Madhusmita, 2012). In addition to macroalgae, presence of green plants in the lagoon may also serve as capable accumulator of rhenium (Novo et al., 2015). Therefore, occurrence of huge biomass in this lagoon can drive significant Re removal through biological activities. The eleven macrophyte samples from the Chilika yield an average Re concentration of 428 ± 259 pg/gm, which is higher than that of the Chilika sediments and UCC (Fig. 5.1.4). This indicates that there is significant Re enrichment in the macrophytes compared to the detrital Re in the sediments and hence, sedimentary Re may not be the only source of rhenium for the macrophytes. If we assume global average Re value for the macroalgae from the Chilika, the Re enrichment in these algal biomass can be higher by three orders of magnitude than the macrophytes. These data comparisons point to significant uptake of dissolved rhenium onto these living organisms. Although little is known about biological fixation of Re by which macroalgae take up perrhenate ions, available a few studies have invoked the possible association of rhenium with amino acids during cellular membrane formation as a pathway for biological removal of perrhenate ions (Xiong, 2003; Prouty et al., 2014; Fig. 5.1.7). To assess this proposition, we investigated the covariation between sedimentary Re with total nitrogen (TN) concentrations (Fig. 5.1.6C). The TN-Re plot shows a significant positive correlation, indicating that the increase in the Re concentrations in the Chilika sediments are associated with the sedimentary nitrogen concentration. Further, the riverine samples in this plot fall closer to the lowest Re and TN zone. Hence, the observed Re and N enrichments in the Chilika, in excess to riverine input, are mostly via lagoonal processes and not linked with detrital sources. Based on these observations, we establish that significant fraction of dissolved Re have been removed from the Chilika lagoon *via* biological uptake during cellular formation of coastal macrophytes and/or macroalgae.

5.1.4. Re burial rate and its significance

Efforts were made in this study to estimate the burial rate of rhenium in the Chilika lagoon through different pathways, such as detrital and authigenic (ion-exchange and biological uptake) processes. The authigenic (Re_{auth}) and detrital (Re_{det}) fractions of sedimentary Re and corresponding burial rates were estimated using the following equations. For these calculations, the Ti-normalized ratios (instead of Al) have been preferred mainly due to possible involvement of sedimentary Al in cation exchange processes (Tanaka et al., 2019).

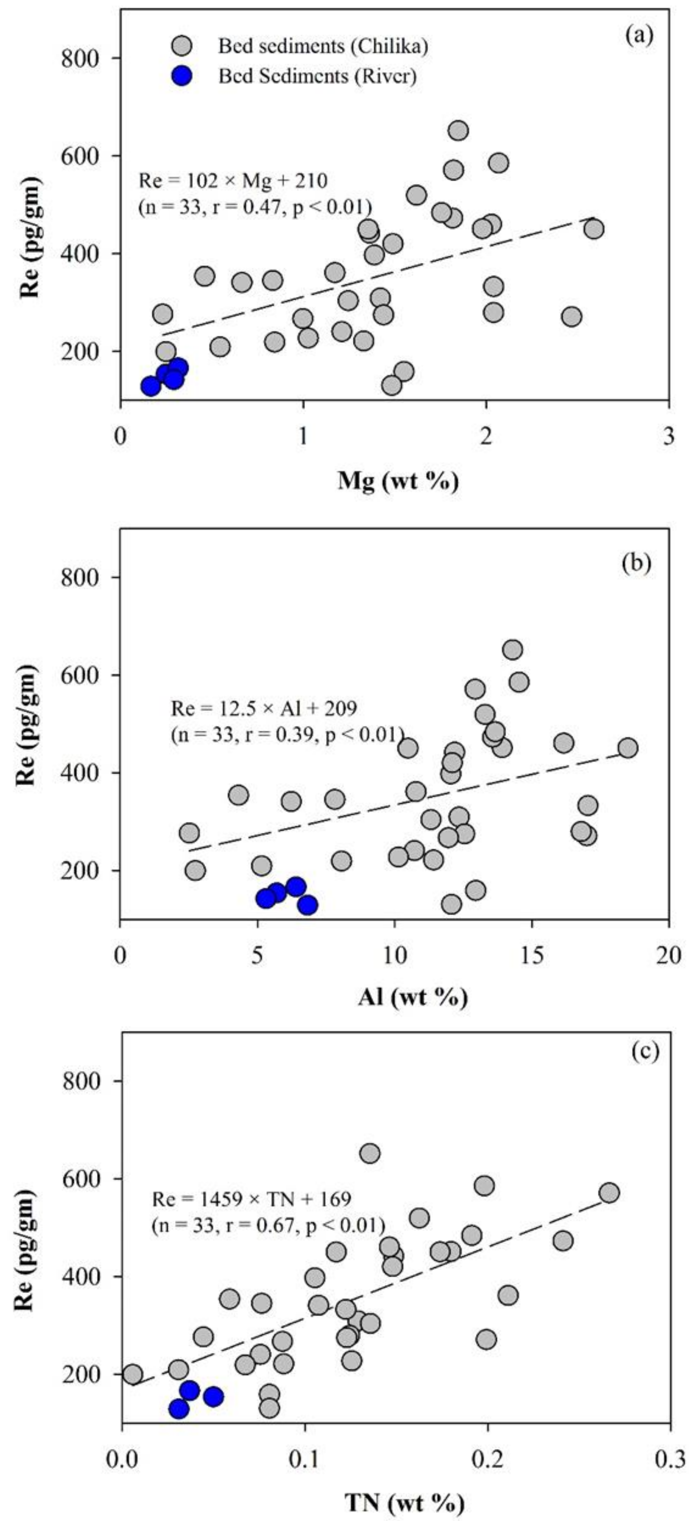

Figure 5.1.6. Correlation of sedimentary Re with (a) Mg, (b) Al and (c) TN (total nitrogen) concentrations for the Chilika lagoon. The river samples consistently show lower concentrations for all the parameters. The significant positive correlation with Mg and Al point to accumulation of rhenium via clay adsorption, whereas the Re-TN covariation hints at biological uptake by amino acids during cellular membrane formations.

$$Re_{det} = Ti_{Chilika} \times (Re/Ti)_{riv} \tag{1}$$

$$Re_{auth} = Re_{Chilika} - Re_{det} \tag{2}$$

$$Re_{det}\ (or, Re_{auth})\, burial\, rate = Re_{det}\ (or, Re_{auth}) \times DBD \times SR \tag{3}$$

where, DBD and SR stand for dry bulk density of sediments and average sedimentation rate for the Chilika lagoon. In absence of these data, we have used earlier reported average sedimentation rate for the Chilika (~0.056 cm/yr; Zachmann et al., 2009) and representative dry bulk density values (~0.61 gm/cc; Bhushan et al., 2001) for coastal regions of India.

The calculated Re_{det} for the Chilika varies from 130 to 287 pg/g, with an average value of 179 ± 36 pg/gm (n = 36). This average value is found to be consistent with the y-intercept value (~169 pg/gm; Fig. 5.1.6C) in the TN-Re plot for the Chilika. Considering all riverine samples fall closer to near-zero nitrogen value (Fig. 5.1.6C), the y-intercept value in this plot may also provide a rough estimate of average detrital Re concentration. The average Re_{det} value (~179 pg/gm) accounts for about half of the bulk sedimentary Re content (354 pg/gm). These average values further indicate that remaining half of rhenium in the Chilika sediments (Re_{auth} ~175 pg/gm) are authigenic in nature. The authigenic rhenium removal, as discussed earlier, may occur through both clay adsorption and biological uptake mechanisms. The adsorptive rhenium amount can be estimated from difference of Re concentrations in exchangeable fractions of the Chilika (~141 pg/gm) and river (~33 pg/gm) sediments. These data indicate that the sedimentary Re derived through clay adsorption may equal to 108 pg/gm. Knowing total Re_{auth} concentration (~175 pg/gm), the amount of Re scavenged through biological (macroalgae/macrophytes) uptake, therefore, is found to be 68 pg/gm. These estimates, therefore, confirm that about 60 % of Re_{auth} has been removed through clay adsorption, whereas remaining 40 % gets incorporated during the biological activities. These calculated Re concentrations for different pathways has been used in equation (3) to estimate the respective burial rates.

Figure 5.1.7 depicts rate and mechanism of Re removal from the Chilika lagoon. The estimated bulk Re burial rate for the Chilika lagoon is 1.2×10^{-2} ng/cm^2/yr, out of which both detrital (6.05×10^{-3} ng/cm^2/yr) and authigenic (5.95×10^{-3} ng/cm^2/yr) processes contribute equally. Among the authigenic mechanisms, the burial rate for the Re adsorption onto clay particles (3.65×10^{-3} ng/cm^2/yr) is found to be ~20% higher than the uptake rate of Re *via* biological activities (2.30×10^{-3} ng/cm^2/yr; Fig. 5.1.7). Based on previous discussion, we show that adsorptive removal of Re onto clay particles are mainly associated with replacement of ReO_4^- with available anions (OH^-) in Mg-Al rich (montmorillonite) clays, whereas Re uptake in biological processes involves bonding with amino acids during cellular membrane formation (Fig. 5.1.7). Our estimated Re burial rates *via* authigenic process is found to be about four times higher than that reported for oxic marine sediments (1.6×10^{-3} ng/cm^2/yr; Sheen et al., 2018) globally, underscoring importance of these coastal Re sinks. The observed Re sinks involving clay adsorption and biological uptake in coastal regimes are currently not part of global Re budget. Outcomes of this study, considering large areal extent of coastal lagoons (700,000 km^2; Herdendorf, 1982), warrant the need to revisit the oceanic Re budget by incorporating these redox-sensitive sinks.

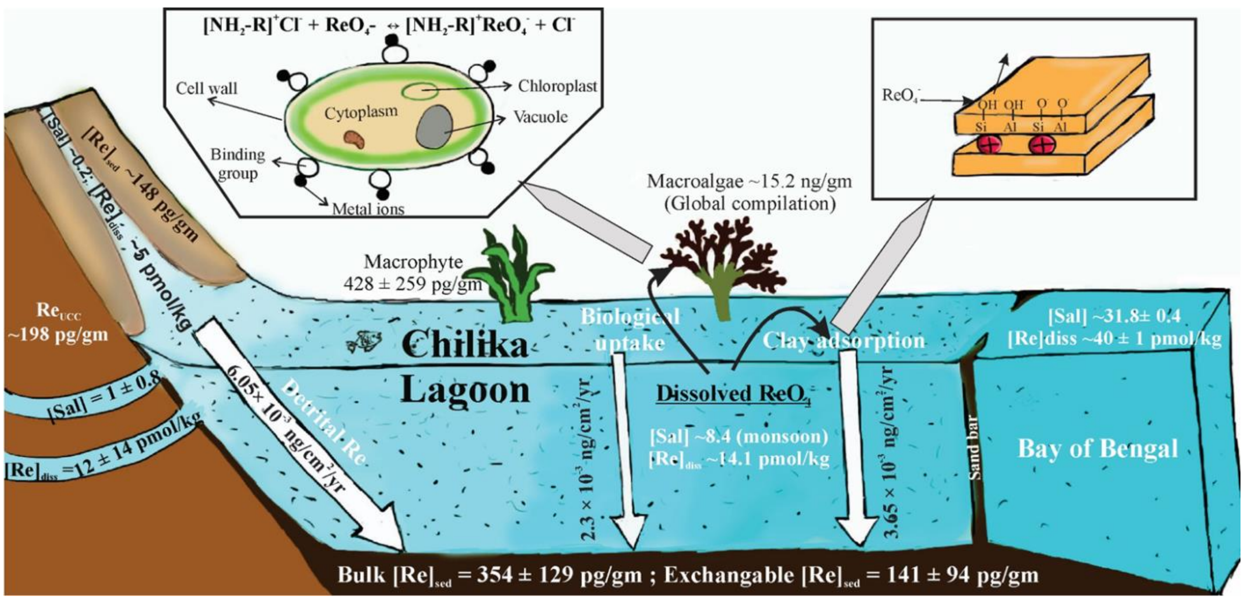

Figure 5.1.7. Sources and cycling of rhenium in the Chilika lagoon, India. The figure depicts all possible pathways (e.g. clay adsorption and biological uptake) and rates of Re removal from this coastal system.

5.2. Stable carbon isotopic systematics of the Chilika lagoon system

5.2.1. $\delta^{13}C_{DIC}$ of dissolved inorganic carbon (DIC)

The $\delta^{13}C_{DIC}$ and DIC compositions have been widely used for understanding the biogeochemical cycling of carbon and tracing the sources, sinks and transformations of carbon in coastal water bodies at the global and regional scale (Alling et al 20012; Samanta et al., 2015; Burt et al. 2016; Bhavya et al., 2018; Cotocvicz et al., 2019; 2020). The $\delta^{13}C_{DIC}$ values are often characterized with distinct isotopic signatures for their major sources (Geogenic (−12‰ to 5‰), Atmospheric (−15% to 8‰), and Biogenic (−26 to −18‰)) and hence, serve as useful proxy to trace the sources of DIC (Campeau et al., 2017). Available studies show both conservative behavior (De la Paz et al., 2008; Pencharee et al., 2012; Cauwet and Sidorov, 1996) and non-conservative (Samanta et al., 2015; Alling et al., 2012; Bhavya et al., 2017 and Dutta et al., 2019) behavior of DIC in coastal oceans/estuaries. The non-conservative behavior of DIC have been attributed to several factors, which includes photosynthetic uptake of CO_2, degradation of organic matter, CO_2 exchange with the atmosphere and/or dissolution/precipitation of carbonate minerals (Finlay and Kendall, 2007). We have assessed co-variation of water salinity with DIC and $\delta^{13}C_{DIC}$ of the Chilika lagoon to constrain their sources and internal cycling of inorganic carbon in the lagoon.

5.2.1.1. Source composition*:* DIC concentrations of river sample (salinity ~0.26) from the Chilika lagoon system is found to be 1299 µmol/kg, which is comparable with that reported earlier for these basins (1170 µmol/kg; Gupta et al., 2008) (Table A4). These concentrations are systematically higher than the global average DIC value for rivers (~900 µmol/kg; Meybeck and Vörösmarty, 1999). The $\delta^{13}C_{DIC}$ value for this sample is -0.55 ‰ (Table A4). The salinities of the groundwater samples vary from 0.27 to 3.02 (Table A4), with their corresponding DIC concentration varying from 2136 to 12142 µmol/kg (mean: 4718 ± 3495 mmol/kg; n = 7). Average $\delta^{13}C_{DIC}$ values for these samples is -5.5 ± 1.9 ‰ (n = 7).

5.2.2.2. Chilika composition*:* The spatial distribution of DIC concentrations and $\delta^{13}C_{DIC}$ compositions for the Chilika lagoon samples show wide variations. These DIC concentrations vary between 630 and 2566 µmol/kg (Table 5.2.1), which are consistent with that reported earlier for the Chilika (310 to 2570 µmol/kg; Muduli et al., 2013). The DIC of the northern sector samples (Mean: 1460 ± 364 µmol/kg) were lower than that observed for the central (Mean: 1808

± 197 μmol/kg) and southern (Mean: 2137 ± 118 ± 197) sectors during monsoon season (Table 5.2.1). The lagoon also exhibits similar DIC trends during the pre-monsoon and post-monsoon seasons.

Table 5.2.1. Average data and ranges of DIC, $\delta^{13}C_{DIC}$ and other parameters investigated in the waters of Chilika for all seasons. The details data of these parameters are provided in the supplementary material.

		Pre-monsoon (May,2017)	Monsoon (August, 2017)	Post-monsoon (January, 2018)
Temp. (^{o}C)	Average	30.1 ± 1.9	31.2 ± 1.3	22 ± 1.7
	range	26.8 - 35.9	28 - 33.6	18.7 - 24.4
pH	Average	8.2 ± 0.5	8.2 ± 0.4	8.5 ± 0.8
	range	7.4 - 9.7	7 - 9.1	7 - 10.2
Salinity	Average	14.4 ± 11.1	5.1 ± 6.4	2.7 ± 3.1
	range	0.2 - 36.3	0.1 - 20.1	0.3 - 8.4
DIC (μmol/kg)	Average	1812 ± 600	1671 ± 403	1887 ± 300
	range	630 - 2566	1019 - 2501	1018 - 2540
$\delta^{13}C_{DIC}$ (‰)	Average	-5.2 ± 3.1	-3.7 ± 1.9	-4.5 ± 2.8
	range	-12.2 - 1.2	-6.67 – 1.8	-10.7 - -0.41

The $\delta^{13}C_{DIC}$ values for the Chilika ranges from -6.7 ‰ to 1.8 ‰ with an average of -3.7 ± 1.9 ‰ (n = 39) during monsoon season. The average $\delta^{13}C_{DIC}$ values for the pre-monsoon (mean: -5.2 ± 3.1 ‰) and post-monsoon (mean: -4.5 ± 2.8 ‰) seasons are found to be systematically depleted compared to the monsoon $\delta^{13}C_{DIC}$ values. Figure 5.2.1 compares the DIC and $\delta^{13}C_{DIC}$ data for several rivers and estuaries from India. The Chilika lagoon has been observed to have moderately high DIC and enriched $\delta^{13}C_{DIC}$ value compared to those from other basins. We have also carried out two-hourly analyses of the DIC and $\delta^{13}C_{DIC}$ at the Chilika outflow to assess the impact of semi-diurnal tidal cycle on these parameters (Fig. 5.2.2). These two-hourly resolution data show that the DIC concentrations during the monsoon show about ~10% variation with an average value of 1692 ± 163 μmol/kg, whereas during pre-monsoon this variations is only ~2% (2602 ± 43 μmol/kg) (Fig. 5.2.2.). Similar elemental variations have also been observed for the Sr concentration (cf. chapter 3), which has been attributable to seawater incursion into the lagoon during semi-diurnal tidal cycle. The $\delta^{13}C_{DIC}$ values at outflow vary from -4.81 to -1.83 ‰, with the highest value being observed for the sample with highest salinity (9.2) during monsoon season (Fig. 5.2.3).

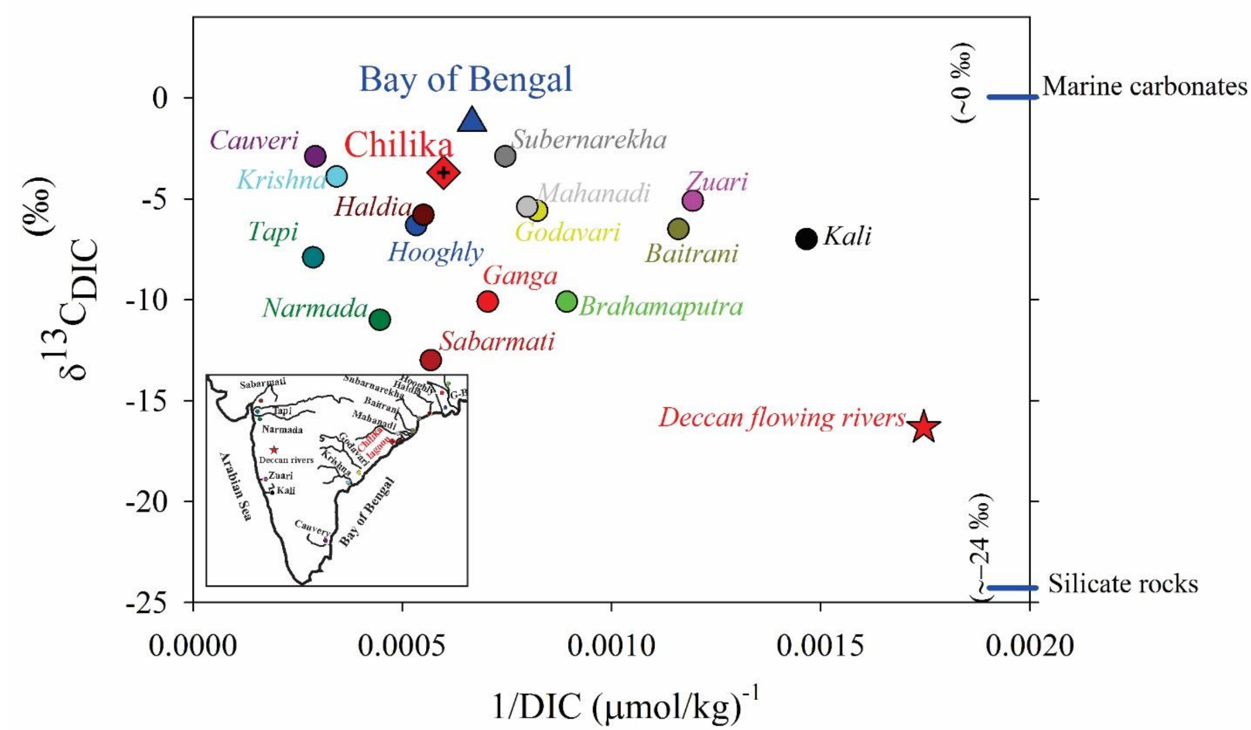

Figure 5.2.1. Comparison of DIC and $\delta^{13}C_{DIC}$ values of Chilika Lagoon with other rivers/estuaries and carbonate-silicate sources. The compiled data and their references are given in the supplementary material.

Figure 5.2.3. shows the relationship of DIC and $\delta^{13}C_{DIC}$ with salinity during the three seasons. Non-conservative behavior of DIC has been observed for all three seasons. During pre-monsoon season most of the samples mainly fall below the river-seawater mixing line, suggested loss of DIC in the lagoon. Conversely, addition of DIC in lagoon samples has been observed for the monsoon and post-monsoon season. In case of $\delta^{13}C_{DIC}$, the $\delta^{13}C_{DIC}$ values are found mostly depleted compared to conservative line for all the seasons. Several factors can contribute for these non-conservative behavior of DIC and $\delta^{13}C_{DIC}$ values in the Chilika lagoon, which includes (i) degradation of terrestrially-derived OC (Alling et al., 2012; Samanta et al., 2015) (ii) biological productivity (Herczeg, 1987; Hollander and Mckenzie, 1991; Wang and Veizer, 2000; Muduli et al., 2013; Bhavya et al., 2018; Dutta et al., 2019) (iii) Outgassing of CO_2 (Cotovicz et al., 2020) (iv) carbonate precipitation/dissolution and submarine groundwater discharge. All these processes influence the DIC and $\delta^{13}C_{DIC}$ values differently. The carbonate precipitation, productivity and outgassing reduces the DIC, whereas the carbonate dissolution and degradation

of terrestrially-derived OC lead to increase in DIC. For $\delta^{13}C_{DIC}$, the isotopic fractionation during biological productivity, outgassing and carbonate dissolution processes enrich the water column isotopically, whereas the degradation of terrestrially-derived OC depleted the water column isotopically. We computed the deviation of DIC (ΔDIC) and $\delta^{13}C_{DIC}$ ($\Delta\delta^{13}C_{DIC}$) for each samples from the "theoretical" conservative line and these values are plotted in Fig. 4. This plot shows that most of monsoon samples fall in a quadrant which is more indicative of organic matter degradation. The pre-monsoon samples fall in both organic matter degradation and calcite precipitation quadrant. Further, the SGD is another possible source of DIC to this coastal lagoon (Samanta et al., 2015). To examine this, we computed a first-order estimation of SGD-derived DIC flux to the Chilika lagoon using the groundwater DIC (Mean: 4718 µmol/kg for monsoon) data and the SGD (1.51×10^6 m^3/day; Danish et al., 2019) flux. There exist no information for the SGD flux for the monsoon season and hence, the SGD value available for the pre-monsoon season has been used here. These data shows that the SGD-derived DIC flux to the Chilika during monsoon is 7.13×10^6 mol/day, which is only ~3 % of the riverine DIC (2.5×10^8 mol/day) to the lagoon. This estimation, therefore, indicates that the SGD contribution for the DIC to the Chilika lagoon is only minimal.

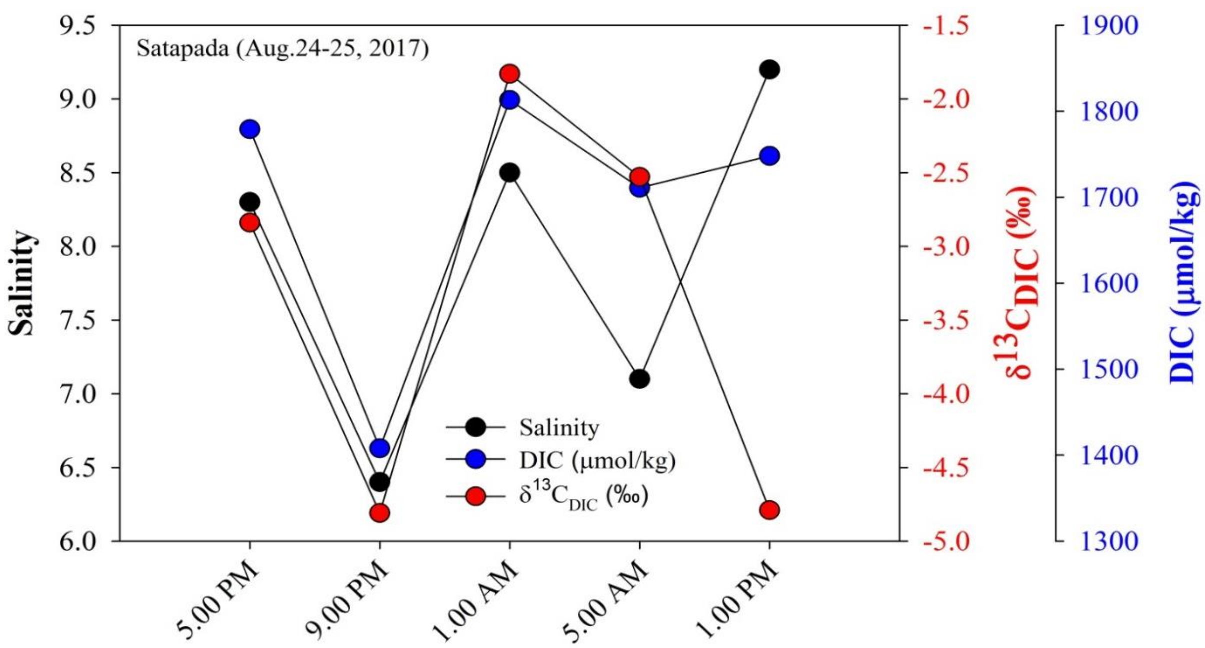

Figure 5.2.2. Two-hourly variations in salinity, DIC and $\delta^{13}C_{DIC}$ concentrations (selected samples 5 out of 12) show impact of seawater exchange with the lagoon during semi-diurnal tidal cycles.

The above discussion based on SGD-flux calculation and ΔDIC-Δ $\delta^{13}C_{DIC}$ distribution, therefore, indicates that different processes regulate the inorganic carbon cycling of the Chilika lagoon. In addition to river and seawater fluxes, the inorganic carbon cycle of the Chilika is dominantly regulated by organic matter degradation during monsoon, whereas calcite precipitation may have key role in regulating $\delta^{13}C_{DIC}$ during lean flow (pre-monsoon) stages.

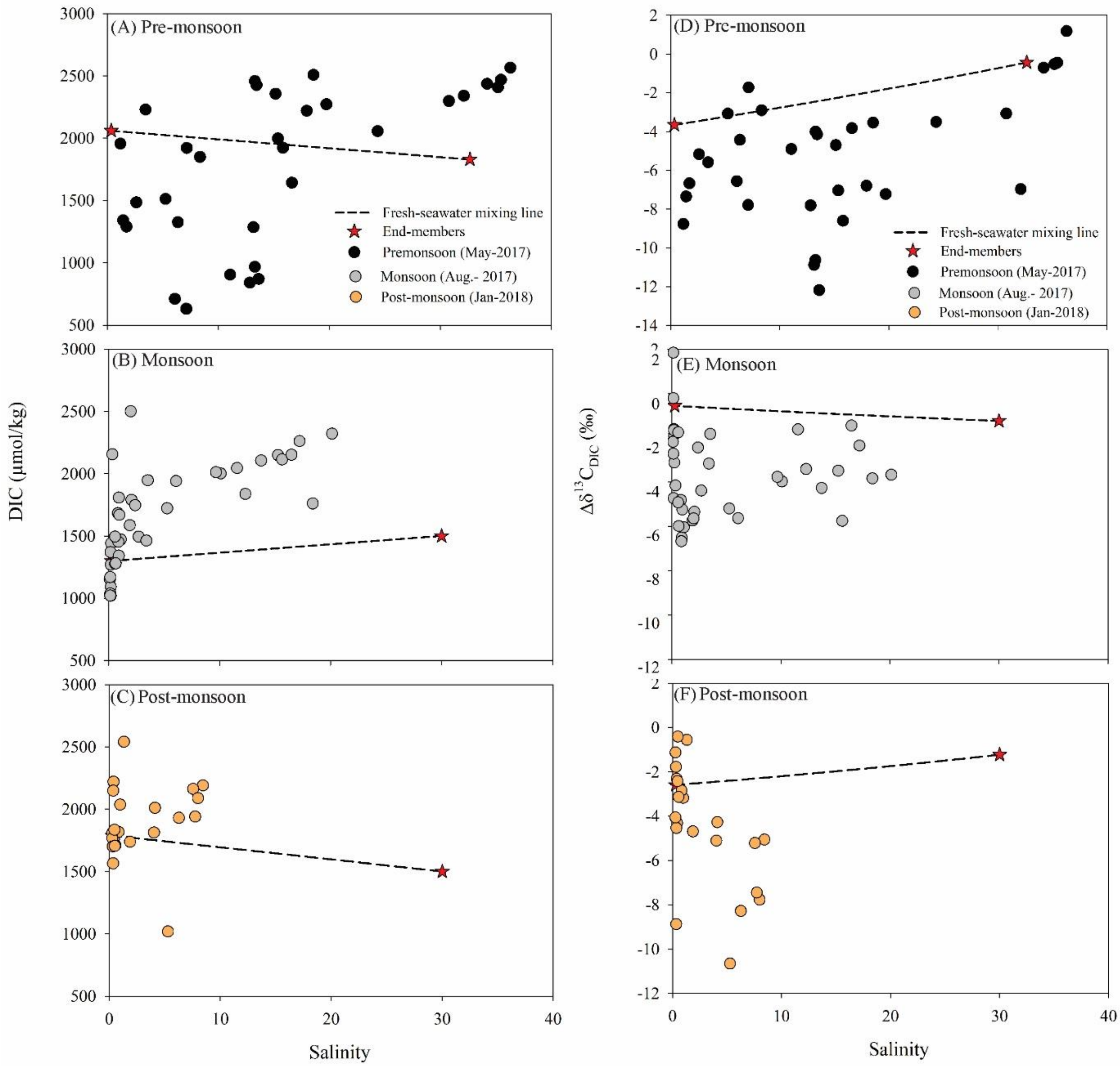

Figure 5.2.3. DIC distribution along the salinity gradient in the Chilika lagoon is shown in the left panel and $\delta^{13}C_{DIC}$ signatures along the salinity gradient is present in right panel. The dotted line presents the conservative mixing between river and seawater, data which is used to construct this line is provided in Table A4.

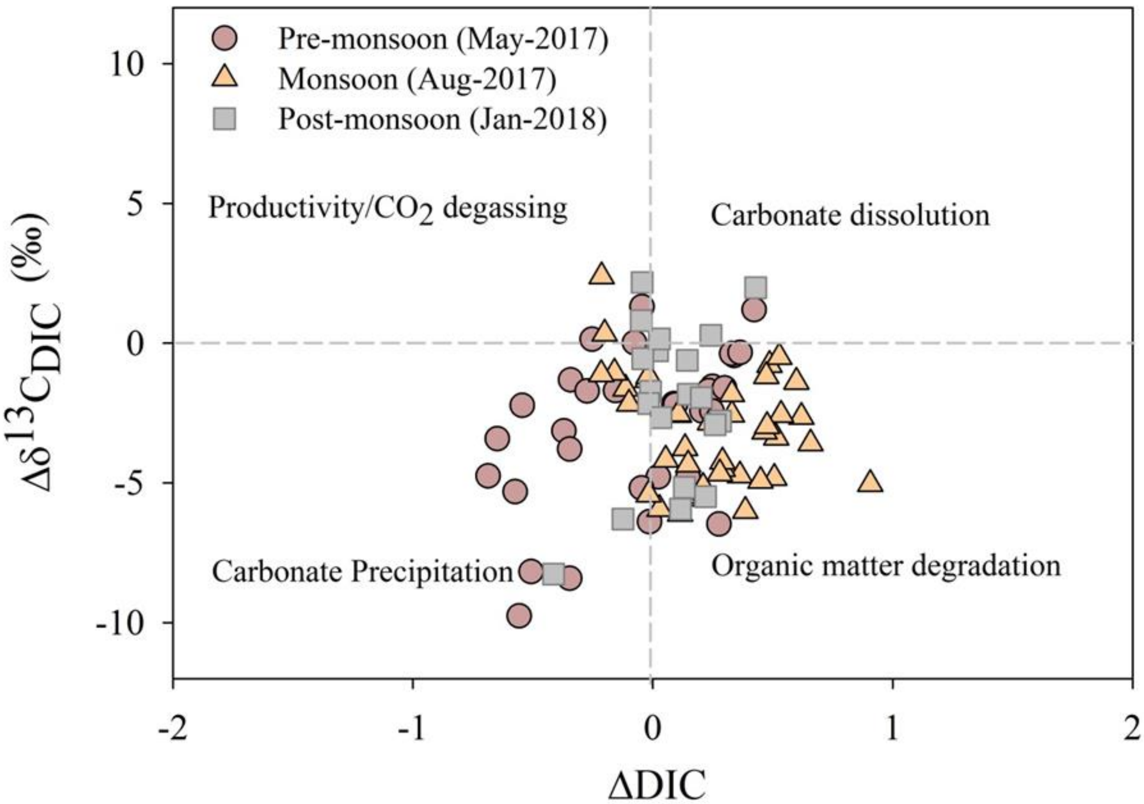

Figure 5.2.4. Plot shows the deviations from conservative mixing lines of $\delta^{13}C_{DIC}$ ($\Delta\delta^{13}C_{DIC}$) as a function of DIC (ΔDIC) for the Chilika lagoon. Different colors represent the sampling campaigns. The origin represents the conservative mixing between fresh-seawater end-members. The four quadrants indicate biogeochemical processes which are responsible for affecting the DIC and $\delta^{13}C_{DIC}$ values. The quadrant of primary production/ CO_2 degassing is indicative of decrease of DIC concentration and increase of $\delta^{13}C_{DIC}$ values. The quadrant of calcite dissolution represents the enrichment of DIC concentrations and $\delta^{13}C_{DIC}$ values. The quadrant of calcite precipitation is representative of depletion of DIC concentrations and $\delta^{13}C_{DIC}$ values. The quadrant of the degradation of organic carbon indicates the enrichment of DIC concentration and depletion of $\delta^{13}C_{DIC}$ values.

5.3. TOC and $\delta^{13}C_{Org}$ of sedimentary organic carbon

The organic carbon content of river bed samples varies from 0.5 to 1.3 wt. % (Table A5), in the range with those reported earlier for these river samples (Amir et al., 2019, 2020, Nazneen et al., 2017).The organic carbon (TOC) abundances ranged from 0.3 to 3.2 wt. % with an average value of 1.3 ± 0.7 wt. % in the Chilika sediments (Table A5). Lower TOC content (0.3 wt. %) was observed in the southern sector of lagoon, whereas higher values (3.2 wt. %) was observed in the northern sector due to the supply of terrestrial derived OC via the river in this zone. The average composition of TOC found in this study (1.3 ± 0.7 %) is slightly higher to those reported earlier (~0.9 %, Amir et al., 2020; Nazneen et al., 2017). Although, similar range of TOC was reported in the slope sediments of east coast of India (Krishna et al., 2013). The $\delta^{13}C_{org}$ signature for river bed samples varies from -27.2 to -23.8 ‰ with an average value of -26 ± 2 ‰, consistent with the previous reports (Amir et al., 2019, 2020). Although this mean value is intermediate to the C3 (~-27 ‰ (range: -35 to -20 ‰)) and C4 (~-13 ‰ (range: -16 to -10 ‰)) vegetation (Tipple

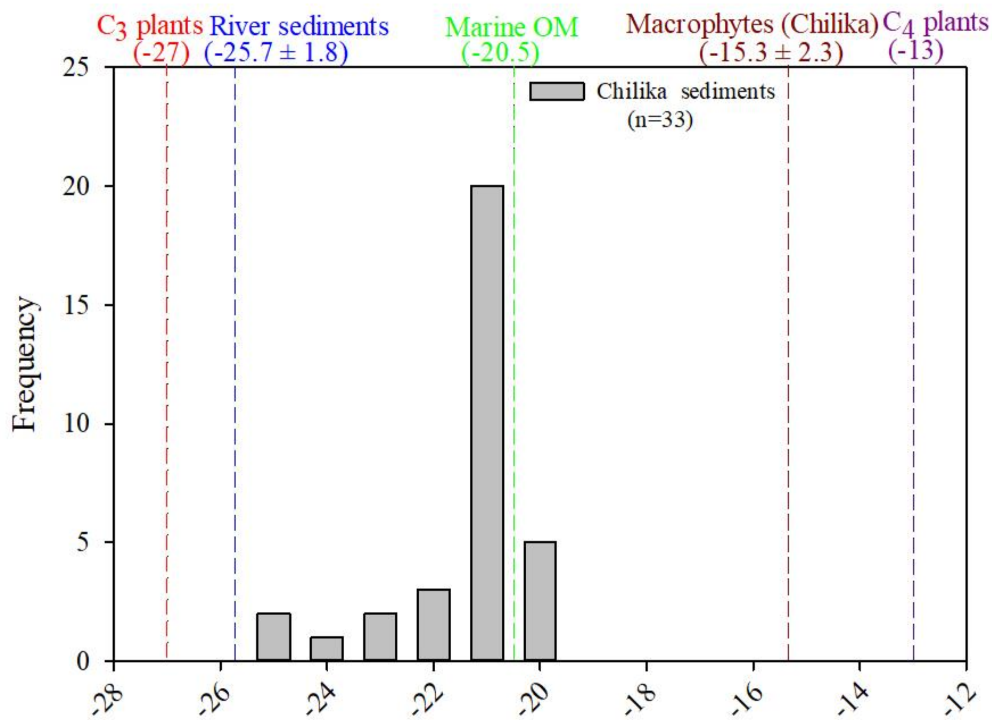

Figure 5.3.1. Frequency distribution of sedimentary organic carbon isotopic composition of the Chilika lagoon. For references, the average isotopic values for river sediments (this study). C3 and C4 plans (Tipple and Pagani, 2007), typical marine organic matter (Ramaswamy et al., 2008) and macrophytes (Amir et al., 2019) from the Chilika lagoon is also shown.

and Pagani, 2007), indicating organic carbon in these river sediments is dominantly supplied from continental C3 vegetation. The $\delta^{13}C_{org}$ values of the lagoon sediments ranges from -25.9 to -20.3 with an average value of -21.8 ± 1.3 ‰, relatively enriched compared to that of the river bed sediments (-26 ± 2 ‰) (Table A5). This $\delta^{13}C_{org}$ value of lagoon samples might be influence by marine organic matter (supplied from the Bay of Bengal) and/or submerged macrophytes from the lagoon itself. The submerged macrophytes of Chilika lagoon and organic matter from the Bay of Bengal have average value of ~-15 ‰ and ~-20.5 ‰, respectively (Ramaswamy et al., 2008, Amir et al., 2019). Based on these observations, we conclude that the Chilika lagoon organic matter mainly supplied through the riverine input.

5.4. Conclusion

Spatial and seasonal distributions of rhenium concentrations along the salinity gradient of the Chilika lagoon, India show non-conservative addition/removal of dissolved Re from this coastal ocean system. The salinity-Re covariation show gain of rhenium in the low-saline regimes during pre-monsoon seasons, attributable to additional Re supply via submarine groundwater discharge during lean flow stages. Additional to this gain, removal of dissolved rhenium has been observed across all the salinity range and during three seasons. Removal mechanism and its rate have been established by comparing Re abundances in particulate phases (such as, river and lagoonal sediments (in their bulk, clay and exchangeable fractions) and coastal macrophytes) and by assessing its correlation with other key elements (Mg, Al and N). These data show that the sedimentary Re in the Chilika has been scavenged by both detrital and authigenic pathways, in near equal proportions. Among the authigenic processes, about 60 % of Re has been scavenged *via* its incorporation on to Mg-Al rich clay substrates, whereas the remaining 40 % of Re follows biotic removal by its adsorption onto amino acids during cellular membrane formation of coastal macroalgae/macrophytes. The estimated authigenic burial rate of Re in the Chilika lagoon (~6×10^{-3} ng/cm^2/yr) is about 5 times higher than that reported for modern oxic sediments (~1.3×10^{-3} ng/cm^2/yr), underscoring importance of this coastal sink in oceanic rhenium cycle. Similar to Re, the DIC and $\delta^{13}C_{DIC}$ compositions also show the non-conservative behavior. In addition to river-seawater mixing, the DIC dynamic in the Chilika lagoon is mainly regulated by organic matter degradation. Impacts of other processes (CO_2 degasing/biological productivity and carbonate dissolution/precipitation) have also been observed on the DIC and $\delta^{13}C_{DIC}$ distributions.

Chapter 6
Conclusion and future perspectives

The major objective of this thesis work was to investigate biogeochemical cycling of trace elements in a large tropical coastal lagoon system (Chilika lagoon, India). Towards this, we have investigated chemical (B, Ba, Re and Sr) and isotopic ($^{87}Sr/^{86}Sr$, $\delta^{13}C$) compositions of Chilika lagoon system during four different periods (January-2018, May-2017, June-2016, August-2017). Additional to seasonal sampling, we have also collected two-hourly time resolution samples to assess impact of semi-diurnal tidal cycles on the elemental abundances of the lagoon. This comprehensive geochemistry study relies on diverse type of samples (lagoon water and its possible source waters (river, rain, ground and seawater), bed and suspended sediments and macrophytes. Chemical and isotopic data of these samples were used to quantify various coastal processes (ion-exchange processes, biological uptake and submarine groundwater discharge) and their impact on lagoon hydrochemistry. The Sr isotopic variations along the salinity gradient of the Chilika were useful in recognizing impact of SGD in supplying ^{87}Sr flux to the lagoon. We have used mass balance calculations involving Sr and $^{87}Sr/^{86}Sr$ ratio to estimate the SGD to the lagoon. Spatial distribution of key elements (boron and barium) in the Chilika lagoon indicated the impact of ion-exchange processes in supplying/removing trace elements to/from the lagoon. In addition, impact of biological processes on lagoon chemistry was evident from the spatio-seasonal distribution of stable carbon isotopes and rhenium concentrations. Key findings from this thesis work have been outlined below.

6.1.1. Estimation of submarine groundwater discharge (SGD) to the Chilika using Sr isotopic approach: Dissolved Sr and $^{87}Sr/^{86}Sr$ ratios of the Chilika lagoon and its possible sources have been investigated for three different seasons to infer coastal behavior of Sr along the salinity gradient. The Sr concentrations co-vary with salinities, as expected for conservative mixing between river and seawater. The mixing trends between 1/Sr and $^{87}Sr/^{86}Sr$ ratios, however, point to non-conservativeness of Sr isotopes in this lagoon during pre-monsoon and monsoon seasons. Based on sediment chemistry data, the non-conservativeness of Sr isotopes during monsoon period have been attributed to additional ^{87}Sr supply via subsurface ion-exchange processes to the lagoon. The non-conservative behavior of $^{87}Sr/^{86}Sr$ during pre-monsoon is due to SGD supply to the Chilika and this flux has been estimated following mass balance calculations using variable groundwater compositions along the salinity gradient. These results indicate that ~20% of hydrological inputs to the lagoon are derived from SGD, which accounts for a SGD flux of 1.51×10^6 m^3/d to the Chilika. The Sr isotopic value of SGD to the lagoon during pre-monsoon season (0.715) is higher than the present-day seawater ratio (~0.7092). The $^{87}Sr/^{86}Sr$ data from this and earlier studies for SGD to the eastern coast of India confirm that the SGD-derived Sr fluxes through large river systems from the Himalayas and Peninsular India regions would have minimal (and may also have opposite) impact on reducing the present-day oceanic imbalance.

6.1.2. Coastal behavior of dissolved B and Ba in the Chilika lagoon:

Detailed spatial and seasonal distributions of dissolved boron and barium in the Chilika have been investigated to infer their coastal behavior and controlling factors. Linear co-variation between boron and salinity of the samples from the monsoon season confirms conservative mixing of river and sea water within this coastal regime. On the contrary, the pre-monsoon samples exhibit non-conservative nature of boron in the Chilika with its significant removal from the low-saline (with salinity < 15) water samples. These removals are mainly due to adsorption of dissolved boron on to particulate phases (clay and/or oxyhydroxides). Higher water residence time during pre-monsoon season through increased particulate-water interaction time seem to regulate the adsorptive removal intensity. Comparison of boron abundances during diurnal and fortnight timescales show strong influence of tidal cycles on lagoon chemistry. However, the behavior of boron remains less influenced due to tidal forces and related seawater influx variations. Outcomes of this study underscore adsorptive removal of boron from coastal regimes and its importance in understanding authigenic boron distribution in clay-rich sedimentary archives from near-shore settings.

Dissolved barium along the salinity gradient of the Chilika lagoon show its non-conservative release with a mid-salinity peak during all study periods. Based on comprehensive datasets of barium in different phases (dissolved, suspended, clay fractions, and exchangeable fractions), the observed barium production has been linked with Ba desorption from the particulate matter by cationic (Mg) replacement during monsoon and post-monsoon seasons. Additionally, the barium supply via SGD has also been inferred for the pre-monsoon samples. In addition to the broad increasing trend, low-saline samples from the monsoon and post-monsoon seasons also show low-saline Ba removal through its adsorption on Fe-Mn hydroxides and/or organic matter. These observations establish the dominats role of ion-exchange processes in changing the riverine input of trace elements and their ultimate delivery to the open ocean.

6.1.3. Re concentrations and stable carbon isotopic study of the Chilika lagoon:

Rhenium concentrations and stable carbon isotopic compositions of the Chilika lagoon and its possible sources have been investigated for three different seasons. The Re concentrations do not follow the river-seawater mixing line, confirming the non-conservative gain/removal of Re in the Chilika. This gain in low-saline regimes during pre-monsoon season has been linked to the additional Re supply via submarine groundwater discharge. Besides the gain of Re, removal of dissolved Re has been observed across all the salinity range during three seasons. Based on the comprehensive datasets (such as, river and lagoonal sediments (in their bulk, clay and exchangeable fractions) and coastal macrophytes)), observed non-conservative removal of Re attributed to the adsorption of Re from the water column onto the Mg-Al rich clay and the uptake of Re by the macrophytes. These data show that the sedimentary Re in the Chilika has been scavenged by both detrital and authigenic pathways, in near equal proportions. Among the authigenic processes, about 60 % of Re has been scavenged *via* its incorporation on to Mg-Al rich clay substrates, whereas the remaining 40 % of Re follows biotic removal by its adsorption onto amino acids during cellular membrane formation of coastal macroalgae/macrophytes. The estimated authigenic burial rate of Re in the Chilika lagoon (~6×10^{-3} ng/cm^2/yr) is about 5 times higher than that reported for modern oxic sediments (~1.3×10^{-3} ng/cm^2/yr), underscoring importance of this coastal sink in oceanic rhenium cycle. Similar to rhenium, the seasonal and spatial distribution of DIC and $\delta^{13}C_{DIC}$ also show non-conservative behavior. The non-conservativeness of these two parameters is attributable to organic matter degradation and calcite precipitation in the Chilika lagoon. Additionally, sedimentary TOC and $\delta^{13}C_{org}$ values constrain that the organic matter buried in the lagoon are mainly supplied through terrestrial sources with minimal contribution from marine sources.

6.2. Future directions

Detailed investigation of selected trace elements and their isotopes (B, Ba, Re Sr, $\delta^{13}C$ and $^{87}Sr/^{86}Sr$) analysed in this study has led us to characterize and quantify the impact of coastal processes (SGD, ion-exchange, and biological process) affecting their distribution in the near-shore environments. During this thesis work, we realized that there exists future scope of research on the following few key aspects.

1. The quantification of SGD flux to coastal ocean depends greatly on the Sr isotopic composition of subsurface groundwater samples. Existing studies have mostly assumed that the SGD is characterized by fixed Sr and $^{87}Sr/^{86}Sr$ values. However, this thesis work shows that the SGD composition is highly variable in terms of Sr elemental and isotopic values in coastal regions. Therefore, it is crucial to better understand the subsurface processes that regulate variable isotopic composition for SGD and its precise flux estimation using Sr isotopes. This effort will also help in better constraining the role of SGD in explaining the existing oceanic imbalance.
2. This thesis work establishes authigenic boron removal onto clay surfaces in coastal lagoon systems. This observation led us to propose that the exchangeable-boron fraction in clays can retain authigenic oceanic signature and hence, can be used for paleo-pH reconstruction. This proposition may be validated by comparing boron isotopic values of foraminifera and exchangeable-B of clay minerals. A future study in this aspect will be useful in establishing potential of authigenic-boron (over analytical challenging foraminifera picking and cleaning approaches) for paleo-pH studies.
3. Significant scavenging of rhenium via macroalgae/macrophytes has been observed in this and a few earlier studies. This coastal sink for rhenium is currently not part of global ocean budget. It is important to carry more research on coastal behavior of rhenium and its biological uptake to better constrain the present-day oceanic Re budget.

References

Akhand, A., Chanda, A., Dutta, S., and Hazra, S. (2012). Air–water carbon dioxide exchange dynamics along the outer estuarine transition zone of Sundarban, northern Bay of Bengal, India. *Indian Journal of Marine Science*, 41 (2), 111-116.

Allègre, C. J., Louvat, P., Gaillardet, J., Meynadier, L., Rad, S. and Capmas, F. (2010). The fundamental role of island arc weathering in the oceanic Sr isotope budget. *Earth and Planetary Science Letters.*, 292, 51-56.

Alling, V., Porcelli, D., Morth C.M., Anderson L.G., Sanchez-Garcia L., Gustafsson O., Andersson P. S., and Humborg C. (2012). Degradation of terrestrial organic carbon, primary production and out-gassing of CO_2 in the Laptev and East Siberian Seas as inferred from $\delta^{13}C$ values of DIC. *Geochimica et Cosmochimica Acta*, 95, 143–159.

Amir, M., Paul, D., and Samal, R. N. (2019). Sources of organic matter in Chilika lagoon, India inferred from stable C and N isotopic compositions of particulates and sediments. *Journal of Marine System*, 194, 81-90.

Amir, M., Paul, D., and Malik, J. N. (2020). Geochemistry of Holocene sediments from Chilika Lagoon, India: inferences on the sources of organic matter and variability of the Indian summer monsoon. *Quaternary International*.

Anand, S., Rahaman, W., Lathika, N., Thamban, M., Patil, S. and Mohan, R. (2019). Trace elements and Sr, Nd isotope compositions of surface sediments in the Indian Ocean: An evaluation of sources and processes for sediment transport and dispersal. *Geochemistry, Geophysics, Geosystems*, 20 (6), 3090-3112.

Anbar, A. D., Creaser, R. A., Papanastassiou, D. A. and Wasserburg, G. J. (1992). Rhenium in seawater: Confirmation of generally conservative behavior. *Geochimica et Cosmochimica Acta*, *56*(11), 4099-4103.

Anderson, R. F., and Henderson, G. M. (2005). GEOTRACES. *Oceanography*, *18*(3), 76.

Andersson, P. S., Wasserburg, G. J., Ingri, J. and Stordal, M. C. (1994). Strontium, dissolved and particulate loads in fresh and brackish waters: the Baltic Sea and Mississippi Delta. *Earth and Planetary Science Letters*, 124, 195-210.

Bahr, A., Schönfeld, J., Hoffmann, J., Voigt, S., Aurahs, R., Kucera, M., Flögel, S., Jentzen, A. and Gerdes, A. (2013). Comparison of Ba/Ca and δOWATER18 as freshwater proxies: A multi-species core-top study on planktonic foraminifera from the vicinity of the Orinoco River mouth. *Earth and Planetary Science Letters*, *383*, 45-57.

Banerjee, K., Paneerselvam, A., Ramachandran, P., Ganguly, D., Singh, G., and Ramesh, R. (2018). Seagrass and macrophyte mediated CO_2 and CH_4 dynamics in shallow coastal waters. *PloS one*, 13(10), e0203922.

Barik, S. K., Bramha, S. N., Mohanty, A. K., Bastia, T. K., Behera, D., and Rath, P. (2016). Sequential extraction of different forms of phosphorus in the surface sediments of Chilika Lake. *Arabian Journal of Geosciences*, *9*(2), 135.

Barik, S. K., Bramha, S. N., Mohanty, A. K., Bastia, T. K., Behera, D., and Rath, P. (2016). Sequential extraction of different forms of phosphorus in the surface sediments of Chilika Lake. *Arabian Journal of Geosciences*, *9*(2), 135.

Barik, S. K., Muduli, P. R., Mohanty, B., Behera, A. T., Mallick, S., Das, A., Samal, R.N., Rastogi, G., and Pattnaik, A. K. (2017). Spatio-temporal variability and the impact of Phailin on water quality of Chilika lagoon. *Continental Shelf Research*, *136*, 39-56.

Barik, S. K., Muduli, P. R., Mohanty, B., Rath, P., and Samanta, S. (2018). Spatial distribution and potential biological risk of some metals in relation to granulometric content in core sediments from Chilika Lake, India. *Environmental Science and Pollution Research*, *25*(1), 572-587.

Barik, S. S., Prusty, P., Singh, R. K., Tripathy, S., Farooq, S. H., and Sharma, K. (2020). Seasonal and spatial variations in elemental distributions in surface sediments of Chilika Lake in response to change in salinity and grain size distribution. *Environmental Earth Sciences*, *79*(269), 269.

Barnes, R.S.K. (1980). Coastal Lagoons. *Cambridge University Press, Cambridge*, UK, 106.

Barth, S. (1998). $^{11}B/^{10}B$ variations of dissolved boron in a freshwater-seawater mixing plume (Elbe Estuary, North Sea). *Marine Chemistry*, 62, 1-14

Basu, A. R., Jacobsen, S. B., Poreda, R. J., Dowling, C. B. and Aggarwal, P. K. (2001). Large groundwater strontium flux to the oceans from the Bengal Basin and the marine strontium isotope record. *Science*, 293, 1470-1473.

Baudron, P., Cockenpot, S., Lopez-Castejon, F., Radakovitch, O., Gilabert, J., Mayer, A. and Claude, C. (2015). Combining radon, short-lived radium isotopes and hydrodynamic modeling to assess submarine groundwater discharge from an anthropized semiarid watershed to a Mediterranean lagoon (Mar Menor, SE Spain). *Journal of Hydrology*, 525, 55-71.

Beck, A. J., Charette, M. A., Cochran, J. K., Gonneea, M. E. and Peucker-Ehrenbrink, B. (2013). Dissolved strontium in the subterranean estuary–implications for the marine strontium isotope budget. *Geochimica et Cosmochimica Acta*, *117*, 33-52.

Berner, R. A. (1982). Burial of organic carbon and pyrite sulfur in the modern ocean: its geochemical and environmental significance. *American Journal of Science*, 282.

Bhavya, P. S., Kumar, S., Gupta, G. V. M., Sudharma, K. V., and Sudheesh, V. (2018). Spatio-temporal variation in $\delta^{13}C_{DIC}$ of a tropical eutrophic estuary (Cochin estuary, India) and adjacent Arabian Sea. *Continental Shelf Research*, 153, 75-85.

Bhushan, R., (2008). Geochemical and isotopic studies in sediments and waters of the northern Indian ocean. *Ph. D. Thesis, MS University of Baroda*, Vadodara, 137 pp.

Bhushan, R., Dutta, K., and Somayajulu, B. L. K. (2001). Concentrations and burial fluxes of organic and inorganic carbon on the eastern margins of the Arabian Sea. *Marine Geology*, *178*(1-4), 95-113.

Bourg, A.C. (1987). Trace metal adsorption modelling and particle-water interactions in estuarine environments. *Continental Shelf Research*, 7, 1319-1332.

Bowden, K. F. (1963). The mixing processes in a tidal estuary. *International Journal of Air and Water Pollution*, *7*(4–5), 343-356.

Boyle, E., Collier, R., Dengler, A. T., Edmond, J. M., Ng, A. C. and Stallard, R. F. (1974). Chemical mass balance in estuaries. *Geochimica et Cosmochimica Acta,* 38, 1719–1728.

Boyle, E.A., Edmond, J.M., and Sholkovitz, E.R. (1977). The mechanism of iron removal in estuaries. *Geochimica et Cosmochimica Acta*, 41, 1313-1324.

Broecker, Wallace S. and Tsung-Hung Peng (1982). *"Tracers in the Sea."* 125-159.

Brunskill, G.J., Zagorskis, I. and Pfitzner, J. (2003). Geochemical mass balance for lithium, boron, and strontium in the Gulf of Papua, Papua New Guinea (Project TROPICS). *Geochimica et Cosmochimica Acta*, 67, 3365-3383.

Burnett W. C., Cable J. E. and Corbett D. R. (2003). Radon tracing of submarine groundwater discharge in coastal environments. *In*: Land and Marine Hydrogeology (eds. M. Taniguchi, K. Wang and T. Gamo). *Elsevier Publications, Amsterdam, The Netherlands*, 25–43.

Burt, W.J., Thomas, H., Hagens, M., Pätsch, J., Clargo, N.M., Salt, L.A., Winde, V., and Böttcher, M.E., (2016). Carbon sources in the North Sea evaluated by means of radium and stable carbon isotope tracers. *Limnology and Oceanography*, 61, 666–683.

Cai, W.J., Hu, X., Huang, W.J., Murrell, M.C., Lehrter, J.C., Lohrenz, S.E., Chou, W.C., Zhai, W., Hollibaugh, J.T., Wang, Y. and Zhao, P., (2011). Acidification of subsurface coastal waters enhanced by eutrophication. *Nature geoscience*, *4*(11), 766-770.

Calvert, S. E., and Pedersen, T. F. (1993). Geochemistry of recent oxic and anoxic marine sediments: implications for the geological record. *Marine geology*, *113*(1-2), 67-88.

Campeau, A., Wallin, M. B., Giesler, R., Löfgren, S., Mörth, C. M., Schiff, S., Venkiteswaran, J.J., and Bishop, K. (2017). Multiple sources and sinks of dissolved inorganic carbon across Swedish streams, refocusing the lens of stable C isotopes. *Scientific Reports*, 7(1), 1-14.

Carrano, C.J., Schellenberg, S., Amin, S.A., Green, D.H. and Küpper, F. C. (2009). Boron and marine life: a new look at an enigmatic bioelement. *Marine Biotechnology* , 11, 431.

Carroll, J., Brown, E. T., and Moore, W. S. (1993). The role of the Ganges-Brahmaputra mixing zone in supplying barium and ^{226}Ra to the Bay of Bengal. *Geochimica et Cosmochimica Acta*, 57(13), 2981-2990.

Carter, S. C., Paytan, A., and Griffith, E. M. (2020). Toward an Improved Understanding of the Marine Barium Cycle and the Application of Marine Barite as a Paleoproductivity Proxy. *Minerals*, 10(5), 421.

Cauwet, G., and Sidorov, I. (1996). The biogeochemistry of Lena River: organic carbon and nutrients distribution. *Marine Chemistry*, 53(3-4), 211-227.

Chakrabarti, R., Mondal, S., Acharya, S. S., Lekha, J. S. and Sengupta, D. (2018). Submarine groundwater discharge derived strontium from the Bengal Basin traced in Bay of Bengal water samples. *Scientific Reports*, 8 (1), 4383.

Chakrapani, G. J., and Subramanian, V. (1990). Preliminary studies on the geochemistry of the Mahanadi river basin, India. *Chemical Geology*, 81(3), 241-253.

Charette, M. A., Buesseler, K. and Andrews, J. (2001). Utility of radium isotopes for evaluating the input and transport of groundwater-derived nitrogen to a Cape Cod estuary. *Limnology and Oceanography*, 46, 465-470.

Charette, M. A., Moore, W. S. and Burnett, W. C. (2008). Uranium-and thorium-series nuclides as tracers of submarine groundwater discharge. *In*: U-Th series nuclides in Aquatic systems Edited by S. Krishnaswami and J. K. Cochran, *Journal of Environmental Radioactivity*, *13*, 155-191.

Charette, M.A. and Sholkovitz, E.R., (2006). Trace element cycling in a subterranean estuary: Part 2. Geochemistry of the pore water. *Geochimica et Cosmochimica Acta*, *70*(4), 811-826.

Charette, M.A., Lam, P.J., Lohan, M.C., Kwon, E.Y., Hatje, V., Jeandel, C., Shiller, A.M., Cutter, G.A., Thomas, A., Boyd, P.W. and Homoky, W.B., (2016). Coastal ocean and shelf-sea biogeochemical cycling of trace elements and isotopes: lessons learned from GEOTRACES. *Philosophical Transactions of the Royal Society A: Mathematical, Physical and Engineering Sciences*, *374*(2081), 20160076.

Charette, M.A., Sholkovitz, E.R., and Hansel, C.M. (2005). Trace element cycling in a subterranean estuary: Part 1. Geochemistry of the permeable sediments. *Geochimica et Cosmochimica Acta*, 69, 2095-2109.

Chaudhuri S. and Clauer N. (1986). Fluctuations of isotopic composition of strontium in seawater during the Phanerozoic Eon. *Chemical Geology* 59, 293–303.

Chetelat, B., Liu, C. Q., Gaillardet, J., Wang, Q. L., Zhao, Z. Q., Liang, C. S., and Xiao, Y. K. (2009). Boron isotopes geochemistry of the Changjiang basin rivers. *Geochimica et Cosmochimica Acta*, 73(20), 6084-6097.

Cho, H.M., Kim, G., Kwon, E.Y., Moosdorf, N., Garcia-Orellana, J. and Santos, I.R. (2018). Radium tracing nutrient inputs through submarine groundwater discharge in the global ocean. *Scientific reports*, *8*(1), 1-7.

Coffey, M., Dehairs, F., Collette, O., Luther, G., Church, T. and Jickells, T. (1997). The behavior of dissolved barium in estuaries. *Estuarine, Coastal and Shelf Science*, 45, 113-121.

Colodner, D., Sachs, J., Ravizza, G., Turekian, K., Edmond, J. and Boyle, E. (1993). The geochemical cycle of rhenium: a reconnaissance. *Earth and Planetary Science Letters*, 117(1-2), 205-221.

Cooper, L. W., McClelland, J. W., Holmes, R. M., Raymond, P. A., Gibson, J. J., Guay, C. K., and Peterson, B. J. (2008). Flow weighted values of runoff tracers ($\delta^{18}O$, DOC, Ba, alkalinity) from the six largest Arctic rivers. *Geophysical Research Letters*, 35(18).

Costa, K.M., Anderson, R.F., McManus, J.F., Winckler, G., Middleton, J.L. and Langmuir, C.H., 2018. Trace element (Mn, Zn, Ni, V) and authigenic uranium (aU) geochemistry reveal sedimentary redox history on the Juan de Fuca Ridge, North Pacific Ocean. *Geochimica et Cosmochimica Acta*, *236*, pp.79-98.

Cotovicz Jr, L. C., Knoppers, B. A., Deirmendjian, L., and Abril, G. (2019). Sources and sinks of dissolved inorganic carbon in an urban tropical coastal bay revealed by $\delta^{13}C$-DIC signals. *Estuarine, Coastal and Shelf Science*, 220, 185-195.

Cotovicz Jr, L. C., Vidal, L. O., de Rezende, C. E., Bernardes, M. C., Knoppers, B. A., Sobrinho, R. L., Cardoso, R.P., Muniz, M., dos Anjos, R.M., Biehler, A., and Abril, G. (2020). Sources and sinks of CO_2 in the delta of the Paraíba do Sul River (Southeastern Brazil) modulated by carbonate thermodynamics, gas exchange and ecosystem metabolism during estuarine mixing. *Marine Chemistry*, 103869.

Crusius, J., Calvert, S., Pedersen, T. and Sage, D. (1996). Rhenium and molybdenum enrichments in sediments as indicators of oxic, suboxic and sulfidic conditions of deposition. *Earth and Planetary Science Letters*, 145(1-4), 65-78.

Cullings, K. W. (1992). Design and testing of a plant-specific PCR primer for ecological and evolutionary studies. *Molecular Ecology*, 1(4), 233-240.

Dalai, T. K., Singh, S. K., Trivedi, J. R. and Krishnaswami, S. (2002). Dissolved rhenium in the Yamuna River System and the Ganga in the Himalaya: Role of black shale weathering on the budgets of Re, Os, and U in rivers and CO_2 in the atmosphere. *Geochimica et Cosmochimica Acta*, 66(1), 29-43.

Danish, M., Tripathy, G. R., Panchang, R., Gandhi, N. and Prakash, S. (2019). Dissolved boron in a brackish-water lagoon system (Chilika lagoon, India): Spatial distribution and coastal behavior. *Marine Chemistry*, 214, 103663.

Danish, M., Tripathy, G. R., and Rahaman, W. (2020). Submarine groundwater discharge to a tropical coastal lagoon (Chilika lagoon, India): An estimation using Sr isotopes. *Marine Chemistry*, 103816.

Das, A. and Krishnaswami, S., (2006). Barium in Deccan Basalt Rivers: its abundance, relative mobility and flux. *Aquatic Geochemistry*, *12*(3), 221-238.

de la Paz, M., Gómez-Parra, A., and Forja, J. (2008). Tidal-to-seasonal variability in the parameters of the carbonate system in a shallow tidal creek influenced by anthropogenic inputs, Rio San Pedro (SW Iberian Peninsula). *Continental Shelf Research*, 28(10-11), 1394-1404.

Dean, W.E., Gardner, J.V. and Piper, D.Z., (1997). Inorganic geochemical indicators of glacial-interglacial changes in productivity and anoxia on the California continental margin. *Geochimica et Cosmochimica Acta*, *61*(21), 4507-4518.

Debnath, P., Das, K., Mukherjee, A., Ghosh, N. C., Rao, S., Kumar, S., Krishan, G. and Joshi, G. (2019). Seasonal-to-diurnal scale isotopic signatures of tidally-influenced submarine groundwater discharge to the Bay of Bengal: Control of hydrological cycle on tropical oceans. *Journal of Hydrology,* 571, 697-710.

Dehairs F., Chesselet R. and Jedwab J. (1980). Discrete suspended particles of barite and the barium cycle in the open ocean. *Earth and Planetary Science Letters,* 49, 528–550.

Doyle, J. J., and Doyle, J. L. (1987). A rapid DNA isolation procedure for small quantities of fresh leaf tissue. *Phytochem. Bull.*, 19:11–15.

Drever, J.I., (1988). The geochemistry of natural waters. *Englewood Cliffs: prentice Hall*.

Du Laing, G., Rinklebe, J., Vandecasteele, B., Meers, E. and Tack, F.M., (2009). Trace metal ehaviour in estuarine and riverine floodplain soils and sediments: a review. Sci Total Environ., 407, 3972-3985.

Duinker, J.C. and Nolting, R.F., (1978). Mixing, removal and mobilization of trace metals in the Rhine estuary. *Netherlands Journal of Sea Research*, (2).

Dutta, M. K., Kumar, S., Mukherjee, R., Sanyal, P., and Mukhopadhyay, S. K. (2019). The post-monsoon carbon biogeochemistry of the Hooghly–Sundarbans estuarine system under different levels of anthropogenic impacts. *Biogeosciences*, 16(2), 289-307.

Dyer, K.R., (1974). The salt balance in stratified estuaries. *Estuarine and coastal marine science*, *2*(3), 273-281.

Dymond, J., Suess, E. and Lyle, M. (1992). Barium in deep-sea sediment: A geochemical proxy for paleoproductivity. *Paleoceanography*, *7*(2), 163-181.

Edmond J. M., Boyle E. D., Drummond D., Grant B. and Mislick T. (1978). Desorption of barium in the plume of the Zaire (Congo) River. *Netherlands Journal of Sea Research,* 12, 324–328.

Edmond, J.M., Spivack, A., Grant, B.C.,Ming-Hui, H., Zexiam, C., Sung, C., and Xiushau, Z. (1985). Chemical dynamics of the Changjiang estuary. *Continental Shelf Research*, 4, 17-36.

Falkner K. K., Klinkhammer G. P., Bowers T. S., Todd J. F., Lewis B. L., Landing W. M. and Edmond J. M. (1993). The behavior of barium in anoxic marine waters. *Geochimica et Cosmochimica Acta,* 57, 537–544.

Fanning, K.A. and Maynard, V. I. (1978). Dissolved boron and nutrients in the mixing plumes of major tropical rivers. *Netherlands Journal of Sea Research*, 12, 345-354.

Feely, R.A., Alin, S.R., Newton, J., Sabine, C.L., Warner, M., Devol, A., Krembs, C. and Maloy, C. (2010). The combined effects of ocean acidification, mixing, and respiration on pH and carbonate saturation in an urbanized estuary. *Estuarine, Coastal and Shelf Science*, *88*(4), 442-449.

Finlay, J. C., and Kendall, C. (2007). Stable isotope tracing of temporal and spatial variability in organic matter sources to freshwater ecosystems. *Stable isotopes in ecology and environmental science*, 2, 283-333.

Flegal, A.R., Smith, G.J., Gill, G.A., Sanudo-Wilhelmy, S. and Anderson, L.C.D. (1991). Dissolved trace element cycles in the San Francisco Bay estuary. *Marine Chemistry*, 36, 329-363.

Francois, R., Honjo, S., Manganini, S.J. and Ravizza, G.E., 1995. Biogenic barium fluxes to the deep sea: Implications for paleoproductivity reconstruction. *Global Biogeochemical Cycles*, *9*(2), pp.289-303.

Gaillardet, J. and Lemarchand, D., (2018). Boron in the weathering environment. In *Boron Isotopes* (163-188). Springer, Cham.

Gaillardet, J., Lemarchand, D., Göpel, C., and Manhès, G. (2001). Evaporation and sublimation of boric acid: application for boron purification from organic rich solutions. Geostandards Newsletter, 25(1), 67-75.

Garcia-Solsona, E., Masqué, P., Garcia-Orellana, J., Rapaglia, J., Beck, A. J., Cochran, J. K., Bokuniewicz, H., Zaggia, L. and Collavini, F. (2008). Estimating submarine groundwater discharge around Isola La Cura, northern Venice Lagoon (Italy), by using the radium quartet. *Marine Chemistry*, 109 (3-4), 292-306.

Gat, J. and Gonfiantini, R. (1981). Stable isotope hydrology: Deuterium and Oxygen-18 in the water cycle. IAEA technical report, 210, 339 pp.

Gattuso, J.P., Frankignoulle, M. and Wollast, R., (1998). Carbon and carbonate metabolism in coastal aquatic ecosystems. *Annual Review of Ecology and Systematics*, *29*(1), 405-434.

GEOTRACES, (2006). GEOTRACES Science Plan. http://www.geotraces.org/libraries/documents/Science_plan.pdf.

Ghosh, A. K., Pattnaik, A. K. and Ballatore, T. J. (2006). Chilika Lagoon: Restoring ecological balance and livelihoods through re-salinization. *Lakes and Reservoirs: Research and Management*, 11 (4), 239-255.

Ghosh, S.K. and Jana, T.K. (1993) Boron-boric acid complexes in estuarine water of River Hugli, east coast of India. *Indian Journal of Marine Sciences*, 22, 225-226.

Goldberg, S. (1997). Reactions of boron with soils. *Plant and soil*, 193(1), 35-48.

Goldstein, S.J. and Jacobsen, S.B., (1988). Nd and Sr isotopic systematics of river water suspended material: implications for crustal evolution. *Earth and Planetary Science Letters*, *87*(3), 249-265.

Gonneea, M. E., and Paytan, A. (2006). Phase associations of barium in marine sediments. *Marine Chemistry*, 100(1-2), 124-135.

Gonneea, M. E., Charette, M. A., Liu, Q., Herrera-Silveira, J. A., and Morales-Ojeda, S. M. (2014). Trace element geochemistry of groundwater in a karst subterranean estuary (Yucatan Peninsula, Mexico). *Geochimica et Cosmochimica Acta*, 132, 31-49.

Gonneea, M. E., Mulligan, A. E., and Charette, M. A. (2013). Seasonal cycles in radium and barium within a subterranean estuary: Implications for groundwater derived chemical fluxes to surface waters. *Geochimica et Cosmochimica Acta*, 119, 164-177.

Goswami, V., Singh, S. K. and Bhushan, R. (2014). Impact of water mass mixing and dust deposition on Nd concentration and ε_{Nd} of the Arabian Sea water column. *Geochimica et Cosmochimica Acta*, 145, 30-49.

Goswami, V., Singh, S. K. and Bhushan, R. (2012). Dissolved redox sensitive elements, Re, U and Mo in intense denitrification zone of the Arabian Sea. *Chemical Geology*, 291, 256-268.

Griffin, D.A. and LeBlond, P.H., (1990). Estuary/ocean exchange controlled by spring-neap tidal mixing. *Estuarine, Coastal and Shelf Science*, *30*(3), 275-297.

Guay, C. K., and Falkner, K. K. (1998). A survey of dissolved barium in the estuaries of major Arctic rivers and adjacent seas. *Continental Shelf Research*, 18(8), 859-882.

Gupta, G.V.M., Sarma, V.V.S.S., Robin, R.S., Raman, A.V., Kumar, M.J., Rakesh, M., and Subramanian, B.R. (2008). Influence of net ecosystem metabolism in transferring riverine organic carbon to atmospheric CO_2 in a tropical coastal lagoon (Chilka Lake, India). *Biogeochemistry*, 87, 265-285.

Gupta, S. K. and Chen, K. Y. (1975). Partitioning of trace metals in selective chemical fractions of nearshore sediments. *Environmental Research Letters*, 10(2), 129-158.

Hanor, J. S., and Chan, L. H. (1977). Non-conservative behavior of barium during mixing of Mississippi River and Gulf of Mexico waters. *Earth and Planetary Science Letters*, 37(2), 242-250.

Harriss, R. C. (1969). Boron regulation in the oceans. *Nature*, 223 (5203), 290.

Helz, G. R., and Dolor, M. K. (2012). What regulates rhenium deposition in euxinic basins?. *Chemical Geology*, *304*, 131-141.

Henkel R (1952). Ernährungsphysiologische Untersuchungen an Meeresalgen, insbesondere an *Bangia pumila*. Kiel Meeresforsch 8:192–211.

Herczeg, A. L., & Fairbanks, R. G. (1987). Anomalous carbon isotope fractionation between atmospheric CO_2 and dissolved inorganic carbon induced by intense photosynthesis. *Geochimica et Cosmochimica Acta*, 51(4), 895-899.

Herdendorf. C. (1982). Largest lakes of the world. *Journal of Great Lakes Research*, 8, 379-412.

Hollander, D. J., and McKenzie, J. A. (1991). CO_2 control on carbon-isotope fractionation during aqueous photosynthesis: A paleo-pCO_2 barometer. *Geology*, 19(9), 929-932.

Horner, T., Little, S., Conway, T., Farmer, J., Hertzberg, J., Lough, A., Mckay, J., Tessin, A., Galer, S., Jaccard, S. and Lacan, F., 2020. Bioactive trace metals and their isotopes as paleoproductivity proxies: An assessment using GEOTRACES-era data.

Hsieh, Y.T. and Henderson, G.M., (2017). Barium stable isotopes in the global ocean: Tracer of Ba inputs and utilization. *Earth and Planetary Science Letters*, *473*, 269-278.

Huang, K. F. and You, C. F. (2007). Tracing freshwater plume migration in the estuary after a typhoon event using Sr isotopic ratios. *Geophysical Research Letters*, *34*(2).

Huang, K. F., You, C. F., Chung, C. H. and Lin, I. T. (2011). Nonhomogeneous seawater Sr isotopic composition in the coastal oceans: A novel tool for tracing water masses and submarine groundwater discharge. *Geochemistry, Geophysics, Geosystems*, 12 (5), 1-14.

Ilina, S. M., Viers, J., Lapitsky, S. A., Mialle, S., Mavromatis, V., Chmeleff, J. and Pokrovsky, O. S. (2013). Stable (Cu, Mg) and radiogenic (Sr, Nd) isotope fractionation in colloids of boreal organic-rich waters. *Chemical Geology*, 342, 63-75.

Ingram, B. L. and Sloan, D. (1992). Strontium isotopic composition of estuarine sediments as paleosalinity-paleoclimate indicator. *Science*, 255 (5040), 68-72.

Ingri, J., Widerlund, A., Suteerasak, T., Bauer, S., and Elming, S. Å. (2014). Changes in trace metal sedimentation during freshening of a coastal basin. *Marine Chemistry*, 167, 2-12.

Jain, S.K., Agarwal, P.K. and Singh, V.P. (2007) Hydrology and water resources of India (Vol.57). Springer publishers, The Netherlands, 1258.

Jeandel, C., Dupré, B., Lebaron, G., Monnin, C., and Minster, J. F. (1996). Longitudinal distributions of dissolved barium, silica and alkalinity in the western and southern Indian Ocean. *Deep-Sea Research Part I: Oceanographic Research Papers*, 43(1), 1-31.

Ji, T., Du, J., Moore, W. S., Zhang, G., Su, N. and Zhang, J. (2013). Nutrient inputs to a Lagoon through submarine groundwater discharge: The case of Laoye Lagoon, Hainan, China. *Journal of Marine system*, 111, 253-262.

Joung, D., and Shiller, A. M. (2014). Dissolved barium behavior in Louisiana Shelf waters affected by the Mississippi/Atchafalaya River mixing zone. *Geochimica et Cosmochimica Acta*, 141, 303-313.

Kanuri, V.V., Muduli, P.R., Robin, R.S., Patra, S., Gupta, G.V.M., Rao, G.N., Raman, A.V. and Subramanian, B.R., (2018). Bioavailable dissolved organic matter and its spatio-temporal variation in a river dominated tropical brackish water Lagoon, India. *Marine pollution bulletin*, *131*, 460-467.

Kendall, B., Creaser, R. A. and Selby, D. (2009). ^{187}Re-^{187}Os geochronology of Precambrian organic-rich sedimentary rocks. *Geological Society, London, Special Publications*, -326(1), 85-107.

Keren, R. and Mezuman, U. (1981). Boron adsorption by clay minerals using a phenomenological equation. *Clays Clay Minerals*, 29, 198-204.

Knee, K. and Paytan, A., (2011). Submarine groundwater discharge: a source of nutrients, metals, and pollutants to the Coastal Ocean. *Treatise on Estuarine and Coastal Science*, *4*, 205-234.

Krishna, M.S., Naidu, S.A., Subbaiah, C.V., Sarma, V.V.S.S. and Reddy, N.P.C., (2013). Distribution and sources of organic matter in surface sediments of the eastern continental margin of India. *Journal of Geophysical Research: Biogeosciences*, *118*(4), pp.1484-1494.

Kumar, A., Equeenuddin, S. M., Mishra, D. R., and Acharya, B. C. (2016). Remote monitoring of sediment dynamics in a coastal lagoon: Long-term spatio-temporal variability of suspended sediment in Chilika. *Estuarine, Coastal and Shelf Science*, 170, 155-172.

Kwon, E. Y., Kim, G., Primeau, F., Moore, W. S., Cho, H. M., DeVries, T. and Cho, Y. K. (2014). Global estimate of submarine groundwater discharge based on an observationally constrained radium isotope model. *Geophysical Research Letters*, 41 (23), 8438-8444.

Lea, D. and Boyle, E. (1989). Barium content of benthic foraminifera controlled by bottom-water composition. *Nature*, 338(6218), 751.

Lécuyer, C., Bodergat, A.M., Martineau, F., Fourel, F., Gürbüz, K. and Nazik, A., (2012). Water sources, mixing and evaporation in the Akyatan lagoon, Turkey. Estuarine, *Coastal and Shelf Science*, 115,200-209.

Lee, K., Kim, T.W., Byrne, R.H., Millero, F.J., Feely, R.A. and Liu, Y.M. (2010) The universal ratio of boron to chlorinity for the North Pacific and North Atlantic oceans. *Geochimica et Cosmochimica Acta*, 74, 1801-1811.

Leeman, W.P., and Sisson, V.B., (1996). Geochemistry of boron and its implications for crustal and mantle processes. In: Grew, E.S., Anovitz, L.M. (Eds.), Boron: Mineralogy, Petrology and Geochemistry. *Reviews in Mineralogy and Geochmistry*, 33: 644–707.

Lemarchand, D., Gaillardet, J., Lewin, E. and Allegre, C. J. (2000) The influence of rivers on marine boron isotopes and implications for reconstructing past ocean pH. *Nature*, 408, 951-954.

Lemarchand, D., Gaillardet, J., Lewin, E. and Allegre, C.J., (2002). Boron isotope systematics in large rivers: implications for the marine boron budget and paleo-pH reconstruction over the Cenozoic. *Chemical Geology*, *190*(1-4), 123-140.

Li Y. H., Burkhardt L. and Teraoka H. (1984). Desorption and coagulation of trace elements during estuarine mixing. *Geochimica et Cosmochimica Acta*, 48, 1879–1884.

Li, Y. H. and Chan, L. H. (1979). Desorption of Ba and ^{226}Ra from river-borne sediments in the Hudson estuary. *Earth and Planetary Science Letters*, 43(3), 343-350.

Liddicoat, M.I., Turner, D.R. and Whitfield, M. (1983). Conservative behavior of boron in the Tamar Estuary. *Estuarine, Coastal and Shelf Science*, 17, 467-472.

Liss, P.S. and Pointon, M.J. (1973). Removal of dissolved boron and silicon during estuarine mixing of sea and river waters. *Geochimica et Cosmochimica Acta*, 37, 1493-1498.

Luoma, S.N., (1983). Bioavailability of trace metals to aquatic organisms-a review. *Science of the total environment*, *28*(1-3), 1-22.

Madhusmita, T. (2012). Biodiversity of Chilika and its conservation, Odisha, India. *International Research Journal of Environmental Sciences*, 1 (5), 54-57.

Mahanty, M.M., Mohanty, P.K., Panda, U.S., Pradhan, S., Samal, R.N. and Rao, V.R. (2015). Characterization of tidal and non-tidal variations in the Chilika lagoon on the east coast of India. *International journal of scientific and engineering research*, 6, 564-571.

Mahanty, M.M., Mohanty, P.K., Pattnaik, A.K., Panda, U.S., Pradhan, S. and Samal, R.N. (2016). Hydrodynamics, temperature/salinity variability and residence time in the Chilika lagoon during dry and wet period: Measurement and modeling. *Continental Shelf Research*, 125, 28-43.

Mao, H. R., Liu, C. Q., and Zhao, Z. Q. (2019). Source and evolution of dissolved boron in rivers: Insights from boron isotope signatures of end-members and model of boron isotopes during weathering processes. *Earth Science Reviews*, 190, 439-459.

McManus, J.F., Oppo, D.W. and Cullen, J.L., (1999). A 0.5-million-year record of millennial-scale climate variability in the North Atlantic. *Science*, *283*(5404), 971-975.

McManus, J.F., Oppo, D.W. and Cullen, J.L., (1999). A 0.5-million-year record of millennial-scale climate variability in the North Atlantic. *Science*, *283*(5404), 971-975.

Meybeck, M., and Vörösmarty, C. (1999). Global transfer of carbon by rivers. *Global Change Newsletter*, 37, 18-19.

Miller, C. A., Peucker-Ehrenbrink, B. and Schauble, E. A. (2015). Theoretical modeling of rhenium isotope fractionation, natural variations across a black shale weathering profile, and potential as a paleoredox proxy. *Earth and Planetary Science Letters*, 430, 339-348.

Miller, C. A., Peucker-Ehrenbrink, B., Walker, B. D. and Marcantonio, F. (2011). Re-assessing the surface cycling of molybdenum and rhenium. *Geochimica et Cosmochimica Acta*, 75(22), 7146-7179.

Mishra, S.P. and Jena, J.G. (2013). Characteristics of western catchment and their inflow contribution to Chilika Lagoon, Odisha (India). *International Journal of Lakes and Rivers*, 6(2), 119-129.

Moon S., Huh Y., Qin J. and van Pho N. (2007). Chemical weathering in the Hong (Red) River basin: rates of silicate weathering and their controlling factors. *Geochimica et Cosmochimica Acta* 71, 1411–1430.

Moore, W. S. (1996). Large groundwater inputs to coastal waters revealed by ^{226}Ra enrichments. *Nature*, 380 (6575), 612.

Moore, W. S. (1997). High fluxes of radium and barium from the mouth of the Ganges-Brahmaputra River during low river discharge suggest a large groundwater source. *Earth and Planetary Science Letters*, 150 (1-2), 141-150.

Moore, W. S. (1999). The subterranean estuary: a reaction zone of ground water and sea water. *Marine Chemistry*, 65 (1-2), 111-125.

Moore, W. S. (2010). The effect of submarine groundwater discharge on the ocean. *Annual Review of Marine Science*, *2*, 59-88.

Moore, W.S. (1999) The subterranean estuary: a reaction zone of ground water and sea water. *Marine Chemistry*, 65, 111-125.

Morel, F.M. and Price, N.M., (2003). The biogeochemical cycles of trace metals in the oceans. *Science*, *300*(5621), 944-947.

Morford, J. L., Emerson, S. R., Breckel, E. J., and Kim, S. H. (2005). Diagenesis of oxyanions (V, U, Re, and Mo) in pore waters and sediments from a continental margin. *Geochimica et Cosmochimica Acta*, *69*(21), 5021-5032.

Morford, J. L., Martin, W. R., and Carney, C. M. (2012). Rhenium geochemical cycling: Insights from continental margins. *Chemical Geology*, *324*, 73-86.

Morford, J.L., Russell, A.D. and Emerson, S. (2001). Trace metal evidence for changes in the redox environment associated with the transition from terrigenous clay to diatomaceous sediment, Saanich Inlet, BC. *Marine Geology* 174, 355–369.

Muduli, P.R., Kanuri, V.V., Robin, R.S., Kumar, B.C., Patra, S., Raman, A.V., and Subramanian, B.R. (2013). Distribution of dissolved inorganic carbon and net ecosystem production in a tropical brackish water lagoon, India. *Continental Shelf Research*, 64, 75-87.

Muduli, P.R., Kanuri, V.V., Robin, R.S., Kumar, B.C., Patra, S., Raman, A.V., Rao, G.N. and Subramanian, B.R., (2012). Spatio-temporal variation of CO_2 emission from Chilika Lake, a tropical coastal lagoon, on the east coast of India. *Estuarine, Coastal and Shelf Science*, *113*, 305-313.

Mukherjee, R., Kumar, S. and Muduli, P.R., (2019). Spatial variation of nitrogen uptake rates in the largest brackish water lagoon of Asia (Chilika, India). *Estuarine, Coastal and Shelf Science*, *216*, 87-97.

Murray, J.W., (1987). Mechanisms controlling the distribution of trace elements in oceans and lakes. *American Chemical Society.*

Nameroff, T.J., Balistrieri, L.S. and Murray, J.W., (2002). Suboxic trace metal geochemistry in the eastern tropical North Pacific. *Geochimica et Cosmochimica Acta*, *66*(7), 1139-1158.

Narvekar, P.V. and Zingde, M.D. (1987). Behavior of boron, calcium and magnesium in Purna and Auranga estuaries (Gujarat), west coast of India. *Indian Journal of Marine Science*, 16, 46-50.

Narvekar, P.V., Zingde, M.D. and Dalal, V.K. (1983). Behavior of boron, calcium and magnesium in a polluted estuary. *Estuarine, Coastal and Shelf Science*, 16, 9-16.

Narvekar, P.V., Zingde, M.D. and Dalal, V.N. (1981). Behavior of Boron, Calcium & Magnesium in Mindola River Estuary (Gujarat). *Indian Journal of Marine Sciences*, 10, 90-92.

Nayak, B.K., Acharya, B.C., Panda, U.C., Nayak, B.B. and Acharya, S.K., (2004). Variation of water quality in Chilika lake, Orissa. *Indian Journal of Marine Sciences*, 33, 164-169.

Nazneen, S. and Raju, N.J., 2017. Distribution and sources of carbon, nitrogen, phosphorus and biogenic silica in the sediments of Chilika lagoon. *Journal of Earth System Science*, *126*(1), 13.

Négrel, P., Allègre, C. J., Dupré, B. and Lewin, E. (1993). Erosion sources determined by inversion of major and trace element ratios and strontium isotopic ratios in river water: the Congo Basin case. *Earth and Planetary Science Letters*, 120 (1-2), 59-76.

Nepf, H.M. and Geyer, W.R., (1996). Intratidal variations in stratification and mixing in the Hudson estuary. *Journal of Geophysical Research: Oceans*, *101*(C5), 12079-12086.

Nicholls, R.J., Wong, P.P., Burkett, V., Codignotto, J., Hay, J., McLean, R., Ragoonaden, S., Woodroffe, C.D., Abuodha, P.A.O., Arblaster, J. and Brown, B., (2007). *Coastal systems and low-lying areas*.

Novo, L. A., Mahler, C. F., and González, L. (2015). Plants to harvest rhenium: scientific and economic viability. *Environmental Chemistry Letters*, 13 (4), 439-445.

Nozaki, Y., Yamamoto, Y., Manaka, T., Amakawa, H., and Snidvongs, A. (2001). Dissolved barium and radium isotopes in the Chao Phraya River estuarine mixing zone in Thailand. *Continental Shelf Research*, 21(13-14), 1435-1448.

Olafsson, J., and Riley, J. P. (1972). Some data on the marine geochemistry of rhenium. *Chemical Geology*, *9*(1-4), 227-230.

Padmavathi, D. and Satyanarayana, D. (1999). Distribution of nutrients and major elements in riverine, estuarine and adjoining coastal waters of Godavari, Bay of Bengal. *Indian Journal of Marine Sciences*, 28, 345-354.

Panchang, R., and Nigam, R. (2012). High resolution climatic records of the past~ 489 years from Central Asia as derived from benthic foraminiferal species, Asterorotalia trispinosa. *Marine Geology*, 307, 88-104.

Panigrahi, S., Acharya, B.C., Panigrahy, R.C., Nayak, B.K., Banarjee, K. and Sarkar, S.K. (2007). Anthropogenic impact on water quality of Chilika lagoon RAMSAR site: a statistical approach. *Wetlands Ecology and Management*, *15*(2), 113-126.

Panigrahi, S., Wikner, J., Panigrahy, R.C., Satapathy, K.K. and Acharya, B.C. (2009). Variability of nutrients and phytoplankton biomass in a shallow brackish water ecosystem (Chilika Lagoon, India). *Limnology*, 10, 73-85.

Panigrahi, S., Wikner, J., Panigrahy, R.C., Satapathy, K.K. and Acharya, B.C. (2009) Variability of nutrients and phytoplankton biomass in a shallow brackish water ecosystem (Chilika Lagoon, India). *Limnology*, 10, 73-85.

Park, H. and Schlesinger, W.H. (2002). Global biogeochemical cycle of boron. *Global Biogeochemical Cycles*, 16, 1072.

Patra, S., Ganguly, D., Tiwari, M., Kanuri, V., Muduli, P.R., Robin, R.S., Abhilash, K.R., Charan Kumar, B., Nagoji, S.S., Raman, A.V. and Subramanian, B.R., (2017). Isotopic composition (C & N) of the suspended particles and N uptake by phytoplankton in a shallow tropical coastal lagoon. *Chemistry and Ecology*, *33*(8), 708-724.

Patra, S., Raman, A.V., Ganguly, D., Robin, R.S., Muduli, P.R., Kanuri, V., Abhilash, K.R., Kumar, B.C. and Subramanian, B.R., (2016). Influence of suspended particulate matter on nutrient biogeochemistry of a tropical shallow lagoon, Chilika, India. *Limnology*, *17*(3), 223-238.

Paytan, A. and Kastner, M., 1996. Benthic Ba fluxes in the central Equatorial Pacific, implications for the oceanic Ba cycle. *Earth and Planetary Science Letters*, *142*(3-4), pp.439-450.

Paytan, A., Kastner, M. and Chavez, F.P., (1996). Glacial to interglacial fluctuations in productivity in the equatorial Pacific as indicated by marine barite. *Science*, *274*(5291), 1355-1357.

Pelletier, E. and Lebel, J. (1978). Détermination du bore inorganique dans l'Estuaire du Saint-Laurent. *Canadian Journal of Earth Sciences*, 15(4), 618-625.

Pencharee, S., Faber, P. A., Ellis, P. S., Cook, P., Intaraprasert, J., Grudpan, K., and McKelvie, I. D. (2012). Underway determination of dissolved inorganic carbon in estuarine waters by gas-diffusion flow analysis with C 4 D detection. *Analytical Methods*, 4(5), 1278-1283.

Petelet-Giraud, E., Klaver, G., and Negrel, P. (2009). Natural versus anthropogenic sources in the surface-and groundwater dissolved load of the Dommel river (Meuse basin): constraints by boron and strontium isotopes and gadolinium anomaly. *Journal of Hydrology*, 369 (3-4), 336-349.

Peucker-Ehrenbrink, B. and Fiske, G. J. (2019). A continental perspective of the seawater $^{87}Sr/^{86}Sr$ record: A review. *Chemical Geology*, 510, 140-165.

Peucker-Ehrenbrink, B. and Jahn, B.M., (2001). Rhenium-osmium isotope systematics and platinum group element concentrations: Loess and the upper continental crust. *Geochemistry, Geophysics, Geosystems*, *2*(10).

Peucker-Ehrenbrink, B., Miller, M.W., Arsouze, T. and Jeandel, C., (2010). Continental bedrock and riverine fluxes of strontium and neodymium isotopes to the oceans. *Geochemistry, Geophysics, Geosystems*, *11*(3).

Planavsky, N. J., Slack, J. F., Cannon, W. F., O'Connell, B., Isson, T. T., Asael, D., Jackson, J.C., Hardisty, D.S., Lyons, T. W. and Bekker, A. (2018). Evidence for episodic oxygenation in a weakly redox-buffered deep mid-Proterozoic ocean. *Chemical Geology*, 483, 581-594.

Pokrovsky, O. S. and Schott, J. (2002). Iron colloids/organic matter associated transport of major and trace elements in small boreal rivers and their estuaries (NW Russia). *Chemical Geology*, 190(1-4), 141-179.

Prouty, N. G., Roark, E. B., Koenig, A. E., Demopoulos, A. W., Batista, F. C., Kocar, B. D., Selby, D., McCarthy, M.D., Mienis, F. and Ross, S. W. (2014). Deep-sea coral record of human impact on watershed quality in the Mississippi River Basin. *Global Biogeochemical Cycles*, 28(1), 29-43.

Rabouille, C., Mackenzie, F.T. and Ver, L.M., (2001). Influence of the human perturbation on carbon, nitrogen, and oxygen biogeochemical cycles in the global coastal ocean. *Geochimica et Cosmochimica Acta*, *65*(21), 3615-3641.

Racionero-Gómez, B., A. D. Sproson, D. Selby, Abdelmouhcine Gannoun, D. R. Gröcke, H. C. Greenwell, and Burton, K. W. (2017). Osmium uptake, distribution, and $^{187}Os/^{188}Os$ and

$^{187}Re/^{188}Os$ compositions in Phaeophyceae macroalgae, Fucus vesiculosus: Implications for determining the $^{187}Os/^{188}Os$ composition of seawater. *Geochimica et Cosmochimica Acta* 199, 48-57.

Racionero-Gómez, B., A. D. Sproson, D. Selby, Abdelmouhcine Gannoun, D. R. Gröcke, H. C. Greenwell, and Burton, K. W. (2017). Osmium uptake, distribution, and $^{187}Os/^{188}Os$ and $^{187}Re/^{188}Os$ compositions in Phaeophyceae macroalgae, Fucus vesiculosus: Implications for determining the $^{187}Os/^{188}Os$ composition of seawater. *Geochimica et Cosmochimica Acta* 199, 48-57.

Racionero-Gómez, B., Sproson, A. D., Selby, D., Gröcke, D. R., Redden, H., and Greenwell, H. C. (2016). Rhenium uptake and distribution in phaeophyceae macroalgae, Fucus vesiculosus. *Royal Society Open Science*, 3(5), 160161.

Rahaman, W. and Singh, S. K. (2012). Sr and $^{87}Sr/^{86}Sr$ in estuaries of western India: Impact of submarine groundwater discharge. *Geochimica et Cosmochimica Acta*, 85, 275-288.

Rahaman, W., and Singh, S. K. (2010). Rhenium in rivers and estuaries of India: Sources, transport and behavior. *Marine Chemistry*, 118 (1-2), 1-10.

Rahaman, W., Singh, S. K. and Raghav, S. (2011). Dissolved Mo and U in rivers and estuaries of India: Implication to geochemistry of redox sensitive elements and their marine budgets. *Chemical Geology*, 278, 160-172.

Rahaman, W., Singh, S. K., and Shukla, A. D. (2012). Rhenium in Indian rivers: Sources, fluxes, and contribution to oceanic budget. *Geochemistry, Geophysics, Geosystems*, 13(8).

Rajagopal, M.D., Rajendran, A. and Reddy, C.V.G. (1981) Distribution of dissolved boron in the waters of the Zuari estuary (Goa). *Indian Journal of Marine Sciences*, 10, 20-23.

Ramaswamy, V., Gaye, B., Shirodkar, P.V., Rao, P.S., Chivas, A.R., Wheeler, D. and Thwin, S., 2008. Distribution and sources of organic carbon, nitrogen and their isotopic signatures in sediments from the Ayeyarwady (Irrawaddy) continental shelf, northern Andaman Sea. *Marine Chemistry*, *111*(3-4), pp.137-150.

Rath, J., and Adhikary, S. P. (2005). Distribution of marine macro-algae at different salinity gradients in Chilika lake, east coast of India. *Indian Journal of Marine Sciences*, 34 (2), 237-241.

Ravizza, G., and Turekian, K. K. (1989). Application of the ^{187}Re-^{187}Os system to black shale geochronometry. *Geochimica et Cosmochimica Acta*, 53 (12), 3257-3262.

Regnier, P., Friedlingstein, P., Ciais, P., Mackenzie, F.T., Gruber, N., Janssens, I.A., Laruelle, G.G., Lauerwald, R., Luyssaert, S., Andersson, A.J. and Arndt, S., (2013). Anthropogenic perturbation of the carbon fluxes from land to ocean. *Nature geoscience, 6*(8), 597-607.

Rengarajan, R. and Sarma, V. V. S. S. (2015). Submarine groundwater discharge and nutrient addition to the coastal zone of the Godavari estuary. *Marine Chemistry*, 172, 57-69.

Richter, F.M., Rowley, D.B. and DePaolo, D.J., (1992). Sr isotope evolution of seawater: the role of tectonics. *Earth and Planetary Science Letters*, *109*(1-2), 11-23.

Rodellas, V., Garcia-Orellana, J., Masque, P., Feldman, M. and Weinstein, Y. (2015). Submarine groundwater discharge as a major source of nutrients to the Mediterranean Sea. *Proc. Natl. Acd. Sci*., 112, 3926-3930.

Rooney, A. D., Selby, D., Lloyd, J. M., Roberts, D. H., Lückge, A., Sageman, B. B., and Prouty, N. G. (2016). Tracking millennial-scale Holocene glacial advance and retreat using osmium isotopes: Insights from the Greenland ice sheet. *Quaternary Science Reviews*, 138, 49-61.

Rubin, S. I., King, S. L., Jahnke, R. A., and Froelich, P. N. (2003). Benthic barium and alkalinity fluxes: Is Ba an oceanic paleo-alkalinity proxy for glacial atmospheric CO_2?. *Geophysical Research Letters*, 30 (17).

Rudnick, R.L. and Gao, S. (2003). Composition of the continental crust. *Treatise on Geochemistry*, 3, 1-65.

Russak, A., Sivan, O. and Yechieli, Y. (2016). Trace elements (Li, B, Mn and Ba) as sensitive indicators for salinization and freshening events in coastal aquifers. *Chemical Geology*, 441, 35 46.

Sahu, B.K., Pati, P. and Panigrahy, R.C. (2014). Environmental conditions of Chilika Lake during pre and post hydrological intervention: an overview. *Journal of Coastal Conservation* , 18, 285-297.

Saldi, G., Noireaux, J., Louvat, P., Faure, L., Balan, E., Schott, J. and Gaillardet, J. (2018). Boron isotopic fractionation during adsorption by calcite-implication for the seawater pH proxy. *Geochimica et Cosmochimica Acta*, 240, 255-273.

Salomons, W. (1980). Adsorption processes and hydrodynamic conditions in estuaries. *Environmental technology*, 1, 356-365.

Samanta, S. and Dalai, T.K. (2016). Dissolved and particulate Barium in the Ganga (Hooghly) River estuary, India: Solute-particle interactions and the enhanced dissolved flux to the oceans. *Geochimica et Cosmochimica Acta*, 195, 1-28.

Samanta, S., Dalai, T. K., Pattanaik, J. K., Rai, S. K., and Mazumdar, A. (2015). Dissolved inorganic carbon (DIC) and its $\delta^{13}C$ in the Ganga (Hooghly) River estuary, India: Evidence of DIC generation via organic carbon degradation and carbonate dissolution. *Geochimica et Cosmochimica Acta*, 165, 226-248.

Santos, I.R., Burnett, W.C., Misra, S., Suryaputra, I.G.N.A., Chanton, J.P., Dittmar, T., Peterson, R.N. and Swarzenski, P.W., (2011). Uranium and barium cycling in a salt wedge subterranean estuary: the influence of tidal pumping. *Chemical Geology*, *287*(1-2), 114-123.

Sánchez-Quiles, D., Marbà, N. and Tovar-Sánchez, A., (2017). Trace metal accumulation in marine macrophytes: hotspots of coastal contamination worldwide. *Science of The Total Environment*, *576*, pp.520-527.

Sarkar, S., Bhattacharya, A., Bhattacharya, A., Satapathy, K., Mohanty, A. and Panigrahi, S. (2012). Chilika Lake. In: Encylopedia of lakes and reservoirs, 148-156. Springer publications, Dordrecht.

Schlesinger, W.H. and Vengosh, A. (2016). Global boron cycle in the Anthropocene. *Global Biogeochemical Cycles.*, 30, 219-230.

Schwarcz, H., Agyei, E. and McMullen, C. (1969). Boron isotopic fractionation during clay adsorption from sea-water. *Earth and Planetary Science Letters*, 6, 1-5.

SCOR Working Group, (2007). GEOTRACES–An international study of the global marine biogeochemical cycles of trace elements and their isotopes. *Geochemistry*, *67*(2), 85-131.

Sengupta, S., Parekh, A.; Chakraborty, S., Ravi Kumar, K. and Bose, T. (2013). Vertical variation of oxygen isotope in Bay of Bengal and its relationships with water masses. *Journal of Geophysical Research: Oceans*, 118, 6411-6424.

Sharma, M., Balakrishna, K., Hofmann, A. W. and Shankar, R. (2007). The transport of osmium and strontium isotopes through a tropical estuary. *Geochimica et Cosmochimica Acta*, 71 (20), 4856-4867.

Sheen, A. I., Kendall, B., Reinhard, C. T., Creaser, R. A., Lyons, T. W., Bekker, A., Poulton, W.S. and Anbar, A. D. (2018). A model for the oceanic mass balance of rhenium and implications for the extent of Proterozoic ocean anoxia. *Geochimica et Cosmochimica Acta*, 227, 75-95.

Shibahara, Y., Takaishi, H., Nishizawa, K. and Fujii, T. (2002). Strontium isotope effects in ligand exchange reaction. *Journal of Nuclear Science and Technology*, 39 (4), 451-456.

Shirodkar, P.V. and Anand, S.P. (1985). Behavior of boron in Mandovi Estuary (Goa). *Mahasagar*, 18, 439-448.

Siddiqui, S.Z. and Rama Rao, K.V. (1995) Limnology of Chilika lake. Director of Zoological Survey of India (Calcutta)(ed) Fauna of Chilika lake (Wetland Ecosystem Series I). *Zoological Survey of India*, Calcutta.

Singh, A., Jani, R. A. and Ramesh, R. (2010) Spatiotemporal variations of the δ 18 O–salinity relation in the northern Indian Ocean. Deep-Sea Research Part I: Oceanographic Research Papers, 57, 1422-1431.

Singh, S. K., Rai, S. K. and Krishnaswami, S. (2008). Sr and Nd isotopes in river sediments from the Ganga Basin: sediment provenance and spatial variability in physical erosion. *Journal of Geophysical Research*, 113 (F3), 1-18.

Singh, S. P., Singh, S. K., and Bhushan, R. (2011). Behavior of dissolved redox sensitive elements (U, Mo and Re) in the water column of the Bay of Bengal. *Marine Chemistry,* 126 (1-4), 76-88.

Singh, S.P., Singh, S.K. and Bhushan, R. (2013). Dissolved boron in the Tapi, Narmada and the Mandovi estuaries, the western coast of India: Evidence for conservative behavior. Estuaries and Coasts, 37, 1017-1027.

Smith, S.V. and Hollibaugh, J.T., (1993). Coastal metabolism and the oceanic organic carbon balance. *Reviews of Geophysics*, *31*(1), 75-89.

Sproson, A. D., Selby, D., Gannoun, A., Burton, K. W., Dellinger, M., and Lloyd, J. M. (2018). Tracing the Impact of Coastal Water Geochemistry on the Re-Os Systematics of Macroalgae: Insights From the Basaltic Terrain of Iceland. *Journal of Geophysical Research: Biogeosciences*, 123 (9), 2791-2806.

Sproson, A. D., Selby, D., Suzuki, K., Oda, T., and Kuroda, J. (2020). Anthropogenic Osmium in Macroalgae from Tokyo Bay Reveals Widespread Contamination from Municipal Solid Waste. *Environmental Science & Technology*, 54 (15), 9356-9365.

Stecher H. A. and Kogut M. B. (1999). Rapid barium removal in the Delaware estuary. *Geochimica et Cosmochimica Acta*, 63, 1003–1012.

Street, J., Knee, K., Grossman, E. and Paytan, A. (2008). Submarine groundwater discharge and nutrient addition to the coastal zone and coral reefs of leeward Hawi'i. *Marine Chemistry*, 109, 355-376.

Stumm, W. and Morgan, J.J., (2012). *Aquatic chemistry: chemical equilibria and rates in natural waters* (Vol. 126). John Wiley & Sons.

Swarzenski, P.W. and Baskaran, M., (2007). Uranium distribution in the coastal waters and pore waters of Tampa Bay, Florida. *Marine Chemistry*, *104*(1-2), 43-57.

Tanaka, K., Kozai, N., Ohnuki, T., and Grambow, B. (2019). Study on coordination structure of Re adsorbed on Mg–Al layered double hydroxide using X-ray absorption fine structure. *Journal of Porous Materials*, 26 (2), 505-511.

Taniguchi, M., (2002). Tidal effects on submarine groundwater discharge into the ocean. *Geophysical Research Letters*, *29*(12), 2-1.

Taniguchi, M., Burnett, W. C., Cable, J. E. and Turner, J. V. (2002). Investigation of submarine groundwater discharge. *Hydrological Processes*, 16 (11), 2115-2129.

Tarantola, A. (2005). Inverse problem theory and methods for model parameter estimation (Vol. 89), SIAM Publishers.

Tipple, B.J. and Pagani, M., (2007). The early origins of terrestrial C4 photosynthesis. *Annual Review of Earth and Planetary Sciences*, *35*, pp.435-461.

Trezzi, G., Garcia-Orellana, J., Rodellas, V., Masqué, P., Garcia-Solsona, E. and Andersson, P. S. (2017). Assessing the role of submarine groundwater discharge as a source of Sr to the Mediterranean Sea. *Geochimica et Cosmochimica Acta*, 200, 42-54.

Tribovillard, N., Algeo, T.J., Lyons, T. and Riboulleau, A., (2006). Trace metals as paleoredox and paleoproductivity proxies: an update. *Chemical geology*, *232*(1-2), 12-32.

Tripathy, G. R. and Singh, S. K. (2010). Chemical erosion rates of river basins of the Ganga system in the Himalaya: Reanalysis based on inversion of dissolved major ions, Sr, and $^{87}Sr/^{86}Sr$. *Geochemistry, Geophysics, Geosystems,* 11 (3), 1-20.

Tripathy, G. R. and Das, A. (2014). Modeling geochemical datasets for source apportionment: Comparison of least square regression and inversion approaches. *Journal of Geochemical Exploration*, 144, 144-153.

Tripathy, G. R., Hannah, J. L., and Stein, H. J. (2018). Refining the Jurassic-Cretaceous boundary: Re-Os geochronology and depositional environment of Upper Jurassic shales from the Norwegian Sea. *Palaeogeography, Palaeoclimatology, Palaeoecology*, 503, 13-25.

Tripathy, G. R., Mishra, S., Danish, M. and Ram, K. (2019). Elevated Barium concentrations in rain water from east-coast of India: role of regional lithology. *Journal of Atmospheric Chemistry*, 76 (1), 59-72.

Tripathy, G. R., Singh, S. K. and Krishnaswami, S. (2012). Sr and Nd isotopes as tracers of chemical and physical erosion. In *Handbook of Environmental Isotope Geochemistry* (pp. 521-552). Springer, Berlin, Heidelberg.

Tripathy, G. R., Singh, S. K., and Ramaswamy, V. (2014). Major and trace element geochemistry of Bay of Bengal sediments: Implications to provenances and their controlling factors. *Palaeogeography, Palaeoclimatology, Palaeoecology,* 397, 20-30.

Tripathy, G.R., Goswami, V., Singh, S.K. and Chakrapani, G.J., (2010). Temporal variations in Sr and $^{87}Sr/^{86}Sr$ of the Ganga headwaters: estimates of dissolved Sr flux to the mainstream. *Hydrological Processes: An International Journal*, *24*(9), 1159-1171.

Tripathy, G.R., Singh, S.K. and Krishnaswami, S., (2012). Sr and Nd isotopes as tracers of chemical and physical erosion. In *Handbook of Environmental Isotope Geochemistry* (521-552). Springer, Berlin, Heidelberg.

Trivedi J. R., Pande K., Krishnaswami S. and Sarin M. M. (1995). Sr isotopes in rivers of India and Pakistan: a reconnaissance study. Current Science 69, 171–178.

Vance, D., Teagle, D. A. and Foster, G. L. (2009). Variable Quaternary chemical weathering fluxes and imbalances in marine geochemical budgets. *Nature*, *458*(7237), 493.

Vengosh, A., Heumann, K. G., Juraske, S., and Kasher, R. (1994). Boron isotope application for tracing sources of contamination in groundwater. *Environmental Science & Technology*, 28(11), 1968-1974.

Vengosh, A., Spivack, A. J., Artzi, Y., and Ayalon, A. (1999). Geochemical and boron, strontium, and oxygen isotopic constraints on the origin of the salinity in groundwater from the Mediterranean coast of Israel. *Water Resources Research*, 35(6), 1877-1894.

Venkatarathnam, K. (1970) Formation of the barrier spit and other sand ridges near Chilka Lake on the east coast of India. *Marine Geology*, 9, 101-116.

Wakoff, B., and Nagy, K. L. (2004). Perrhenate uptake by iron and aluminum oxyhydroxides: An analogue for pertechnetate incorporation in Hanford waste tank sludges. *Environmental Science & Technology*, 38 (6), 1765-1771.

Walker, B. D., and Peucker-Ehrenbrink, B. (2004). Rhenium and Molybdenum in Rivers and Estuaries. *In AGU Fall Meeting Abstracts*.

Wang Z., Liu C., Han G. and Xu Z. (2001). Strontium isotopic geochemistry of the Changjiang estuarine waters: implications for water–sediment interaction. *Science in China Series E-Engineering & Material Science* 44, 129–133.

Wang, R. and You, C. (2013). Uranium and strontium isotopic evidence for strong submarine groundwater discharge in an estuary of a mountainous island: A case study in the Gaoping River Estuary, Southwestern Taiwan. *Marine Chemistry*, 157, 106-116.

Wang, R.M., You, C.F., Chu, H.Y. and Hung, J. J. (2009). Seasonal variability of dissolved major and trace elements in the Gaoping (Kaoping) River Estuary, Southwestern Taiwan. *Journal of Marine System,* 76, 444-456.

Wang, X., and Veizer, J. (2000). Respiration–photosynthesis balance of terrestrial aquatic ecosystems, Ottawa area, Canada. *Geochimica et Cosmochimica Acta*, 64(22), 3775-3786.

Weis, D., Kieffer, B., Maerschalk, C., Barling, J., De Jong, J., Williams, G. A., Hanano, D., Pretorius, W., Mattielli, N., Scoates, J., Goolaerts, A., Friedman, R. and Mahoney, J.

(2006). High-precision isotopic characterization of USGS reference materials by TIMS and MC-ICP MS. *Geochemistry, Geophysics, Geosystems,* 7 (8), 1-30.

Xiao, Y., Liao, B., Wang, Z., Wei, H. and Zhao, Z. (2007). Isotopic composition of dissolved boron and its geochemical behavior in a freshwater-seawater mixture at the estuary of the Changjiang (Yangtze) river. *Chinese Journal of Geochemistry*, 26, 105-113.

Xiong, Y. (2003). Solubility and speciation of rhenium in anoxic environments at ambient temperature and applications to the Black Sea. *Deep-Sea Research Part I: Oceanographic Research Papers, 50* (5), 681-690.

Xu, Y. and Marcantonio, F. (2007). Strontium isotope variations in the lower Mississippi River and its estuarine mixing zone. *Marine Chemistry*, 105 (1-2), 118-128.

Yamashita, Y., Takahashi, Y., Haba, H., Enomoto, S., and Shimizu, H. (2007). Comparison of reductive accumulation of Re and Os in seawater–sediment systems. *Geochimica et Cosmochimica Acta*, 71 (14), 3458-3475.

Yang, J. S. (1991). High rhenium enrichment in brown algae: a biological sink of rhenium in the sea? *Hydrobiologia*, 211 (3), 165-170.

Zachmann, D. W., Mohanti, M., Treutler, H. C., and Scharf, B. (2009). Assessment of element distribution and heavy metal contamination in Chilika Lake sediments (India). *Lakes & Reservoirs Research & Management*, 14 (2), 105-125.

Zingde, M.D., Ram, A.L., Sharma, P. and Abidi, S.A.H. (1995). Seawater intrusion and behavior of dissolved boron, fluoride, calcium, magnesium and nutrients in Vashisti estuary. *Society of Biosciences*, Muzaffarnagar, India.

Annexure

Table A1. Data on pH, temperature, salinity, dissolved oxygen (DO), dissolved boron, dissolved barium and geographical coordinates of Chilika lagoon water samples collected during four filed campaigns (January-2018, May-2017, June-2016, August-2017).

	Sample ID	Sampling Date	Lat (°N)	Lon (°E)	Depth (m)	Temp (°C)	pH	Salinity	DO (mg/l)	B (μmol/kg)	Ba (nmol/kg)
Monsoon (July-August, 2017)			-	-	-	-	-	-		-	
Southern	CLK17-M04	30-Jul-17	19.52	85.109	3.2	30.4	8.02	19	6	222 ± 9	687 ± 18
	CLK17-M05	30-Jul-17	19.536	85.121	2.62	29.9	8.09	19.8	6.1	232 ± 4	654 ± 16
	CLK17-M06	30-Jul-17	19.546	85.138	2.74	30.3	8.11	20	6.8	235 ± 3	669 ± 13
	CLK17-M07	30-Jul-17	19.556	85.157	2.74	30.6	8.07	19.7	6.6	239 ± 3	672 ± 13
	CLK17-M08	30-Jul-17	19.568	85.174	3.86	30.7	8.11	19.7	6.7	236 ± 2	677 ± 20
	CLK17-M09	30-Jul-17	19.548	85.176	3.07	30.8	8.11	19.8	6.8	203 ± 3	669 ± 17
	CLK17-M10	30-Jul-17	19.532	85.194	2.29	30.5	7.98	19.5	6.1	245 ± 8	680 ± 18
	CLK17-M11	30-Jul-17	19.519	85.163	2.59	30.5	8.07	20.1	6.7	211 ± 3	701 ± 14
	CLK17-M12	30-Jul-17	19.513	85.144	1.22	30.8	7.89	20	6.1	246 ± 9	719 ± 20
	CLK17-M13	30-Jul-17	19.491	85.134	1.7	31.4	8.09	19.6	6.2	236 ± 6	682 ± 16
	CLK17-M14	30-Jul-17	19.476	85.129	1.14	32.1	8.13	19.5	5.9	237 ± 3	701 ± 12
	CLK17-M15	30-Jul-17	19.522	85.125	2.41	31.8	7.95	19.9	6.4	245 ± 3	715 ± 23
	CLK17-M17	2-Aug-17	19.68	85.204	3.12	30.6	7.97	18.3	5.1	213 ± 3	680 ± 9
	CLK17-M18	2-Aug-17	19.666	85.188	2.92	30.6	8.08	19	5.3	226 ± 3	688 ± 19
	CLK17-M19	2-Aug-17	19.635	85.186	3.28	31	8.1	19.5	5.5	231 ± 3	673 ± 21
	CLK17-M20	2-Aug-17	19.619	85.164	2.87	31	8.13	19.7	5.4	236 ± 3	687 ± 23
	CLK17-M21	2-Aug-17	19.6	85.153	3.18	31.2	8.12	19.7	5.9	227 ± 5	632 ± 16
	CLK17-M22	2-Aug-17	19.589	85.151	3.4	31.4	8.14	18.9	5.7	227 ± 2	647 ± 23
	CLK17-M23	2-Aug-17	19.593	85.182	2.62	31.6	8.12	19.6	5.4	242 ± 2	725 ± 17
	CLK17-M24	2-Aug-17	19.616	85.201	3.35	31.2	8.13	19.5	5.6	231 ± 3	689 ± 11
	CLK17-M25	2-Aug-17	19.641	85.213	2.79	31.7	8.1	19.3	6	231 ± 2	647 ± 12
	CLK17-M26	2-Aug-17	19.66	85.222	3.48	31.2	8.12	19.3	6.1	232 ± 4	693 ± 17

Central	CLK17-M27	4-Aug-17	19.693	85.227	2.79	30.5	8.04	18.4	5.3	224 ± 1	669 ± 13
	CLK17-M28	4-Aug-17	19.684	85.26	2.84	30.2	8.09	18.5	6.8	226 ± 2	672 ± 12
	CLK17-M29	4-Aug-17	19.678	85.29	1.22	30	7.85	18.8	5.4	231 ± 3	680 ± 17
	CLK17-M30	4-Aug-17	19.687	85.328	0.97	29.8	7.99	18.5	5.1	231 ± 2	708 ± 15
	CLK17-M31	4-Aug-17	19.711	85.333	2.01	30.5	8.05	18.8	6.8	228 ± 2	758 ± 14
	CLK17-M32	4-Aug-17	19.732	85.321	2.36	30.3	8.16	16.6	7.4	203 ± 2	921 ± 23
	CLK17-M33	4-Aug-17	19.754	85.307	2.06	30	8.18	9.5	7.4	115 ± 2	766 ± 19
	CLK17-M34	4-Aug-17	19.768	85.293	1.75	30.6	8.02	7.1	7.1	93 ± 1	706 ± 16
	CLK17-M35	4-Aug-17	19.751	85.263	1.96	30.9	8.11	8.2	7.9	100 ± 1	608 ± 13
	CLK17-M36	4-Aug-17	19.721	85.259	2.67	30.8	8.22	14.5	8.1	175 ± 2	777 ± 18
	CLK17-M37	4-Aug-17	19.72	85.227	2.21	31.4	8.12	16.3	8	200 ± 2	736 ± 21
Northern	CLK17-M71	9-Aug-17	19.841	85.448	1.52	30.2	8.7	0.9	6.7	10 ± 0.1	-
	CLK17-M72	9-Aug-17	19.816	85.472	1.57	31	8.66	0.2	6.9	3 ± 0.05	109 ± 3
	CLK17-M73	9-Aug-17	19.786	85.496	1.52	31.9	8.09	0.1	6.1	2 ± 0.03	168 ± 5
	CLK17-M74	9-Aug-17	19.76	85.503	1.75	31.2	7.7	0.2	6.4	4 ± 0.05	132 ± 3
	CLK17-M75	9-Aug-17	19.741	85.47	1.65	32	8.08	0.5	5.6	7 ± 0.1	140 ± 2
	CLK17-M76	9-Aug-17	19.729	85.431	1.7	33.6	8.33	2.7	7.1	30 ± 1	257 ± 5
	CLK17-M77	9-Aug-17	19.715	85.392	1.65	32.9	8.18	12.6	7.1	140 ± 2	832 ± 17
	CLK17-M78	9-Aug-17	19.745	85.374	1.85	32.6	8.1	11.7	6.5	125 ± 1	813 ± 15
	CLK17-M79	9-Aug-17	19.773	85.363	1.55	31.9	7.9	6.8	7	78 ± 1	571 ± 9
	CLK17-M80	9-Aug-17	19.788	85.348	1.57	31.9	8.2	6.7	6.7	69 ± 1	560 ± 14
	CLK17-M81	9-Aug-17	19.819	85.37	1.42	32.1	8.34	1.9	6.6	18 ± 0.1	328 ± 8
	CLK17-M82	9-Aug-17	19.821	85.39	1.52	32.1	8.34	2.1	6.6	25 ± 0.2	318 ± 5
	CLK17-M83	9-Aug-17	19.838	85.406	1.52	31.8	8.14	1.3	6.2	13 ± 0.1	355 ± 9
	CLK17-M84	11-Aug-17	19.838	85.481	1.4	29.9	7.97	0.2	6.2	3 ± 0.03	125 ± 4
	CLK17-M85	11-Aug-17	19.818	85.499	1.75	30	8.05	0.1	7	2 ± 0.1	225 ± 7
	CLK17-M86	11-Aug-17	19.771	85.525	1.75	30.1	8.18	0.2	6.1	2 ± 0.03	134 ± 2
	CLK17-M87	11-Aug-17	19.79	85.543	1.45	30.7	7.94	0.1	7.3	1 ± 0.02	161 ± 3
	CLK17-M88	11-Aug-17	19.812	85.548	1.73	30	8.1	0.1	6.5	2 ± 0.02	192 ± 4
	CLK17-M89	11-Aug-17	19.848	85.559	1.45	31	7.94	0.1	6.1	1 ± 0.02	270 ± 6
	CLK17-M90	11-Aug-17	19.847	85.534	1.32	31.7	7.53	0.1	5.3	1 ± 0.01	284 ± 6

	CLK17-M91	11-Aug-17	19.844	85.51	1.52	30.7	8.33	0.1	6.1	1 ± 0.02	201 ± 4
	CLK17-M94	14-Aug-17	19.81	85.433	-	29.3	8.02	0.3	6.4	7 ± 0.08	201 ± 4
	CLK17-M95	14-Aug-17	19.78	85.402	-	29.1	8.1	0.7	6.3	13 ± 0.21	72 ± 2
Outer channel	CLK17- M107	23-Aug-17	19.69	85.422	-	31.1	8.35	7.8	6.1	91 ± 2	337 ± 10
	CLK17- M108	23-Aug-17	19.672	85.436	-	30.9	8.27	6.9	6.2	86 ± 1	298 ± 9
	CLK17- M109	23-Aug-17	19.684	85.517	-	31	8.22	17.1	6.7	232 ± 5	131 ± 3
	CLK17- M110	23-Aug-17	19.678	85.501	-	31.6	8.27	14.7	6.9	209 ± 3	175 ± 5
	CLK17- M111	23-Aug-17	19.667	85.484	-	32.4	8.29	11.7	7.6	169 ± 4	191 ± 16
	CLK17- M112	23-Aug-17	19.668	85.471	-	32.2	8.29	12.3	6.2	166 ± 5	233 ± 7
Pre-monsoon (April-May, 2017)											
	CLK17-04	27-Apr-17	19.52	85.109	1.98	29.6	8.36	13.4	6	159 ± 2	898 ± 17
	CLK17-05	27-Apr-17	19.536	85.121	1.98	29.8	8.34	13.1	6.7	144 ± 3	881 ± 14
	CLK17-06	27-Apr-17	19.546	85.138	2.13	29.7	8.31	13.3	6.9	163 ± 2	672 ± 16
	CLK17-07	27-Apr-17	19.556	85.157	2.44	30	8.32	13.5	6.4	164 ± 2	914 ± 21
	CLK17-08	27-Apr-17	19.568	85.174	3.05	30.2	8.25	13.7	7.7	166 ± 2	961 ± 19
	CLK17-09	27-Apr-17	19.548	85.176	1.22	29.7	8.36	13.1	9.8	159 ± 1	893 ± 19
	CLK17-10	27-Apr-17	19.534	85.177	1.68	29.6	8.74	13.5	8.7	164 ± 2	896 ± 15
	CLK17-11	27-Apr-17	19.519	85.163	1.52	29.9	8.45	13.7	9.1	168 ± 3	909 ± 31
	CLK17-12	27-Apr-17	19.513	85.144	0.91	30.6	8.57	13.5	11	165 ± 2	582 ± 19
Southern	CLK17-13	27-Apr-17	19.476	85.128	0.61	31.7	8.45	29.7	9.7	364 ± 4	525 ± 13
	CLK17-14	27-Apr-17	19.52	85.126	2.44	30.8	8.37	13.2	8.3	163 ± 2	867 ± 21
	CLK17-15	27-Apr-17	19.492	85.134	1.22	30.2	8.14	27.7	9.1	339 ± 6	633 ± 10
	CLK17-18	29-Apr-17	19.68	85.204	1.83	30.1	8.51	13.6	3.8	158 ± 2	915 ± 21
	CLK17-19	29-Apr-17	19.664	85.18	2.13	30	8.43	13.1	4.2	158 ± 1	961 ± 12
	CLK17-20	29-Apr-17	19.635	85.186	2.13	29.9	8.31	13.2	2.3	167 ± 2	1001 ± 28
	CLK17-21	30-Apr-17	19.619	85.164	3.05	29.8	8.3	13.3	4.2	148 ± 3	911 ± 13
	CLK17-22	30-Apr-17	19.6	85.151	1.83	30	8.31	13.3	7.4	165 ± 2	922 ± 24
	CLK17-23	30-Apr-17	19.589	85.151	2.44	29.8	8.25	13.3	4.4	163 ± 2	943 ± 14
	CLK17-24	30-Apr-17	19.593	85.182	2.13	29.8	8.31	13.5	9.1	168 ± 3	881 ± 15
	CLK17-25	30-Apr-17	19.616	85.201	1.83	30.1	8.26	13.4	7.5	166 ± 3	674 ± 10
	CLK17-26	30-Apr-17	19.641	85.213	2.13	29.8	8.18	13.3	4.6	166 ± 3	870 ± 19

	CLK17-27	30-Apr-17	19.66	85.222	1.22	30.2	8.13	14.5	5	166 ± 2	907 ± 16
Central	CLK17-28	2-May-17	19.693	85.227	4.57	28.5	8.1	18.6	2.9	228 ± 4	601 ± 11
	CLK17-29	2-May-17	19.684	85.26	2.13	26.8	8.3	16.9	4.7	212 ± 2	896 ± 22
	CLK17-30	2-May-17	19.678	85.29	1.22	26.8	8.3	15.8	3	192 ± 2	1435 ± 27
	CLK17-31	2-May-17	19.687	85.328	-	26.6	8.9	17.9	3.4	202 ± 4	594 ± 16
	CLK17-32	2-May-17	19.711	85.333	-	28	8.2	35	7.1	431 ± 6	-
	CLK17-33	2-May-17	19.728	85.311	3.05	28.4	8.4	30.6	6.8	354 ± 5	-
	CLK17-34	2-May-17	19.754	85.307	-	28.8	8.3	13.1	2.6	148 ± 2	815 ± 14
	CLK17-35	2-May-17	19.768	85.293	1.22	29.6	8.36	12.9	4.8	150 ± 2	749 ± 12
	CLK17-36	2-May-17	19.751	85.263	1.83	29.2	8.44	13.9	4.5	166 ± 2	670 ± 15
	CLK17-37	2-May-17	19.721	85.259	3.05	29.5	8.5	18.1	5.8	218 ± 4	656 ± 12
	CLK17-38	2-May-17	19.72	85.227	3.66	30.2	8.7	15.1	4.7	184 ± 2	713 ± 17
	CLK17-77	8-May-17	19.727	85.369	1.83	29.6	8.29	36.3	7	463 ± 7	325 ± 8
	CLK17-78	8-May-17	19.737	85.35	1.52	30	8.24	36.8	5.1	463 ± 9	337 ± 6
	CLK17-79	8-May-17	19.766	85.324	1.22	32.1	9.73	13.6	5.6	155 ± 2	891 ± 23
Northern	CLK17-72	8-May-17	19.832	85.444	0.91	28.6	7.97	13.3	2.9	132 ± 2	1938 ± 40
	CLK17-73	8-May-17	19.803	85.439	1.22	28.8	8.3	15.4	5.8	173 ± 2	1607 ± 26
	CLK17-74	8-May-17	19.774	85.437	1.37	28.9	8.41	24.3	2.3	273 ± 3	2061 ± 23
	CLK17-75	8-May-17	19.743	85.435	1.22	28.3	8.22	32.1	7.8	390 ± 5	870 ± 10
	CLK17-76	8-May-17	19.738	85.409	1.52	29.3	8.22	34.2	3.7	430 ± 6	743 ± 10
	CLK17-80	8-May-17	19.825	85.382	0.91	32	8.85	14.4	5.2	150 ± 2	1660 ± 28
	CLK17-81	8-May-17	19.817	85.394	-	32.1	9.28	15.8	8.4	179 ± 3	1415 ± 35
	CLK17-82	10-May-17	19.843	85.468	1.22	27.7	8.05	11.1	7.3	59 ± 1	1922 ± 33
	CLK17-83	10-May-17	19.844	85.496	-	27.7	8.09	6.3	7.6	47 ± 1	1352 ± 26
	CLK17-84	10-May-17	19.856	85.515	-	26.8	7.87	3.4	4.9	30 ± 0	1117 ± 25
	CLK17-85	10-May-17	19.863	85.531	-	27.7	8.05	1.7	3	10 ± 0	1022 ± 23
	CLK17-86	10-May-17	19.862	85.548	-	29.6	7.98	0.5	5.5	4 ± 0.04	339 ± 7
	CLK17-87	10-May-17	19.877	85.56	-	30.1	8.16	0.2	5	3 ± 0.04	301 ± 6
	CLK17-88	10-May-17	19.842	85.529	-	29.2	8.01	1.2	5.3	5 ± 0.1	769 ± 20
	CLK17-89	10-May-17	19.822	85.518	-	31.3	9.41	1.4	10.2	6 ± 0.1	731 ± 26
	CLK17-90	10-May-17	19.809	85.509	-	29.9	8.63	1.9	6.9	12 ± 0.2	714 ± 21

	CLK17-91	10-May-17	19.802	85.484	-	29	8.82	7.1	8	58 ± 1	1618 ± 21
	CLK17-92	10-May-17	19.813	85.477	-	30.3	8.52	6.1	6.5	51 ± 1	1375 ± 36
	CLK17-93	10-May-17	19.833	85.464	-	30	8.19	12.8	7.3	115 ± 1	2043 ± 52
	CLK17-94	12-May-17	19.807	85.351	-	30.1	7.91	19.7	6.1	207 ± 4	1376 ± 25
	CLK17-95	12-May-17	19.774	85.379	-	30.5	7.37	38.2	6.2	452 ± 7	887 ± 13
	CLK17-96	12-May-17	19.83	85.428	-	32	7.97	16.6	7.5	167 ± 1	2071 ± 42
	CLK17-115	13-May-17	19.734	85.484	-	31.6	8.5	39.9	8.5	414 ± 7	1320 ± 20
	CLK17-116	13-May-17	19.743	85.48	0.91	32.7	8.1	30.5	6.4	340 ± 4	1083 ± 20
	CLK17-117	13-May-17	19.745	85.473	-	34.6	8.1	30.8	6.8	359 ± 5	1097 ± 20
	CLK17-118	13-May-17	19.757	85.475	-	35.9	8.1	18	6.3	193 ± 2	1520 ± 28
	CLK17-132	17-May-17	19.776	85.551	-	30.9	7.42	7.1	6	58 ± 1	768 ± 18
	CLK17-133	17-May-17	19.764	85.532	-	30.6	7.7	2.6	6.5	17 ± 0.2	471 ± 10
	CLK17-134	17-May-17	19.753	85.505	-	31	7.66	5.2	7.3	44 ± 1	732 ± 13
	CLK17-135	17-May-17	19.765	85.507	-	31.3	8.21	5.4	8	37 ± 1	1158 ± 24
	CLK17-136	17-May-17	19.776	85.555	-	31.3	8.01	8.3	6.8	73 ± 1	785 ± 22
Outer channel	CLK17-109	13-May-17	19.684	85.517	-	29.2	7.43	34.5	6.3	468 ± 9	179 ± 5
	CLK17-110	13-May-17	19.678	85.501	-	30.7	7.52	35.3	5.8	477 ± 8	182 ± 5
	CLK17-111	13-May-17	19.667	85.484	-	32.3	7.64	35.1	5.7	468 ± 5	193 ± 4
	CLK17-112	13-May-17	19.668	85.471	-	32.4	7.67	35.2	5.8	472 ± 6	201 ± 4
	CLK17-113	13-May-17	19.69	85.422	-	29.2	7.8	35.8	7.3	473 ± 4	368 ± 4
	CLK17-114	13-May-17	19.672	85.436	-	30.7	7.57	35.5	7.7	476 ± 9	260 ± 4
One-day sampling of the whole lagoon (16th August, 2017)											
Southern	CLKS17-SM05	16-Aug-17	19.675	85.237	-	30.4	8.29	11.6	-	132 ± 2	706 ± 20
	CLKS17-SM06	16-Aug-17	19.646	85.208	-	30.7	8.28	13.7	-	162 ± 2	740 ± 16
	CLKS17-SM07	16-Aug-17	19.613	85.197	-	31.4	8.28	15.3	-	176 ± 2	717 ± 21
	CLKS17-SM08	16-Aug-17	19.585	85.172	-	31.5	8.29	15.6	-	181 ± 2	697 ± 12
	CLKS17-SM09	16-Aug-17	19.547	85.158	-	31.4	8.28	16.5	-	187 ± 5	769 ± 19
	CLKS17-SM10	16-Aug-17	19.519	85.135	-	31.9	8.23	17.2	-	185 ± 2	791 ± 24
Central	CLKS17-SM03	16-Aug-17	19.732	85.332	-	29.8	8.4	6.1	-	73 ± 0.9	489 ± 14
	CLKS17-SM04	16-Aug-17	19.702	85.275	-	30.4	8.32	10.1	-	119 ± 2	647 ± 15
	CLKS17-SM11	16-Aug-17	19.716	85.209	-	32.8	8.34	9.7	-	114 ± 1	648 ± 12

	CLKS17-SM12	16-Aug-17	19.752	85.253	-	33	8.46	3.5	-	45 ± 1	405 ± 9
	CLKS17-SM13	16-Aug-17	19.767	85.281	-	33	8.41	2.4	-	36 ± 1	288 ± 8
	CLKS17-SM18	16-Aug-17	19.712	85.377	-	32	8.2	5.3	-	78 ± 1	2185 ± 50
	CLKS17-SM19	16-Aug-17	19.743	85.359	-	33	8.4	3.4	-	41 ± 1	190 ± 5
Northern	CLKS17-SM01	16-Aug-17	19.822	85.445	-	29.9	8.86	0.2	-	4 ± 0.1	95 ± 3
	CLKS17-SM02	16-Aug-17	19.769	85.388	-	30	8.24	0.9	-	16 ± 0.2	116 ± 2
	CLKS17-SM14	16-Aug-17	19.808	85.47	-	28	7.8	0.8	-	8 ± 0.2	267 ± 7
	CLKS17-SM15	16-Aug-17	19.768	85.477	-	29	8.3	0.2	-	3 ± 0.04	98 ± 2
	CLKS17-SM16	16-Aug-17	19.73	85.433	-	31	8.1	0.2	-	3 ± 0.04	107 ± 3
	CLKS17-SM17	16-Aug-17	19.84	85.455	-	32	8.2	0.6	-	6 ± 0.1	150 ± 3
	CLKS17-SM20	16-Aug-17	19.779	85.325	-	32	8.5	1.9	-	28 ± 0.4	107 ± 3
	CLKS17-SM21	16-Aug-17	19.802	85.353	-	31	8.2	1.1	-	18 ± 0.3	94 ± 3
	CLKS17-SM22	16-Aug-17	19.817	85.371	-	32	8.6	1	-	13 ± 0.1	177 ± 5
	CLKS17-SM23	16-Aug-17	19.838	85.398	-	33	8.2	0.9	-	6 ± 0.1	304 ± 7
	CLKS17-SM24	16-Aug-17	19.847	85.41	-	32	7.2	0.6	-	2 ± 0.04	440 ± 10
	CLKS17-SM25	16-Aug-17	19.853	85.444	-	30.3	6.96	2	-	18 ± 0.2	706 ± 17
	CLKS17-SM26	16-Aug-17	19.839	85.47	-	29.6	7.36	0.6	-	3 ± 0.05	212 ± 4
	CLKS17-SM27	16-Aug-17	19.818	85.508	-	30.6	7.27	0.1	-	2 ± 0.02	292 ± 5
	CLKS17-SM28	16-Aug-17	19.792	85.549	-	31.1	7.26	0.2	-	2 ± 0.04	234 ± 7
	CLKS17-SM29	16-Aug-17	19.822	85.555	-	32	7.38	0.1	-	2 ± 0.02	220 ± 4
	CLKS17-SM30	16-Aug-17	19.852	85.527	-	32.7	9.14	0.1	-	2 ± 0.03	209 ± 4
	CLKS17-SM31	16-Aug-17	19.88	85.51	-	32	6.98	0.3	-	4 ± 0.1	199 ± 4
Post-monsoon(January, 2018)											
Southern	CLK18-Ja04	1/3/2018	19.52	85.11	-	22	8.51	10.1	9.2	-	444 ± 11
	CLK18-Ja05	1/3/2018	19.54	85.12	-	21.7	8.47	9.9	7.9	-	455 ± 12
	CLK18-Ja06	1/3/2018	19.55	85.14	-	21.7	8.45	9.6	8.4	-	442 ± 9
	CLK18-Ja07	1/3/2018	19.56	85.16	-	21.8	8.47	9.5	9.2	-	454 ± 8
	CLK18-Ja08	1/3/2018	19.64	85.17	-	21.7	8.38	9.7	7	-	457 ± 8
	CLK18-Ja09	1/3/2018	19.6	85.15	-	21.7	8.42	9.1	6.7	-	434 ± 9
	CLK18-Ja10	1/3/2018	19.62	85.17	-	21.6	8.47	9.1	7.3	-	418 ± 11
	CLK18-Ja11	1/3/2018	19.64	85.19	-	21.8	8.32	8.7	6.2	-	376 ± 7

	CLK18-Ja12	1/3/2018	19.66	85.19	-	21.9	8.33	8.4	5.6	-	355 ± 6
	CLK18-Ja13	1/3/2018	19.64	85.21	-	21.6	8.47	7.3	5.2	-	313 ± 12
	CLK18-Ja14	1/3/2018	19.62	85.2	-	22	8.44	7.6	5.1	-	320 ± 6
	CLK18-Ja15	1/3/2018	19.59	85.18	-	22.3	8.47	8.4	5.3	-	374 ± 4
	CLK18-Ja16	1/3/2018	19.57	85.18	-	22.7	8.54	9.6	5.3	-	379 ± 11
	CLK18-Ja17	1/3/2018	19.55	85.18	-	22.6	8.57	9.7	9	-	459 ± 10
	CLK18-Ja18	1/3/2018	19.53	85.16	-	22.7	8.62	9.8	5.2	-	481 ± 9
	CLK18-Ja19	1/3/2018	19.51	85.15	-	22.8	8.87	10	5.9	-	411 ± 8
	CLK18-Ja20	1/3/2018	19.5	85.14	-	23.1	8.98	10.2	5.6	-	486 ± 11
	CLK18-Ja21	1/3/2018	19.49	85.14	-	22.8	9.24	12.3	5.2	-	507 ± 9
	CLK18-Ja22	1/3/2018	19.52	85.12	-	23	8.8	10.4	5.5	-	431 ± 9
	CLK18-Ja36	1/5/2018	19.68	85.2	-	21.5	8.33	7.5	7.9	-	294 ± 6
	CLK18-Ja37	1/5/2018	19.68	85.24	-	21.5	8.46	7	8.8	-	304 ± 8
	CLK18-Ja38	1/5/2018	19.68	85.27	-	21	9.17	6.1	8.5	-	226 ± 5
	CLK18-Ja39	1/5/2018	19.68	85.29	-	21.5	9.28	5.6	8	-	236 ± 7
	CLK18-Ja40	1/5/2018	19.68	85.33	-	21.7	8.47	6.7	9.6	-	350 ± 6
	CLK18-Ja41	1/5/2018	19.72	85.34	-	21.6	8.25	6.8	8.4	-	318 ± 9
	CLK18-Ja42	1/5/2018	19.74	85.33	-	21.5	9.5	7.6	10.4	-	304 ± 7
Central	CLK18-Ja43	1/5/2018	19.77	85.32	-	21.5	9.14	7.4	10.9	-	390 ± 10
	CLK18-Ja44	1/5/2018	19.76	85.27	-	21.6	8.28	7.1	8.2	-	329 ± 9
	CLK18-Ja45	1/5/2018	19.75	85.25	-	21.6	8.51	7.2	9.2	-	311 ± 10
	CLK18-Ja46	1/5/2018	19.73	85.25	-	22.1	8.44	7.4	9.8	-	313 ± 7
	CLK18-Ja47	1/5/2018	19.72	85.22	-	22.2	8.52	7.4	9.9	-	302 ± 10
	CLK18-Ja72	1/7/2018	19.72	85.38	-	23.2	8.52	6.3	7.5	-	232 ± 6
	CLK18-Ja73	1/7/2018	19.74	85.37	-	22.7	8.3	7.6	7	-	322 ± 8
	CLK18-Ja66	1/7/2018	19.84	85.44	-	19.4	8.1	1	6.5	-	206 ± 6
	CLK18-Ja67	1/7/2018	19.77	85.41	-	20	8.34	0.4	7.6	-	102 ± 2
Northern	CLK18-Ja68	1/7/2018	19.78	85.46	-	20.5	8.23	0.8	7.6	-	103 ± 3
	CLK18-Ja69	1/7/2018	19.76	85.48	-	20.5	8.24	0.6	7.6	-	107 ± 2
	CLK18-Ja70	1/7/2018	19.74	85.46	-	21.7	8.26	1.9	7.9	-	181 ± 5
	CLK18-Ja71	1/7/2018	19.73	85.42	-	23.6	8.3	4	7.9	-	176 ± 6

	CLK18-Ja74	1/7/2018	19.77	85.36	-	23.3	8.41	8	8.5	-	311 ± 10
	CLK18-Ja75	1/7/2018	19.79	85.34	-	21	8.31	7.9	8.3	-	328 ± 10
	CLK18-Ja76	1/7/2018	19.81	85.37	-	23.9	9.75	7.7	13.1	-	131 ± 5
	CLK18-Ja77	1/7/2018	19.8	85.4	-	23.1	10.18	5.3	11	-	350 ± 6
	CLK18-Ja78	1/7/2018	19.82	85.41	-	23.9	9.89	4.1	14.4	-	335 ± 11
	CLK18-Ja79	1/7/2018	19.84	85.41	-	23.2	8.45	5.7	6.5	-	1130 ± 19
	CLK18-Ja80	1/8/2018	19.85	85.48	-	19.4	7.87	1.3	6	-	324 ± 7
	CLK18-Ja81	1/8/2018	19.84	85.5	-	19.7	8.37	0.5	10.3	-	187 ± 3
	CLK18-Ja82	1/8/2018	19.86	85.52	-	18.7	6.97	0.4	0.8	-	263 ± 5
	CLK18-Ja83	1/8/2018	19.87	85.53	-	19.8	7.8	0.4	7	-	260 ± 7
	CLK18-Ja84	1/8/2018	19.86	85.55	-	21.7	7.29	0.3	5.9	-	358 ± 12
	CLK18-Ja85	1/8/2018	19.84	85.53	-	21.9	7.28	0.3	5.6	-	387 ± 5
	CLK18-Ja86	1/8/2018	19.81	85.53	-	21.2	8.41	0.3	10.3	-	230 ± 9
	CLK18-Ja87	1/8/2018	19.79	85.53	-	21.8	8.91	0.3	7.9	-	104 ± 3
	CLK18-Ja88	1/8/2018	19.77	85.52	-	22.8	8.36	0.5	8.9	-	203 ± 4
	CLK18-Ja89	1/8/2018	19.71	85.51	-	23.1	8.38	0.3	9.8	-	130 ± 4
	CLK18-Ja90	1/8/2018	19.8	85.49	-	24.4	9.34	0.3	10.8	-	72 ± 3
	CLK18-Ja91	1/8/2018	19.8	85.44	-	23.5	8.54	0.5	10.3	-	77 ± 2
Outer channel	CLK18-Ja103	13/1/2018	19.69	85.42	-	22.5	8.01	6.1	10.1	-	171 ± 6
	CLK18-Ja104	13/1/2018	19.67	85.44	-	22.7	8.16	6	9.1	-	229 ± 6
	CLK18-Ja105	13/1/2018	19.68	85.52	-	-	-	14.8	-	-	-
	CLK18-Ja106	13/1/2018	19.68	85.5	-	24.3	8.01	15.2	-	-	-
	CLK18-Ja107	13/1/2018	19.67	85.48	-	24.4	8.2	7.5	-	-	-
	CLK18-Ja108	13/1/2018	19.67	85.47	-	24.4	8.26	6.6	-	-	-
One-day sampling of the whole lagoon (10th January, 2018)											
Southern	CLK18-SJa7	1/10/2018	19.66	85.21	-	22.3	8.38	8.3	-	-	198 ± 6
	CLK18-SJa8	1/10/2018	19.62	85.19	-	22.3	8.34	9.1	-	-	219 ± 6
	CLK18-SJa9	1/10/2018	19.57	85.17	-	22.4	8.53	9.5	-	-	259 ± 7
	CLK18-SJa10	1/10/2018	19.54	85.14	-	23.1	8.61	10.7	-	-	263 ± 10
	CLK18-SJa4	1/10/2018	19.76	85.34	-	21.1	8.38	8	-	-	255 ± 9
Central	CLK18-SJa5	1/10/2018	19.74	85.3	-	21.7	8.12	8.2	-	-	232 ± 8

	CLK18-SJa6	1/10/2018	19.7	85.27	-	21.8	8.29	8.2	-	-	207 ± 7
	CLK18-SJa1	1/10/2018	19.85	85.44	-	19.2	7.34	1.4	-	-	329 ± 9
Northern	CLK18-SJa2	1/10/2018	19.81	85.44	-	19.6	10.11	0.9	-	-	105 ± 4
	CLK18-SJa3	1/10/2018	19.8	85.39	-	20.1	10.1	5.8	-	-	319 ± 10
	CLK18-SJa11	1/10/2018	19.84	85.5	-	20.3	7.89	0.6	-	-	163 ± 4
	CLK18-SJa12	1/10/2018	19.81	85.51	-	20.2	7.77	0.3	-	-	202 ± 7
	CLK18-SJa13	1/10/2018	19.79	85.51	-	19.3	7.81	0.3	-	-	145 ± 7
	CLK18-SJa14	1/10/2018	19.77	85.51	-	20.1	7.75	0.4	-	-	162 ± 5
	CLK18-SJa15	1/10/2018	19.75	85.48	-	20.4	7.78	0.6	-	-	105 ± 3
	CLK18-SJa16	1/10/2018	19.74	85.46	-	20.9	7.84	1.8	-	-	209 ± 8
	CLK18-SJa17	1/10/2018	19.72	85.43	-	22	7.66	2.2	-	-	-
	CLK18-SJa18	1/10/2018	19.71	85.39	-	22	8.8	6.5	-	-	237 ± 6
	CLK18-SJa19	1/10/2018	19.74	85.38	-	21.9	8.55	7.5	-	-	281 ± 6
	CLK18-SJa20	1/10/2018	19.78	85.35	-	21.8	8.28	8	-	-	217 ± 6
	CLK18-SJa21	1/10/2018	19.81	85.36	-	22	9.43	8	-	-	-
	CLK18-SJa22	1/10/2018	19.82	85.38	-	23.6	9.94	8.1	-	-	282 ± 14
	CLK18-SJa23	1/10/2018	19.84	85.41	-	21.6	8.38	6.5	-	-	991 ± 24

Onset of Monsoon (June, 2016)

Southern	CLK16-02	18-Jun-16	19.7	85.2	2.48	30.5	7.64	22.6	5.7	257 ± 3	-
	CLK16-03	18-Jun-16	19.65	85.18	2.7	30.8	7.79	21.9	5.9	251 ± 4	-
	CLK16-04	18-Jun-16	19.62	85.17	2	30.7	7.76	22.2	6.2	260 ± 4	-
	CLK16-05	18-Jun-16	19.58	85.15	2.9	30.6	7.78	20.1	5.9	249 ± 4	-
	CLK16-06	18-Jun-16	19.65	85.22	2.92	30.6	7.8	20.3	6.7	266 ± 2	-
	CLK16-07	18-Jun-16	19.7	85.2	1.78	30.6	7.67	23.4	6.1	286 ± 5	-
	CLK16-10	19-Jun-16	19.52	85.1	2.23	31	7.79	20.5	5.7	254 ± 5	-
	CLK16-11	19-Jun-16	19.52	85.13	2.06	30.5	7.71	18.5	6	246 ± 2	-
	CLK16-12	19-Jun-16	19.53	85.12	2.3	30.9	7.73	18.7	6.4	246 ± 4	-
	CLK16-14	20-Jun-16	19.69	85.24	2.33	30.6	7.85	24.2	5.7	301 ± 6	-
	CLK16-15	20-Jun-16	19.68	85.3	2.07	30.1	7.8	23.2	6	283 ± 4	-
Central	CLK16-16	20-Jun-16	19.68	85.33	0.8	31.7	7.53	22.1	6.4	281 ± 5	
	CLK16-17	20-Jun-16	19.72	85.33	1.87	31.3	7.63	22.7	6.2	309 ± 3	-

	CLK16-18	20-Jun-16	19.74	85.33	2	31.1	7.78	25	5.8	330 ± 3	-
	CLK16-19	20-Jun-16	19.78	85.34	1.55	32	7.74	27.2	6.4	386 ± 7	-
	CLK16-20	20-Jun-16	19.8	85.33	1.32	31.7	7.7	29.2	6	364 ± 4	-
	CLK16-21	20-Jun-16	19.78	85.3	1.39	32	7.86	25.9	7	317 ± 5	-
	CLK16-22	20-Jun-16	19.75	85.26	1.9	31.7	7.78	23.4	6.7	311 ± 5	-
	CLK16-23	20-Jun-16	19.73	85.24	2.06	31.6	7.8	24.8	6.7	302 ± 4	-
	CLK16-24	20-Jun-16	19.71	85.21	1.93	31.8	7.81	21.7	7	293 ± 5	-
	CLK16-25	21-Jun-16	19.67	85.43	2.09	31.5	7.87	32.1	6.2	418 ± 5	-
	CLK16-26	21-Jun-16	19.7	85.4	1.53	32.2	8.06	31.5	5.2	408 ± 7	-
Northern	CLK16-27	21-Jun-16	19.73	85.43	1.95	32.7	8.07	31.7	5.6	411 ± 5	-
	CLK16-28	21-Jun-16	19.75	85.45	1.82	32.4	8.08	31.3	5.8	416 ± 6	-
	CLK16-29	21-Jun-16	19.78	85.48	1.71	32.6	7.74	23.3	5.4	293 ± 4	-
	CLK16-30	21-Jun-16	19.8	85.48	1.58	32.8	7.78	19.3	5.5	246 ± 5	-
	CLK16-31	21-Jun-16	19.8	85.48	1.64	32.5	7.9	15.6	5.3	199 ± 4	-
	CLK16-32	21-Jun-16	19.82	85.5	1.17	32.7	7.8	12.1	5.5	160 ± 2	-
	CLK16-33	21-Jun-16	19.817	85.517	-	32.2	7.76	7.5	5.1	92 ± 1	-
	CLK16-34	21-Jun-16	19.83	85.48	1.4	32.7	7.85	13.9	5.9	182 ± 2	-
	CLK16-35	21-Jun-16	19.78	85.43	1.52	32.9	7.78	29.2	5.1	411 ± 5	-
	CLK16-36	21-Jun-16	19.73	85.42	1.91	32.2	7.68	31	5.7	408 ± 7	-
	CLK16-43	22-Jun-16	19.883	85.507	1	33.6	6.89	8	3	105 ± 1	-
	CLK16-44	22-Jun-16	19.868	85.516	2	33	7.02	9.3	2.4	115 ± 1	-

Table A2. Data on salinity, Sr, Re, DIC, $^{87}Sr/^{86}Sr$, and $\delta^{13}C_{DIC}$ of Chilika lagoon samples collected during three filed campaigns (January-2018, May-2017, August-2017).

Sample ID	Salinity	Sr (μmol/kg)	$^{87}Sr/^{86}Sr$*	Re (pmol/kg)	DIC (μmol/kg)	$\delta^{13}C_{DIC}$ (‰)
Pre-monsoon (April-May, 2017)						
CLK17-06	13.3	35 ± 1	0.709908	15.8	-	-
CLK17-25	13.4	35.7 ± 0.5	0.709538	16	-	-
CLK17-28	18.6	50 ± 1	0.709773	13.5	-	-
CLK17-34	13.1	35.4 ± 0.5	0.709656	13.2	-	-
CLK17-38	15.1	41 ± 1	0.70951	17.1	-	-
CLK17-79	13.6	37.1 ± 0.5	0.709643	14.6	-	-
CLK17-80	14.4	38 ± 1	0.709733	12.6	-	-
CLK17-82	11.1	28 ± 1	0.710145	12.1	-	-
CLK17-84	3.4	9.6 ± 0.1	0.711895	9.8	-	-
CLK17-87	0.2	1.29 ± 0.04	0.717062	6.1	-	-
CLK17-88	1.2	3.7 ± 0.1	0.714342	8.3	-	-
CLK17-91	7.1	18.7 ± 0.4	0.710778	11.7	-	-
CLK17-94	19.7	52 ± 1	0.709495	20.9	-	-
CLK17-118	18	47 ± 1	0.709679	20.7	-	-
CLK17-132	7.1	19.1 ± 0.4	0.710436	14.3	-	-
CLK17-134	5.2	14.5 ± 0.3	0.71084	12.6	-	-
CLK17-136	8.3	22 ± 1	0.710224	15	-	-
CLK17-133	2.6	6.6 ± 0.2	0.712565	-	-	-
CLK17-111	35.1	90 ± 2	0.709184	-	-	-
CLK17-113	35.8	93 ± 1	0.709192	-	-	-
Monsoon (July-August, 2017)						
CLK17-M11	20.1	54 ± 1	0.709383	-	2322	-3.67
CLK17-M14	19.5	-	-	19.3	-	-
CLK17-M17	18.3	-	-	17.2	-	-
CLK17-M27	18.4	50 ± 1	0.709379	-	1761	-3.83
CLK17-M32	16.6	-	-	14.8	-	-
CLK17-M33	9.5	25.6 ± 0.4	0.709754	9.3	-	-
CLK17-M34	7.1	19.8 ± 0.2	0.709823	7.1	-	-
CLK17-M35	8.2	-	-	7.4	-	-
CLK17-M36	14.5	-	-	12.4	-	-
CLK17-M71	0.9	2.7 ± 0.1	0.711667	4.5	1808	-6.57
CLK17-M72	0.2	1.16 ± 0.02	0.71505	-	1442	-3.12
CLK17-M73	0.1	1.01 ± 0.01	0.716344	-	-	-
CLK17-M74	0.2	1.15 ± 0.03	0.715177	-	-	-
CLK17-M75	0.5	1.98 ± 0.05	0.712862	-	-	-
CLK17-M76	2.7	7.0 ± 0.1	0.710456	7.6	1494	-4.38
CLK17-M77	12.6	-	-	13.7	-	-
CLK17-M79	6.8	-	-	9.8	-	-
CLK17-M81	1.9	4.8 ± 0.1	0.710891	3.8	-	-
CLK17-M82	2.1	5.7 ± 0.1	0.710688	5.8	1789	-5.34
CLK17-M83	1.3	4.0 ± 0.1	0.711071	4.1	-	-

CLK17-M84	0.2	1 ± 0.02	0.714573	6.9	1269	-1.87
CLK17-M85	0.1	0.81 ± 0.03	0.717901	-	1151	-2.18
CLK17-M86	0.2	1.16 ± 0.02	0.71559	-	1369	-4.72
CLK17-M88	0.1	-	-	5.8	-	-
CLK17-M94	0.3	1.15 ± 0.02	0.712746	-	2156	-4.15
CLK17- M112	12.3	33 ± 1	0.709362	-	1837	-3.41
One-day sampling (16th August, 2017)						
CLKS17-SM05	11.6	31.2 ± 0.4	0.709497	11.2	2046	-1.61
CLKS17-SM06	13.7	38.1 ± 0.5	0.709437	12.6	2106	-4.26
CLKS17-SM07	15.3	42 ± 1	0.709416	14.7	2149	-3.48
CLKS17-SM08	15.6	43.4 ± 0.4	0.709405	15.5	2114	-5.75
CLKS17-SM09	16.5	46 ± 1	0.709425	-	2153	-1.44
CLKS17-SM10	17.2	44 ± 1	0.709411	16.6	2261	-2.35
CLKS17-SM03	6.1	18.3 ± 0.2	0.709745	7.7	1941	-5.62
CLKS17-SM04	10.1	27.7 ± 0.5	0.709541	10.3	2003	-3.97
CLKS17-SM11	9.7	28 ± 1	0.709574	9.6	2013	-3.76
CLKS17-SM12	3.5	10.1 ± 0.1	0.710082	5.7	1948	-1.82
CLKS17-SM13	2.4	6.9 ± 0.1	0.71029	5.4	1748	-2.44
CLKS17-SM18	5.3	16.8 ± 0.4	0.709786	8.9	1723	-5.19
CLKS17-SM19	3.4	8.4 ± 0.2	0.710196	-	1463	-3.16
CLKS17-SM01	0.2	0.92 ± 0.01	0.714629	-	-	-
CLKS17-SM02	0.9	2.81 ± 0.05	0.711368	-	1341	-6.5
CLKS17-SM14	0.8	2.26 ± 0.04	0.712091	-	1683	-4.81
CLKS17-SM15	0.2	0.9 ± 0.01	0.716252	4.9	1091	-1.6
CLKS17-SM16	0.2	1.24 ± 0.02	0.716322	-	1019	-1.65
					1278	-1.75
CLKS17-SM20	1.9	4.4 ± 0.1	0.710501	6.2	1586	-5.74
CLKS17-SM21	1.1	2.6 ± 0.1	0.710976	-	1471	-6.04
CLKS17-SM22	1	2.88 ± 0.05	0.71126	5	1669	-5.24
CLKS17-SM23	0.9	2.72 ± 0.03	0.711684	-	1453	-6.67
CLKS17-SM24	0.6	1.78 ± 0.03	0.712548	2.1	1279	-5.98
CLKS17-SM25	2	5.9 ± 0.1	0.710672	2.8	2501	-5.64
CLKS17-SM26	0.6	0.88 ± 0.01	0.712865	-	1494	-4.91
CLKS17-SM27	0.1	0.9 ± 0.02	0.718276	4	1038	-0.21
CLKS17-SM28	0.2	0.97 ± 0.02	0.717303	-	-	-
CLKS17-SM29	0.1	0.82 ± 0.01	0.717736	-	1021	1.84
CLKS17-SM30	0.1	0.79 ± 0.01	0.717625	-	1169	-2.72
CLKS17-SM31	0.3	0.85 ± 0.01	0.713723	-	-	-
Post-monsoon (Jan, 2018)						
CLK18-Ja68	0.8	2.23 ± 0.04	0.712589	3.3	1818	-2.84
CLK18-Ja69	0.6	1.91 ± 0.04	0.714229	3.4	1710	-3.13
CLK18-Ja70	1.9	4.8 ± 0.1	0.711399	4.4	1738	-4.69
CLK18-Ja71	4	10.6 ± 0.2	0.710273	6.3	1812	-5.11
CLK18-Ja72	6.3	16 ± 0.3	0.709874	7.3	-	-
CLK18-Ja76	7.7	20.1 ± 0.3	0.70968	8.4	1940	-7.46
CLK18-Ja77	5.3	13.4 ± 0.5	0.710183	6.1	1018	-10.66
CLK18-Ja78	4.1	10.9 ± 0.2	0.710392	4.5	2010	-4.28
CLK18-Ja79	5.7	15.1 ± 0.4	0.710134	5.9	-	-
CLK18-Ja86	0.3	1.33 ± 0.02	0.716971	2.5	-	-

CLK18-Ja12	8.43	-	-	-	2190	-5.06
CLK18-Ja72	6.27	-	-	-	1930	-8.29
CLK18-Ja73	7.56	-	-	-	2162	-5.22
CLK18-Ja66	0.98	-	-	-	2036	-3.18
CLK18-Ja67	0.43	-	-	-	1768	-4.32
CLK18-Ja74	7.99	-	-	-	2088	-7.78
CLK18-Ja80	1.32	-	-	-	2540	-0.56
CLK18-Ja82	0.38	-	-	-	2220	-2.31
CLK18-Ja83	0.36	-	-	-	2148	-4.54
CLK18-Ja85	0.27	-	-	-	1808	-4.06
CLK18-Ja87	0.28	-	-	-	1766	-1.12
CLK18-Ja88	0.46	-	-	-	1834	-2.42
CLK18-Ja89	0.32	-	-	-	1700	-1.78
CLK18-Ja90	0.34	-	-	-	1564	-8.88
CLK18-Ja91	0.49	-	-	-	1704	-0.41

**Errors on $^{87}Sr/^{86}Sr$ data are better than 10 ppm*

Table A3. Two-hourly data for pH, temperature, salinity, DIC, elemental (B, Ba, Re, Sr) and isotopic composition ($^{87}Sr/^{86}Sr$, $\delta^{13}C_{DIC}$) at two locations (Outer (Satapada) and southern (Barkul) sectors) of the Chilika lagoon during pre-monsoon, monsoon and post-monsoon seasons.

Sample id	Date and time of collection	Temp. (°C)	pH	Salinity	B (µmol/kg)	Ba (nmol/kg)	Re (pmol/kg)	Sr (µmol/kg)	$^{87}Sr/^{86}Sr$	DIC (µmol/kg)	$\delta^{13}C_{DIC}$ (‰)
Satapada (Outer channel; 19.669 °N; 85.437 °E)			-	-	-						
Monsoon (August, 2017)											
CLK17-M113	Aug-24-2017; 5:00 PM	32.7	8.5	8.3	114 ± 2	271 ± 12	10.7	19	0.709533	1779	-2.84
CLK17-M114	Aug-24-2017; 7:00 PM	32	8.47	7.3	101 ± 1	311 ± 10	10	20	0.70962	-	-
CLK17-M115	Aug-24-2017; 9:00 PM	31.9	8.41	6.4	92 ± 1	321 ± 9	9.5	18	0.709609	1408	-4.81
CLK17-M116	Aug-24-2017; 11:00 PM	31.6	8.41	7.4	85 ± 2	297 ± 9	9.7	20	0.70961	-	-
CLK17-M117	Aug-25-2017; 1:00 AM	31.9	8.35	8.5	119 ± 2	291 ± 8	11.4	24	0.709513	1813	-1.83
CLK17-M118	Aug-25-2017; 3:00 AM	30.6	8.34	8.4	110 ± 2	287 ± 16	10.9	22	0.709525	-	-
CLK17-M119	Aug-25-2017; 5:00 AM	30.9	8.34	7.1	105 ± 1	270 ± 24	10.1	21	0.709561	1711	-2.53
CLK17-M120	Aug-25-2017; 7:00 AM	31	8.26	7.3	99 ± 1	290 ± 13	9.6	20	0.709587	-	-
CLK17-M121	Aug-25-2017; 9:00 AM	31.3	8.33	6.7	97 ± 2	300 ± 12	9.5	19	0.70963	-	-
CLK17-M122	Aug-25-2017; 11:00 AM	31.2	8.5	7.9	105 ± 2	225 ± 7	10.2	21	0.709591	-	-
CLK17-M123	Aug-25-2017; 1:00 PM	31.3	8.66	9.2	120 ± 2	261 ± 9	11.3	24	0.709494	1748	-4.79
CLK17-M124	Aug-25-2017; 3:00 PM	31.3	8.4	8.9	116 ± 2	289 ± 9	11.6	24	0.709522	-	-
Pre-monsoon (May, 2017)											
CLK17-119	May-15-2017; 8:00 AM	29.7	7.65	36.6	455 ± 6	347 ± 5	-	93	0.709198	2605	-1.89
CLK17-120	May-15-2017; 10:00 AM	30.3	7.63	36	466 ± 5	175 ± 4	-	93	0.709205	-	-
CLK17-121	May-15-2017; 12:00 PM	31.3	7.59	35.4	456 ± 6	139 ± 3	-	90	0.709189	-	-
CLK17-122	May-15-2017; 2:00 PM	32.3	7.64	35.3	450 ± 4	413 ± 8	-	90	0.709177	2678	-1.04
CLK17-123	May-15-2017; 4:00 PM	32.3	7.62	35.1	446 ± 4	147 ± 5	-	90	0.709179	2551	-0.55
CLK17-124	May-15-2017; 6:00 PM	31.6	7.6	35.2	442 ± 7	133 ± 3	-	89	0.709181	2589	-1.62

CLK17-125	May-15-2017; 8:00 PM	30.9	7.59	35.4	447 ± 3	227 ± 5	-	93	0.709197	-	-
CLK17-126	May-15-2017; 10:00 PM	31.1	7.55	35.4	443 ± 5	321 ± 8	-	95	0.709202	-	-
CLK17-127	May-16-2017; 12:00 AM	30.4	8.4	36.3	451 ± 7	133 ± 4	-	92	0.709192	-	-
CLK17-128	May-16-2017; 2:00 AM	29.8	8.3	35.7	443 ± 8	95 ± 3	-	89	0.709184	2575	-0.95
CLK17-129	May-16-2017; 4:00 AM	29.6	8.3	35.2	450 ± 5	87 ± 2	-	90	0.709197	-	-
CLK17-130	May-16-2017; 6:00 AM	31.1	-	36.2	444 ± 6	293 ± 4	-	92	0.709189	2615	-2.72
Post-monsoon (January,2018)											
CLK18-Ja109	Jan-13-2018; 6:00 AM	24.4	7.1	6.2	-	693 ± 30	-	-	-	-	-
CLK18-Ja110	Jan-13-2018; 8:00 AM	24.4	8.49	6.2	-	671 ± 14	-	-	-	-	-
CLK18-Ja111	Jan-13-2018; 10:00 AM	24.4	8.13	6.3	-	660 ± 19	-	-	-	-	-
CLK18-Ja112	Jan-13-2018; 12:00 PM	24.5	8.38	6.2	-	547 ± 11	-	-	-	-	-
CLK18-Ja113	Jan-13-2018; 2:00 PM	24.5	8.33	6.4	-	484 ± 11	-	-	-	-	-
CLK18-Ja114	Jan-13-2018; 4:00 PM	24.5	8.37	6.4	-	735 ± 13	-	-	-	-	-
CLK18-Ja115	Jan-13-2018; 6:00 PM	24.2	8.45	6.6	-	441 ± 10	-	-	-	-	-
CLK18-Ja116	Jan-13-2018; 8:00 PM	24.2	8.38	6.6	-	530 ± 18	-	-	-	-	-
CLK18-Ja117	Jan-13-2018; 10:00 PM	24.3	8.37	6.2	-	612 ± 15	-	-	-	-	-
CLK18-Ja118	Jan-14-2018; 12:00 AM	24.3	8.49	6.2	-	nm	-	-	-	-	-
CLK18-Ja119	Jan-14-2018; 2:00 AM	24	8.43	6.2	-	646 ± 9	-	-	-	-	-
Barkul (Southern sector; *19.707* °N; 85.194 °E)											
Monsoon (August, 2017)											
CLK17-M38	Aug-05-2017; 12:00 PM	32.2	8.13	16.6	195 ± 3	698 ± 22	-	45	0.709406	-	-
CLK17-M39	Aug-05-2017; 2:00 PM	32.4	8.36	16.6	198 ± 2	635 ± 19	-	46	0.709405	-	-
CLK17-M40	Aug-05-2017; 4:00 PM	31.5	8.29	16.6	197 ± 2	635 ± 18	-	47	0.709402	-	-
CLK17-M41	Aug-05-2017; 6:00 PM	29.7	8.2	16.1	206 ± 3	615 ± 17	-	47	0.709402	-	-
CLK17-M42	Aug-05-2017; 8:00 PM	30.5	8.09	16.1	207 ± 2	602 ± 9	-	44	0.709392	-	-
CLK17-M43	Aug-05-2017; 10:00 PM	30.6	8.07	16.1	210 ± 3	604 ± 15	-	46	0.7094	-	-
CLK17-M44	Aug-06-2017; 12:00 AM	30.4	8.17	16	206 ± 2	640 ± 22	-	46	0.709392	-	-
CLK17-M45	Aug-06-2017; 2:00 AM	30.4	8.05	15.9	212 ± 3	657 ± 15	-	47	0.70939	-	-
CLK17-M46	Aug-06-2017; 4:00 AM	30.2	8.02	16.1	210 ± 2	661 ± 16	-	46	0.709389	-	-
CLK17-M47	Aug-06-2017; 6:00 AM	30.1	7.86	15.9	205 ± 3	635 ± 21	-	-	-	-	-
CLK17-M48	Aug-06-2017; 8:00 AM	30.8	8.12	15.7	203 ± 3	648 ± 43	-	-	-	-	-

CLK17-M49	Aug-06-2017; 10:00 AM	33.7	8.23	13.2	174 ± 2	nm	-	-	-	-	-
Pre-monsoon (May, 2017)											
CLK17-39	May-03-2017; 3:00 PM	33.3	8.83	14.3	160 ± 2	863 ± 13	-	35	0.709557	-	-
CLK17-40	May-03-2017; 5:00 PM	32.1	8.89	15	176 ± 3	869 ± 19	-	37	0.709544	-	-
CLK17-41	May-03-2017; 7:00 PM	31.2	8.3	15.6	185 ± 1	859 ± 27	-	40	0.709554	-	-
CLK17-42	May-03-2017; 9:00 PM	30.6	8.8	14.6	168 ± 3	849 ± 27	-	37	0.709557	-	-
CLK17-43	May-03-2017; 11:00 PM	30.2	8.78	14.2	167 ± 1	849 ± 19	-	36	0.709563	-	-
CLK17-44	May-04-2017; 1:00 AM	30.2	8.78	13.8	171 ± 2	835 ± 21	-	38	0.709559	-	-
CLK17-45	May-04-2017; 5:00 AM	29	8.8	13.6	165 ± 3	871 ± 25	-	36	0.709563	-	-
CLK17-46	May-04-2017; 7:00 AM	31.4	8.28	13.5	164 ± 2	815 ± 26	-	35	0.709572	-	-
CLK17-47	May-04-2017; 9:00 AM	30.8	8.18	13.6	166 ± 3	844 ± 19	-	36	0.70957	-	-
CLK17-48	May-04-2017; 11:00 AM	32.8	8.5	14.1	170 ± 3	827 ± 20	-	37	0.709569	-	-
CLK17-49	May-04-2017; 1:00 PM	33.6	8.52	14	177 ± 1	3157 ± 81	-	38	0.709583	-	-
Post-monsoon (January, 2018)											
CLK18-Ja48	Jan-5-2018; 2:00 PM	21.8	7.87	7.9	-	379 ± 11	-	-	-	-	-
CLK18-Ja49	Jan-5-2018; 6:00 PM	21.8	9.07	8	-	513 ± 9	-	-	-	-	-
CLK18-Ja50	Jan-5-2018; 8:00 PM	21.3	9.47	7.1	-	1068 ± 56	-	-	-	-	-
CLK18-Ja51	Jan-5-2018; 10:00 PM	21.6	9.41	7.8	-	918 ± 42	-	-	-	-	-
CLK18-Ja52	Jan-6-2018; 12:00 AM	21.6	9.12	7.8	-	426 ± 12	-	-	-	-	-
CLK18-Ja53	Jan-6-2018; 2:00 AM	21.8	8.98	7.7	-	943 ± 47	-	-	-	-	-
CLK18-Ja54	Jan-6-2018; 4:00 AM	21.5	8.82	7.9	-	426 ± 11	-	-	-	-	-
CLK18-Ja55	Jan-6-2018; 6:00 AM	21.7	8.79	7.8	-	455 ± 10	-	-	-	-	-
CLK18-Ja56	Jan-6-2018; 8:00 AM	21.4	9.1	7.9	-	414 ± 7	-	-	-	-	-
CLK18-Ja57	Jan-6-2018; 10:00 AM	21.9	9.5	7.8	-	418 ± 8	-	-	-	-	-
CLK18-Ja58	Jan-6-2018; 12:00 AM	24	9.6	8.1	-	405 ± 11	-	-	-	-	-

Table A4. Data on pH, temperature, salinity, DIC, geographical coordinates and elemental (B, Sr, Re, Ba) and isotopic composition ($^{87}Sr/^{86}Sr$ and $\delta^{13}C_{DIC}$) of source (river/rivulets, rain, groundwater, coastal and western Bay of Bengal, Palur canal) water samples collected during all filed campaigns.

Sample ID	Date of collection	Lat	Long	pH	Temp (°C)	Salinity	B (μmol/kg)	Ba (nmol/kg)	Re (pmol/kg)	Sr (μmol/kg)	$^{87}Sr/^{86}Sr$	DIC (μmol/kg)	$\delta^{13}C_{DIC}$ (‰)
						Groundwater Samples							
						Pre-monsoon (May, 2017)							
CLK17-17	28-Apr-17	19.51	85.09	7.26	28	0.81	7 ± 0.1	4055 ± 45	-	11	0.71494	-	-
CLK17-50	5-May-17	19.67	85.16	7.14	28.4	1.21	23 ± 0.3	1141 ± 17	-	13	0.71607	-	-
CLK17-52	5-May-17	19.62	85.12	7.6	28.6	0.28	4 ± 0.1	1006 ± 18	-	1	-	-	-
CLK17-54	5-May-17	19.57	85.1	7	29.2	0.35	10 ± 0.2	662 ± 14	-	4	0.71877	-	-
CLK17-55	5-May-17	19.54	85.09	7.1	27.9	0.62	9 ± 0.2	-	-	6	0.71919	-	-
CLK17-56	5-May-17	19.47	85.09	7.6	29.3	1.04	55 ± 1	551 ± 10	20	6	0.71574	-	-
CLK17-57	5-May-17	19.45	85.12	6.8	29.2	0.43	14 ± 0.2	160 ± 3	-	3	0.71523	-	-
CLK17-58	5-May-17	19.5	85.19	7.7	29.4	0.74	21 ± 0.3	62 ± 2	38	3	-	-	-
CLK17-59	5-May-17	19.59	85.25	7.6	32.1	1.05	88 ± 1	323 ± 8	-	5	0.71652	-	-
CLK17-60	5-May-17	19.62	85.31	7.2	29	8.18	239 ± 3	344 ± 5	-	22	0.70993	-	-
CLK17-61	5-May-17	19.65	85.38	7.5	29.9	0.92	31 ± 1	286 ± 4	-	4	0.71313	-	-
CLK17-63	5-May-17	19.82	85.27	7.7	29.1	0.4	6 ± 0.1	-	-	6	0.71349	-	-
CLK17-64	5-May-17	19.84	85.28	6.6	28.9	0.15	3 ± 0.1	778 ± 15	-	1	0.71623	-	-
CLK17-65	5-May-17	19.71	85.19	7.12	31.5	0.79	8 ± 0.1	-	-	1	-	-	-
CLK17-69	5-May-17	19.76	85.21	7.4	31.6	0.54	3 ± 0.07	35 ± 1	-	6	0.71056	-	-
CLK17-97	13-May-17	19.82	85.33	6.87	30.5	1.37	34 ± 1	-	-	2	0.71349	-	-
CLK17-98	13-May-17	19.92	85.43	7.18	30.4	0.72	2 ± 0.02	516 ± 10	4	1	0.71632	-	-
CLK17-99	13-May-17	19.94	85.45	6.2	30.3	0.5	4 ± 0.1	258 ± 5	-	4	0.72228	-	-
CLK17-100	13-May-17	19.93	85.5	7.1	30.31	1.59	17 ± 0.2	302 ± 5	-	7	0.71619	-	-
CLK17-101	13-May-17	19.97	85.53	6.96	30.5	0.19	4 ± 0.1	553 ± 12	2	2	-	-	-
CLK17-103	13-May-17	19.95	85.66	6.86	30.2	3	41 ± 0.5	2630 ± 59	-	35	0.86605	-	-
CLK17-105	13-May-17	19.88	85.69	7.1	30.4	2.06	18 ± 0.3	4428 ± 70	0.25	21	0.71187	-	-
CLK17-107	13-May-17	19.81	85.65	7.32	30.5	0.85	22 ± 0.2	4390 ±	-	4	0.71073	-	-

CLK17-108	13-May-17	19.79	85.61	7.39	30.1	1.41	53 ± 1	464 ± 7	-	11	0.71537	-	-
CLK17-131	17-May-17	19.69	85.47	7.21	29.1	0.23	12 ± 0.2	424 ± 10	-	0.35	-	-	-
Monsoon (May, 2017)													
CLK17-M16	1-Aug-17	19.51	85.09	7.26	28	0.81	7 ± 0.08	1915 ± 33	16	11	0.71524	-	-
CLK17-M50	7-Aug-17	19.65	85.4	7.12	30.9	0.95	18 ± 0.2	422 ± 9	-	6	-	-	-
CLK17-M51	7-Aug-17	19.62	85.31	6.51	30.2	4.32	123 ± 1	497 ± 8	-	19	-	-	-
CLK17-M52	7-Aug-17	19.53	85.25	7.43	31.8	1.21	89 ± 1	298 ± 5	-	8	0.7159	-	-
CLK17-M53	7-Aug-17	19.5	85.19	7.58	30.3	0.75	19 ± 0.3	87 ± 2	-	3	-	-	-
CLK17-M55	7-Aug-17	19.45	85.12	-	-	0.41	13 ± 0.1	159 ± 3	4	3	0.71499	4051	-6.11
CLK17-M56	7-Aug-17	19.47	85.09	7.53	30.2	0.99	45 ± 0.6	373 ± 6	-	5	-	-	-
CLK17-M57	7-Aug-17	19.54	85.09	7.51	29.7	0.51	6 ± 0.1	1200 ± 12	13	5	-	-	-
CLK17-M58	7-Aug-17	19.57	85.1	7.23	31.2	0.12	3 ± 0.03	335 ± 5	-	1	-	-	-
CLK17-M60	7-Aug-17	19.62	85.12	6.85	29.5	0.13	2 ± 0.03	740 ± 18	-	1	-	-	-
CLK17-M62	7-Aug-17	19.67	85.16	7.43	30.3	0.41	7 ± 0.1	701 ± 12	-	5	0.71606	-	-
CLK17-M63	7-Aug-17	19.71	85.19	7.63	29.7	0.75	8 ± 0.1	20 ± 0	-	4	-	12142	-9.11
CLK17-M66	7-Aug-17	19.76	85.21	6.99	29.5	0.39	2 ± 0.03	66 ± 1	-	5	-	-	-
CLK17-M68	7-Aug-17	19.82	85.27	7.44	29.4	0.38	5 ± 0.05	22 ± 0	-	6	0.7127	-	-
CLK17-M69	7-Aug-17	19.84	85.28	5.96	29.6	0.16	4 ± 0.1	931 ± 15	-	1	-	-	-
CLK17-M92	13-Aug-17	19.85	85.37	-	-	0.14	2 ± 0.03	134 ± 2	-	1	-	-	-
CLK17-M96	16-Aug-17	19.92	85.43	5.61	29.3	0.17	1 ± 0.01	641 ± 10	-	1	-	-	-
CLK17-M97	16-Aug-17	19.94	85.45	6.77	29.9	0.38	4 ± 0.07	163 ± 4	-	3	0.73335	3556	-3.98
CLK17-M98	16-Aug-17	19.93	85.5	7.02	30.5	1.37	18 ± 0.3	483 ± 7	-	6	0.71693	-	-
CLK17-M99	16-Aug-17	19.97	85.35	6.86	28.6	0.27	4 ± 0.1	520 ± 9	2	2	0.71201	2459	-5.09
CLK17-M101	16-Aug-17	19.95	85.66	7.17	29.7	3.02	42 ± 1	675 ± 23	0.28	34	0.71564	2136	-4.57
CLK17-M103	16-Aug-17	19.88	85.69	7.55	29.8	2.01	18 ± 0.2	2001 ± 60	-	21	0.71189	2876	-6.04
CLK17-M105	16-Aug-17	19.81	85.65	7.56	29.9	0.97	23 ± 0.3	1917 ± 34	35	4	0.71074	-	-
CLK17-M106	16-Aug-17	19.79	85.61	7.6	30	1.57	44 ± 1	585 ± 10	-	14	0.71551	5810	-3.46
CLK17- M125	27-Aug-17	19.69	85.47	6.71	29.5	nm	11 ± 0.1	384 ± 5	-	0.4	-	-	-
Post-monsoon (May, 2017)													
CLK18-Ja23	4-Jan-18	19.51	85.09	7.34	23.1	0.8	-	1373 ± 32	-	6	-	-	-

CLK18-Ja24	4-Jan-18	19.47	85.09	8.06	23.4	1.27	-	432 ± 11	-	6	-	-	-
CLK18-Ja25	4-Jan-18	19.45	85.12	6.77	23.6	0.44	-	166 ± 3	-	3	-	-	-
CLK18-Ja27	4-Jan-18	19.5	85.19	8.03	23.3	1.46	-	132 ± 2	-	4	-	-	-
CLK18-Ja28	4-Jan-18	19.59	85.25	7.88	23.5	1.29	-	339 ± 8	-	5	-	-	-
CLK18-Ja29	4-Jan-18	19.62	85.31	7.35	23	3.92	-	367 ± 6	-	13	-	-	-
CLK18-Ja30	4-Jan-18	19.65	85.4	7.4	22.7	0.7	-	217 ± 3	-	2	-	-	-
CLK18-Ja31	4-Jan-18	19.57	85.1	7.99	22.8	0.75	-	1441 ± 28	-	5	-	-	-
CLK18-Ja33	4-Jan-18	19.6	85.12	7.56	22.6	0.18	-	996 ± 17	-	1	-	-	-
CLK18-Ja35	4-Jan-18	19.66	85.15	8.18	22.6	0.95	-	950 ± 28	-	15	-	-	-
CLK18-Ja59	6-Jan-18	19.71	85.19	7.95	23	1	-	nm	-	5	-	-	-
CLK18-Ja62	6-Jan-18	19.76	85.21	7.18	23	0.63	-	60 ± 1	-	7	-	-	-
CLK18-Ja64	6-Jan-18	19.82	85.27	7.62	22.9	0.45	-	nm	-	7	-	-	-
CLK18-Ja65	6-Jan-18	19.84	85.28	7.22	23	0.17	-	668 ± 17	-	1	-	-	-
CLK18-Ja92	12-Jan-18	19.92	85.43	6.72	24.1	0.32	-	289 ± 8	-	2	-	-	-
CLK18-Ja93	12-Jan-18	19.94	85.45	6.27	24.1	6.27	-	416 ± 10	-	-	-	-	-
CLK18-Ja94	12-Jan-18	19.93	85.5	7.01	24.1	0.43	-	183 ± 7	-	3	-	-	-
CLK18-Ja95	12-Jan-18	19.97	85.35	7.33	24.3	1.23	-	387 ± 12	-	5	-	-	-
CLK18-Ja96	12-Jan-18	19.95	85.66	7.43	24.3	0.32	-	590 ± 17	-	3	-	-	-
CLK18-Ja99	12-Jan-18	19.88	85.69	7.44	24.3	2.39	-	2236 ± 56	-	-	-	-	-
CLK18-Ja101	12-Jan-18	19.81	85.65	7.77	24.4	1.58	-	1864 ± 56	-	4	-	-	-
CLK18-Ja102	12-Jan-18	19.79	85.61	7.84	24.2	1.96	-	625 ± 18	-	15	-	-	-
CLK18-Ja120	14-Jan-18	19.69	85.47	8.66	24.2	0.4	-	177 ± 4	-	-	-	-	-

Onset of monsoon (June, 2016)

CLK16-8	19-Jun-16	19.52	85.09	7.38	30.6	1.46	39 ± 1	-	-	-	-	-	-
CLK16-9	19-Jun-16	19.54	85.1	7.3	29.6	1.25	20 ± 0.4	-	-	-	-	-	-
CLK16-37	22-Jun-16	19.74	85.57	6.23	30.6	1.48	28 ± 0.4	-	-	-	-	-	-
CLK16-41	22-Jun-16	19.93	85.51	7.28	32	1.85	12 ± 0.1	-	-	-	-	-	-
CLK16-42	22-Jun-16	19.93	85.51	7.64	32.2	1.38	8 ± 0.1	-	-	-	-	-	-

Rivers/Rivulets (Draining into Chilika)

Mahanadi Distributaries

Pre-monsoon (May, 2017)

CLK17-102 (Daya R.)	12-May-17	19.97	85.62	7.32	30.5	0.13	2 ± 0.04	583 ± 11	6.17	-	-	-	-
CLK17-104 (Luna R.)	12-May-17	19.95	85.67	7.67	30.5	0.16	2 ± 0.03	293 ± 6	5.74	-	-	-	-
CLK17-106 (Bhargavi R.)	12-May-17	19.86	85.66	7.8	30.5	0.12	2 ± 0.03	319 ± 7	6.53	-	-	-	-
Monsoon (May, 2017)													
CLK17-M100 (Daya R.)	16-Aug-17	19.97	85.62	*7.45*	*31.6*	0.12	0.5 ± 0.01	324 ± 5	4.59	0.9	0.71912	-	-
CLK17-M102 (Luna R.)	16-Aug-17	19.95	85.67	7.22	31.4	0.26	1 ± 0.02	264 ± 3	3.47	1	0.71896	1299	-0.55
CLK17-M104 (Bhargavi R.)	16-Aug-17	19.86	85.66	7.23	31.6	0.16	2 ± 0.03	274 ± 4	4.05	1	0.71942	-	-
Post-monsoon (May, 2017)													
CLK18-Ja97 (Daya)	12-Jan-18	19.97	85.62	7.5	24.1	0.28	-	256 ± 6	-	-	-	-	-
CLK18-Ja98 (Luna)	12-Jan-18	19.95	85.67	7.6	24.3	0.52	-	436 ± 9	-	-	-	-	-
CLK18-Ja100 (Bhargavi)	12-Jan-18	19.86	85.66	8	24.4	0.34	-	322 ± 8	-	-	-	-	-
Onset of monsoon (June, 2016)													
CLK16-38 (Bhargavi R.)	22-Jun-16	19.86	85.66	7.12	32.8	0.15	3 ± 0.04	-	-	-	-	-	-
CLK16-39 (Luna R.)	22-Jun-16	19.95	85.67	7.12	31.6	0.94	3 ± 0.1	-	-	-	-	-	-
CLK16-40 (Daya R.)	22-Jun-16	19.97	85.62	7.25	33.4	0.26	2 ± 0.03	-	-	-	-	-	-
Rivulet/sewage from western catchments													
Pre-monsoon (May, 2017)													
CLK17-51	5-May-17	19.66	85.15	7.39	30.2	6.95	82 ± 4	1124 ± 16	-	-	-	-	-
CLK17-53	5-May-17	19.6	85.12	7.8	29.9	nm	29 ± 0.4	2233 ± 40	-	-	-		
CLK17-62	5-May-17	19.79	85.22	7.48	31.1	0.13	1 ± 0.03	446 ± 4	-	-	-	-	-
CLK17-66	5-May-17	19.72	85.19	7.37	31.5	14.64	167 ± 2	2100 ± 20	-	-	-	-	-
CLK17-67	5-May-17	19.73	85.2	7.5	31	0.34	1 ± 0.03	283 ± 3	-	-	-	-	-
CLK17-68	5-May-17	19.74	85.2	7.15	31	0.34	1 ± 0.02	-	-	-	-	-	-
CLK17-70	5-May-17	19.84	85.35	7.8	31.2	0.22	3 ± 0.06	1507 ± 22	-	-	-	-	-

CLK17-71	5-May-17	19.87	85.38	7.6	30.6	0.16	2 ± 0.03	701 ± 12	-	-	-	-	-
Monsoon (May, 2017)													
CLK17-M59	7-Aug-17	19.6	85.12	7.45	32	0.11	2 ± 0.03	392 ± 7	-	-	-	-	-
CLK17-M61	7-Aug-17	19.66	85.15	7.66	31.8	0.12	2.7 ± 0.03	572 ± 11	-	-	-	-	-
CLK17-M64	7-Aug-17	19.73	85.2	7.77	32.6	0.09	1 ± 0.02	331 ± 5	-	-	-	-	-
CLK17-M67	7-Aug-17	19.78	85.23	7.82	31.7	0.11	1 ± 0.01	201 ± 3	-	-	-	1697	-6.16
CLK17-M70	7-Aug-17	19.72	85.2	7.98	28.9	0.62	7 ± 0.1	718 ± 15	-	-	-	-	-
CLK17-M93	13-Aug-17	19.84	85.35	-	-	0.13	2 ± 0.02	217 ± 5	-	0.8	0.71782	-	-
Post-monsoon (May, 2017)													
CLK18-Ja32	4-Jan-18	19.66	85.15	8.37	22.4	0.37	-	569 ± 13	-	-	-	-	-
CLK18-Ja34	4-Jan-18	19.6	85.12	8.08	22.1	0.6	-	851 ± 16	-	-	-	-	-
CLK18-Ja60	6-Jan-18	19.72	85.2	8.21	22.6	0.1	-	293 ± 4	-	-	-	-	-
CLK18-Ja61	6-Jan-18	19.73	85.2	7.66	22.8	0.42	-	811 ± 32	-	-	-	-	-
CLK18-Ja63	6-Jan-18	19.79	85.22	8.09	22.8	0.17	-	372 ± 9	-	-	-	-	-
Onset of monsoon (June, 2016)													
CLK16-13	19-Jun-16	19.605	85.117	7.22	30.4	20.17	164 ± 2	-	-	-	-	-	-
Other East-flowing rivers (Rushikulya; near mouth)													
CLK17-M01	29-Jul-17	19.49	84.91	7.97	33.3	0.34	4 ± 0.03	415 ± 11	-	-	-	-	-
CLK17-M03	29-Jul-17	19.38	85.04	8.35	30.4	0.33	1 ± 0.02	330 ± 5	-	-	-	-	-
CLK17-01	26-Apr-16	19.49	84.91	8.1	33.9	0.75	4 ± 0.03	572 ± 10	-	-	-	-	-
CLK17-03	26-Apr-16	19.38	85.04	8.22	31.2	26.72	322 ± 5	1718 ± 39	-	-	-	-	-
CLK18-Ja1	2-Jan-18	19.49	84.91	8.86	24.5	0.28	-	423 ± 13	-	-	-	-	-
CLK18-Ja3	2-Jan-18	19.38	85.04	8.16	23.9	8.22	-	553 ± 23	-	-	-	-	-
Bay of Bengal (Nov.- Dec., 2013)													
Leg 2 - 01	-	7.116	85.416	-	-	31.9	399 ± 6	30	39	-	-	-	-
Leg 2 - 02	-	8.411	85.897	-	-	32.8	391 ± 5	-	-	-	-	-	-
Leg 2 - 03	-	9.611	86.343	-	-	33.1	413 ± 6	33	-	-	-	-	-
Leg 2 - 04	-	10.213	86.568	-	-	31.5	406 ± 6	39	41	-	-	-	-
Leg 2 - 05	-	12.09	87.271	-	-	32.6	407 ± 4	35	-	85	0.7092	-	-
Leg 2 - 06	-	12.715	87.508	-	-	30.5	406 ± 3	-	-	-	-	-	-

Leg 2 - 07	-	13.965	87.979	-	-	31.7	400 ± 6	-	-	-	-	-	-
Leg 2 - 08	-	14.904	88.335	-	-	32.3	406 ± 7	45	41	-	-	-	-
Leg 2 - 09	-	16.47	88.933	-	-	30.7	382 ± 3	45	-	-	-	-	-
Leg 2 - 10	-	17.098	89.175	-	-	30.3	393 ± 6	42	-	-	-	-	-
Leg 2 - 12	-	17.599	89.2	-	-	32.2	401 ± 7	37	39	-	-	-	-
Leg 2 - 13	-	17.135	88.655	-	-	31.5	395 ± 6	43	-	82	0.70919	-	-
Leg 2 - 14	-	16.672	88.11	-	-	30.9	403 ± 6	37	-	-	-	-	-
Leg 2 - 15	-	16.378	87.567	-	-	32	414 ± 7	31	-	-	-	-	-
Leg 2 - 16	-	15.747	87.019	-	-	31.2	439 ± 6	53	38	-	-	-	-
Leg 2 - 18	-	14.82	85.931	-	-	32	400 ± 8	30	39	-	-	-	-
Leg 2 - 19	-	14.357	85.388	-	-	32.8	416 ± 5	30	-	-	-	-	-
Leg 2 - 20	-	13.437	85.295	-	-	33.6	426 ± 6	-	-	87	0.70918	-	-
Leg 2 - 22	-	8.822	88.563	-	-	32.5	420 ± 6	38	-	-	-	-	-
							<u>Coastal Bay of Bengal (January, 2018)</u>						
BoB18-01	-	19.678	85.562	-	-	27.1	349 ± 5	105	-	-	-	-	-
BoB18-2	-	19.672	85.569	-	-	27	347 ± 4	72	-	-	-	-	-
BoB18-3	-	19.66	85.567	-	-	27	346 ± 4	172	-	-	-	-	-
BoB18-5	-	19.638	85.567	-	-	26.5	338 ± 5	93	-	-	-	-	-
BoB18-6	-	19.641	85.565	-	-	26.7	342 ± 6	135	31	-	-	-	-
BoB18-7	-	19.645	85.564	-	-	26.7	341 ± 6	87	33	-	-	-	-
BoB18-8	-	19.651	85.562	-	-	26.4	344 ± 5	109	31	-	-	-	-
BoB18-9	-	19.658	85.561	-	-	27.2	349 ± 5	95	30	-	-	-	-
BoB18-10	-	19.664	85.558	-	-	26.5	350 ± 7	90	31	-	-	-	-
OD14-R1 (Rushikulya) (upper reaches)	-	-	-	-	-	-	0.73 ± 0.39	-	-	-	-	-	-
OD14-R2 (Rushikulya) (Jarao Tributary)		-	-	-	-	-	2.27 ± 0.05	-	-	-	-	-	-

OD14-R3 (Rushikulya) (after Jarao confl.)	-	-	-	-	-	1.96 ± 0.02	-	-	-	-	-	-
OD14-R6 (Rushikulya) (after Badanadi confl.)	-	-	-	-	-	1.54 ± 0.02	-	-	-	-	-	-
OD14-V2 (Vamsadhara)	-	-	-	-	-	0.83 ± 0.02	-	-	-	-	-	-
OD14-N1 (Nagavalli)	-	-	-	-	-	0.88 ± 0.02	-	-	-	-	-	-
RW17-M9 (Damodar)	-	-	-	-	-	1.52 ± 0.04	-	-	-	-	-	-
RW17-M10 (Swarnarekha)	-	-	-	-	-	1.58 ± 0.03	-	-	-	-	-	-
RW17-M11 (Brahamani)	-	-	-	-	-	1.12 ± 0.02	-	-	-	-	-	-
RW17-M12 (Mahanadi)	-	-	-	-	-	1.31 ± 0.03	-	-	-	-	-	-
Palur canal												
CLK17-M02	-	-	-	-	32	349 ± 4	-	-	-	-	-	-
CLK17-M54	-	-	-	-	18.5	207 ± 3	-	-	-	-	-	-
CLK17-02	-	-	-	-	33.5	396 ± 5	-	-	-	-	-	-
CLK17-16	-	-	-	-	34.3	409 ± 9	-	-	-	-	-	-
Rainwater (2016-2017)												
BRW17-01	-	-	-	-	-	2.92±0.04	-	-	-	-	-	-
BRW17-2	-	-	-	-	-	1.36±0.02	-	-	-	-	-	-
BRW17-3	-	-	-	-	-	0.186±0.004	-	-	-	-	-	-
BRW17-4	-	-	-	-	-	0.65 ± 0.02	-	-	-	-	-	-
BRW17-5	-	-	-	-	-	0.38 ± 0.01	-	-	-	-	-	-
BRW17-6	-	-	-	-	-	0.47 ± 0.01	-	-	-	-	-	-
BRW17-7	-	-	-	-	-	0.5 ± 0.01	-	-	-	-	-	-
BRW17-8	-	-	-	-	-	0.48 ± 0.01	-	-	-	-	-	-

BRW17-9	-	-	-	-	-	0.21 ± 0.01	-	-	-	-	-	-
BRW17-10	-	-	-	-	-	0.207±0.005	-	-	-	-	-	-
BRW17-11	-	-	-	-	-	1.22 ± 0.03	-	-	-	-	-	-
BRW17-12	-	-	-	-	-	0.97 ± 0.01	-	-	-	-	-	-
BRW17-13	-	-	-	-	-	0.76 ± 0.02	-	-	-	-	-	-
BRW17-14	-	-	-	-	-	0.49 ± 0.01	-	-	-	-	-	-
BRW17-15	-	-	-	-	-	0.42 ± 0.01	-	-	-	-	-	-
BRW17-16	-	-	-	-	-	0.42 ± 0.01	-	-	-	-	-	-
BRW17-17	-	-	-	-	-	0.71 ± 0.02	-	-	-	-	-	-
BRW17-18	-	-	-	-	-	0.47 ± 0.01	-	-	-	-	-	-
BRW17-19	-	-	-	-	-	0.33 ± 0.01	-	-	-	-	-	-
BRW17-20	-	-	-	-	-	0.47 ± 0.01	-	-	-	-	-	-
BRW17-21	-	-	-	-	-	1.3 ± 0.03	-	-	-	-	-	-
BRW17-22	-	-	-	-	-	0.93 ± 0.01	-	-	-	-	-	-
BRW17-23	-	-	-	-	-	0.59 ± 0.01	-	-	-	-	-	-
BRW17-24	-	-	-	-	-	0.37 ± 0.01	-	-	-	-	-	-
BRW17-25	-	-	-	-	-	0.33 ± 0.01	-	-	-	-	-	-
BRW17-26	-	-	-	-	-	0.7 ± 0.02	-	-	-	-	-	-
BRW17-27	-	-	-	-	-	0.82 ± 0.02	-	-	-	-	-	-
BRW17-28	-	-	-	-	-	0.39 ± 0.01	-	-	-	-	-	-
CLK17-RW1	-	-	-	-	-	0.42 ± 0.01	-	-	-	-	-	-
CLK17-RW2	-	-	-	-	-	0.29 ± 0.01	-	-	-	-	-	-
CLK16-RW1	-	-	-	-	-	0.21 ± 0.004	-	-	-	-	-	-

Table A5. Data on elements (Major and trace elements), clay abundances, TOC, TN, P, and $\delta^{13}C_{org}$ isotopic data for bed sediments from the Chilika lagoon and bed sediments from the rivers.

Sample List	Na	K	Ca	Mg	Al	Fe	Ti	Clay (%)	P	TOC	TN	B	V	Mn	Co	Zn	Sr	Mo	Ba	U	$\delta^{13}C_{org}$
	wt%											µg/g									(‰)
CLK16-02	0.9	2.2	0.7	1.4	12.4	5.9	0.7	76.4	0.1	1.3	0.1	10	123	490	20	90	109	1.5	611	2.3	-21.5
CLK16-3	1.0	2.3	0.3	1.6	13.0	6.3	0.6	99.6	0.2	1.0	0.1	15	135	740	22	92	75	1.3	382	2.4	-21.6
CLK16-4	0.8	2.4	0.4	1.2	10.7	5.3	0.6	68.0	0.2	0.7	0.1	12	111	577	18	76	82	0.8	467	2.4	-21.4
CLK16-5	0.9	2.1	0.3	1.5	12.1	5.9	0.5	87.0	0.2	0.9	0.1	14	129	995	21	90	77	1.2	382	2.2	-21.2
CLK16-6	1.0	2.3	0.4	1.3	11.4	5.6	0.6	11.7	0.2	0.8	0.1	10	121	596	19	84	77	1.3	423	2.4	-21.4
CLK16-7	0.9	2.1	0.9	1.4	12.2	5.8	0.8	68.2	0.1	1.3	0.1	13	124	519	20	88	113	1.0	557	2.1	-20.6
CLK16-10	1.1	1.8	0.5	1.4	10.5	5.3	0.9	53.6	0.1	0.7	0.1	12	127	722	20	81	77	1.0	327	2.5	-20.9
CLK16-11	0.8	2.5	0.6	0.8	8.1	4.0	0.4	38.3	0.0	0.6	0.1	6	91	479	14	53	98	0.6	592	1.8	-22.8
CLK16-12	2.7	2.8	0.5	2.5	17.0	8.4	0.6	78.9	0.1	1.0	0.2	16	124	1199	22	127	78	1.0	323	2.5	-21.0
CLK16-14	0.4	1.0	0.3	0.2	2.7	2.0	0.9	14.0	0.1	0.3	0.0	5	63	245	7	36	42	0.6	277	1.5	-25.2
CLK16-15	0.5	1.5	0.4	0.5	4.3	2.4	0.6	18.2	0.0	0.5	0.1	5	62	323	8	48	60	0.7	375	1.4	-20.3
CLK16-16	0.4	1.1	0.3	0.2	2.5	1.5	0.5	4.6	0.0	0.6	0.0	4	48	247	6	26	44	0.6	287	1.1	-22.2
CLK16-17	0.6	1.5	0.4	0.5	5.2	2.9	0.7	25.1	0.0	0.4	0.0	8	67	310	9	41	51	0.7	324	1.1	-22.9
CLK16-18	0.9	2.4	1.9	2.0	16.2	8.1	0.6	90.5	0.1	1.2	0.1	14	112	488	18	75	111	0.8	247	3.1	-23.2
CLK16-19	0.9	2.0	3.6	2.0	13.9	7.4	0.5	77.1	0.1	2.3	0.2	14	114	719	19	77	190	0.8	254	2.5	-21.5
CLK16-20	0.9	1.9	2.3	1.8	12.9	7.2	0.5	52.8	0.1	2.8	0.3	16	126	907	21	85	170	0.9	285	2.4	-21.2
CLK16-21	0.8	1.7	2.2	1.8	13.6	6.8	0.4	78.6	0.1	2.8	0.2	15	115	796	20	81	160	0.9	257	2.2	-21.2
CLK16-22	1.8	2.6	1.1	2.6	18.5	8.7	0.6	87.2	0.1	1.0	0.2	14	116	666	20	81	89	0.8	265	3.1	-21.1
CLK16-23	1.7	2.3	1.7	2.1	14.5	7.6	0.6	86.0	0.1	1.6	0.2	12	115	633	19	79	105	0.9	271	2.7	-21.0
CLK16-24	0.8	2.0	1.0	1.8	13.7	6.5	0.5	86.1	0.1	1.7	0.2	14	104	545	18	75	88	0.7	275	2.2	-21.2
CLK16-25	0.8	2.1	0.3	0.8	7.8	3.9	0.6	51.7	0.1	0.7	0.1	7	90	411	14	65	80	0.8	502	1.6	-21.3
CLK16-26	0.7	1.7	0.3	0.7	6.2	3.2	0.5	40.2	0.0	1.0	0.1	7	77	406	12	49	68	0.8	415	1.5	-23.9
CLK16-27	1.2	2.2	0.3	1.6	13.3	7.1	0.5	77.3	0.1	1.5	0.2	9	137	772	23	89	72	1.0	332	2.8	-21.6
CLK16-28	1.0	2.7	0.8	2.0	16.8	8.9	0.7	85.6	0.1	1.4	0.1	11	130	1137	21	85	77	0.9	317	3.3	-21.6

CLK16-29	1.1	2.7	0.8	2.0	17.0	8.9	0.7	82.3	0.1	1.0	0.1	7	135	1090	22	91	82	1.1	345	3.4	-20.4
CLK16-30	0.8	2.1	0.9	1.4	12.1	6.5	0.5	74.7	0.1	1.3	0.1	7	123	1179	21	83	94	1.1	399	2.4	-21.8
CLK16-31	0.6	2.0	0.6	1.4	12.6	6.8	0.5	82.3	nd	1.0	0.1	9	123	1245	21	82	81	0.7	381	2.6	-21.1
CLK16-32	0.9	2.1	0.5	1.0	12.0	6.3	0.5	49.7	0.1	1.9	0.1	6	123	1142	26	85	82	1.1	580	3.4	-24.7
CLK16-34	0.7	2.0	0.5	1.2	11.3	6.2	0.5	83.2	0.1	1.2	0.1	10	125	2190	21	80	81	0.9	407	2.4	-21.7
CLK16-35	1.2	1.9	0.5	1.5	12.1	6.4	0.5	85.8	0.1	0.9	0.1	10	135	1052	22	87	81	1.0	340	2.4	-21.2
CLK16-36	1.1	2.3	0.4	1.8	14.3	7.4	0.5	77.0	0.1	1.1	0.1	10	127	784	21	86	68	0.8	288	2.8	-21.1
CLK16-43	0.7	1.9	1.1	1.0	10.1	9.4	0.5	59.7	0.2	2.3	0.1	6	115	3384	25	76	86	1.0	388	2.7	-21.0
CLK16-44	0.8	2.0	0.6	1.2	10.8	7.0	0.5	68.1	0.2	3.2	0.2	6	113	1724	21	136	79	2.3	428	2.5	-25.9
River sediments																					
CLK16-45	0.5	1.8	0.6	0.2	6.8	8.8	0.5	-	0.2	0.5	0.0	4	175	941	15	44	78	1.9	570	3.2	-24.7
CLK16-46	0.8	2.5	0.7	0.3	5.7	2.4	0.4	-	0.1	1.3	0.0	5	56	493	10	35	110	0.8	704	2.0	-27.2
CLK16-47	0.9	2.7	0.8	0.3	6.4	2.8	0.4	-	0.1	1.3	0.0	4	57	477	10	33	108	0.6	683	2.2	-27.2
CLK16-48	0.9	2.5	0.8	0.3	5.3	3.4	0.6	-	0.1			5	60	1412	12	39	112	0.6	701	2.1	-23.8
Clay (June, 2016)																					
CLK16-03	4.2	2.1	0.2	1.5	12.8	5.9	0.4	-	-	-	-	13	112	578	18	130	53	1.3	280	2.1	-
CLK16-4	2.4	1.4	0.2	1.2	9.4	4.6	0.1	-	-	-	-	11	125	662	22	126	64	1.2	263	1.4	-
CLK16-6	2.4	2.0	0.3	1.7	13.8	6.7	0.4	-	-	-	-	7	128	607	22	705	63	4.2	262	2.3	-
CLK16-11	2.0	2.0	0.3	1.8	13.2	6.5	0.4	-	-	-	-	11	117	693	21	280	65	2.2	275	2.3	-
CLK16-15	2.2	1.9	0.6	1.6	12.5	5.6	0.4	-	-	-	-	7	109	617	21	230	72	1.0	242	2.4	-
CLK16-16	4.1	1.6	0.4	1.2	7.9	4.6	0.1	-	-	-	-	12	106	684	18	169	65	3.3	216	4.0	-
CLK16-18	1.5	1.9	0.5	1.6	13.8	6.2	0.1	-	-	-	-	13	117	647	20	120	69	1.1	247	2.4	-
CLK16-20	1.3	1.8	0.7	1.7	13.3	5.5	0.4	-	-	-	-	11	116	779	21	106	93	1.7	284	2.3	-
CLK16-21	1.7	1.6	0.7	1.7	12.7	5.3	0.4	-	-	-	-	8	111	754	19	129	81	0.8	229	1.9	-
CLK16-22	1.5	1.8	0.4	1.8	13.6	5.2	0.4	-	-	-	-	8	114	635	20	95	65	0.7	252	2.1	-
CLK16-24	2.0	1.7	0.8	1.9	13.0	5.4	0.3	-	-	-	-	13	109	566	19	93	69	2.8	227	2.2	-
CLK16-27	1.1	1.9	0.3	1.5	12.4	6.3	0.5	-	-	-	-	7	136	746	23	106	64	0.9	300	2.7	-
CLK16-29	1.9	1.7	0.4	1.5	13.5	6.7	0.4	-	-	-	-	9	123	882	20	115	58	1.5	208	2.3	-
CLK16-31	3.2	1.5	0.4	1.3	12.2	6.2	0.2	-	-	-	-	10	128	1392	22	115	59	2.1	224	2.4	-
CLK16-34	2.0	1.9	0.7	1.5	12.8	6.4	0.3	-	-	-	-	7	113	1716	19	83	59	3.5	268	2.6	-

CLK16-35	2.3	1.8	0.3	1.5	12.6	6.0	0.2	-	-	-	-	11	130	1031	21	92	63	1.1	271	2.5	-
CLK16-36	2.5	1.8	0.2	1.6	13.1	6.1	0.2	-	-	-	-	13	125	934	21	100	57	2.2	245	2.4	-
CLK16-43	1.9	1.9	0.7	1.3	12.4	7.5	0.5	-	-	-	-	9	141	1545	25	109	71	1.2	371	2.9	-
CLK16-44	3.4	1.6	0.4	1.2	11.1	5.9	0.1	-	-	-	-	10	114	1420	23	104	52	0.9	297	2.4	-

Table A6. Data on Re content in the bulk bed sediments and clay fractions are listed in this table. This tables also includes data on the exchangeable fraction of bed sediments and clay.

Sample List	Re	Re (in Exchangeable fractions of bed Sediments)	Re (in clay fractions)	Re (in Exchangeable fractions of clay fractions)
	pg/gm			
Bed Sediments (June, 2016)				
CLK16-02	309	-	298	-
CLK16-3	159	37	321	166
CLK16-4	240	-	-	-
CLK16-5	130	-	350	113
CLK16-6	221	-	-	-
CLK16-7	441	-	-	-
CLK16-10	450	-	495	310
CLK16-11	219	-	-	-
CLK16-12	271	-	-	-
CLK16-14	199	-	927	-
CLK16-15	354	-	-	-
CLK16-16	276	-	-	-
CLK16-17	209	-	470	192
CLK16-18	460	202	-	-
CLK16-19	451	-	354	-
CLK16-20	571	-	464	296
CLK16-21	473	-	412	-
CLK16-22	450	-	-	-
CLK16-23	585	-	790	600
CLK16-24	484	-	-	-
CLK16-25	345	122	-	-
CLK16-26	341	-	388	
CLK16-27	519	-	-	-
CLK16-28	279	-	578	287
CLK16-29	332	-	-	-
CLK16-30	397	-	532	407
CLK16-31	274	-	-	-
CLK16-32	267	-	531	-
CLK16-34	304	-	444	231
CLK16-35	420	-	725	508
CLK16-36	652	268	473	220
CLK16-43	227	74	472	

CLK16-44	361	-	-	-
River sediments				
CLK16-45	129	-	-	-
CLK16-46	154	33	-	-
CLK16-47	166	-	-	-
CLK16-48	142	-	-	-

Table A7. Elemental and Sr isotopic data for suspended sediments and exchangeable fractions from the Chilika lagoon.

Sample ID	Ca	Fe	Al	Sr	Mn	Ba	$^{87}Sr/^{86}Sr$
Bulk sediments		*(wt%)*			*(µg/g)*		
Suspended sediments (Chilika Lagoon)							
CLK17-M72_SS	0.5	6.6	13.9	91	1739	229	0.73142
CLK17-M72_SS (R)	-	-	-	-	-	-	0.73142
CLK17-M73_SS	0.4	6.9	13.2	88	1950	253	0.72917
CLK17-M74_SS	0.5	7.3	14.9	96	1253	257	0.73317
CLK17-M75_SS	0.3	6.1	13.4	83	954	140	0.7291
CLK17-M81_SS	0.2	6.3	13.8	88	2192	198	0.7207
CLK17-M82_SS	0.3	6.6	14.2	95	2954	216	0.72942
CLK17-M83_SS	0.3	7.3	13.8	102	4148	261	0.7284
CLK17-M84_SS	0.5	6.9	13.7	97	1765	274	0.7334
CLK17-M85_SS	0.6	7.1	13.6	109	2229	353	0.73739
CLK17-M86_SS	0.5	7	14.1	97	1539	267	0.73498
Exchangeable fractions *(all major and trace elements in µg/g)*							
CLK17-M72_SS	-	26.1	-	33	78	38.6	0.71504
CLK17-M72_SS (R)	-	-	-	-	-	-	0.71502
CLK17-M73_SS	-	8	-	28	101	47.9	0.71647
CLK17-M74_SS	-	11	-	36	76	45.0	0.71528
CLK17-M75_SS	-	10	-	31	48	21.0	0.71292
CLK17-M81_SS	-	49	-	44	264	22.7	0.71102
CLK17-M82_SS	-	11	-	32	200	17.8	0.71097
CLK17-M83_SS	-	17	-	33	300	23.3	0.71123
CLK17-M84_SS	-	56	-	33	111	41.4	0.71469
CLK17-M85_SS	-	63	-	32	138	79.2	0.71801
CLK17-M86_SS	-	10	-	35	84	44.3	0.71567

Table A8. Stable oxygen isotopic data for the Chilika lagoon water collected during June, 2016. The $\delta^{18}O$ values for the source water (river, rain and ground water) samples are also included.

Sample ID	$\delta^{18}O$ (‰)
Chilika Lagoon samples	
CLK16-02	2.34 ± 0.06
CLK16-03	2.38 ± 0.1
CLK16-04	2.67 ± 0.11
CLK16-05	2.81 ± 0.07
CLK16-06	2.41 ± 0.08
CLK16-07	2.51 ± 0.08
CLK16-10	3.07 ± 0.07
CLK16-11	3.27 ± 0.02
CLK16-12	3.08 ± 0.07
CLK16-14	2.48 ± 0.07
CLK16-15	2.59 ± 0.09
CLK16-16	2.77 ± 0.06
CLK16-17	2.41 ± 0.1
CLK16-18	2.34 ± 0.09
CLK16-19	2.21 ± 0.12
CLK16-20	1.92 ± 0.1
CLK16-21	2.86 ± 0.07
CLK16-22	2.85 ± 0.05
CLK16-23	2.86 ± 0.05
CLK16-24	2.51 ± 0.13
CLK16-25	0.64 ± 0.07
CLK16-26	0.74 ± 0.02
CLK16-27	0.95 ± 0.06
CLK16-28	0.89 ± 0.04
CLK16-29	1.9 ± 0.07
CLK16-30	2.22 ± 0.08
CLK16-31	2.24 ± 0.04
CLK16-32	1.98 ± 0.11
CLK16-33	1.83 ± 0.04
CLK16-34	2.58 ± 0.06
CLK16-35	1.27 ± 0.12
CLK16-36	1.11 ± 0.1
CLK16-43	2.18 ± 0.1

CLK16-44	2.28 ± 0.06
Groundwater	
CLK16-08	-4.33 ± 0.07
CLK16-09	-5.09 ± 0.07
CLK16-41	-3.03 ± 0.05
CLK16-42	-3.67 ± 0.02
CLK16-37	-4.69 ± 0.09
River/Rivulet water	
CLK16-38 (Bhargavi R.)	0.85 ± 0.07
CLK16-39 (Luna R.)	2.32 ± 0.09
CLK16-40 (Daya R.)	-1.68 ± 0.08
CLK16-13	3.89 ± 0.12
OD14-R1 (Rushikulya)	-5.33 ± 0.07
OD14-R2 (Jarao trib.)	-3.67 ± 0.09
OD14-R3 (Rushikulya after Jarao)	-3.35 ± 0.06
OD14-R6 (Rushikulya at Aska)	-3.39 ± 0.04
RW17-52 (Mahanadi)	-3.33 ± 0.07
Rain water	
Barkul	0.09 ± 0.06

Table A9. Sequences of the primer pairs used for amplification of genomic DNA from different plant accessions.

Primer pair	**Primer name**	**Primer sequence**	Samples
Pair I	ITS1	5'-TCCGTAGGTGAACCTGCGG-3'	CLK17-MP6
	ITS4	5'-TCCTCCGCTT ATTGATATGC-3'	
Pair II	17 SE	5’- ACGAATTCATGGTCCGGTGAAGTGTTCG-3’	CLK17-MP5, MP10
	26SE	5’- TAGAATTCCCCGGTTCGCTCGCCGTTAC-3’	
Pair III	18s rRNA- F	5’-AACCTGGTTGATCCTGCCAG-3’	CLK17-MP1, MP2, MP3, MP4, MP7, MP8, MP9, MP11
	18s rRNA- R	5’-CACCAGACTTGCCCTCCA-3’	

Table A10. Blast result of the DNA sequences showing similarity with different plant species. DNA sequences obtained from the amplified product of the respective plant samples collected from the Chilika lagoon were subjected to BLAST. BLAST result showing the percentage query cover, percent identity, E-value and identity of the plant samples.

Sr. No.	Sample	Description	Re pg/gm	Query Cover (%)	Identity (%)	E Value
1	CLK17- MP1	*Polygala alba*	684	97	84.18	2.30E-08
2	CLK17- MP2	*Panicum hallii*	446	97	94.7	0
3	CLK17- MP3	*Phyllostachys heteroclada*	838	89	92.31	0
4	CLK17- MP4	*Panicum hallii*	792	100	97.32	0
5	CLK17- MP5	*Stukenia pectinata*	580	52	92.18	1.60E-04
6	CLK17- MP6	*Stukenia pectinata*	318	100	99.2	0
7	CLK17- MP7	*Stukenia pectinata*	168	97	91.52	0.00E+00
8	CLK17- MP8	*Stukenia pectinata*	174	98	98.82	0
9	CLK17- MP9	*Enteromorpha intestinalis*	169	30	80.85	0.003
10	CLK17- MP10	*Stuckenia pectinata*	171	100	92.9	0
11	CLK17- MP11	*Panicum hallii*	369	92	93.12	2.30E-08

List of Publications

Danish, M., Tripathy, G. R., Panchang, R., Gandhi, N., and Prakash, S. (2019). Dissolved boron in a brackish-water lagoon system (Chilika lagoon, India): Spatial distribution and coastal behavior. Marine Chemistry, 103663.

Tripathy, G. R., Mishra, S., **Danish, M.**, and Ram, K. (2019). Elevated Barium concentrations in rain water from east-coast of India: role of regional lithology. Journal of Atmospheric Chemistry, 76(1), 59-72.

Danish, M., Tripathy, G. R., and Rahaman, W (2020). Submarine groundwater discharge to a tropical coastal lagoon (Chilika lagoon, India): An estimation using Sr isotopes. Marine chemistry, 103816.

Das, S., Tripathy, G. R., Rai S. K., **Danish, M.**, Thakur, D., Dutt, S., and Sarangi, S. The Role of Sulfuric Acid in Continental Weathering: Insights from Dissolved major ions and inorganic carbon isotopes of the Teesta River, lower Brahmaputra system. Geochemistry Geophysics Geosystems (Under review)

Danish, M., Tripathy, G. R., Mitra, S., and Raskar, S. Non-conservative removal of dissolved rhenium from a coastal lagoon: Clay adsorption versus biological uptake Chemical Geology (Under review).

Abstracts (Conference and Meeting):

Danish, M., Tripathy, G. R., and Panchang, R. (2017). Isotope hydrology of a tropical coastal lagoon: Evaporative loss estimates (Goldschmidt Abstract)

Danish, M., Tripathy, G. R., and Rahaman, W (2019). Tracing submarine groundwater discharge to a coastal lagoon system using Sr isotopes. Presented in the Asia GEOTRACES Workshop, China.

Danish, M. and Tripathy, G. R. Distribution and cycling of barium in the tropical coastal lagoon (Chilika, India): Role of ion-exchange process and sediments resuspension in 36th International Geological Congress.

Marine Chemistry 214 (2019) 103663

Contents lists available at ScienceDirect

Marine Chemistry

journal homepage: www.elsevier.com/locate/marchem

Dissolved boron in a brackish-water lagoon system (Chilika lagoon, India): Spatial distribution and coastal behavior

Mohd Danish[a], Gyana Ranjan Tripathy[a,*], Rajani Panchang[a,b], Naveen Gandhi[c], Satya Prakash[d]

[a] Department of Earth and Climate Science, Indian Institute of Science Education and Research, Dr. Homi Bhabha Road, Pune 411008, India
[b] Department of Environmental Sciences, Savitribai Phule Pune University, Pune 411007, India
[c] Indian Institute of Tropical Meteorology, Pune 411008, India
[d] Indian National Centre for Ocean Information Services, Hyderabad 500090, India

ARTICLE INFO

Keywords:
Conservative behavior
Salinity
Trace elements
Adsorption
Tides

ABSTRACT

Boron is a bio-essential metalloid and its concentrations as well as isotopic compositions are useful tracers for various environmental processes; however, its oceanic budget is not yet well-constrained. In this contribution, spatial and seasonal distribution of dissolved boron of the Chilika lagoon, India (Asia's largest brackish-water lagoon) and its possible source waters have been investigated to constrain its coastal behavior and chemical budget. Further, oxygen isotopic analyses of selected samples were carried out to quantify the evaporation process. The boron concentrations show significant spatial variations (0.6–246 μmol/kg; for monsoon (Aug., 2017) season), with the lower values being observed in the river-dominated northern sector of the lagoon. The area-weighted boron concentration of the Chilika during monsoon (128 μmol/kg) is found intermediate to that of the riverine (1.7 ± 0.8 μmol/kg), groundwater (25 ± 38 μmol/kg) and oceanic (406 ± 13 μmol/kg) water sources. In contrast to boron, the average $\delta^{18}O$ value (2.2 ± 0.7‰) for the lagoon samples is significantly enriched than their source waters. Calculations based on the $\delta^{18}O$ and salinity data estimate about 40% loss of surface water via evaporation. Co-variation between boron and salinity of the samples establishes conservative behavior during onset of the monsoon (June) and also, in the monsoon (Aug) seasons. The boron-salinity trend and boron/salinity ratios of pre-monsoon (May) samples, however, point to its non-conservative behavior with significant boron removal at low-saline regime through ion-exchange (adsorption) processes. Removal of boron is mostly limited to salinity < 15 psu and the intensity (in %) of removal increases steadily with decrease in salinity. These adsorptive losses of boron during pre-monsoon period are mostly dependent on the water residence time; higher residence time allows efficient particulate-water interaction, which possibly intensifies the removal. Further, the boron concentrations show significant changes on diurnal and fortnightly timescales due to tide/ebb cycles. However, the coastal behavior of boron, despite of large concentration changes, remains invariant due to tidal forcing. Outcomes of this study underscore adsorptive removal of boron from coastal regimes and its importance in understanding authigenic boron distribution in clay-rich sedimentary archives from near-shore settings.

1. Introduction

The freshwater-seawater interface, a biogeochemically active aquatic regime, regulates the ultimate delivery of dissolved solutes from rivers to the ocean. Conservative elements supplied by rivers mix with the ocean without any discernible loss/gain in this zone. Several chemical elements, however, behave non-conservatively and their dissolved concentrations either increase or decrease in the salinity gradient due to contributions from additional sources (i.e. submarine groundwater discharge (SGD) (Moore, 1999; Rahaman and Singh, 2012; Beck et al., 2013), desorption and anthropogenic supplies (Coffey et al., 1997; Vengosh et al., 1999; Petelet-Giraud et al., 2009; Samanta and Dalai, 2016) and/or removal through particulate-water interactions (e.g. adsorption, biological activities) (Boyle et al., 1977; Edmond et al., 1985; Bourg, 1987; Charette et al., 2005). Relative contributions from these sources/sinks to the coastal hydrochemistry vary both at spatial and seasonal scales. These variations are complicatedly regulated by various parameters, which include water pH (Bourg, 1987), hydraulic gradient and salinity (Flegal et al., 1991; Gonneea et al., 2014), abundance and composition of suspended sediments (Samanta

* Corresponding author.
E-mail address: grtripathy@iiserpune.ac.in (G.R. Tripathy).

https://doi.org/10.1016/j.marchem.2019.103663
Received 6 November 2018; Received in revised form 2 May 2019; Accepted 26 May 2019
Available online 28 May 2019

and Dalai, 2016), and turbidity, redox state, and biological activities (Du Laing et al., 2009). Proper quantification of these coastal processes and their spatial and seasonal variations are crucial for balance in marine chemical budgets.

One such imbalance in oceanic budget has been observed for boron, which has been widely used as a valuable tracer for different environmental and/or geological processes. For instance the boron isotopic composition of marine biogenic carbonates serves as a reliable paleo-pH proxy (Lemarchand et al., 2000; Park and Schlesinger, 2002; Carrano et al., 2009; Gaillardet and Lemarchand, 2018; Saldi et al., 2018). The present-day seawater boron concentration is nearly uniform globally (433 ± 2 μmol/kg; Lee et al., 2010), consistent with its higher residence time (~10 Myr; Gaillardet and Lemarchand, 2018) compared to the average ocean mixing time (~1500 years; Broecker and Peng, 1982). In contrast to open ocean, existing studies on the behavior of boron in coastal realm report both conservative (Fanning and Maynard, 1978; Liddicoat et al., 1983; Barth, 1998; Xiao et al., 2007; Wang et al., 2009; Singh et al., 2013) and non-conservative (Liss and Pointon, 1973; Pelletier and Lebel, 1978; Narvekar et al., 1981, 1983; Narvekar and Zingde, 1987; Rajagopal et al., 1981; Shirodkar and Anand, 1985; Ghosh and Jana, 1993; Zingde et al., 1995; Padmavathi and Satyanarayana, 1999; Brunskill et al., 2003; Russak et al., 2016) nature. The exact cause(s) for these diverging results is unclear. The non-conservative behavior has often been linked to the removal of dissolved boron through its adsorption onto clay minerals, hydrous oxides of Fe and Al, and organic matters (Liss and Pointon, 1973; Keren and Mezuman, 1981; Goldberg, 1997). The amount of boron removal is typically 10–30% in most of these estuaries. Contrary to this behavior, boron has been reported to be conservative in several estuaries, including those of certain large rivers (e.g., Zaire, Changjiang, Magdalena, Narmada, Tapi and Tamar). Prolonged river water-suspended load interaction in these large river basins may reduce the adsorptive capacity of sediments, which in turn may lead to conservative mixing of boron in large estuaries (Barth, 1998). The above discussion indicates that our understanding on boron behavior in coastal oceans is elusive and has mainly been limited to estuarine zones.

Coastal lagoons are another important component of coastal systems and occupy ~13% of world's coastline (Barnes, 1980). The behavior of boron in these shallow and highly productive regions has not yet been studied. In this contribution, the sources and behavior of boron have been investigated along the salinity gradient of the Chilika lagoon (India), the largest brackish-water lagoon in Asia (Herdendorf, 1982). Towards this, about 200 surface water samples from three different months (June-2016, May-2017, and August-2017) were measured for their boron abundances. These three sampling periods (May (Pre-monsoon), June (Onset of monsoon) and August (Monsoon)) represent different seasons. Surface water samples (n = 47) were also collected at 2-h' time interval for 1 day at two locations during both monsoon (August) and pre-monsoon (May) seasons to assess tidal impact on lagoon chemistry. Additionally, several water samples (n = 152) from possible sources (rain, river, ground and sea water) were also analyzed during this study. Outcomes of this detailed geochemical research show seasonality in behavior of boron in the Chilika lagoon with conservative behavior during the monsoon season and non-conservative removal of boron during pre-monsoon period through ion-exchange processes.

2. Study area

The Chilika lagoon, a polymictic and shallow (mean water depth~ 2 m) brackish water lagoon, is situated parallel to east coast of India between the Eastern Ghat and the Bay of Bengal (Fig. 1). The lagoon was formed about 3750 years ago as a consequence of sea level rises and subsequent land emergence due to minor tectonic uplift (Venkatarathnam, 1970). The coastal lagoon is about 65 km in length with a variable width reaching up to 20 km (Fig. 1; Sarkar et al., 2012). It contains about 2.06×10^{12} L volume of water. Its size varies seasonally with a maximum area (1165 km^2) during the monsoon which decreases to 950 km^2 during the non-monsoon period (Siddiqui and Rama Rao, 1995). Based on hydrology, the lagoon has been divided into four sectors, i.e. northern, central, southern and outer sectors (Fig. 1). The northern sector receives most of the fresh water from the distributaries of the Mahanadi river (e.g. Bhargavi, Daya, Nuna, Makara), whereas the outer sector exchanges seawater from the Bay of Bengal with the lagoon (Fig. 1). The southern sector is connected with the Bay through a small channel, Palur canal. During 1980s and 1990s, the ecology of the lagoon deteriorated significantly due to siltation and northward shifting of its inlet. A new mouth in the outer sector was dredged during September 2000 for efficient seawater exchange, which in turn improved the fishery production, reduction in weed infestation, and increase in population of migratory birds (Sahu et al., 2014). Water circulation within the lagoon is mostly dominated by wind and tidal forces. In addition, fresh water discharge also influences the circulation pattern during the monsoon period (Mahanty et al., 2016). The residence time (RT) of lagoon water varies both spatially and seasonally (Gupta et al., 2008; Mahanty et al., 2016). The RT is lowest (4–5 days) in the outer channel due to efficient water exchange between the lagoon and the sea. In the northern sector, this varies widely from 132 days during the dry periods (November–June) to 8 days during the monsoon (July–October; Mahanty et al., 2016).

The catchment area of the lagoon is about 4406 km^2 and falls in tropical climate with average annual rainfall of 1240 mm (Sahu et al., 2014). The rocks present in the catchment area are mostly Precambrian granites and charnokites. The average fresh water influx to the lagoon is 5.1×10^{12} L/y (Fig. 2), of which 60–80% is supplied by the Mahanadi distributaries from the northern catchment and most of the remaining water, is supplied by several small streams from the western catchment (Sahu et al., 2014). There is almost no fresh water influx to the lagoon during the drier seasons. The lagoon also receives significant anthropogenic supplies (~550 million L/day) from agriculture, aqua-culture and domestic practices (Panigrahi et al., 2009). Depending on the seasonal agricultural practices, these supplies to the Chilika are expected to show large monthly variations. These flux data at monthly timescale, however, are unavailable in the literature. The Chilika is also responsible for huge fishery production (10,000 Mt. per annum) and also, supports tourism greatly. For this, about 6640 boats operate daily inside the lagoon (Mahanty et al., 2016), which may also contribute to the lagoon hydrochemistry.

3. Material and methods

Spatial sampling of water samples from the Chilika lagoon and their possible sources (rain, river, and ground water) were conducted during three field trips (May-2017, June-2016, and August-2017). There was no significant delay in monsoon arrival at this location during 2016 (2nd week of June) and 2017 (3rd week of June). The samples collected during May and August represent the pre-monsoon and monsoon seasons respectively, whereas the June samples were collected immediately after the onset of the monsoon. The lagoon receives about 21% of its annual riverine discharge during August (monsoon), and about 1% during both May (pre-monsoon) and June months (Fig. 2; Muduli et al., 2012). A total of 247 lagoon water and 152 source water samples were investigated in this study. Spatial collection of surface water samples throughout this lagoon using a boat took around 2–3 weeks during each campaign. The fortnightly tidal cycle may influence the water chemistry within the total sampling period of 2–3 weeks. Realizing this, we have also sampled the whole lagoon (with limited spatial resolution) within 1 day during the monsoon season for comparison. A total of thirty-one water samples throughout the Chilika lagoon were collected on 16th August 2017. Further, water samples at two different locations (Satapada (outer sector), Barkul (southern sector); Fig. 1) were also collected at 2-h interval for 24 h during the monsoon (August) and pre-monsoon (May) seasons. Several sea water

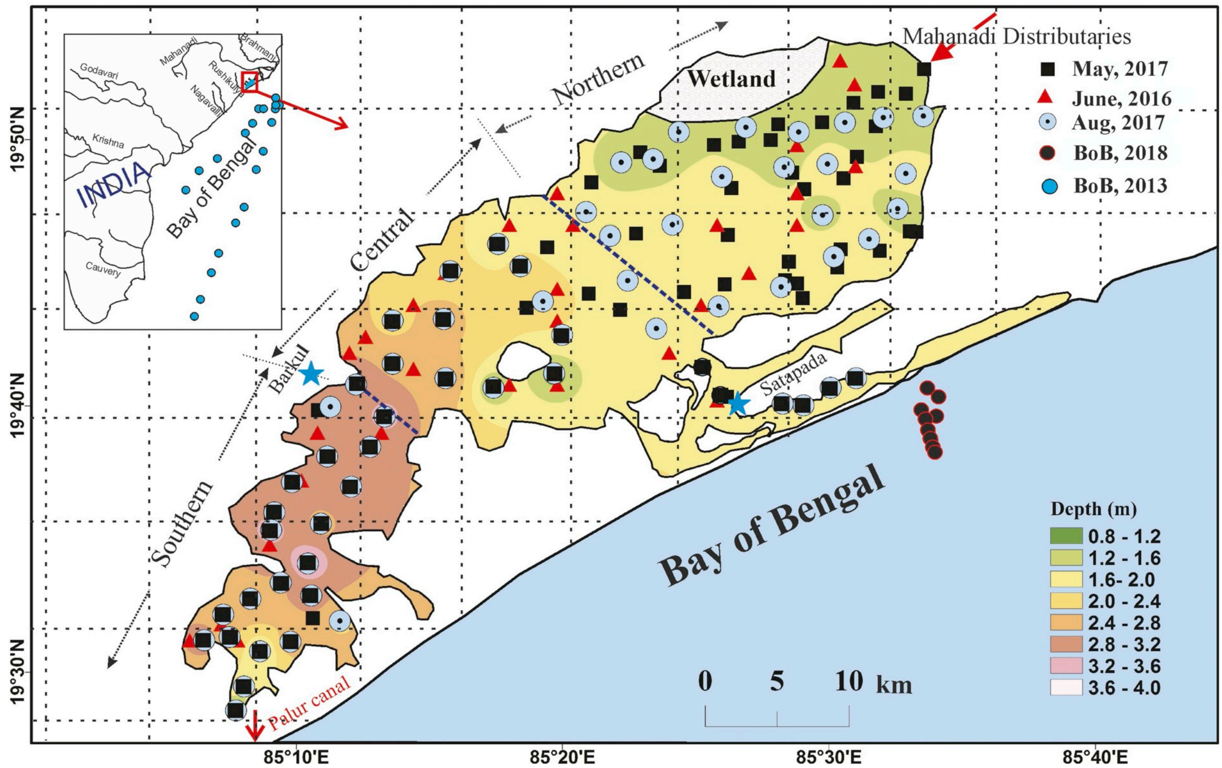

Fig. 1. Map showing the samples collected from the Chilika lagoon during the three field trips (August-2017, May-2017, June-2016). Several seawater samples from the coastal and western Bay of Bengal (BoB) were also collected and their locations are shown. The symbol of blue stars represents the two locations (Barkul and Satapada) where the diurnal sampling of 2-h resolution were carried out. Contours shown in the figure reflect water depth of the lagoon during the monsoon season. The dotted lines represent the 7 km × 7 km grids identified for homogenous spatial analyses of the datasets. The wetland area in the north-east part of the lagoon is also highlighted. (For interpretation of the references to colour in this figure legend, the reader is referred to the web version of this article.)

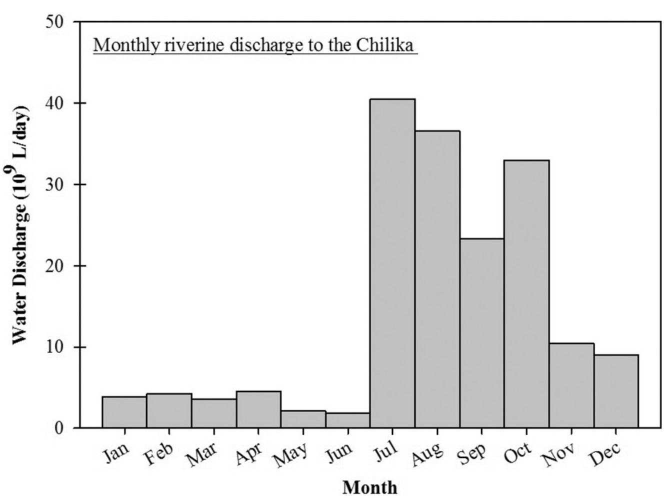

Fig. 2. Monthly distribution of riverine discharge to the Chilika lagoon (Muduli et al., 2012).

samples from the coastal (collected during Jan., 2018) and western (collected during the RR1317 cruise (Nov-Dec, 2013)) Bay of Bengal were also used to constrain the source composition. The river and groundwater samples from the drainage basins were collected during the three filed trips (May, June and Aug). The rain water samples were collected at a nearby location (Berhampur, Odisha) during the southwest monsoon period of 2017 (Tripathy et al., 2019). In addition to water samples, bed sediments ($n = 33$) corresponding to the June samples were also collected manually using a plastic scoop. Four (bed) sediments from the source rivers were sampled to constrain the source composition.

Sampling of water samples were conducted following the approach adopted by Rahaman and Singh (2010). Surface water samples were collected in 10 L plastic containers, after rinsing them with the ambient water. Water temperature, pH, salinity and dissolved oxygen (DO) of the samples were measured on-board using portable multi-parameter probes. In addition, the total water depth of the lagoon at the sampling sites was also measured manually using a graduated wooden pole. Salinities and DO of reference solutions and pH of buffer solutions were constantly monitored for the data accuracy. The collected samples were filtered on the same day (or, within 24 h for few samples) through 0.45 μm nylon filters using vacuum filtration system. We have used HDPE bottles for sample storage and prior to sampling, these bottles were soaked with 1 N HCl at room temperature for 2–3 days and rinsed thoroughly using MilliQ water. About 500 mL of filtered water were acidified to pH~2 using nitric acid and stored in the pre-cleaned bottles. Dissolved boron concentrations of these samples were measured using the quadrupole-ICP MS (Thermo iCAP-Q) facility at IISER, Pune. The salinity of the samples varied significantly and hence, the samples were appropriately diluted to minimize the matrix effect. The boron concentrations of all the samples in 0.32 N HNO_3 medium were analyzed using a standard calibration method. Each sample was measured 10 times and the average is reported here. The relative standard deviation for these 10 analyses is about ± 2%. The background counts were always insignificant compared to signal observed for the samples. Several samples were measured in replicate and the average precision of these measurements is ± 3% ($n = 28$). International seawater (NASS-7) and natural (NIST 1640a) water reference materials were measured to check the accuracy for boron measurements. The measured boron concentrations of NASS-7 (3877 ± 307 μg/kg; $n = 4$) and NIST 1640a (293 ± 20 μg/kg; $n = 3$) were found consistent with its reported values (3670 ± 120 μg/kg (https://www.nrc-cnrc.gc.ca/eng/

solutions/advisory/crm/certificates/nass_7.html); 301 ± 3 μg/kg (https://www-s.nist.gov/srmors/certificates/1640a.pdf)), respectively. In addition, the lagoon and its possible source water samples collected during June 2016 were also investigated for their oxygen isotopic compositions. Details on the methodology adopted for these analyses are provided in Sengupta et al. (2013). Briefly, the filtered water samples, after equilibration with CO_2, were analyzed for their oxygen isotopic composition using a Thermo Delta V Plus isotope ratio mass spectrometer. The accuracy and precision of these analyses was monitored using in-house NARM and IITM-B standards. The measured $\delta^{18}O$ for these standards (−4.43 ± 0.12‰ (NARM); −1.79 ± 0.11‰ (IITM-B), $n = 4$) were consistent with its reported values (−4.52 ± 0.09‰; −1.90 ± 0.13‰; Sengupta et al., 2013). The measured oxygen isotopic data are reported here in ‰ units with reference to V-SMOW. The precision of these $\delta^{18}O$ measurements is better than 0.13‰.

Boron and aluminum concentrations of bed sediments from the Chilika lagoon and near-by rivers from its drainage basins were analyzed during this study. The clay fractions from these sediments were separated using conventional gravity separation approach and its abundance was quantified (Panchang and Nigam, 2012). The bulk and clay fractions of the sediments were thoroughly powdered using an agate mortar and pestle. About 0.1 g of water-washed aliquot of these powdered samples were completely dissolved using HF-HNO_3-HCl acids. The dissolved solutions, stored in 0.32 N HNO_3 medium, were used for their chemical analyses. B and Al concentrations of these solutions were measured using standard-calibration approach in the Quadrupole ICPMS instrument. Replicate analyses of five sediments samples constrained the precision of Al (< ± 8%) and B (< ± 10%) measurements. Chemical analyses of a USGS reference material (W-2) were carried out for accuracy check. The measured Al concentration (8.5 ± 0.3 wt%) matches well with its reported value (8.2 ± 0.1 wt%; https://crustal.usgs.gov/geochemical_reference_standards/pdfs/diabase.pdf). The measured B concentrations (10.5 ± 1.5 μg/g) overlap with its information value (12 μg/g; https://crustal.usgs.gov/geochemical_reference_standards/pdfs/diabase.pdf).

4. Results

Chemical Data on dissolved boron and other relevant parameters for the Chilika lagoon, its source waters and sediments are provided in supplementary materials (Tables S1–S6). Table 1 summarizes the spatial and seasonal distribution of boron in the Chilika lagoon system. Average chemical compositions of possible major source waters to the lagoon are provided in Table 2. The river water samples with salinities ≤0.5 psu have been used to constrain the average riverine composition. The samples with higher (> 0.5 psu) salinities are expected to have appreciable seawater influence and hence, are excluded in finding the average value for this end-member. We have conducted various statistical analyses (e.g. *t*-test, F-test, ANOVA and Kolmogorov-Smirnov (K–S) test) of the boron and salinity datasets; results from these analyses are listed in Table 3.

4.1. Composition of source waters

Boron concentrations of seawater samples from the coastal and western Bay of Bengal vary between 338 and 439 μmol/kg (average: 387 ± 31 μmol/kg ($n = 28$)), whereas their corresponding salinity ranges from 26.4 to 33.6 psu (Table S2). Average salinity and boron concentration of these samples are 30 ± 3 psu and 387 ± 31 μmol/kg respectively. Considering these average values, the B value for the Bay of Bengal samples when extrapolated to a salinity of 35 psu is found to be 448 ± 13 μmol/kg, which is consistent (within 3%) with that reported earlier for the open ocean (433 ± 2 μmol/kg; Lee et al., 2010). Boron concentrations of rain water samples ($n = 31$) collected near the Chilika coast varied from 0.2 μmol/kg to 2.9 μmol/kg (Table S3). Most (27 out of 31) of these samples have concentrations < 1 μmol/kg, with an average value of 0.5 ± 0.2 μmol/kg. This average boron value is consistent with that reported earlier for global marine sites (~0.6 μmol/kg; Schlesinger and Vengosh, 2016). The lagoon is connected with the Mahanadi distributaries and also, several small rivulets which are often anthropogenic-influenced. The dissolved boron concentrations of these streams (samples with salinity < 0.5 psu) range between 0.5 μmol/kg and 3.0 μmol/kg (Table S3); their average value (1.7 ± 0.7 μmol/kg; $n = 18$) is marginally lower than that reported earlier for Indian rivers (~2.4 μmol/kg; Singh et al., 2013). These samples do not show any systematic seasonal variation. The salinities of the groundwater (GW) samples vary widely from 0.12 psu to 8.2 psu. The average salinity and boron concentration of low-saline (with salinity < 0.5 psu) GW samples were 0.28 ± 0.12 psu and 6 ± 4 μmol/kg ($n = 18$), respectively. Higher salinity (0.50–8.18 psu) and boron concentrations (2.0–239.0 μmol/kg; $n = 36$) were observed for several GW samples, attributable to anthropogenic seepage and/or seawater incursion into the coastal aquifer through tidal pumping. It is worth mentioning here that two GW samples with higher salinities (4.32 and 8.18 psu) are characterized with disproportionally higher B concentration (123 and 239 μmol/kg) than that expected for river-seawater mixing (55 and 104 μmol/kg), indicating supply of B from additional sources. These additional sources could be possible seepage of anthropogenic supplies into the aquifer (Vengosh et al., 1994, 1999; Petelet-Giraud et al., 2009) and/or groundwater interaction with the aquifer lithology.

4.2. Composition of the Chilika lagoon

The pH of the lagoon samples varies from 6.9 to 9.7, with an average value of 8.1 ± 0.4 ($n = 250$). The lowest pH value is observed for the sample collected near the wetland area, whereas the sample with the highest value is sampled close to the river (Mahanadi distributaries) mouth during the pre-monsoon season. Large variations in the salinity of the lagoon (August (11.5 ± 8 psu; $n = 62$), May (17.2 ± 11 psu; $n = 73$) and June (22 ± 7 psu; $n = 34$)) are observed during the three field campaigns (Fig. 3). The northern sector of the lagoon receives large riverine influx and exhibits estuarine characteristics. The salinities of the northern sector samples were, therefore, lower than that observed for the other sectors (Fig. 3). The salinity of the northern Chilika vary between 0.1 and 12.6 psu (3 ± 4 psu; $n = 25$) during the monsoon season, systematically lower than that observed for the pre-monsoon season (14 ± 12 psu; $n = 31$). The lagoon salinities in the southern sector show limited spread during August (~2% (19.5 ± 0.4 psu; $n = 22$)) and June (~11% (21 ± 2 psu; $n = 11$)) months, compared to the pre-monsoon (May) samples (~30% (15 ± 5 psu; $n = 22$)). The spatial distribution of the boron concentrations by and large follows the salinity trend (Fig. 3) and the B-salinity relationships are statistically significant for $p < .05$ (c.f. Fig. 5 for Pearson's correlation values). The boron concentrations of the Chilika lagoon vary widely from 1.0 to 477 μmol/kg. Few non-monsoon samples ($n = 9$) with higher boron concentrations than that of the Bay of Bengal are also characterized with higher salinity values (36 ± 1 psu), attributable to evaporation effect. The average boron content for the Chilika was 139 ± 99 μmol/kg ($n = 62$) during the monsoon and 203 ± 143 μmol/kg ($n = 73$) for the pre-monsoon season. Similar to salinity trend, systematically lower boron concentrations were observed for samples from the northern sector (Fig. 3). Fig. 4 depicts the spatial and seasonal variations in boron/salinity ratios for the Chilika lagoon (Fig. 4). These variations are statistically significant both at seasonal and spatial scale (c.f. Table 3 for statistical analysis details). Average boron/salinity ratios for the pre-monsoon (11 ± 2 μmol/kg/psu (May 2017); $n = 73$), onset-of-monsoon (12.8 ± 0.6 μmol/kg/psu (June 2016); $n = 34$) and monsoon (12 ± 2 μmol/kg/psu (August 2017); $n = 62$) samples were comparable with that of the Bay of Bengal (12.8 ± 0.4 μmol/kg/psu; Table S2) and open ocean (12.36 ± 0.03 μmol/kg/psu; Lee et al., 2010). Few

Table 1
Dissolved boron and salinity data for the Chilika lagoon samples collected during three field trips (viz. May 2017; Aug, 2017; June 2016).

Lagoon sector		Depth (m)	Temp (°C)	pH	Salinity (psu)	B (μmol/kg)	B/Salinity (μmol/kg/psu)	DO (mg/l)
Monsoon (July–August 2017)								
Southern (n = 22)	Min	1.14	29.9	7.89	18.3	203	10.3	5.06
	Max	3.86	32.1	8.14	20.1	246	12.5	6.8
	Average	2.8 ± 0.7	31 ± 0.5	8.1 ± 0.1	19.5 ± 0.4	231 ± 11	11.8 ± 0.5	6 ± 0.5
Central (n = 11)	Min	0.97	29.8	7.85	7.1	93	12.1	5.14
	Max	2.84	31.4	8.22	18.8	231	13.1	8.06
	Average	2.1 ± 0.6	30.5 ± 0.5	8.1 ± 0.1	15 ± 5	184 ± 55	12.3 ± 0.3	7 ± 1
Northern (n = 25)	Min	1.32	30	7.7	0.1	2	11	5.61
	Max	1.85	32	8.7	16.6	203	22.2	8.06
	Average	1.6 ± 0.1	30.9 ± 0.7	8.2 ± 0.3	7 ± 7	83 ± 83	14 ± 3	7 ± 0.8
Monsoon (16th August 2017)								
Southern (n = 6)	Min	–	30.4	8.23	11.6	132	10.8	–
	Max	–	31.9	8.29	17.2	187	11.8	–
	Average	–	31.2 ± 0.6	8.28 ± 0.02	15 ± 2	171 ± 21	11 ± 0	–
Central (n = 7)	Min	–	29.8	8.2	2.4	36	11.8	–
	Max	–	33	8.46	10.1	119	15.1	–
	Average	–	32 ± 1	8.4 ± 0.1	6 ± 3	72 ± 34	13 ± 1	–
Northern (n = 18)	Min	–	28	6.96	0.1	2	3.2	–
	Max	–	33	9.14	2	28	20	–
	Average	–	31 ± 1	7.9 ± 0.7	1 ± 1	8 ± 8	13 ± 5	–
Pre-monsoon (April–May 2017)								
Southern (n = 22)	Min	0.61	29.6	8.13	13.1	144	11	2.31
	Max	3.05	31.7	8.74	29.7	364	12.7	11.0
	Average	1.9 ± 0.6	30.1 ± 0.5	8.3 ± 0.1	15 ± 5	179 ± 56	12.1 ± 0.4	7 ± 2
Central (n = 14)	Min	1.22	26.6	8.1	12.9	148	11.3	2.64
	Max	4.57	32.1	9.73	36.8	463	12.8	7.11
	Average	2 ± 1	29 ± 2	8.5 ± 0.4	21 ± 9	255 ± 119	12 ± 0.5	5 ± 2
Northern (n = 37)	Min	0.91	26.8	7.37	0.2	3	4.3	2.31
	Max	1.52	35.9	9.41	39.9	477	15	10.21
	Average	1.2 ± 0.2	30 ± 2	8.1 ± 0.5	17 ± 14	198 ± 180	10 ± 3	6 ± 2
Onset of Monsoon (June 2016)								
Southern (n = 11)	Min	1.78	30.1	7.64	18.5	246	11.4	5.67
	Max	2.92	31	7.85	24.15	301	13.3	6.74
	Average	2.3 ± 0.4	30.6 ± 0.2	7.8 ± 0.1	21 ± 2	264 ± 19	12 ± 1	6 ± 0.3
Central (n = 11)	Min	0.8	31.1	7.53	21.7	281	12.2	5.22
	Max	2.09	32.2	8.06	32.1	418	14.2	7.03
	Average	1.7 ± 0.4	31.7 ± 0.3	7.8 ± 0.1	26 ± 4	338 ± 48	13 ± 1	6.3 ± 0.5
Northern (n = 12)	Min	1	32.2	6.89	7.49	92	12.3	2.4
	Max	2	33.6	8.08	31.7	416	14.1	5.89
	Average	1.6 ± 0.3	32.7 ± 0.4	7.7 ± 0.4	19 ± 10	253 ± 130	13 ± 0.5	5 ± 1

samples, particularly from the pre-monsoon (May) season, are also characterized with lower boron/salinity ratio compared to their source waters (Figs. 4 and 5D).

4.3. Chemical composition of Chilika sediments

The size fraction of bed sediments from the Chilika lagoon is dominated by clay (64 ± 26 wt%; n = 33) fractions. Aluminum concentrations of the river sediments from the Chilika drainage basin vary between 5.3 and 6.8 wt% (average: 6.1 ± 0.7 wt%; n = 4; Table S6). These values are consistent with that reported earlier for sediments from the Mahanadi river (6.22 wt%; Chakrapani and Subramanian, 1990). The Al concentrations of river sediments are found systematically lower than that of the bed sediments from the Chilika lagoon (12 ± 4 wt%; n = 33) and their clay fractions (12 ± 1 wt%; n = 19). Boron concentrations of riverine (bed) sediments vary between 3.5 and 5.3 μg/g (mean: 4 ± 1 μg/g; Table S6). This average B concentration is lower than that reported for upper continental crust (17 μg/g; Rudnick and Gao, 2004), but consistent with average B content for igneous rocks (< 10 μg/g; Mao et al., 2019). Similar to Al, the boron concentrations of the Chilika bed sediments (10 ± 4 μg/g; n = 33) and their clay fractions (10 ± 2 μg/g; n = 19) are also higher than that of the river

Table 2
Data on elemental boron, oxygen isotopes and salinity for possible source waters to the Chilika lagoon.

	Salinity (psu)	Boron (μmol/kg)	B/salinity (μmol/kg/psu)	$\delta^{18}O$ (‰)
Bay of Bengal	32 ± 1 (n = 19)	406 ± 13 (n = 19)	12.8 ± 0.4 (n = 19)	−0.3 ± 0.1[a]
Open ocean	35	433 ± 2[b]	12.36 ± 0.03	0
Ground water	1 ± 1 (n = 54)	25 ± 38 (n = 54)	22 ± 16 (n = 54)	−4.2 ± 0.8 (n = 5)
River/Rivulets[c]	0.17 ± 0.08 (n = 18)	1.73 ± 0.75 (n = 18)	12 ± 6 (n = 18)	1.3 ± 2.4 (n = 4)
Nearby river basins[c]	0.34 ± 0.01 (n = 2)	1.56 ± 0.9 (n = 12)	7 ± 6 (n = 2)	−3.8 ± 0.9 (n = 5)
Rain water	–	0.6 ± 0.5 (n = 31)	–	0.1 ± 0.1 (n = 1)

River samples with higher salinities (> 0.5 psu) are expected to have seawater influence and hence, not included in constraining the average riverine composition.
[a] Singh et al. (2010).
[b] Lee et al. (2010).
[c] Samples with salinity ≤ 0.5 psu.

Table 3
Results comparison of statistical analyses using various approaches of spatial and seasonal distribution of B, salinity and B/salinity values of the Chilika lagoon.

	ANOVA	t-test	F-test	K-S test
Salinity data comparison				
Within the sectors (Pre-monsoon; May)	**2.9**	–	–	–
Within the sectors (Onset-monsoon; June)	124.7	–	–	–
Within the sectors (Monsoon; August)	173.5	–	–	–
Within May, June and Aug sampling	15.5	–	–	–
May vs June	5.9	2.4	2.7	0.5
May vs Aug	11.4	3.4	1.7	0.3
June vs Aug	41.7	6.5	**1.6**	0.7
Aug vs 16th Aug	17.6	4.2	2.0	0.4
Boron data comparison				
Within the sectors (Pre-monsoon; May)	4.2	–	–	–
Within the sectors (Onset-monsoon; June)	3.5	–	–	–
Within the sectors (Monsoon; August)	184.7	–	–	–
Within May, June and Aug sampling	16.7	–	–	–
May vs June	9.2	3	2.6	0.6
May vs Aug	8.9	3	2.1	0.3
June vs Aug	50.4	7.1	**1.2**	0.8
Aug vs 16th Aug	18.6	4.3	2.2	0.5
B/salinity ratio comparison				
Within the sectors (Pre-monsoon; May)	21.7	–	–	–
Within the sectors (Onset-monsoon; June)	102	–	–	–
Within the sectors (Monsoon; August)	**1.54**	–	–	–
Within May, June and Aug sampling	12.9	–	–	–
May vs June	20.9	4.6	12.8	0.5
May vs Aug	15.4	3.9	**1.2**	0.2
June vs Aug	**0.24**	**0.5**	15.1	0.5
Aug vs 16th Aug	**0.004**	**0.07**	2.0	**0.3**

Bold numbers show significant similarity within the sample groups for $p < .05$.The t, F and K−S tests were carried out using the PAST software, whereas ANOVA analysis were done using MS-Office.

sediments (4 ± 1 μg/g; Table S6).

4.4. $\delta^{18}O$ values of the Chilika system

The $\delta^{18}O$ value of the rain water sample from this coastal location is found to be 0.09 ± 0.06‰ (Table S5). The average $\delta^{18}O$ values of the groundwater (−4.2 ± 0.8‰) samples are found similar to that of the river samples from the drainage basin of the Chilika (−3.8 ± 0.9‰; $n = 5$) (Table 2). The $\delta^{18}O$ values of the lagoon samples collected varies from 0.6 to 3.3‰, with an average value of 2.2 ± 0.7‰ ($n = 34$). These isotopic compositions are highly enriched compared to its source waters (Table 2). The $\delta^{18}O$ values were found to be least for the northern sector (1.8 ± 0.6‰; $n = 11$) and highest for the southern sector samples (2.7 ± 0.3‰; $n = 12$). A few river samples collected near the lagoon are found to have enriched $\delta^{18}O$ values (1.3 ± 2.4‰; $n = 4$), indicating incursion of lagoon water during tidal periods.

5. Discussion

5.1. Hydrology of the lagoon: evaporative loss estimates

The hydrology of the Chilika is mainly regulated by mixing of source waters (e.g. river, rain, groundwater and seawater) and/or evaporation process. The relative contributions from river and sea water to the lagoon are by and large reflected in the spatial distribution of salinities (Fig. 3). Interestingly, salinities of few (13 out of 73) samples from the pre-monsoon season (May 2017) were higher than those reported for the Bay of Bengal (~32 psu; Table S2), attributable to evaporative loss of the lagoon water. We have analyzed $\delta^{18}O$ values of samples collected only during June 2016 to assess the impact of evaporation on the Chilika hydrology. Average $\delta^{18}O$ values of these samples (2.2 ± 0.7‰; Table S5) is found enriched compared to that reported for the Bay of Bengal (−0.3 ± 0.1‰; Singh et al., 2010), indicating evaporative loss of water from the lagoon. Efforts were made in this study to estimate the evaporative water loss using salinity and $\delta^{18}O$ values of the water samples. Towards this, we employed an iterative approach involving mass balance (Eqs. (1)–(2)) and Rayleigh fractionation (Eq. (3)) equations.

$$S_{Chilika} = S_{river} \times f_{river} + S_{BoB} \times (1 - f_{river}) \tag{1}$$

$$\delta^{18}O_{calc} = \delta^{18}O_{river} \times f_{river} + \delta^{18}O_{BoB} \times (1 - f_{river}) \tag{2}$$

$$\delta^{18}O_{meas} = (\delta^{18}O_{calc} + 1000) \times f_{Ev}^{(\alpha-1)} - 1000 \tag{3}$$

where, $S_{Chilika}$, S_{river} and S_{BoB} stand for salinities of the Chilika, riverine supply and the Bay of Bengal respectively. $\delta^{18}O_{river}$ and $\delta^{18}O_{BoB}$ represent the oxygen isotopic compositions of the river and sea water respectively. The $\delta^{18}O_{calc}$ and $\delta^{18}O_{meas}$ are the calculated (i.e. expected value before evaporation) and measured oxygen isotopic value for the sample respectively. The f_{river} is the fraction of water supplied by the rivers, whereas f_{Ev} reflects the fraction of water remained in the lagoon after evaporation. A value of 0.9908 is used for the fractionation factor, α (at 25 °C; Gat and Gonfiantini, 1981). The mass balance calculation (Eqs. (1)–(3)) considers that the Chilika receives waters from rivers and Bay of Bengal, and assumes insignificant supply of groundwater (GW) to the lagoon. The assumption on negligible GW supply may not be strictly valid. Although there is lack of GW flux data for the Chilika, radium isotopic investigations have computed a submarine groundwater discharge of (1.55–7.44) × 10^6 m^3/d for a nearby river (Guatami) estuaries (Rengarajan and Sarma, 2015). These SGD fluxes are of similar order when compared with the riverine discharge (3.1 × 10^6 m^3/d; Gupta et al., 2008) to the Chilika during the non-monsoon periods. We, therefore, recognize that omission of GW flux from the mass balance calculation based on two end-member mixing equations (Eqs. (1)–(3)) may overestimate the riverine contribution to the Chilika. However, this approach will have minimal influence on the estimation of evaporation rates. This is mainly due to similar $\delta^{18}O$ composition of the river (−3.8 ± 0.9‰; $n = 5$ (collected in June)) and groundwater samples (−4.2 ± 0.8‰; $n = 5$) from the basin and our evaporation rate estimation largely depends Rayleigh isotopic fractionation of oxygen isotopes.

Table 2 lists the salinity and $\delta^{18}O$ values for source waters used for the estimating the evaporation rates. The average salinity and $\delta^{18}O$ values for the sea water were constrained using the data reported for the Bay of Bengal (Singh et al., 2010). The mass balance equations for salinity (Eq. (1)) and $\delta^{18}O$ (Eq. (2)) values were used for estimating the expected pre-evaporation $\delta^{18}O$ (i.e. $\delta^{18}O_{calc}$) values for the lagoon water samples. The measured $\delta^{18}O$ value represents the post-evaporation value of the sample and hence, a Rayleigh fractionation calculation using the $\delta^{18}O_{calc}$ and $\delta^{18}O_{meas}$ values (Eq. (3)) was carried out to find the fraction of water lost during evaporation. However, the measured salinity is already influenced by evaporation and hence, the pre-evaporation salinity (S_{calc}) value is computed (Eq. (4)). The estimated S_{calc} is iteratively used in Eqs. (1)–(3) to estimate the fraction of water lost from the lagoon during the month of June.

$$S_{calc} = \frac{S_{Chilika}}{(1 - f_{Ev})} \tag{4}$$

The amount of surface water lost from the lagoon during June month varies from 14% to 48%, with an average value of 38 ± 9% ($n = 34$). The evaporative loss was highest for the southern sector (43 ± 3%; $n = 11$) compare to the central (36 ± 10%; $n = 11$) and northern (35 ± 11%; $n = 12$) sectors. Relatively higher evaporation in the southern sector is consistent with limited water exchange from fresh and sea water sources. There is lack of estimates on evaporative loss of water for coastal lagoons in India for comparison with the present results. The present estimates, however, are of similar order (up to 70%) that reported earlier for coastal lagoons from along the Mediterranean

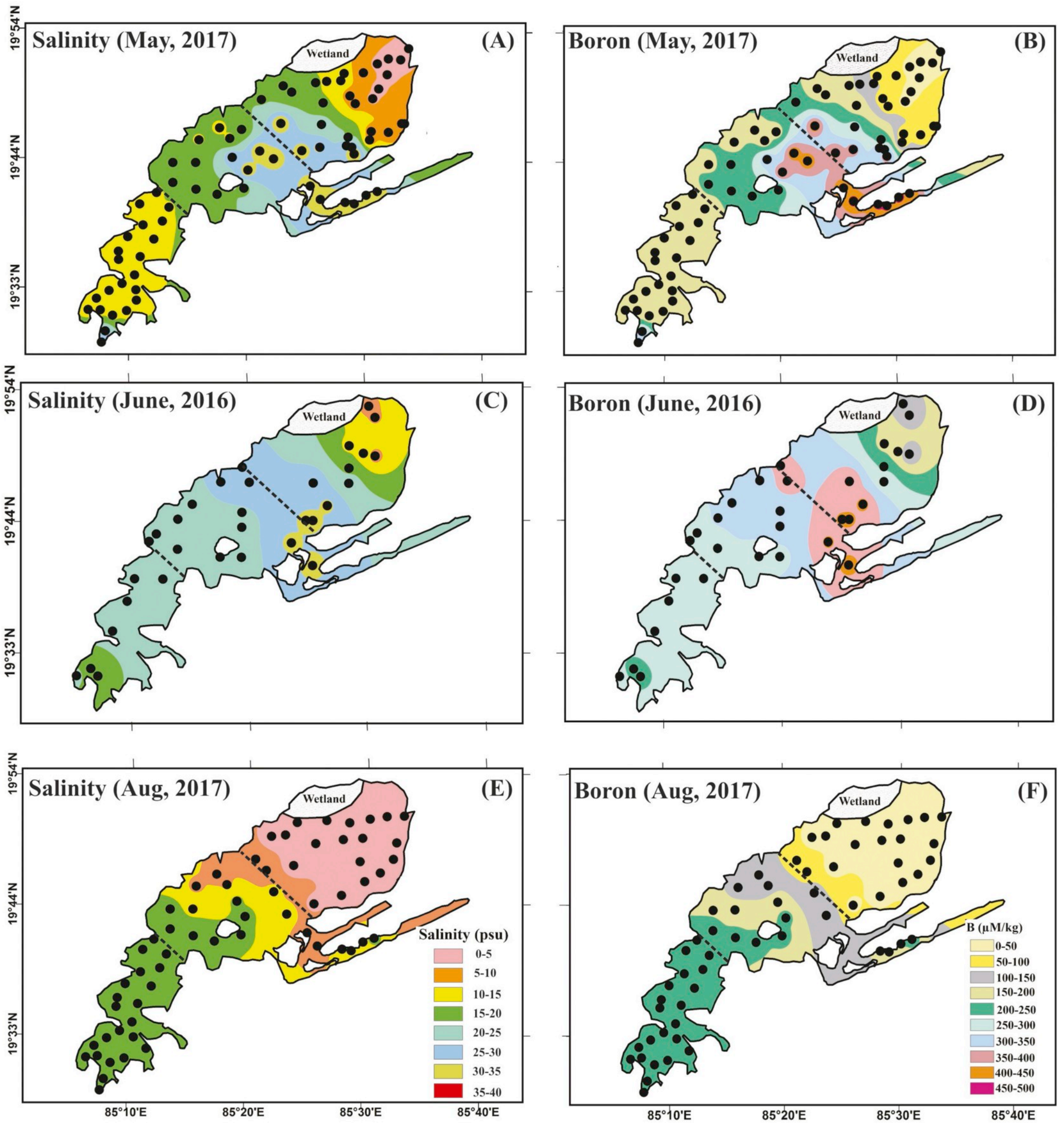

Fig. 3. Contour map showing the salinity and boron distributions of the Chilika lagoon during different seasons: pre-monsoon (May-2017; inset A-B), onset of monsoon (June-2016; inset C-D) and monsoon (August-2017; inset E-F). The dotted lines in each figure inset represent the sector (i.e. southern, central and northern) boundaries. Spatial distribution of boron concentration follows that of the salinity pattern.

coast (Lécuyer et al., 2012). The estimated evaporative loss of ~40% from the Chilika is higher compared to insignificant evaporation (0.31%; Gupta et al., 2008) water loss from the Chilika during the monsoon season and lower as compared to annual evapotranspiration loss (~57%) reported for a nearby river (Subernarekha) basin (Jain et al., 2007). Our estimate is based on oxygen isotopic composition of the surface water and hence, precise estimation of the evaporative loss will also require $\delta^{18}O$ data for the benthic water of the lagoon.

5.2. Variation of boron with salinity

We have investigated the co-variations between boron and salinity of the lagoon samples collected during three different seasons to infer sources and behavior of dissolved boron in this tropical coastal lagoon (Fig. 5). Towards this, data on average compositions for river and sea water were required to constrain the theoretical mixing line. Average salinity (0.2 ± 0.1 psu) and boron (1.7 ± 0.8 μmol/kg) concentrations of the rivers draining into the Chilika were used as the riverine end-member composition (Table 2). The average salinity (32 ± 1 psu) and boron concentration (406 ± 13 μmol/kg) of the Bay of Bengal samples analyzed during this study is used as the seawater end-member composition (Table 2). As mentioned earlier, the average boron concentration of the Bay of Bengal samples (448 ± 13 μmol/kg (normalized to salinity of 35 psu)) matches well with the reported boron data for global ocean (433 ± 2 μmol/kg; Lee et al., 2010). Considering these B and salinity concentrations, the mixing between river and Bay of Bengal waters should yield a B/salinity ratio of 12.7 (Fig. 5). In addition, salinity (1 ± 1 psu) and B (25 ± 38 μmol/kg) composition of the groundwater fluxes can also contribute to the B-salinity trend of the Chilika. Fig. 5 depicts the salinity-boron relationship for the Chilika lagoon during the three seasons sampled. The figure also shows the characterized values for river, ground and sea water for reference. Samples from all the seasons show strong linearity ($r^2 \geq 0.97$; $p < .05$) between the two parameters, pointing to dominant contributions from river and seawater to the lagoon chemistry. The slope of the regression lines for the pre-monsoon (May; 13.0 ± 0.2), onset of monsoon (June; 13.2 ± 0.4) and monsoon (August; 12.0 ± 0.2) seasons are found comparable with that expected (12.7) for river-sea water mixing line (Fig. 5). This indicates a conservative behavior of boron in the coastal lagoon system and hence, the supply of boron is delivered to the Chilika mainly through river and sea water. The conservative B-salinity mixing trends, further, corroborates that the boron supply from any other

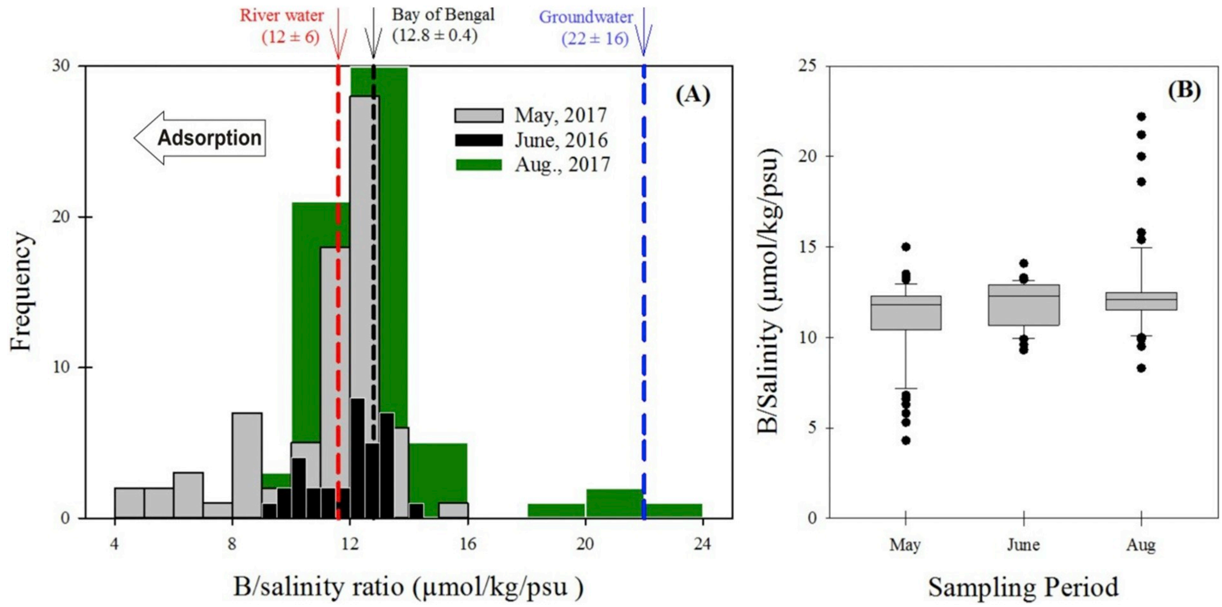

Fig. 4. (A) Frequency distribution of the boron/salinity ratio (in μmol/kg/psu units) during different seasons. The frequency in this histogram stands for the count of the samples within the given bin of B/salinity ratio. The boron/salinity ratios of most of the samples fall between of the Bay of Bengal (12.8 ± 0.4 μmol/kg/psu) and riverine (11.6 ± 6 μmol/kg/psu) input. Several pre-monsoon (May) samples show relatively lower B/salinity ratios than that of its possible sources. This observation indicates removal of dissolved boron from the lagoon which we interpret as ion-exchange (i.e. adsorption) processes. (B) Box plot showing the B/salinity distribution for three different months. The pre-monsoon (May) samples with relatively lower B/salinity ratios are mostly from the northern sector of the lagoon. This B/salinity decline has been attributed to adsorptive removal of boron from the Chilika.

(groundwater and anthropogenic) sources is only minimal. This behavior of boron is consistent with an earlier reported study for large estuary systems from the western India (Singh et al., 2013).

The pre-monsoon samples although show a linear trend between boron and salinity, several data systematically fall below the theoretical mixing line (Fig. 5D). Fig. 5D presents the B-salinity trend for low-saline (< 15 psu) samples collected during the pre-monsoon (May) period. All these samples fall systematically below the river-seawater mixing line. The B/salinity for most (40 out of 42; Fig. 5D) of these samples vary between 4.3 and 12.5, which is lower compared to the ratio expected (12.7; Fig. 5) for river and seawater mixing. These systematically lower ratios demand an additional source/sink to explain their boron distribution. These additional sources/sinks for the Chilika could be influx from SGD and/or removal of boron through ion-exchange (adsorption) mechanisms. The B and salinity data for the groundwater influx falls above the river-seawater mixing line (Fig. 5D), which is consistent with its higher B/salinity ratio (Fig. 4). Any solute supply through this pathway, therefore, is expected to elevate the B/salinity ratio of the lagoon, which is clearly in contrast with the observed lower values for the low-saline samples from May. These observations point to non-conservative behavior of boron in the coastal regime with appreciable amount of boron removal from the lagoon during the pre-monsoon period. The boron-salinity trends of the Chilika, therefore, indicate seasonality in the behavior of boron in the coastal system with conservative nature during the monsoon and non-conservative nature during the pre-monsoon period.

Efforts are made to quantify the amount of boron lost from the low-saline regions during May 2017. Towards this, the expected boron for the given salinity of a sample was computed from the river-sea water mixing equation. The difference between measured and expected boron is used as a measure of loss of boron in the lagoon. This estimation of boron loss, however, will be an underestimation, in case of appreciable water supply from any additional (groundwater/anthropogenic) sources to the lagoon. The estimated boron removal from the Chilika for the May samples is presented in Fig. 6. Consistent with our earlier observation, strong removal of boron from the low-saline samples (< 15 psu) was observed. The amount of boron removal (in %) show a decreasing trend from ~60% to zero in the 0–15 psu salinity zone. This decreasing trend is consistent with earlier reported trend of adsorptive removal of elements from estuaries with salinity (Salomons, 1980; Bourg, 1987). Samples from the higher saline zone do not show any B loss (Fig. 6), indicating dominance of river and sea water mixing in this zone. As the lesser-saline samples are more restricted to the northern sector (strongly influenced by freshwater influx), the non-conservativeness is more pronounced in this river-dominated part of the lagoon. In concurrence with this, the amount of loss of boron (in %) in the southern (1 ± 3%; $n = 22$) and central (2 ± 4%; $n = 14$) sectors are found statistically similar ($F = 1.34$; $t = 0.68$) for $p < .05$. However, the boron loss in the northern sector (25 ± 21%; $n = 31$) is found statistically different when compared with that from the central ($F = 26.8$; $t = 4.05$) and southern ($F = 35.9$; $t = 5.27$) sectors. Possible mechanisms contributing to the boron removal from the Chilika are discussed below.

5.2.1. Possible causes for removal of dissolved boron

Removal of dissolved boron from coastal lagoon can be regulated by several factors, which includes volatilization of boron complexes (Chetelat et al., 2009; Gaillardet and Lemarchand, 2018), biological activities (Harriss, 1969; Park and Schlesinger, 2002) and adsorption on to the surface of clays (Liss and Pointon, 1973; Salomons, 1980), and/or organic matter (Goldberg, 1997). Earlier studies have shown that boric acid, which constitutes about 90% of seawater B, is highly volatile in nature and it contributes significant fraction of the B present in the atmosphere (Gaillardet et al., 2001; Xiao et al., 2007; Gaillardet and Lemarchand, 2018). This removal mechanism involving evaporative loss of boron is expected to be uniform across different salinity gradient, which is in clear contrast to observed preferential removal of boron only from the low-saline (< 15 psu) regimes of the Chilika (Fig. 5D). Minimal impact of B volatilization from the Chilika is also evident from the observed conservative mixing of boron (Fig. 5B) during the month of June, when significant evaporation impact on the lagoonal hydrology has already been established (cf. Section 5.1). Although available dataset from this study does not allow proper evaluation of impact of biological matter on removal of boron from the Chilika, co-variation of

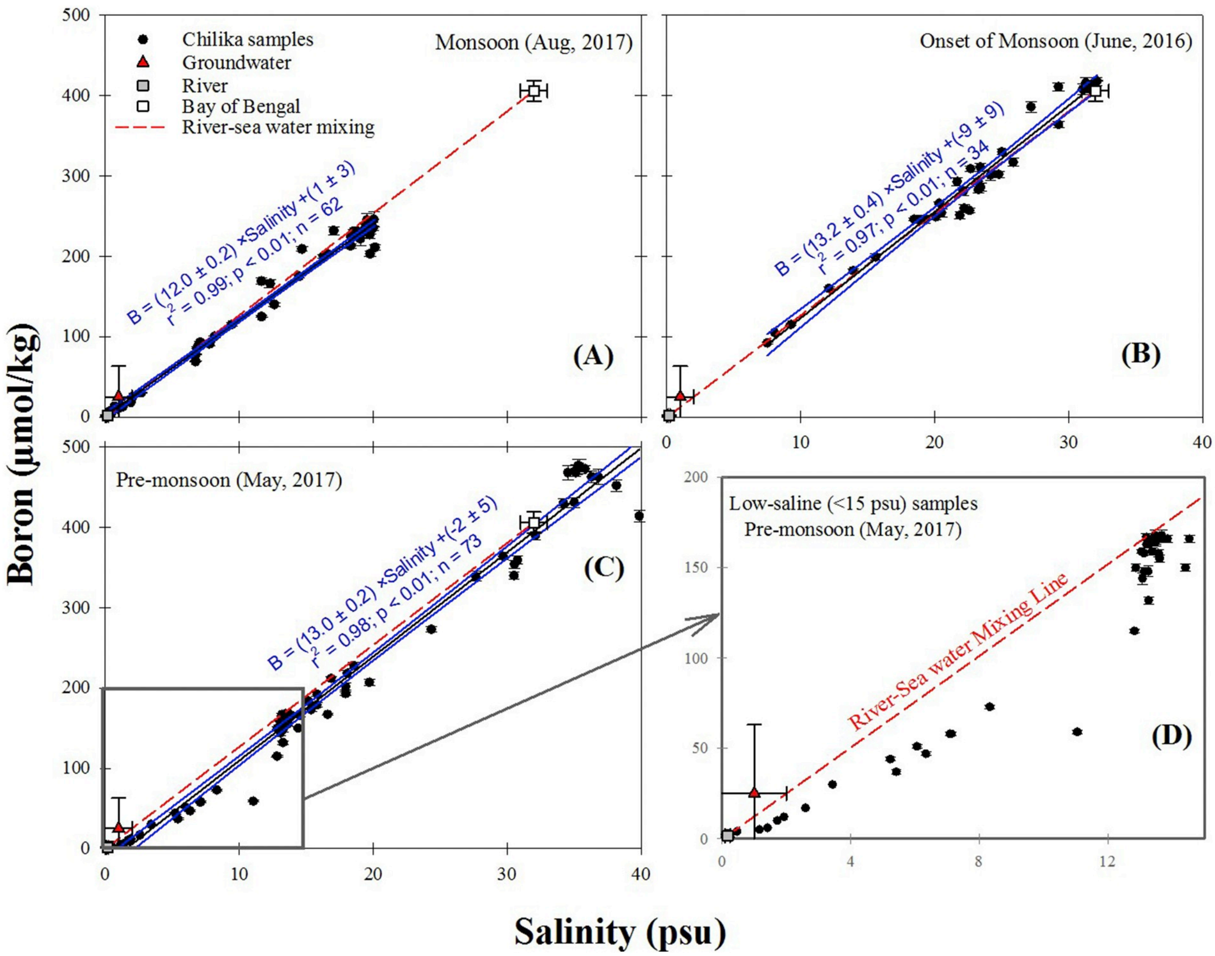

Fig. 5. Co-variation between salinity and boron concentrations of the lagoon during (A) monsoon (Aug), (B) onset of monsoon (June) and (C) pre-monsoon (May) seasons. Error bars here represent the uncertainty associated with the boron measurements. The end-member compositions for the river (gray squares) and Bay of Bengal (open squares) waters are shown here. The dotted (red) line reflects the theoretical river-sea water mixing line. Average groundwater composition (red triangle) is also shown for comparison. The linear regression line of the dataset (bold black) and the corresponding 95% confidence level (blue dotted line) are also shown. (D) B-salinity trend of low-saline samples with salinity < 15 psu from the pre-monsoon (May) season. Most of these data fall below the theoretical mixing line for river and sea water. (For interpretation of the references to colour in this figure legend, the reader is referred to the web version of this article.)

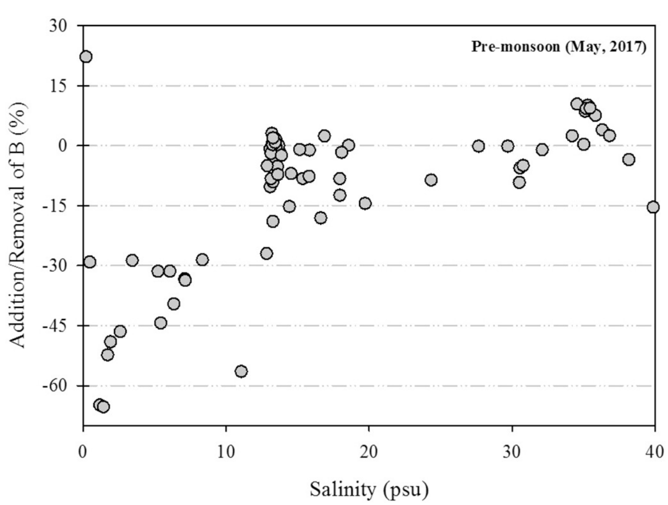

Fig. 6. Estimated dissolved boron removal (in %) with respect to salinity of the lagoon during the pre-monsoon (May) period. The removal process is restricted mostly to the low saline regime of the Chilika.

boron with dissolved oxygen (a possible proxy for biological activities) was assessed for this purpose. The boron concentrations of the Chilika samples from the month of May show insignificant correlation with their dissolved oxygen concentrations ($r = 0.05$; $n = 73$; $p > .05$; Fig. S1 (cf. Supplementary material)), pointing to limited role of biological activities in the boron loss. However, more rigorous data analysis of boron distribution with other key biological proxies (e.g. suspended organic matter, organic carbon isotopes) can provide more insight on the removal of boron through biological pathways.

Particulate-water interaction has been recognized to be the primary process that removes boron from aquatic systems (Schwarcz et al., 1969; Liss and Pointon, 1973; Salomons, 1980). The observed boron removal from the Chilika during the month of May, therefore, can be attributed to adsorptive processes. Earlier studies have shown removal of boron from water column through its adsorption onto clay minerals (more readily to illites) and/or oxides of Fe and Al (Liss and Pointon, 1973). Consistent with this removal process, boron concentration in clay minerals (up to 1000 µg/g) are always higher than that of the continental crust (10 µg/g) (Gaillardet and Lemarchand, 2018). Average B concentrations in the Chilika bed sediments (10 ± 4 µg/g; $n = 33$) and their clay fractions (10 ± 2 µg/g; $n = 19$) are higher than their riverine source value (4 ± 1 µg/g; $n = 4$; Table 2). We estimated the enrichment factors (EF) for the bulk and clay fractions of the bed sediments with respect to their riverine input using the following

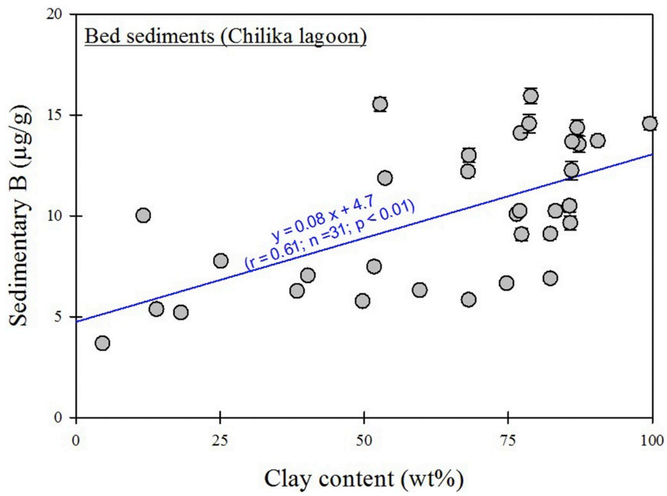

Fig. 7. Correlation between boron concentration (in bulk fraction of sediments) and clay abundance of the bed sediments from the Chilika lagoon.

equation. The EF values are calculated based on Al-normalized ratios to take care of size-sorting chemical changes and hence, provides a good measure of elemental enrichment in sedimentary basins (Tripathy et al., 2018).

$$EF = \frac{\left({}^{B}\!/_{Al}\right)_{Chilika}}{\left({}^{B}\!/_{Al}\right)_{river}} \quad (5)$$

By the definition (Eq. (5)), the average EF for the river sediment is 1. Average EF of boron in the bulk (1.3 ± 0.4 ($n = 33$)) and clay (1.7 ± 0.5 ($n = 19$)) fractions of the Chilika bed sediments are about 30% and 70% higher than the riverine EF value (~1), respectively. This boron enrichment hints at possible removal of this element through their adsorption onto clay particles. To evaluate this proposition, co-variation between the clay and boron abundances of the Chilika bed sediments were evaluated (Fig. 7). The clay content of these sediments vary from 5 and 100 wt%, with a median value of 76 wt%. Despite of this large variation, the clay abundance of these samples show significant correlation with their boron concentrations, corroborating again the possibility of boron removal from the Chilika lagoon through their adsorption onto clay surfaces.

Various factors can control the adsorptive removal of elements in the coastal regions, which include salinity, pH, turbulence and sediment abundances (Bourg, 1987). No significant correlation between pH and dissolved boron is observed, pointing to minimal role of pH in regulating the ion-exchange process. The intensity of elemental removal through adsorption generally shows an inverse relation with salinity (Bourg, 1987). Further, turbulence and sediment abundances are other possible controlling factors for adsorptive removal. These parameters (salinity, turbulence and sediment load) are expected to be more influential during the monsoon seasons. This is not consistent with the conservative behavior of boron during monsoon with no significant removal. This observation points to minimal role of these parameters in controlling removal of boron from the Chilika. Higher removal of boron during the pre-monsoon seasons can be due to higher residence time of the water during this period. The water residence time of the lagoon is significantly higher during the pre-monsoon season than that during the monsoon period. Higher residence time would increase the particulate-water interaction time, which in turn can increase the adsorption removal of boron from the Chilika. Intensity of this adsorptive process is also supported by re-suspension of fine sediments due to low depth of the lagoon and churning of the water column by winds (Kumar et al., 2016).

5.3. Impact of tides on the boron distribution

Tides in the Chilika are pre-dominantly semi-diurnal (12.4 h) and fortnightly (12 days periodicity) in nature (Mahanty et al., 2015). The water level of the lagoon at its inlet (near Satapada) varies by ~1 m (between 0.84 and 1.92 m) during the non-monsoon and by ~1.5 m (between 1.07 and 2.53 m) during the monsoon season (Mahanty et al., 2016). These tidal cycling introduce temporal changes in the seawater incursion into the lagoon and hence, can influence the lagoon chemistry. In particular, collection of water samples throughout this large lagoon generally took 2–3 weeks' time during each field trip and hence, some of the observed boron variations can be attributed to variation in the tide/ebb intensity within the lagoon. In order to assess tidal influence at semi-diurnal timescale, water samples at two locations (i.e. Barkul and Satapada; Fig. 1) were collected on 2-hourly interval basis for a duration of 1-day during monsoon and pre-monsoon seasons. The salinity at Barkul (from southern sector) within 1 day varies by about 6% (mean: 16 ± 1 psu) during the monsoon season. Considering average salinity of river and seawater (Table 2), this salinity change accounts for variation in seawater contribution from 41% to 52% to the lagoon (estimated using Eq. (1)). A similar degree (~5%) of salinity change at Barkul was also observed for the pre-monsoon season. However, the salinity changes at Satapada (near the Chilika inlet) during the pre-monsoon season were only limited (1.4%). On the contrary, the salinity at Satapada varies from 6.4 to 9.2 psu over duration of 1-day during the monsoon season (Fig. 8A). These changes in salinity indicate variation in seawater water supply from 19.6 to 28.6% (Fig. 8A). These changes in seawater influx to the lagoon are linked with the tide and ebb cycle of the lagoon system. Similar to salinity, the boron concentrations of these samples also show significant diurnal variation due to tidal changes. Despite these variations, Boron concentrations of these samples co-vary with their corresponding salinity and show conservative behavior (Fig. 8B). The boron-salinity regression equation yields a boron concentration of 440 µmol/kg for a salinity of 35 psu, consistent (within 1.6%) with that of the global ocean value (433 ± 2 µmol/kg; Lee et al., 2010). These observations confirm conservative behavior of boron during different tidal conditions of the lagoon. This evidence of conservative river-seawater mixing, further, points to minimal impact of groundwater influx to the lagoon during tidal pumping.

To assess the tidal impact on lagoon chemistry at fortnightly timescales, the spatial sampling of the whole lagoon during the monsoon season has been carried out two times. In addition to high-resolution ($n = 62$) spatial sampling over a period of 2–3 weeks' time (Table 1), the whole lagoon with limited spatial resolution ($n = 31$) was also collected within 1 day on a waning crescent moon phase day (16th August 2017; 9th day after full moon). The boron concentrations of the 1-day sampling varies widely between 2 and 187 µmol/kg with a salinity-weighted average value of 74 µmol/kg, which is about 63% lower than that of the high-resolution spatial sampling of the lagoon (203 µmol/kg) during the same season. Further, attempts were made to compare the spatial boron data during the two sampling trips for the monsoon. For this, we identified grids at 7 km × 7 km areal resolution for the Chilika lagoon and these grids are shown in Fig. 1. The salinity-weighted average boron concentrations of all the points within a given grid during both of the sampling trips are compared in Fig. 9. The boron abundance of the 1-day sampling data is found consistently lower (by ~34%; Fig. 9) than that of the high-resolution spatial sampling of the lagoon. This difference in boron abundance is mainly due to the degree of seawater exchange into the lagoon during the different tidal stages. Despite these differences in boron concentrations, the linearity between boron and salinity and hence, conservative nature of boron during monsoon period persists for both the sampling durations. This observation indicates that boron concentration of the Chilika and its spatial distribution depends on the tidal/ebb cycle and related seawater exchange. However, the coastal behavior of boron remains invariant during different tidal phases.

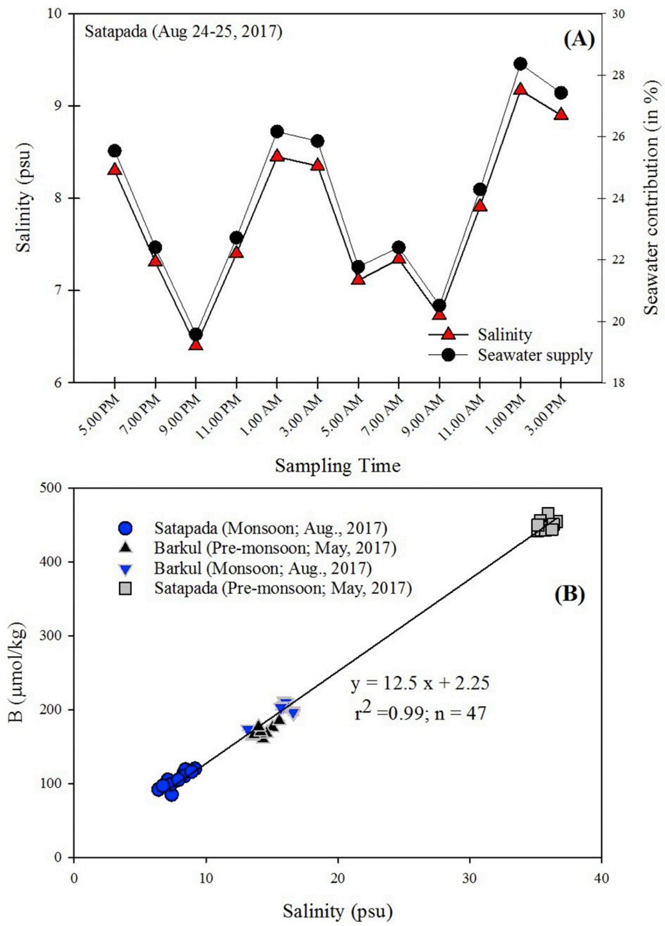

Fig. 8. (A) Two-hourly data for salinity and relative contribution from seawater to the lagoon at Satapada (outer channel) during the monsoon season. Variation in these datasets points to fluctuation of Bay of Bengal water influx into the Chilika due to tidal cycle. (B) Combined salinity and boron data on 2-h basis sampling at two different locations (Barkul and Satapada) for two seasons (monsoon and non-monsoon) show a conservative behavior. Analytical uncertainties associated with these two parameters are smaller than the symbol size.

5.4. Boron budget of the Chilika lagoon

The salinity and boron budgets of the Chilika lagoon for the monsoon (August) period are presented in Fig. 10. For this, the hydrological data are taken from Gupta et al. (2008), whereas the salinity and boron data are from this study. There exists no literature data for SGD flux to the Chilika. Assuming the SGD value for the Chilika is similar to that (1.55–7.44 × 10^6 m^3/d; Rengarajan and Sarma, 2015) reported for a nearby river (Guatami) estuary, the submarine groundwater discharge to this lagoon is found ~1–4% of the river water supply (167 × 10^6 m^3/d; Fig. 10) during the monsoon. Further, the conservative B-salinity trend ensures minimal impact of SGD on the Chilika boron budget. We, however, recognize here that precise SGD flux estimation for the lagoon can provide better constrains on the chemical budget. The salinity and boron compositions for the tide and ebb are computed from the diurnal data (Fig. 8) obtained at the Chilika outflow (Satapada). Area-weighted salinity and boron concentrations for the lagoon presented in Fig. 10 were estimated by considering surface area, average salinity and boron of all of the identified grids in Fig. 1. The average salinity of the lagoon is found to be 10.5 psu, which corresponds to about 30% of seawater influx to the Chilika. Average boron content of the Chilika lagoon (128 µmol/kg) corresponds to a total B inventory of 2.85 × 10^6 kg. Similar to salinity, mass balance calculation show about 70% of boron in

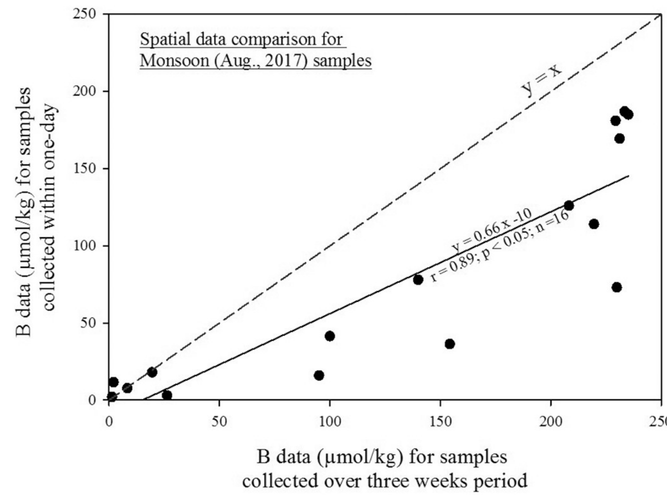

Fig. 9. Spatial correlation of boron data between monsoon samples for two different spatial sampling (1-day sampling versus spatial sampling over ~3 weeks' time). We compare here salinity-weighted boron data for each grid (7 km × 7 km) shown in Fig. 1 for the two sampling trips in the same season. The boron concentrations for the 1-day sampling are different than those collected by spatial sampling in about 3 weeks duration, attributable to tidal effect on water chemistry.

the Chilika is supplied through the freshwater sources.

In addition to these sources, the samples from the month of May also show removal of dissolved boron from low-saline (< 15 psu) regions of the Chilika through adsorptive processes (cf. Section 5.2.). Gridded data analysis of these samples provides an area-weighted average boron concentration of 226 µmol/kg for the lagoon, whereas the low-saline (< 15 psu) regions yield a B content of 117 µmol/kg. This analysis also provides an estimation of adsorptive B removal of 13 µmol/kg from the low-saline regions, which is only 3% of the open seawater boron value. Although extrapolating these regional data at global scales is likely to yield large uncertainties, we used the present data to compute total boron removal from the coastal lagoons worldwide. Available global database for total area (700,000 km^2) and volume (104,000 km^3) of saline lakes (Herdendorf, 1982) were used for this estimation. These data yield a total boron loss of 1.5 × 10^{10} kg from coastal lagoons globally, which is lower by few orders of magnitude than the total boron inventory in seawater (6.32 × 10^{15} kg). The adsorptive removal of boron from coastal lagoons, therefore, seems to have insignificant impact on global oceanic boron budget. This minimal impact is mainly due to lower concentration of boron in the low-saline regions by 1–2 orders of magnitude when compared with open ocean values. Outcomes of this study, however, provide "proof of a chemical process" involving removal of dissolved boron through ion-exchange mechanism. This observation can find implications in understanding authigenic boron distribution in clay-rich sedimentary archives and its applications to paleo-fluvial processes in continental/near-shore settings.

6. Conclusions

Detailed spatial and seasonal distributions of dissolved boron of a large brackish-water lagoon system (Chilika, India) have been investigated to infer its coastal behavior and controlling factors. Linear co-variation between boron and salinity of the samples from the monsoon season confirm conservative mixing of river and sea water within this coastal regime. On the contrary, the pre-monsoon samples exhibit non-conservative nature of boron in the Chilika with its significant removal from the low-saline (with salinity < 15 psu) water samples. These removals are mainly due to adsorption of dissolved boron on to particulate phases (clay and/or oxyhydroxides). Higher water residence time during pre-monsoon season through increased particulate-water

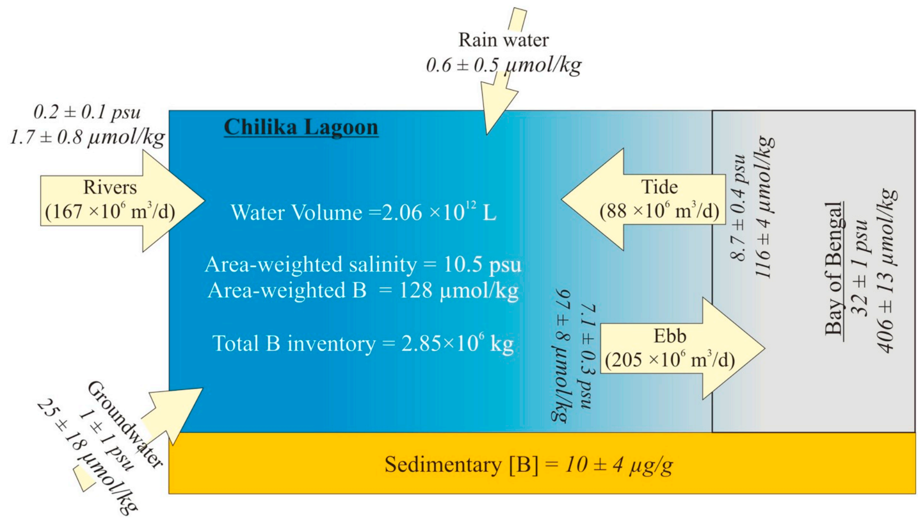

Fig. 10. Boron budget of the Chilika lagoon for the monsoon season. The boron and salinity data shown here from this study, whereas the hydrological data are from Gupta et al. (2008). Please note that the arrow size does not reflect the water volume of the sources to the lagoon.

interaction time seem to regulate the adsorptive removal intensity. Comparison of boron abundances during diurnal and fortnight time-scales show strong influence of tidal cycles on lagoon chemistry. However, the behavior of boron remains less influenced due to tidal forces and related seawater influx variations.

Acknowledgment

This research was financially supported by SERB Early career research award (ECS/2016/001884) to GRT. We thank Sharala Das, Anirban Mandal and Anupam Samanta for their help during collection of samples. Discussion with Devapriya Chattopadhyay during this work was beneficial. We sincerely acknowledge the local support received from Ramachandra, Avinash and Sanjay during the field trips. We thank Prof. Thomas Bianchi, the editor and two anonymous reviewers for their thorough and constructive reviews.

Appendix A. Supplementary data

Supplementary data to this article can be found online at https://doi.org/10.1016/j.marchem.2019.103663.

References

Barnes, R.S.K., 1980. Coastal Lagoons. Cambridge University Press, Cambridge, UK (106 pp.).
Barth, S., 1998. $^{11}B/^{10}B$ variations of dissolved boron in a freshwater-seawater mixing plume (Elbe Estuary, North Sea). Mar. Chem. 62, 1–14.
Beck, A.J., Charette, M.A., Cochran, J.K., Gonneea, M.E., Peucker-Ehrenbrink, B., 2013. Dissolved strontium in the subterranean estuary–implications for the marine strontium isotope budget. Geochim. Cosmochim. Acta 117, 33–52.
Bourg, A.C., 1987. Trace metal adsorption modelling and particle-water interactions in estuarine environments. Cont. Shelf Res. 7, 1319–1332.
Boyle, E.A., Edmond, J.M., Sholkovitz, E.R., 1977. The mechanism of iron removal in estuaries. Geochim. Cosmochim. Acta 41, 1313–1324.
Broecker, W.S., Peng, T.H., 1982. Tracers in the Sea. Eldigio Press, Lamont Doherty Geological Observatory, pp. 690.
Brunskill, G.J., Zagorskis, I., Pfitzner, J., 2003. Geochemical mass balance for lithium, boron, and strontium in the Gulf of Papua, Papua New Guinea (Project TROPICS). Geochim. Cosmochim. Acta 67, 3365–3383.
Carrano, C.J., Schellenberg, S., Amin, S.A., Green, D.H., Küpper, F.C., 2009. Boron and marine life: a new look at an enigmatic bioelement. Mar. Biotechnol. 11, 431.
Chakrapani, G.J., Subramanian, V., 1990. Preliminary studies on the geochemistry of the Mahanadi river basin, India. Chem. Geol. 81 (3), 241–253.
Charette, M.A., Sholkovitz, E.R., Hansel, C.M., 2005. Trace element cycling in a subterranean estuary: part 1. Geochemistry of the permeable sediments. Geochim. Cosmochim. Acta 69, 2095–2109.
Chetelat, B., Liu, C.Q., Gaillardet, J., Wang, Q.L., Zhao, Z.Q., Liang, C.S., Xiao, Y.K., 2009. Boron isotopes geochemistry of the Changjiang basin rivers. Geochim. Cosmochim. Acta 73 (20), 6084–6097.
Coffey, M., Dehairs, F., Collette, O., Luther, G., Church, T., Jickells, T., 1997. The behaviour of dissolved barium in estuaries. Estuar. Coast. Shelf Sci. 45, 113–121.
Du Laing, G., Rinklebe, J., Vandecasteele, B., Meers, E., Tack, F.M., 2009. Trace metal ehaviour in estuarine and riverine floodplain soils and sediments: a review. Sci. Total Environ. 407, 3972–3985.
Edmond, J.M., Spivack, A., Grant, B.C., Ming-Hui, H., Zexiam, C., Sung, C., Xiushau, Z., 1985. Chemical dynamics of the Changjiang estuary. Cont. Shelf Res. 4, 17–36.
Fanning, K.A., Maynard, V.I., 1978. Dissolved boron and nutrients in the mixing plumes of major tropical rivers. Neth. J. Sea Res. 12, 345–354.
Flegal, A.R., Smith, G.J., Gill, G.A., Sanudo-Wilhelmy, S., Anderson, L.C.D., 1991. Dissolved trace element cycles in the San Francisco Bay estuary. Mar. Chem. 36, 329–363.
Gaillardet, J., Lemarchand, D., 2018. Boron in the weathering environment. In: Marschall, H., Foster, G. (Eds.), Boron Isotopes: The Fifth Element. Springer International Publishing, pp. 163–188.
Gaillardet, J., Lemarchand, D., Göpel, C., Manhès, G., 2001. Evaporation and sublimation of boric acid: application for boron purification from organic rich solutions. Geostand. Newslett. 25 (1), 67–75.
Gat, J., Gonfiantini, R., 1981. Stable isotope hydrology: deuterium and Oxygen-18 in the water cycle. IAEA Tech. Rep. 210, 339.
Ghosh, S.K., Jana, T.K., 1993. Boron-boric acid complexes in estuarine water of River Hugli, east coast of India. Indian J. Mar. Sci. 22, 225–226.
Goldberg, S., 1997. Reactions of boron with soils. Plant Soil 193 (1), 35–48.
Gonneea, M.E., Charette, M.A., Liu, Q., Herrera-Silveira, J.A., Morales-Ojeda, S.M., 2014. Trace element geochemistry of groundwater in a karst subterranean estuary (Yucatan Peninsula, Mexico). Geochim. Cosmochim. Acta 132, 31–49.
Gupta, G.V.M., Sarma, V.V.S.S., Robin, R.S., Raman, A.V., Kumar, M.J., Rakesh, M., Subramanian, B.R., 2008. Influence of net ecosystem metabolism in transferring riverine organic carbon to atmospheric CO_2 in a tropical coastal lagoon (Chilka Lake, India). Biogeochemistry 87, 265–285.
Harriss, R.C., 1969. Boron regulation in the oceans. Nature 223 (5203), 290.
Herdendorf, C.E., 1982. Large lakes of the world. J. Great Lakes Res. 8, 379–412.
Jain, S.K., Agarwal, P.K., Singh, V.P., 2007. Hydrology and Water Resources of India. vol. 57. Springer publishers, The Netherlands, pp. 1258.
Keren, R., Mezuman, U., 1981. Boron adsorption by clay minerals using a phenomenological equation. Clay Clay Miner. 29, 198–204.
Kumar, A., Equeenuddin, S.M., Mishra, D.R., Acharya, B.C., 2016. Remote monitoring of sediment dynamics in a coastal lagoon: long-term spatio-temporal variability of suspended sediment in Chilika. Estuar. Coast. Shelf Sci. 170, 155–172.
Lécuyer, C., Bodergat, A.M., Martineau, F., Fourel, F., Gürbüz, K., Nazik, A., 2012. Water sources, mixing and evaporation in the Akyatan lagoon, Turkey. Estuar. Coast. Shelf Sci. 115, 200–209.
Lee, K., Kim, T.W., Byrne, R.H., Millero, F.J., Feely, R.A., Liu, Y.M., 2010. The universal ratio of boron to chlorinity for the North Pacific and North Atlantic oceans. Geochim. Cosmochim. Acta 74, 1801–1811.
Lemarchand, D., Gaillardet, J., Lewin, E., Allegre, C.J., 2000. The influence of rivers on marine boron isotopes and implications for reconstructing past ocean pH. Nature 408, 951–954.
Liddicoat, M.I., Turner, D.R., Whitfield, M., 1983. Conservative behaviour of boron in the Tamar Estuary. Estuar. Coast. Shelf Sci. 17, 467–472.
Liss, P.S., Pointon, M.J., 1973. Removal of dissolved boron and silicon during estuarine mixing of sea and river waters. Geochim. Cosmochim. Acta 37, 1493–1498.
Mahanty, M.M., Mohanty, P.K., Panda, U.S., Pradhan, S., Samal, R.N., Rao, V.R., 2015. Characterization of tidal and non-tidal variations in the Chilika lagoon on the east coast of India. Int. J. Sci. Eng. Res. 6, 564–571.
Mahanty, M.M., Mohanty, P.K., Pattnaik, A.K., Panda, U.S., Pradhan, S., Samal, R.N.,

2016. Hydrodynamics, temperature/salinity variability and residence time in the Chilika lagoon during dry and wet period: measurement and modeling. Cont. Shelf Res. 125, 28–43.
Mao, H.R., Liu, C.Q., Zhao, Z.Q., 2019. Source and evolution of dissolved boron in rivers: insights from boron isotope signatures of end-members and model of boron isotopes during weathering processes. Earth Sci. Rev. 190, 439–459.
Moore, W.S., 1999. The subterranean estuary: a reaction zone of ground water and sea water. Mar. Chem. 65, 111–125.
Muduli, P.R., Kanuri, V.V., Robin, R.S., Kumar, B.C., Patra, S., Raman, A.V., Rao, G.N., Subramanian, B.R., 2012. Spatio-temporal variation of CO_2 emission from Chilika Lake, a tropical coastal lagoon, on the east coast of India. Estuar. Coast. Shelf Sci. 113, 305–313.
Narvekar, P.V., Zingde, M.D., 1987. Behaviour of boron, calcium and magnesium in Purna and Auranga estuaries (Gujarat), west coast of India. Indian J. Mar. Sci. 16, 46–50.
Narvekar, P.V., Zingde, M.D., Dalal, V.N., 1981. Behaviour of boron, Calcium & Magnesium in Mindola River Estuary (Gujarat). Indian J. Mar. Sci. 10, 90–92.
Narvekar, P.V., Zingde, M.D., Dalal, V.K., 1983. Behaviour of boron, calcium and magnesium in a polluted estuary. Estuar. Coast. Shelf Sci. 16, 9–16.
Padmavathi, D., Satyanarayana, D., 1999. Distribution of nutrients and major elements in riverine, estuarine and adjoining coastal waters of Godavari, Bay of Bengal. Indian J. Mar. Sci. 28, 345–354.
Panchang, R., Nigam, R., 2012. High resolution climatic records of the past~ 489 years from Central Asia as derived from benthic foraminiferal species, *Asterorotalia trispinosa*. Mar. Geol. 307, 88–104.
Panigrahi, S., Wikner, J., Panigrahy, R.C., Satapathy, K.K., Acharya, B.C., 2009. Variability of nutrients and phytoplankton biomass in a shallow brackish water ecosystem (Chilika lagoon, India). Limnology 10, 73–85.
Park, H., Schlesinger, W.H., 2002. Global biogeochemical cycle of boron. Glob. Biogeochem. Cycles 16, 1072.
Pelletier, E., Lebel, J., 1978. Détermination du bore inorganique dans l'Estuaire du Saint-Laurent. Can. J. Earth Sci. 15 (4), 618–625.
Petelet-Giraud, E., Klaver, G., Negrel, P., 2009. Natural versus anthropogenic sources in the surface-and groundwater dissolved load of the Dommel river (Meuse basin): constraints by boron and strontium isotopes and gadolinium anomaly. J. Hydrol. 369 (3–4), 336–349.
Rahaman, W., Singh, S.K., 2010. Rhenium in rivers and estuaries of India: sources, transport and behaviour. Mar.Chem. 118, 1–10.
Rahaman, W., Singh, S.K., 2012. Sr and 87Sr/86Sr in estuaries of western India: impact of submarine groundwater discharge. Geochim. Cosmochim. Acta 85, 275–288.
Rajagopal, M.D., Rajendran, A., Reddy, C.V.G., 1981. Distribution of dissolved boron in the waters of the Zuari estuary (Goa). Indian J. Mar. Sci. 10, 20–23.
Rengarajan, R., Sarma, V.V.S.S., 2015. Submarine groundwater discharge and nutrient addition to the coastal zone of the Godavari estuary. Mar.Chem. 172, 57–69.
Rudnick, R.L., Gao, S., 2004. Composition of the continental crust. Treatise Geochem. 3, 1–65.
Russak, A., Sivan, O., Yechieli, Y., 2016. Trace elements (Li, B, Mn and Ba) as sensitive indicators for salinization and freshening events in coastal aquifers. Chem. Geol. 441, 35 46.
Sahu, B.K., Pati, P., Panigrahy, R.C., 2014. Environmental conditions of Chilika Lake during pre and post hydrological intervention: an overview. J. Coast. Conserv. 18, 285–297.
Saldi, G.D., Noireaux, J., Louvat, P., Faure, L., Balan, E., Schott, J., Gaillardet, J., 2018. Boron isotopic fractionation during adsorption by calcite–implication for the seawater pH proxy. Geochim. Cosmochim. Acta 240, 255–273.
Salomons, W., 1980. Adsorption processes and hydrodynamic conditions in estuaries. Environ. Technol. 1, 356–365.
Samanta, S., Dalai, T.K., 2016. Dissolved and particulate Barium in the Ganga (Hooghly) River estuary, India: solute-particle interactions and the enhanced dissolved flux to the oceans. Geochim. Cosmochim. Acta 195, 1–28.
Sarkar, S., Bhattacharya, A., Bhattacharya, A., Satapathy, K., Mohanty, A., Panigrahi, S., 2012. Chilika lake. In: Encylopedia of Lakes and Reservoirs. Springer publications, Dordrecht, pp. 148–156.
Schlesinger, W.H., Vengosh, A., 2016. Global boron cycle in the Anthropocene. Glob. Biogeochem. Cycles 30, 219–230.
Schwarcz, H., Agyei, E., McMullen, C., 1969. Boron isotopic fractionation during clay adsorption from sea-water. Earth Planet. Sci. Lett. 6, 1–5.
Sengupta, S., Parekh, A., Chakraborty, S., Ravi Kumar, K., Bose, T., 2013. Vertical variation of oxygen isotope in Bay of Bengal and its relationships with water masses. J. Geophys. Res. Oceans 118, 6411–6424.
Shirodkar, P.V., Anand, S.P., 1985. Behaviour of boron in Mandovi Estuary (Goa). Mahasagar 18, 439–448.
Siddiqui, S.Z., Rama Rao, K.V., 1995. Limnology of Chilika lake. In: Director of Zoological Survey of India (Calcutta) (Ed.), Fauna of Chilika Lake (Wetland Ecosystem Series I). Zoological Survey of India, Calcutta.
Singh, A., Jani, R.A., Ramesh, R., 2010. Spatiotemporal variations of the δ 18 O–salinity relation in the northern Indian Ocean. Deep Sea Res. Part 1 Oceanogr. Res. Pap. 57, 1422–1431.
Singh, S.P., Singh, S.K., Bhushan, R., 2013. Dissolved boron in the Tapi, Narmada and the Mandovi estuaries, the western coast of India: evidence for conservative behavior. Estuaries Coast. 37, 1017–1027.
Tripathy, G.R., Hannah, J.L., Stein, H.J., 2018. Refining the Jurassic-Cretaceous boundary: Re-Os geochronology and depositional environment of upper Jurassic shales from the Norwegian Sea. Palaeogeogr. Palaeoclimatol. Palaeoecol. 503, 13–25.
Tripathy, G.R., Mishra, S., Danish, M., Ram, K., 2019. Elevated barium concentrations in rain water from east-coast of India: role of regional lithology. J. Atmos. Chem. 1–14.
Vengosh, A., Heumann, K.G., Juraske, S., Kasher, R., 1994. Boron isotope application for tracing sources of contamination in groundwater. Environ. Sci. Technol. 28 (11), 1968–1974.
Vengosh, A., Spivack, A.J., Artzi, Y., Ayalon, A., 1999. Geochemical and boron, strontium, and oxygen isotopic constraints on the origin of the salinity in groundwater from the Mediterranean coast of Israel. Water Resour. Res. 35 (6), 1877–1894.
Venkatarathnam, K., 1970. Formation of the barrier spit and other sand ridges near Chilka Lake on the east coast of India. Mar. Geol. 9, 101–116.
Wang, R.M., You, C.F., Chu, H.Y., Hung, J.J., 2009. Seasonal variability of dissolved major and trace elements in the Gaoping (Kaoping) river estuary, Southwestern Taiwan. J. Mar. Syst. 76, 444–456.
Xiao, Y., Liao, B., Wang, Z., Wei, H., Zhao, Z., 2007. Isotopic composition of dissolved boron and its geochemical behavior in a freshwater-seawater mixture at the estuary of the Changjiang (Yangtze) river. Chin. J. Geochem. 26, 105–113.
Zingde, M.D., Ram, A.L., Sharma, P., Abidi, S.A.H., 1995. Seawater Intrusion and Behaviour of Dissolved Boron, Fluoride, Calcium, Magnesium and Nutrients in Vashisti Estuary. Society of Biosciences, Muzaffarnagar, India.

Marine Chemistry 224 (2020) 103816

Contents lists available at ScienceDirect

Marine Chemistry

journal homepage: www.elsevier.com/locate/marchem

Submarine groundwater discharge to a tropical coastal lagoon (Chilika lagoon, India): An estimation using Sr isotopes

Mohd Danish[a,*], Gyana Ranjan Tripathy[a], Waliur Rahaman[b]

[a] Department of Earth and Climate Science, Indian Institute of Science Education and Research, Dr. Homi Bhabha Road, Pune 411008, India
[b] National Centre for Polar and Ocean Research (NCPOR), Ministry of Earth Sciences, Vasco-da-Gama, Goa 403804, India

ARTICLE INFO

Keywords:
Coastal lagoon
Water chemistry
Salinity
$^{87}Sr/^{86}Sr$
SGD

ABSTRACT

Submarine groundwater discharge (SGD) is an important component of the marine $^{87}Sr/^{86}Sr$ budget, which is currently in an imbalance with a missing source. In this contribution, dissolved Sr concentrations and $^{87}Sr/^{86}Sr$ of the Chilika lagoon (India), the largest brackish-water lagoon in Asia, have been investigated for three different seasons (pre-monsoon (May 2017), monsoon (Aug., 2017) and post-monsoon (Jan., 2018)) to infer coastal behavior of Sr and estimate the SGD fluxes to the coastal ocean. Major source waters (groundwater, river and seawater) and suspended sediments from the lagoon system have also been analyzed for source characterization. Salinity and Sr concentrations of the Chilika samples show wide variations during pre-monsoon (0.2–35.8; 1–93 μmol/kg), monsoon (0.1–20.1; 0.8–55 μmol/kg) and post-monsoon (0.3–7.7; 1–20 μmol/kg) seasons. Despite of these variations, salinity and Sr concentrations of the lagoon co-vary linearly as expected for conservative mixing between river and seawater. In contrast, the mixing plot between 1/Sr and $^{87}Sr/^{86}Sr$ during the monsoon and pre-monsoon seasons deviate from the river-seawater mixing trend, indicating an additional source/sink of ^{87}Sr to this lagoon. The non-conservative behavior of $^{87}Sr/^{86}Sr$ during monsoon has largely been restricted to low salinity ($< \sim 2$) regime, which could be attributed to subsurface ion-exchange process. During the pre-monsoon, the SGD can explain the non-conservative isotopic behavior that requires additional water supply with higher $^{87}Sr/^{86}Sr$ ratios. The SGD fluxes have been estimated using two separate approaches, (i) using an inverse model with fixed SGD composition and (ii) using a source-mixing computation using variable SGD compositions within the lagoon. These computations estimate that the SGD contributes ~20% of total water supplied to the Chilika lagoon during the pre-monsoon season. This SGD contribution corresponds to a flux of 1.51×10^6 m^3/d to the lagoon. Data from this and earlier studies indicate that the $^{87}Sr/^{86}Sr$ ratios of the SGD to the western Bay of Bengal, which receives water from several large rivers from the Himalaya and Peninsular Indian regions, are relatively higher (~0.715) than the seawater value (0.7092). The SGD flux to the east coast of India, therefore, would not contribute in reducing the oceanic imbalance, which requires a less-radiogenic source.

1. Introduction

Submarine groundwater discharge (SGD) is comprised of subsurface seepage of fresh groundwater and wave/tide-induced recycled seawater through porous terrestrial rocks or sediment aquifers to the coastal ocean (Burnett et al., 2003; Moore, 2010; Knee and Paytan, 2011). This source has been recognized as an important source of nutrients and trace metals (e.g. carbon, nitrogen, alkaline earth metals and rare earth elements) to the coastal ecosystem (Charette et al., 2001; Street et al., 2008; Rodellas et al., 2015). Precise estimation of the SGD and associated chemical fluxes is often complicated due to its non-point and spatio-temporal behavior (Taniguchi et al., 2002; Charette et al., 2008). In this context, source-mixing calculations for chemical tracers (e.g. Ra, Rn and Sr isotopes) and associated "flux-by-difference" approaches have been successful in quantifying the SGD to different coastal regimes (Moore, 1996; Charette et al., 2008). Available global estimates on meteoric (2.4×10^{15} L/y) and brackish ($2–5 \times 10^{16}$ L/y) SGD are found comparable with the global river discharge (3.89×10^{16} L/y; Beck et al., 2013 and references therein). Furthermore, a recent continental-scale study based on Ra isotopic data from the Atlantic and the Indo-Pacific oceans estimate that the SGD flux (12×10^{16} L/yr) is higher than the riverine flux (3×10^{16} L/yr; Kwon et al., 2014) to these oceans and hence, warrants detailed investigation to assess importance of SGD in global chemical budgets for different elements.

* Corresponding author.
E-mail address: mohd.danish@students.iiserpune.ac.in (M. Danish).

https://doi.org/10.1016/j.marchem.2020.103816
Received 24 September 2019; Received in revised form 31 March 2020; Accepted 4 May 2020
Available online 13 May 2020

The SGD serves as an important source in regulating past and contemporary oceanic Sr budgets (Chaudhuri and Clauer, 1986; Basu et al., 2001; Beck et al., 2013). The oceanic Sr isotopic budget is currently in an imbalance with missing flux from less radiogenic Sr sources (Vance et al., 2009; Allègre et al., 2010; Tripathy et al., 2012; Peucker-Ehrenbrink and Fiske, 2019). The global lithology-weighted average $^{87}Sr/^{86}Sr$ ratio for SGD (0.7089) is lower compared to the present-day seawater ratio (0.7092) and hence, may account for a part of the missing less radiogenic component (Beck et al., 2013). Recent estimates indicate that the range of SGD-derived Sr flux is 7–28 × 10^9 mol/yr, which is about one-third of the riverine flux (47.6× 10^9 mol/yr; Peucker-Ehrenbrink and Fiske, 2019) and can account for 13–30% of the present-day seawater $^{87}Sr/^{86}Sr$ budget (Beck et al., 2013). Available SGD estimates based on Sr isotopes are mainly based on the non-conservativeness of $^{87}Sr/^{86}Sr$ in estuaries/coastal oceans (Huang et al., 2011; Rahaman and Singh, 2012; Beck et al., 2013; Trezzi et al., 2017; Chakrabarti et al., 2018). These non-conservative behaviors of Sr isotopes are mostly attributed to isotope exchange from aquifer solids to groundwater without changing the Sr content (Rahaman and Singh, 2012). Existing Sr isotopic studies in global estuaries report both conservative (Ingram and Sloan, 1992; Andersson et al., 1994; Sharma et al., 2007) and non-conservative (Wang et al., 2001; Rahaman and Singh, 2012; Beck et al., 2013) behavior in the coastal regions. Although the exact cause is not clear, these contrasting behaviors could be attributed to variable efficiency of particulate-water interaction in these river basins and their estuaries (Barth, 1998).

Earlier studies on $^{87}Sr/^{86}Sr$ have largely been restricted to estuaries but not extended to coastal lagoons, whose areal extent account for ~13% of total coastline area globally (Barnes, 1980). Considering this, the objectives for this study are identified as (i) to assess the coastal behavior of Sr and $^{87}Sr/^{86}Sr$ in a large tropical coastal lagoon system and (ii) to estimate SGD-derived Sr fluxes to the coastal ocean. Spatial distributions of dissolved Sr and $^{87}Sr/^{86}Sr$ ratios of the Chilika lagoon (the largest brackish water lagoon in Asia; Herdendorf, 1982) have been investigated in this study for three seasons (pre-monsoon (April–May 2017); monsoon (July-Aug., 2017); post-monsoon (Jan., 2018)). Further, possible source waters (river, groundwater and seawater) to the lagoon were also measured for their Sr concentration and isotopic compositions. The SGD flux were estimated using two approaches, (i) an inverse model approach assuming fixed groundwater composition (Rahaman and Singh, 2012) and (ii) source-mixing approach using variable groundwater compositions across salinity gradient. Although variable SGD compositions within a coastal system have already been reported elsewhere (Charette et al., 2008; Debnath et al., 2019), its impact on SGD estimations have not yet been assessed thoroughly.

2. Study area

Hydrogeological details about the Chilika lagoon, India are part of several earlier publications (Gupta et al., 2008; Sarkar et al., 2012; Danish et al., 2019). Briefly, it is the largest brackish water lagoon in Asia and a wetland of international importance (Ramsar site) with rich biodiversity. This tropical coastal lagoon (annual rainfall ~1240 mm) is situated between the Eastern Ghat and the Bay of Bengal (Fig. 1). The lagoon is separated by a long (approx. 60 km length) sand bar and connected to the Bay of Bengal by a narrow opening from the eastern side. A small canal (namely, Palur canal) also connects the southern part of the lagoon to the Bay (Fig. 1). The drainage basin of the Chilika, including the lagoon itself, covers an area of ~4406 km^2 and is mostly composed of metamorphic Precambrian rocks (gneisses, quartzites and charnockites). The areal extent of the lagoon is ~1165 km^2 during the monsoon period, which reduces by ~20% during non-monsoon season. The pear-shaped, shallow (~2 m deep) lagoon is approximately 65 km long with a maximum width of 20 km. The Chilika receives freshwater discharge of ~5.1 × 10^{12} L annually from its north-eastern (via Mahanadi distributaries) and western catchments. The major water source for this discharge is the south-west rainfall during the monsoon season, which accounts for about 60% of the annual freshwater influx to the lagoon (Muduli et al., 2012). The lagoon exhibits an estuarine characteristic with lower salinity in the northern sector compared to that in the central and southern sectors. Its hydrology is significantly influenced by the semi-diurnal (12.4 h) and fortnightly (12 days) tides. The lagoon is dominated by evaporation over precipitation during drier seasons (Danish et al., 2019). The water residence times for the northern (8 days) and southern (35 days) sectors during monsoon period (Mahanty et al., 2016) are distinctly different, with the later sector being less-readily exchanged. The lagoon receives a significant amount of suspended sediments from both north-eastern (1.2 × 10^6 tons/yr) and western (0.3 × 10^6 tons/yr) catchments (Ghosh et al., 2006).

3. Sampling and analytical methods

Surface water samples from the Chilika lagoon were collected for three different seasons (Fig. 1; Danish et al., 2019), viz. pre-monsoon (April–May 2017), monsoon (July–August 2017) and post-monsoon (January 2018). This spatial sampling using motor boats took around 3-weeks' time during each season. To account for the fortnight tidal cycle of the lagoon, we have also collected an additional set of spatial samples on another day (16th August 2017) during the monsoon season. Furthermore, 2-hr resolution sampling of water samples at two locations (Satapada (outflow) and Barkul (southern sector); Fig. 1) during monsoon and pre-monsoon seasons were conducted to assess the impact of semi-diurnal tidal effect. The post-monsoon samples for this study were collected after two heavy rainfall events [during mid-November (BOB-06 cyclone) and early-December (BOB-08 cyclone); http://www.imd.gov.in] due to low depression developed over the Bay of Bengal. Several groundwater (n = 70), river (n = 4) and seawater (Bay of Bengal; n = 3) samples were also collected to constrain the source compositions. The groundwater samples were mostly collected from open wells with their typical depths varying between 5 and 10 m from the surface. Few groundwater samples were collected from borewells after continuous pumping of about five minutes. Further, ten suspended sediment samples from the northern sector of the lagoon during the monsoon and four bed sediments from the Mahanadi distributaries were also collected.

Sampling protocols adopted during this study are provided in Danish et al. (2019). Briefly, water temperature, pH and salinity were measured on-site using a portable multi-parameter probe. The samples were filtered within 24 h through 0.45 μm nylon filters, acidified to pH ~ 2 using nitric acid and stored in pre-cleaned HDPE bottles. For Sr elemental analyses, the samples were diluted to a salinity of ~1 to minimize matrix effect and these aliquots were measured using Quadrupole-inductively coupled plasma mass spectrometer (Q-ICP MS facility at IISER, Pune) in its kinetic energy discrimination mode. The ^{88}Sr isotopic signals of the samples were quantified using a standard calibration method to compute their Sr concentrations. Average ^{88}Sr counts of the samples (~200, 000 cps) were about four orders of magnitude higher than the background counts (~100 cps) and hence, no noise corrections were done. Sr concentrations of fourteen water samples were measured in replicates to constrain the measurement precision (~4%). Further, a few replicate samples (n = 23) were also measured using internal (indium) standards. The Sr concentrations data yielded from the internal standard approach compare well (± 5%) with that measured using the standard calibration method. The accuracy of Sr measurement was ascertained by analyzing international natural water (NIST-1640a) reference materials. The measured Sr concentrations for NIST-1640a (123 ± 7 μg/kg; (n = 7)) are consistent with its reported values (125.03 ± 0.86 μg/kg). In addition to water, concentrations of selected elements (Sr, Ca, Fe Al) and $^{87}Sr/^{86}Sr$ ratios for ten suspended sediments from the lagoon and four bed sediments from associated

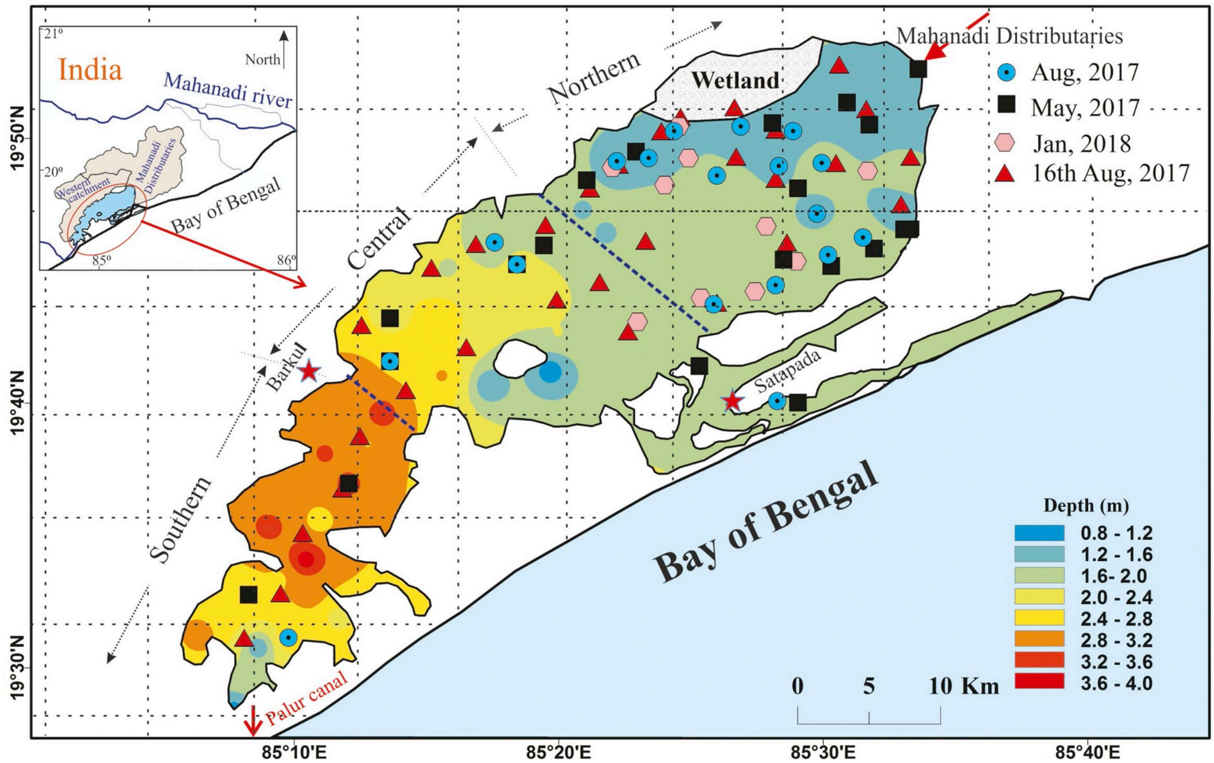

Fig. 1. Locations of the Chilika water samples collected during three seasons (pre-monsoon (May 2017); monsoon (August-2017) and post-monsoon (January 2018)) are shown. The color contour in the map reflects the water depth of the lagoon during the monsoon period. Two-hourly sampling for 1-day during the pre-monsoon and monsoon were carried out at two locations (star symbols) from the southern (Barkul) and outer (Satapada) sectors. The figure inset depicts the catchment area (shaded in gray color) of Mahanadi distributaries and other streams from the western sides to the lagoon.

rivers were measured. These sediments were water-washed and thoroughly homogenized to 100 mesh size using an agate-mortar pestle (Danish et al., 2019). A known amount of powdered aliquots of the bulk sediments were completely digested by repeated treatment with HF-HNO_3-HCl acids. These digested solutions were analyzed for their elemental concentrations using the Q-ICP MS instrument. The exchangeable Sr fraction present in the lagoon sediments were also measured in this study. For this, about 0.5 g of sediments were treated with 1 N ammonium acetate for 16 h at room temperature to extract the exchangeable Sr into solution phase. Sr concentrations of these solutions were measured using a Q-ICP MS.

The Sr isotopic compositions of water (Rahaman and Singh, 2012; Nuruzzama et al., 2020), and bulk and exchangeable fractions of sediment (Singh et al., 2008; Anand et al., 2019) samples were carried out following established protocols. For water (filtered and acidified) samples and exchangeable fractions, about 10–50 g of the aliquot were dried at 80 °C and re-dissolved in 3 N HNO_3 medium. This solution was passed through Eichrom® Sr-Spec resin (50–100 μm) to extract the pure Sr. In case of sediment samples, the acid-digested solutions of the water-washed sediments were passed through a cation-exchange column to collect pure Sr. Isotopic analyses of the Sr fraction were carried out using the multi-collector ICP MS (Neptune Plus, Thermo® Scientific) at NCPOR, Goa. We constantly monitored the signal at mass 85 amu to monitor any ^{87}Rb interference. The isotopic data were corrected for any instrumental fractionation by normalizing the measured $^{86}Sr/^{88}Sr$ ratio to its natural value of 0.1194, and subsequently normalized with the reported value of NIST NBS-987 (0.71025; Weis et al., 2006). The $^{87}Sr/^{86}Sr$ ratio of NBS-987 standard solution was monitored after every five analyses to establish the measurement accuracy. The measured $^{87}Sr/^{86}Sr$ ratio (0.71026 ± 0.00003; 2σ, n = 48) of the NBS-987 is consistent with its reported values. The procedural Sr blank for the isotopic analyses was ~500 pg, which is lower by few orders of magnitude than the total amount of Sr processed (~1 μg) for samples and hence, no blank corrections were made.

4. Results

4.1. Compositions of possible sources

Elemental analyses of three surface water samples from the Bay of Bengal have constrained the average salinity (33 ± 1) and Sr concentrations (85 ± 2 μmol/kg) for the seawater input to the lagoon (Table 1). The average $^{87}Sr/^{86}Sr$ ratio for these Bay samples (0.70919 ± 0.00001; n = 3) is similar to that reported for open ocean (~ 0.70918; Peucker-Ehrenbrink and Fiske, 2019) globally. Average Sr concentration and $^{87}Sr/^{86}Sr$ ratios of four riverine samples from monsoon season were 957 ± 156 nmol/kg and 0.719 ± 0.001, respectively (Table 1). The average Sr concentrations of the less saline (salinity ≤0.3) samples from the Chilika show seasonal variations with lower values during the monsoon (938 ± 265 nmol/kg; n = 15) compared to other seasons (1311 ± 27 nmol/kg; n = 2). However, the $^{87}Sr/^{86}Sr$ ratios of these samples show no significant difference between the monsoon (0.716 ± 0.002) and lean-flow seasons (0.7170 ± 0.0001). The Sr concentration of the groundwater samples (with salinity range of 0.12 to 8.18) vary between 0.35 and 35 μmol/kg with an average value of 7 ± 7 μmol/kg (n = 70; see supplementary materials). We have analyzed thirty-two groundwater samples for Sr isotopic analyses. The $^{87}Sr/^{86}Sr$ ratios of groundwater samples vary between 0.70993 and 0.86605, with an average value of 0.72 ± 0.03 (n = 32; Supplementary Table S3).

4.2. Sr and $^{87}Sr/^{86}Sr$ ratios of the Chilika

Average salinity and Sr concentrations of the lagoon during the monsoon season are 4 ± 6 (range: 0.1–20.1; n = 18) and 12 ± 17 μmol/kg (range: 0.8–54 μmol/kg; n = 18), respectively. The

Table 1
Average chemical (salinity and Sr concentrations) and Sr isotopic data for the Chilika lagoon system.

		Counts	Salinity	Sr (μmol/kg)	$^{87}Sr/^{86}Sr$
Chilika (Spatial Sampling)					
Pre-monsoon (Apr.-May 2017)	*Range*	20	0.2–35.8	1.3–93	0.7092–0.7171
	Average		13 ± 10	34 ± 25	0.711 ± 0.002
Monsoon (Jul.-Aug., 2017)	*Range*	18	0.1–20.1	0.8–54	0.7094–0.7179
	Average		4 ± 6	12 ± 17	0.712 ± 0.003
Monsoon (16th Aug. 2017)	*Range*	30	0.1–17.2	0.8–46	0.7094–0.7183
	Average		5 ± 6	13 ± 16	0.712 ± 0.003
Post-monsoon (Jan., 2018)	*Range*	10	0.3–7.7	1.3–20	0.7097–0.7170
	Average		4 ± 3	10 ± 7	0.712 ± 0.002
Chilika (2-h resolution sampling)					
Barkul (monsoon)	Range	9	15.9–16.6	44–47	0.70939–0.70941
	Average		16.2 ± 0.3	46 ± 1	0.70940 ± 0.00001
Barkul (pre-monsoon)	Range	11	13.5–15.6	35–40	0.70954–0.70958
	Average		14.2 ± 0.6	37 ± 1	0.70956 ± 0.00001
Satapada (Monsoon)	Range	12	6.4–9.2	18–24	0.70949–0.70963
	Average		8 ± 1	21 ± 2	0.70957 ± 0.00005
Satapada (pre-monsoon)	Range	12	35.1–36.6	89–95	0.70918–0.70920
	Average		35.6 ± 0.5	91 ± 2	0.70919 ± 0.00001
Possible major sources					
River water	Range	4	0.12–0.26	0.8–1.1	0.7178–0.7194
	Average		0.17 ± 0.06	1.0 ± 0.2	0.719 ± 0.001
Groundwater (Monsoon)	Range	12	0.27–3.02	2–34	0.7107–0.7334
	Average		1.0 ± 0.8	10 ± 9	0.716 ± 0.006
Groundwater (Pre-monsoon)	Range	20	0.15–8.18	1–35	0.7099–0.8660
	Average		1.4 ± 1.7	9 ± 9	0.723 ± 0.034
Seawater (Bay of Bengal)	Range	3	31.5–33.6	82–87	0.70918–0.70920
	Average		33 ± 1	85 ± 2	0.70919 ± 0.00001
Suspended Sediments (Bulk)	Range	10	–	83–109	0.7207–0.7374
	Average		–	95 ± 8[a]	0.731 ± 0.005
Suspended Sediments (Exchangeable)	Range	10	–	28–44	0.7110–0.7180
	Average		–	34 ± 4[a]	0.714 ± 0.002

[a] Units for particulate Sr are μg/g; Salinity data are from Danish et al. (2019).

northern sector receives dominant amount of the riverine influx to the lagoon and exhibits an estuarine characteristics. Consistent with this, the average Sr concentration of the northern sector samples (3 ± 2 μmol/kg) is lower than that for the other sectors (37 ± 15 μmol/kg) during the monsoon (Fig. 2). The Sr concentrations of the pre-monsoon (1.3–93 μmol/kg; $n = 20$) and post-monsoon (1.3–20 μmol/kg; $n = 10$) samples also show significant spatial distributions (Table 1). Further, the spatial distribution of $^{87}Sr/^{86}Sr$ ratios (Fig. 2) also depicts dominancy of freshwater influxes in the northern sector and seawater fluxes to the central and southern sectors. The $^{87}Sr/^{86}Sr$ ratios of the lagoon during the monsoon vary from 0.70936 to 0.71790, with an average value of 0.712 ± 0.003 (n = 18). This average isotopic value for the spatial sampling over three-weeks' period is similar to that observed for the whole lagoon sampled within 24 h (0.712 ± 0.003; $n = 30$). The $^{87}Sr/^{86}Sr$ ratios for the pre-monsoon (0.70918–0.71706; n = 20) and post-monsoon (0.70968–0.71697; n = 10) seasons also show similar spatial distributions with high radiogenic values in the northern sectors.

Fig. 3 depicts correlation between dissolved Sr concentrations and salinity of the Chilika lagoon during three seasons. The correlation factors for the Sr-salinity linear relationship for the pre-monsoon ($r = 0.999$ (n = 20); $p < .01$), monsoon (r = 0.999 ($n = 48$); p < .01) and post-monsoon (r = 0.999 (n = 10); p < .01) seasons are statistically significant at a confidence level of 99%. Further, the slopes of the regression lines between these two parameters for pre-monsoon (2.6 ± 0.2), monsoon (2.7 ± 0.2) and post-monsoon (2.5 ± 0.3) seasons overlap with that expected (~2.56) for river-seawater mixing line. These observations confirm conservative behavior of Sr concentration in the Chilika lagoon. Two samples from the pre-monsoon season are characterized with relatively higher salinity and Sr concentrations than the Bay of Bengal samples. Although these outliers follow the conservative trend, their higher values are attributable to evaporation effects (Danish et al., 2019). In contrast to Sr concentrations, the $^{87}Sr/^{86}Sr$ ratios show seasonal changes in its coastal behavior (Fig. 4). The post-monsoon samples from the Chilika follow a near linear trend in 1/Sr-versus-$^{87}Sr/^{86}Sr$ ratio plot (Fig. 4), which is consistent with conservative river-seawater mixing line. However, these data for monsoon and pre-monsoon samples deviate from the conservative mixing line (Fig. 4). During the monsoon season, selected samples (mainly from the low-saline region) show non-conservative behavior and fall below the expected binary mixing line. The monsoon samples with relatively higher salinities mostly follow the conservative mixing trend (Fig. 4). These trends are consistent during two different set of monsoon sampling, viz. detailed (over three-week period) spatial (Aug., 2017) and 1-day (16th Aug, 2017) sampling of the lagoon. For the pre-monsoon period, most of the lagoon samples fall above the expected river-seawater mixing line and hence, confirm their non-conservative behavior.

4.2.1. Diurnal variations

The water levels of the lagoon at its outflow are higher during the monsoon (1.07 to 2.53 m) compared to that during the non-monsoon (0.84 to 1.95 m) seasons (Mahanty et al., 2015). These water levels increase during the flood tides by ~1.5 m during the monsoon and ~ 1 m during the non-monsoon seasons with a periodicity of 12.4 h (Mahanty et al., 2015, 2016). We investigated the Sr and $^{87}Sr/^{86}Sr$ ratio of the Chilika at its outflow (Satapada) and in its southern sector (Barkul; Fig. 1) at 2 h interval to assess variation in water chemistry due to tide-ebb related depth fluctuations. At the outflow, the Sr concentrations during the monsoon vary by about 10% with an average value of 21 ± 2 μmol/kg (Fig. 5). The highest Sr concentration was observed for the samples with highest salinity (Fig. 5), confirming seawater incursion into the lagoon during the flood tides. The $^{87}Sr/^{86}Sr$ ratios at Satapada ranged from 0.70949 to 0.70963 (0.70957 ± 0.00005) within 24 h during the monsoon, with the lowest ratio being observed for the highest saline (9.2) sample. In contrast to

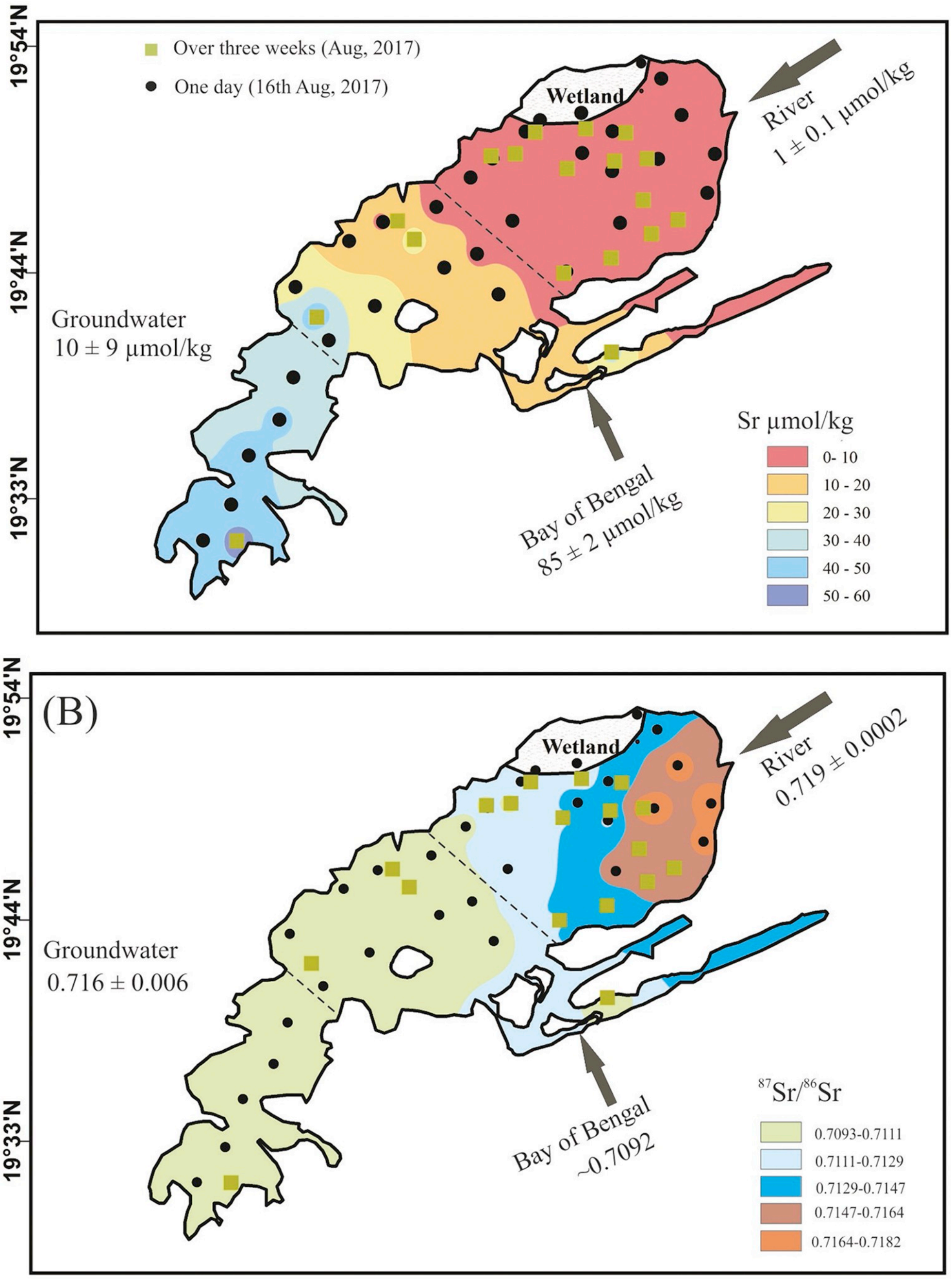

Fig. 2. Spatial distribution of dissolved Sr concentrations and $^{87}Sr/^{86}Sr$ ratios of the Chilika lagoon during monsoon period. For reference, these data for possible source waters (groundwater, river, and sea (Bay of Bengal) water; Table 1) are also shown.

the monsoon, the Sr concentrations only show minimal change (~2%) during the pre-monsoon season. The semi-diurnal tidal impact at the southern sector (Barkul) on lagoon salinity and Sr concentrations is weak (2–4%) during both monsoon and pre-monsoon seasons. The average Sr concentration at Barkul during the monsoon (46 ± 1 µmol/kg) is higher than that during the pre-monsoon (37 ± 1 µmol/kg). The $^{87}Sr/^{86}Sr$ ratios at this location show minimal change during the monsoon (0.70940 ± 0.00001; n = 9) and pre-monsoon (0.70956 ± 0.00001; n = 11) seasons.

4.2.2. Sediment compositions

The Al concentrations of the suspended sediments from the Chilika lagoon (13.2–14.9 wt%; n = 10) are about two times higher than that of the bed sediments of the Mahanadi distributaries (6.1 ± 0.7 wt%; n = 4; see supplementary material). In contrast, the Sr concentrations for the suspended sediments (95 ± 8 µg/g; n = 10) and the river sediments (102 ± 16 µg/g; n = 4) are found to be comparable. The Sr/Al ($\times 10^{-4}$) ratios for the suspended sediments (6.8 ± 0.5) are lower than the bed sediments (17 ± 4); this may be attributed to release of Sr to the dissolved phases. The Sr content of the exchangeable fraction of sediments vary between 28 and 44 µg/g, with an average value of 34 ± 4 µg/g (n = 11; Table S4). This exchangeable Sr content, on average, accounts for ~30% of the bulk Sr concentrations of the suspended sediments. The $^{87}Sr/^{86}Sr$ ratios of the suspended sediments from the Chilika vary between 0.72070 and 0.73739, with an average value of 0.731 ± 0.005. The Sr isotopic values of the exchangeable fractions are less radiogenic (compared to that of the bulk sediments) with their values ranging between 0.71097 and 0.71801. The Sr/Al and $^{87}Sr/^{86}Sr$ ratios of the suspended sediments show a broadly decreasing trend with their corresponding water salinities (Fig. 6). Similar to the

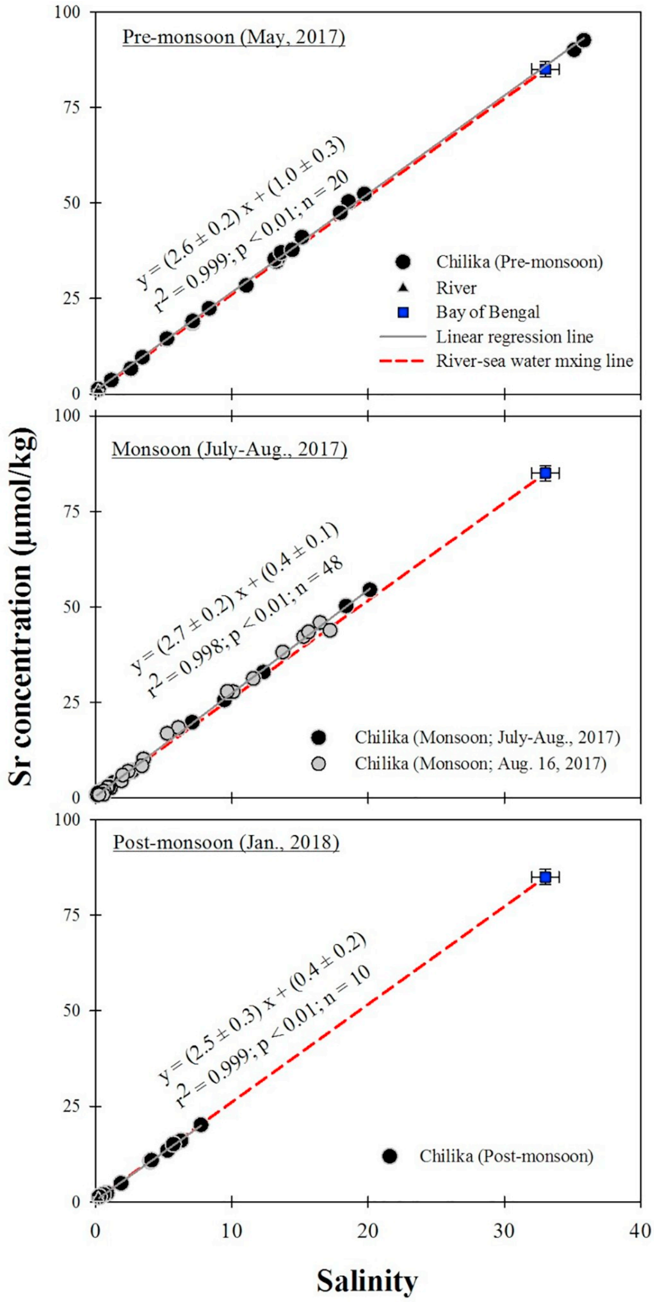

Fig. 3. Significant correlation between water salinity and Sr concentrations confirm conservative behavior of Sr during (i) pre-monsoon, (ii) monsoon and (iii) post-monsoon seasons. The slopes of linear regression lines during the three seasons overlap with that expected (~2.6) for conservative mixing of river and seawater.

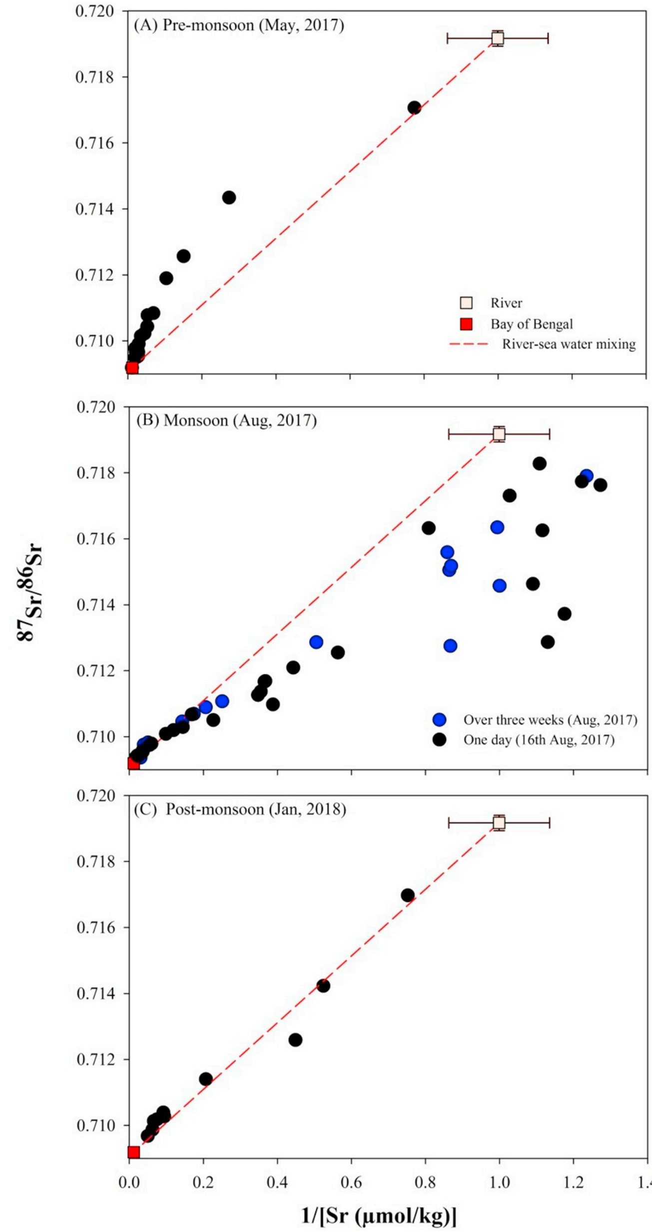

Fig. 4. Mixing diagram between dissolved Sr concentrations and $^{87}Sr/^{86}Sr$ ratios during different seasons. The Sr isotopes behave conservatively during post-monsoon, but non-conservatively during monsoon and pre-monsoon seasons.

Sr/Al ratios, their corresponding Ca/Al and Fe/Al ratios (figure not shown) also show decreasing trends, indicating possible release of Sr through re-dissolution of Ca-rich minerals and Fe-Mn hydroxides to the dissolved phase of the lagoon.

5. Discussion

5.1. Behavior of Sr and $^{87}Sr/^{86}Sr$ along the salinity gradient

Co-variation between salinity and dissolved elemental concentrations in coastal systems serves as a measure for constraining the solute sources (river, seawater, and SGD) and/or internal cycling of elements [such as, ion-exchange, association with biological activities, and re-dissolution of minerals (Fe-Mn oxyhydroxides, carbonates)] (Coffey et al., 1997; Moore, 1999; Samanta and Dalai, 2016; Rahaman et al., 2011; Danish et al., 2019). Linear trend between these two parameters confirms that the elemental distribution along the salinity gradient is regulated only by its supply through river and seawater, whereas deviation of data from the linearity points to either removal or addition of the element through additional sources/sinks. As discussed in the result section, dissolved strontium concentrations of the Chilika samples exhibit significant correlation ($r^2 = 0.999$, $p < .01$; Fig. 3) with salinity during all the three seasons. This linear relationship confirms efficient mixing of river and seawater in regulating the dissolved Sr concentrations within the Chilika. This observation on conservative behavior of strontium along the salinity gradient is consistent with that reported earlier for various estuaries worldwide (Andersson et al., 1994; Wang et al., 2001; Sharma et al., 2007; Rahaman and Singh, 2012; Beck et al., 2013; Wang and You, 2013). Unlike Sr concentrations, Sr isotopic ratios

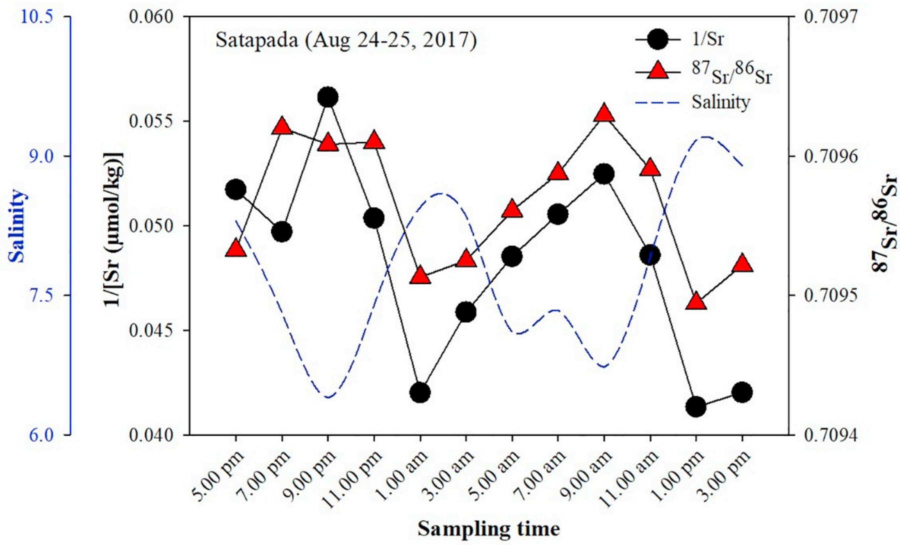

Fig. 5. Two-hourly resolution water salinity, Sr, and $^{87}Sr/^{86}Sr$ data at the Chilika outflow during the monsoon. Variations in salinity show effect of tides and ebb on the lagoon chemistry. The observed variations are due to seawater exchange during semi-diurnal tidal cycles.

in the Chilika lagoon exhibit non-conservative behavior during monsoon and pre-monsoon seasons (Fig. 4). Although the observed non-conservative behavior of Sr isotopes (and conservative behavior for Sr) is consistent with few earlier reports (Rahaman and Singh, 2012; Beck et al., 2013), these results, however, are not in accordance with conservative $^{87}Sr/^{86}Sr$ behavior reported for other global estuaries (Ingram and Sloan, 1992; Andersson et al., 1994; Sharma et al., 2007). Available literature differences on behavior of Sr isotopes along salinity gradient indicate the controlling factors for dissolved $^{87}Sr/^{86}Sr$ vary at regional scales depending on their biogeochemical properties and aquifer conditions.

The non-conservative behavior of $^{87}Sr/^{86}Sr$ ratios during monsoon and pre-monsoon seasons (Fig. 4) could be attributed to various possible mechanisms, which includes (i) removal of dissolved Sr through its incorporation onto Fe-Mn oxyhydroxides (Andersson et al., 1994; Xu and Marcantonio, 2007) and/or calcite precipitation, (ii) desorptive release of Sr from Fe-Mn oxides and/or clay surfaces (Huang and You, 2007; Huang et al., 2011), (iii) re-dissolution of minerals in the coastal regime and/or (iv) Sr supply through SGD to the lagoon (Rahaman and Singh, 2012; Beck et al., 2013; Trezzi et al., 2017). The Sr/Al (and, Ca/Al and Fe/Al) ratio of suspended sediments from the Chilika show a steady decline up to 2 salinity (Fig. 6), and the non-conservative behavior of $^{87}Sr/^{86}Sr$ during monsoon is mostly restricted to these low-salinity regimes. The observed decrease in Sr/Al points to possible release of Sr through re-dissolution of Ca-rich minerals and/or Fe-Mn hydroxides to the dissolved phase of the lagoon. Possible supply of dissolved Sr to the Chilika through re-dissolution of Ca-rich minerals is not supported by the observed decreasing $^{87}Sr/^{86}Sr$ trends for the Chilika sediments (Fig. 6B). The Sr isotopic ratios decrease from 0.73739 to 0.72070 along the salinity gradient of corresponding water samples. Decrease in sedimentary $^{87}Sr/^{86}Sr$ ratios can be attributed to preferential dissolution of minerals with higher Sr isotopic ratios than that of the bulk sediments, which is in clear contrast with less radiogenic Ca-rich minerals. The most likely explanation for the observed non-conservative behavior of $^{87}Sr/^{86}Sr$ during monsoon could be desorptive Sr release from the sediments. This proposition is strongly supported by $^{87}Sr/^{86}Sr$ ratios of exchangeable Sr fraction which steadily decreased from 0.71802 to 0.71097 along the salinity gradient (Fig. 6B). This declining $^{87}Sr/^{86}Sr$ trend is in accordance with the observed lower Sr isotopic ratios (compared to the river-sea water mixing line) during the monsoon period (Fig. 4). Further, the suspended sediments from the Chilika contains appreciable amount of exchangeable Sr (~30%) to promote release of Sr during cation-exchange processes (supplementary Table S2). These observations, which support non-conservative behavior of Sr isotopes, are not in agreement with the conservative behavior of Sr concentrations. One possible explanation for this disagreement could be lack of appreciable impact of these processes in the low-saline regime. The Sr concentrations of low-saline regimes of the Chilika are lower by about two orders of magnitude than the seawater. These large concentration differences among the sources may subdue any difference in slope (Sr/salinity ratio) between regression (~2.7 for monsoon) and conservative (2.56) mixing lines (Fig. 3).

Earlier studies (Rahaman and Singh, 2012; Beck et al., 2013) on non-conservative behavior of $^{87}Sr/^{86}Sr$ in estuaries have invoked possible SGD supply to coastal ocean. These studies have suggested a mechanism involving isotopic exchange between subsurface water and aquifer lithology to explain non-conservative $^{87}Sr/^{86}Sr$ behavior with conservative Sr trends in estuaries (Rahaman and Singh, 2012). The SGD can also serve as a potential source of Sr to the Chilika lagoon. However, the riverine discharge to the Chilika (~167 × 10^6 m^3/d; Gupta et al., 2008) during monsoon is higher by two orders of magnitude than the SGD flux reported for the Gautami estuary (1.34–5.60 × 10^6 m^3/d) (Rengarajan and Sarma, 2015) from the east coast of India. The impact of SGD on Sr behavior during the monsoon season, therefore, is not resolvable within the analytical uncertainty on Sr measurements. However, the SGD can serve as an important source during pre-monsoon season when the riverine discharge (4 × 10^6 m^3/d) is limited. The possible SGD impact on lagoon chemistry during pre-monsoon is evident from non-conservative $^{87}Sr/^{86}Sr$ trends with higher Sr isotopic values compared to conservative mixing line (Fig. 4). This isotopic mixing trend with high $^{87}Sr/^{86}Sr$ ratios (Fig. 4) during pre-monsoon season can not be attributed to cation-exchange processes, which supplies low Sr isotopic values with decreasing trends along the salinity gradient (Fig. 6B).

5.2. Estimation of SGD to the Chilika during the pre-monsoon season

Two different approaches have been adopted in this study to estimate SGD flux to the Chilika during the pre-monsoon season. The first approach involves an inversion modeling of chemical mass balance equations (Rahaman and Singh, 2012), and assumes that the SGD is characterized with a fixed end-member composition throughout the lagoon. Several studies suggest that the SGD chemistry may vary within a coastal system depending on subsurface ion exchange processes and/

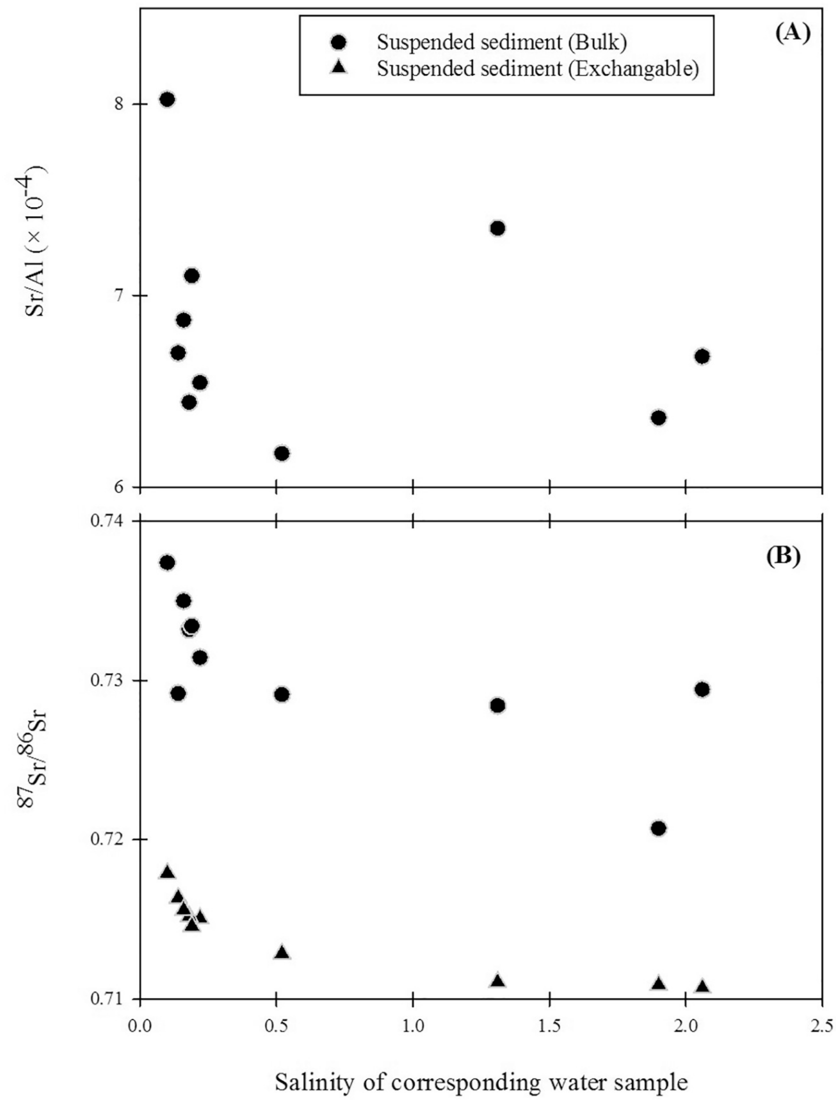

Fig. 6. Variations in (A) Sr/Al and (B) $^{87}Sr/^{86}Sr$ ratios of the suspended sediments (in both bulk and exchangeable fractions) with their corresponding water salinity. These ratios broadly show a declining trend with salinity, indicating release of Sr through ion-exchange (desorptive) processes and/or dissolution of Sr-rich minerals to the Chilika.

or relative contribution from seawater (e.g. Charette et al., 2008; Debnath et al., 2019). There has been limited effort in addressing this aspect of variable composition and its impact on SGD estimation. We, therefore, have also adopted a second approach based on mixing of major source waters to estimate the SGD flux by assuming a variable SGD composition. Details of these approaches and related results have been discussed below.

5.2.1. Inversion approach

Inverse modeling of geochemical datasets have been found successful in apportioning solute source contributions to various aquatic reservoirs (Négrel et al., 1993; Tripathy and Singh, 2010; Goswami et al., 2014). Rahaman and Singh (2012) have used this approach involving mass balance equations for Sr elemental and isotopic compositions in the Narmada estuary to estimate the SGD flux to the west coast of India. We have adopted a similar method in this study for the SGD estimation to the Chilika. As mentioned earlier, two samples are characterized with higher salinity and Sr concentrations than the seawater and have not been used in this model calculation. The inverse method assumes a fixed SGD composition for the whole lagoon. Details about the inverse model and the computational code are provided in Tripathy and Das (2014). Briefly, the model uses a non-linear Quasi-Newton optimization algorithm to find a best-fit between the observed and model parameters. The observed data for this model are the measured salinity, Sr concentration and $^{87}Sr/^{86}Sr$ ratios for the lagoon samples, whereas the model data are those for their possible source waters. A set of mass balance equations relates the observed and model parameters, which are provided below.

$$Sal = \sum_{i=1}^{3} (Sal_i \times f_i) \tag{1}$$

$$Sr = \sum_{i=1}^{3} (Sr_i \times f_i) \tag{2}$$

$$\frac{87_{Sr}}{86_{Sr}} \times Sr = \sum_{i=1}^{3} \left(\left(\frac{87_{Sr}}{86_{Sr}} \right)_i \times Sr_i \times f_i \right) \tag{3}$$

$$1 = \sum_{i=1}^{3} (f_i) \tag{4}$$

where, Sal, Sr and $^{87}Sr/^{86}Sr$ refer to the water salinity, Sr concentration and isotopic composition of the lagoon samples. The subscript, i (= 1, 2,

Table 2
A-priori salinity, Sr and $^{87}Sr/^{86}Sr$ data used in the inverse model for different end-members. These compositions are constrained based on measured data from this study (cf. Supplementary materials).

Source	Salinity	Sr (μmol/kg)	$^{87}Sr/^{86}Sr$
River water	0.2 ± 0.1	1.0 ± 0.2	0.716 ± 0.002
Seawater	33 ± 1	85 ± 2	0.70919 ± 0.00001
SGD[a]	0.8 ± 0.5	4 ± 3	0.715 ± 0.002

[a] After excluding outliers based on Turkey's univariate method.

3) stands for three possible sources, viz. river, seawater and SGD, respectively. The f_i stands for the fractional water contribution from the source, *i*. The Eqs. (1)–(4) are in the form of $d = g(p)$ where, *d* and *p* are the matrices of observed and model parameters respectively. The inverse model iterates to minimize the *d-g(p)* (Tarantola, 2005; Tripathy and Singh, 2010). The iteration algorithm starts from the a-priori data for the model parameters and converge to their *a-posteriori* values, which can best fit the mass balance equations with least residual.

The a-priori data and associated uncertainties used for the model parameters are provided in Table 2, whereas the source-apportionment results obtained from the inversion method are included in Table 3. These results show steady decline in riverine contribution from 96 to 5% with increase in lagoon salinity (range: 0.2–19.7). The SGD contribution to the Chilika varies between 1 and 42% (average: 19 ± 11% (n = 18)), with the maximum contribution at salinity of 18.6. We have used this dataset and the following equation to estimate the absolute SGD flux.

$$Q_{SGD} = \frac{\sum_{j=1}^{18} (f_{SGD})_j}{\sum_{j=1}^{18} (f_{riv})_j} \times Q_{riv} \tag{5}$$

where, the subscript, j (= 1,.., 18) stand for samples collected from the Chilika during the pre-monsoon season. The Q_{riv} and Q_{SGD} refer to the water discharge from the rivers and submarine groundwater discharge to the lagoon during this period, respectively. The lagoon receives water of about 4×10^6 m^3/d during the pre-monsoon (Feb-May) seasons (Muduli et al., 2013) and this value has been used as Q_{riv} for this calculation. The Eq. (5), which is formulated based on cumulative supply of SGD throughout the lagoon, calculates the SGD contribution by comparing riverine discharge and its fractional water contributions at every location. The inversion results and Eq. (5) estimate a SGD contribution of 1.5×10^6 m^3/d to the Chilika lagoon. This estimate is comparable with that reported earlier based on Ra isotopic investigation for few other estuaries linked to the Bay of Bengal (Godavari (1.34–43.02 × 10^6 m^3/d; Rengarajan and Sarma, 2015), Ganga (6.3–63 × 10^6 m^3/d; Moore, 1997)). Implications of these SGD estimations in terms of regional SGD-Sr fluxes and impact of these fluxes in global oceanic budget have been discussed in a subsequent section (cf. section 5.3.).

5.2.2. "Variable SGD end-member" approach

Efforts were also made in this study to estimate SGD flux to the Chilika by assuming a variable composition for this end-member. We have used Sr concentrations of seventy groundwater samples collected over three seasons from the Chilika basin to evaluate variability of groundwater with their salinity (Table S3 (Supplementary materials)). The salinity of these samples varies significantly (0.1–8.2), out of which only eight samples were similar to that of the freshwater (≤ 0.3). Average Sr concentration of the fresh groundwater samples (0.9 ± 0.2 μmol/kg; n = 8) is similar to that of the river water samples (Table 1). The samples with higher salinities may provide a first-order clue for the SGD composition. Fig. 7A confirms that the Sr concentration for the groundwater samples changes with salinity and the Sr concentration of the SGD is highly variable within this coastal lagoon. Most of the groundwater samples from the Chilika basin seem to have higher Sr concentrations (with respect to their salinity) when compared to the river-sea water mixing line (Fig. 7A). Tukey univariate analyses of these 70 samples confirms that samples with high salinities (≥ 3) and with high Sr concentrations (≥ 13 μmol/kg) can be considered as outliers and may be excluded to constrain a general trend. A linear regression between salinity and Sr data for groundwater samples, after excluding outliers in terms of their salinity concentrations, yielded a statistically significant (r = 0.71; p < .01; n = 64) line with a slope of 6.3 ± 0.8. The slope of the regression line (r = 0.54; p < .01; n = 59) changes to 3.5 ± 0.7, if outlier samples in terms of both salinity and Sr concentrations are excluded during regression analyses. These regression slopes are systematically higher than that expected (~2.6) for river-sea water mixing line. Consistent with this observation, higher Sr/salinity slopes for coastal groundwater have also been documented in earlier studies (Vengosh et al., 1999; Trezzi et al., 2017) and has been attributed to several processes, with includes supply of Sr to the groundwater through its release from bedrocks, clay particles, leakage of deeper groundwater or anthropogenic sources. In contrast to Sr concentrations, the Sr isotopes of the groundwater samples show

Table 3
Contributions (in %) of hydrological input from three end-members (river, seawater and SGD) to the Chilika lagoon during the pre-monsoon season. These contributions estimated using both the inversion and variable-SGD approaches are provided below.

Sample ID	Salinity	Inverse model approach			Variable-SGD composition approach		
		River (%)	Seawater (%)	SGD (%)	River (%)	Seawater (%)	SGD (%)
CLK17–06	13.3	43	38	18	54	36	11
CLK17–25	13.4	37	39	24	56	40	4
CLK17–28	18.6	5	53	42	37	53	9
CLK17–34	13.1	36	38	27	55	38	6
CLK17–38	15.1	23	43	34	50	46	4
CLK17–79	13.6	30	39	31	54	40	6
CLK17–80	14.4	37	41	21	52	40	8
CLK17–82	11.1	57	32	12	58	28	14
CLK17–84	3.4	82	10	9	54	6	40
CLK17–87	0.2	96	0	4	100	0	0
CLK17–88	1.2	92	3	5	16	1	84
CLK17–91	7.1	69	20	11	60	16	24
CLK17–94	19.7	8	57	35	37	58	4
CLK17–118	18.0	18	52	30	41	51	7
CLK17–132	7.1	67	20	13	65	18	17
CLK17–133	2.6	92	7	1	47	3	50
CLK17–134	5.2	73	15	13	64	12	23
CLK17–136	8.3	60	24	16	64	22	14

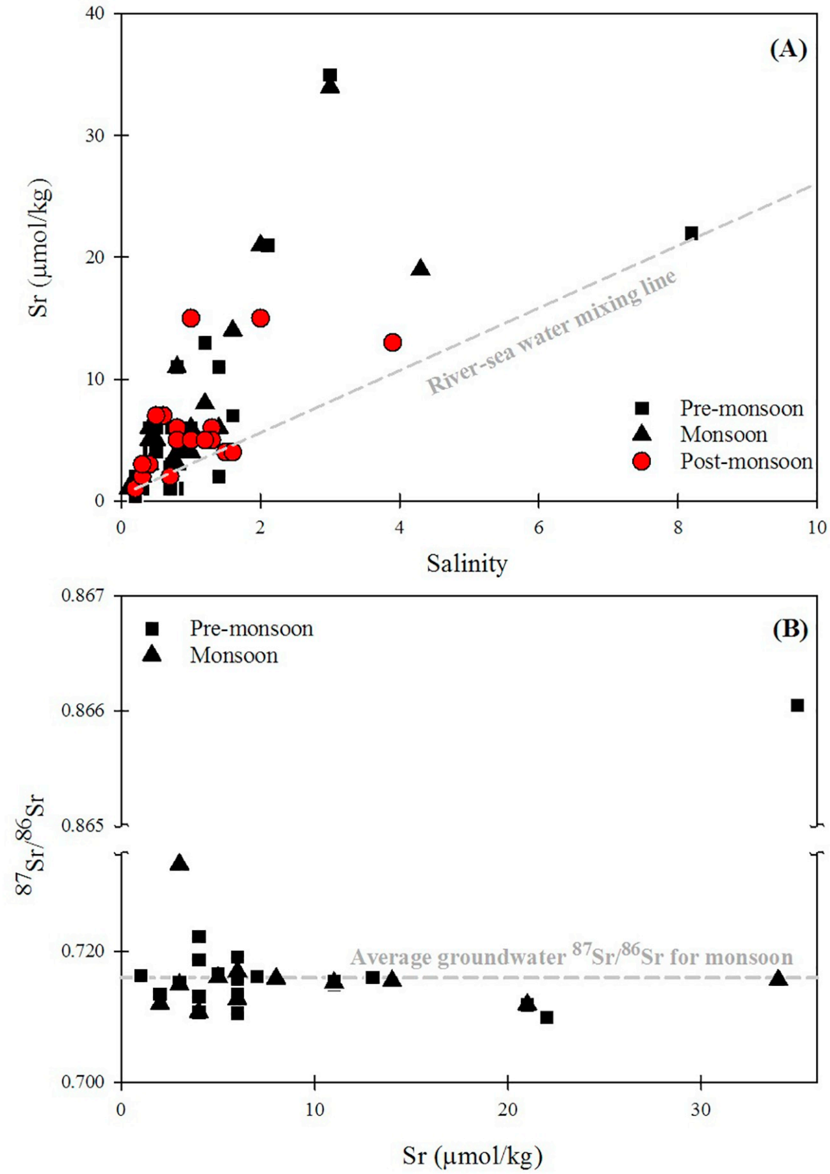

Fig. 7. Co-variation between (A) Sr and salinity, and (B) Sr and $^{87}Sr/^{86}Sr$ ratios of groundwater samples from the Chilika basin. For reference, the conservative mixing line for river and seawater is shown in (A). These plots show variable SGD compostions within the basin. The SGD compositions show variable Sr concentrations with relatively constant $^{87}Sr/^{86}Sr$ ratios.

limited variation (Fig. 7B). The Sr isotopic composition of these samples, after excluding three outliers based on Tukey's method (≥ 0.7215), vary between 0.70993 and 0.70918 with an average value of 0.715 ± 0.002 ($n = 29$). This average value matches well with the riverine $^{87}Sr/^{86}Sr$ ratio for this basin (~0.716; Table 1). The exact cause for anomalously higher $^{87}Sr/^{86}Sr$ ratio observed for three outlier samples is not clear. Possible explanations for these high radiogenic values could be (i) supply of Sr from fertilizers and other agricultural practices, and/or (ii) subsurface leaching of radiogenic Sr from K-rich minerals with faster dissolution kinetics. We recognize here that more studies are required to constrain the exact source(s) of Sr to the coastal groundwater. However, this information on source of groundwater Sr will have limited impact on the SGD estimation.

We have adopted a source-mixing approach with variable SGD composition to estimate the SGD fluxes to the Chilika (Fig. 8). The Sr concentrations and $^{87}Sr/^{86}Sr$ of the Chilika samples were accounted by mixing of (i) a combined river-seawater mixture source, and (ii) the SGD with varying chemistry along the salinity gradient. As discussed earlier, the Sr concentrations of the groundwater from the basin show a steady increase with salinity with limited changes in $^{87}Sr/^{86}Sr$ ratios (Fig. 7B). We have used a constant $^{87}Sr/^{86}Sr$ ratio (0.715 ± 0.002) with varying Sr concentrations for the SGD end member composition. The expected $^{87}Sr/^{86}Sr$ ratios for the combined RW-SW sources (R_{RW-SW}) and SGD (R_{SGD}) sources were computed for the measured Sr concentration of sample using relevant mixing equations (Eqs. (1)–(3)). The R_{RW-SW} was calculated from the river-seawater mixing line, whereas the R_{SGD} was calculated using the variable-SGD equation for the given salinity and Sr concentration (Fig. 8). Considering conservative behavior of Sr concentration, the SGD flux for each sample can be estimated using the following equations:

$$R = [R_{RW-SW} \times Sr_{RW-SW} \times (f_{RW} + (1 - f_{RW}))] + [R_{SGD} \times Sr_{SGD} \times p] \tag{6}$$

For conservative behavior, the Sr concentrations at a given salinity are expected to be same for RW-SW and SGD sources. For same Sr value, the Eq. (6) reduces to:

$$R = [R_{RW-SW} \times (f_{RW} + (1 - f_{RW}))] + [R_{SGD} \times p] \tag{7}$$

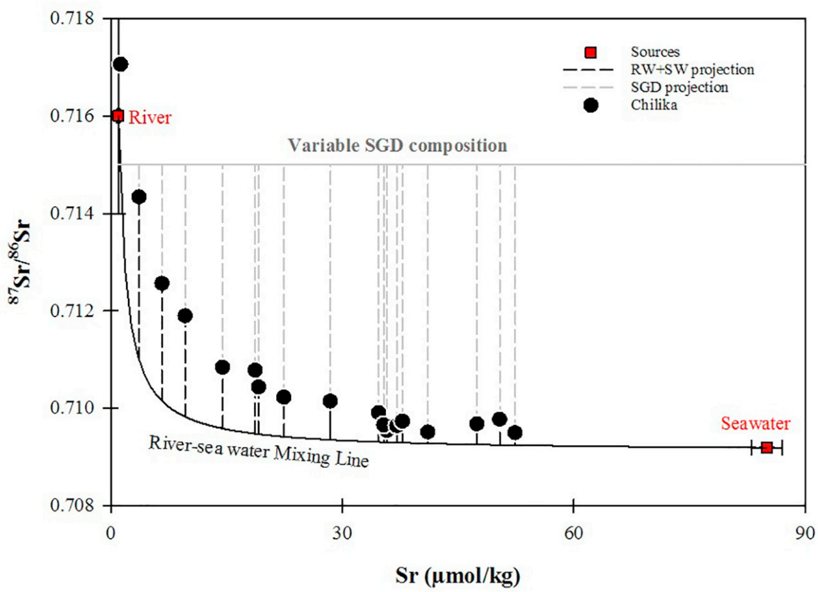

Fig. 8. Mixing plot between Sr concentration and $^{87}Sr/^{86}Sr$ for the Chilika lagoon during pre-monsoon season. For reference, theoretical river-sea water mixing trend and also, variable SGD composition has also been shown. The SGD compositions show an increasing Sr concentrations with salinity (Fig. 7) with a near constant $^{87}Sr/^{86}Sr$ ratio (~0.715 for pre-monsoon season; Table 1). The SGD contribution has been estimated assuming a conservative behavior for Sr element in this lagoon system.

$$Sal = Sal_{RW} \times f_{RW} + Sal_{SW} \times (1 - f_{RW}) \tag{8}$$

where, the subscripts *RW*, *SGD* and *RW-SW* stand for river, SGD and combined river-sea water sources. R represents the $^{87}Sr/^{86}Sr$ ratio. The term, *p* refers to relative water supply from the SGD. The computed f_{SGD} and f_{RW} (after normalizing to unity for all three sources) values were used in Eq. (7) to estimate the absolute SGD to the Chilika. The relative SGD contribution to the Chilika lagoon estimated using this approach varies between 4 and 84% (Table 3), with a steady decline with salinity values. These contributions account for a SGD flux of 1.51 × 10^6 m^3/d to the Chilika lagoon during the pre-monsoon season.

5.3. SGD and related Sr fluxes to the Chilika lagoon

Our estimates using both fixed and variable groundwater compositions show that the Chilika lagoon, on average, receives about 20% of SGD during the pre-monsoon season (Table 3). These estimates can be considered as a lower limit, as desorptive Sr supply with lower $^{87}Sr/^{86}Sr$ ratio (Fig. 6B) may also contribute to the non-conservativeness in Sr isotope mixing. Appreciable SGD signature in the water chemistry during pre-monsoon season could be attributed to intense seawater incursion into the seepage head due to limited freshwater discharge/stream-power during the lean-flow stage (Debnath et al., 2019). The variable SGD approach estimates an absolute SGD flux of 1.51 × 10^6 m^3/d for the pre-monsoon season to the Chilika, which is comparable to that computed (1.5 × 10^6 m^3/d) using a fixed-SGD inverse modeling approach. Although both the approaches yield comparable estimates, we propose that the variable-SGD approach is more robust for better constraining SGD fluxes and in explaining the non-conservative $^{87}Sr/^{86}Sr$ behavior with limited changes in elemental concentrations. The groundwater samples from the Chilika basin depict significant concentration changes with salinity (Fig. 7) and hence, the variable-SGD approach is possibly more appropriate for this kind of aquifer system. We, however, recognize that the better understanding on variability of $^{87}Sr/^{86}Sr$ and Sr concentration in submarine groundwater fluxes is indeed essential for more accurate estimation.

The estimated SGD flux of 1.51 × 10^6 m^3/day for the Chilika lagoon is consistent with that reported earlier for estuaries from the eastern coast of India (Godavari (1.34–43.02 × 10^6 m^3/d; Rengarajan and Sarma, 2015); Ganga (6.3–63 × 10^6 m^3/d; Moore, 1997);) and other lagoons (e.g., Vanice Lagoon (1 to 6 × 10^6 m^3/d; Garcia-Solsona et al., 2008); Mar Menor (1 to 5 × 10^6 m^3/d; Baudron et al., 2015); Laoye Lagoon (4.11× 10^6 m^3/d; Ji et al., 2013)) using Ra isotopes. The *a-posteriori* Sr (13.8 µM) and $^{87}Sr/^{86}Sr$ (0.7155) values of the SGD to the Chilika correspond to an annual Sr flux of 6.9 × 10^6 mol/yr. These SGD fluxes account for ~0.1% of total SGD-Sr fluxes (7.1 × 10^9 mol/yr; Beck et al., 2013) to the global coastal ocean. Considering the SGD flux to the Chilika lagoon is only 0.02% of global SGD flux, the computed Sr fluxes through SGD to the Chilika lagoon is disproportionally higher by an order of magnitude than the global Sr fluxes via SGD. Again, the $^{87}Sr/^{86}Sr$ ratio of the SGD to the eastern coast of India (~0.715; This study; Basu et al., 2001) is significantly higher than reported for the global average SGD value (~0.7089; Beck et al., 2013) and the present-day seawater value of 0.7092. Considering the drainage lithology of Archean rocks, this study indicates that the SGD fluxes from the granitic shield regions are expected to supply relatively higher radiogenic Sr (than the global-average SGD) to the coastal region. Further, the earlier reported Sr isotopic composition of the SGD to the eastern coast of India is always found higher than the global oceanic $^{87}Sr/^{86}Sr$ ratio. It has been well documented that the ^{87}Sr supply via rivers from these regions plays a dominant role in regulating the oceanic Sr isotopes in a global scale (Tripathy et al., 2012 and references therein). The SGD supplies from these basins, however, are relatively highly radiogenic (~0.715) compared to present-day seawater (~0.7092) and will have minimal (and, may also have opposite) impact on reducing the marine imbalance, which requires a missing source with lower $^{87}Sr/^{86}Sr$ ratios than the seawater.

6. Conclusion

Dissolved Sr and $^{87}Sr/^{86}Sr$ ratios of the Chilika lagoon and its possible sources have been investigated for three different seasons to infer coastal behavior of Sr along the salinity gradient. The Sr concentrations co-vary with salinities, as expected for conservative mixing between river and seawater. The mixing trends between 1/Sr and $^{87}Sr/^{86}Sr$ ratios, however, point to non-conservativeness of Sr isotopes in this lagoon during pre-monsoon and monsoon seasons. Based on sediment chemistry data, the non-conservativeness of Sr isotopes during monsoon period have been attributed to additional ^{87}Sr supply via subsurface ion-exchange processes to the lagoon. The non-conservative behavior of $^{87}Sr/^{86}Sr$ during pre-monsoon is due to SGD supply to the Chilika and this flux has been estimated following mass balance calculations using variable groundwater compositions along the salinity gradient. These results indicate that ~20% of hydrological inputs to the lagoon are derived from SGD, which accounts for a SGD flux of

1.51×10^6 m^3/d to the Chilika. The Sr isotopic value of SGD to the lagoon during pre-monsoon season (0.715) is higher than the present-day seawater ratio (~0.7092). The $^{87}Sr/^{86}Sr$ data from this and earlier studies for SGD to the eastern coast of India confirm that the SGD-derived Sr fluxes through large river systems from the Himalayas and Peninsular India regions would have minimal (and may also have opposite) impact on reducing the present-day oceanic imbalance.

Acknowledgement

This work was financial supported by SERB Early career research award (ECR/2016/001884) to GRT. We thank Dr. Rajani Panchang for her valuable inputs throughout this study. Help from Mohd Tarique and Mohammed Nuruzzama during chemical processing of samples is thankfully acknowledged. We also thank Prof. Thomas Bianchi for editorial handling of the manuscript and Prof. Henrietta Dulai (Associate editor) and two anonymous reviewers for their constructive comments and suggestion. NCPOR contribution number is J-9/2020-21.

Appendix A. Supplementary data

Supplementary data to this article can be found online at https://doi.org/10.1016/j.marchem.2020.103816.

References

Allègre, C.J., Louvat, P., Gaillardet, J., Meynadier, L., Rad, S., Capmas, F., 2010. The fundamental role of island arc weathering in the oceanic Sr isotope budget. Earth Planet. Sci. Lett. 292, 51–56.

Anand, S., Rahaman, W., Lathika, N., Thamban, M., Patil, S., Mohan, R., 2019. Trace elements and Sr, Nd isotope compositions of surface sediments in the Indian Ocean: an evaluation of sources and processes for sediment transport and dispersal. Geochem. Geophys. Geosyst. 20 (6), 3090–3112.

Andersson, P.S., Wasserburg, G.J., Ingri, J., Stordal, M.C., 1994. Strontium, dissolved and particulate loads in fresh and brackish waters: the Baltic Sea and Mississippi Delta. Earth Planet. Sci. Lett. 124, 195–210.

Barnes, R.S.K., 1980. Coastal Lagoons. Cambridge University Press, Cambridge, UK (106 pp).

Barth, S., 1998. $^{11}B/^{10}B$ variations of dissolved boron in a freshwater-seawater mixing plume (Elbe Estuary, North sea). Mar. Chem. 62, 1–14.

Basu, A.R., Jacobsen, S.B., Poreda, R.J., Dowling, C.B., Aggarwal, P.K., 2001. Large groundwater strontium flux to the oceans from the Bengal Basin and the marine strontium isotope record. Science 293, 1470–1473.

Baudron, P., Cockenpot, S., Lopez-Castejon, F., Radakovitch, O., Gilabert, J., Mayer, A., Claude, C., 2015. Combining radon, short-lived radium isotopes and hydrodynamic modeling to assess submarine groundwater discharge from an anthropized semiarid watershed to a Mediterranean lagoon (Mar Menor, SE Spain). J. Hydrol. 525, 55–71.

Beck, A.J., Charette, M.A., Cochran, J.K., Gonneea, M.E., Peucker-Ehrenbrink, B., 2013. Dissolved strontium in the subterranean estuary–implications for the marine strontium isotope budget. Geochim. Cosmochim. Acta 117, 33–52.

Burnett, W.C., Cable, J.E., Corbett, D.R., 2003. Radon tracing of submarine groundwater discharge in coastal environments. In: Taniguchi, M., Wang, K., Gamo, T. (Eds.), Land and Marine Hydrogeology. Elsevier Publications, Amsterdam, The Netherlands, pp. 25–43.

Chakrabarti, R., Mondal, S., Acharya, S.S., Lekha, J.S., Sengupta, D., 2018. Submarine groundwater discharge derived strontium from the Bengal Basin traced in bay of Bengal water samples. Sci. Rep. 8 (1), 4383.

Charette, M.A., Buesseler, K., Andrews, J., 2001. Utility of radium isotopes for evaluating the input and transport of groundwater-derived nitrogen to a Cape Cod estuary. Limnol. Oceanogr. 46, 465–470.

Charette, M.A., Moore, W.S., Burnett, W.C., 2008. Uranium-and thorium-series nuclides as tracers of submarine groundwater discharge. In: U-Th series nuclides in aquatic systems edited by S. Krishnaswami and J. K. Cochran. J. Environ. Radioact. 13, 155–191.

Chaudhuri, S., Clauer, N., 1986. Fluctuations of isotopic composition of strontium in seawater during the Phanerozoic eon. Chem. Geol. 59, 293–303.

Coffey, M., Dehairs, F., Collette, O., Luther, G., Church, T., Jickells, T., 1997. The behaviour of dissolved barium in estuaries. Estuar. Coast. Shelf Sci. 45 (1), 113–121.

Danish, M., Tripathy, G.R., Panchang, R., Gandhi, N., Prakash, S., 2019. Dissolved boron in a brackish-water lagoon system (Chilika lagoon, India): spatial distribution and coastal behavior. Mar. Chem. 214, 103663.

Debnath, P., Das, K., Mukherjee, A., Ghosh, N.C., Rao, S., Kumar, S., Krishan, G., Joshi, G., 2019. Seasonal-to-diurnal scale isotopic signatures of tidally-influenced submarine groundwater discharge to the Bay of Bengal: control of hydrological cycle on tropical oceans. J. Hydrol. 571, 697–710.

Garcia-Solsona, E., Masqué, P., Garcia-Orellana, J., Rapaglia, J., Beck, A.J., Cochran, J.K., Bokuniewicz, H., Zaggia, L., Collavini, F., 2008. Estimating submarine groundwater discharge around Isola La Cura, northern Venice lagoon (Italy), by using the radium quartet. Mar. Chem. 109 (3–4), 292–306.

Ghosh, A.K., Pattnaik, A.K., Ballatore, T.J., 2006. Chilika lagoon: restoring ecological balance and livelihoods through re-salinization. Lakes Reserv. Res. Manag. 11 (4), 239–255.

Goswami, V., Singh, S.K., Bhushan, R., 2014. Impact of water mass mixing and dust deposition on Nd concentration and ε_{Nd} of the Arabian Sea water column. Geochim. Cosmochim. Acta 145, 30–49.

Gupta, G.V.M., Sarma, V.V.S.S., Robin, R.S., Raman, A.V., Kumar, M.J., Rakesh, M., Subramanian, B.R., 2008. Influence of net ecosystem metabolism in transferring riverine organic carbon to atmospheric CO_2 in a tropical coastal lagoon (Chilka Lake, India). Biogeochemistry 87, 265–285.

Herdendorf, C., 1982. Largest lakes of the world. J. Great Lakes Res. 8, 379–412.

Huang, K.F., You, C.F., 2007. Tracing freshwater plume migration in the estuary after a typhoon event using Sr isotopic ratios. Geophys. Res. Lett. 34 (2).

Huang, K.F., You, C.F., Chung, C.H., Lin, I.T., 2011. Nonhomogeneous seawater Sr isotopic composition in the coastal oceans: a novel tool for tracing water masses and submarine groundwater discharge. Geochem. Geophys. Geosyst. 12 (5), 1–14.

Ingram, B.L., Sloan, D., 1992. Strontium isotopic composition of estuarine sediments as paleosalinity-paleoclimate indicator. Science 255 (5040), 68–72.

Ji, T., Du, J., Moore, W.S., Zhang, G., Su, N., Zhang, J., 2013. Nutrient inputs to a lagoon through submarine groundwater discharge: the case of Laoye lagoon, Hainan, China. J. Mar. Syst. 111, 253–262.

Knee, K., Paytan, A., 2011. Submarine groundwater discharge: a source of nutrients, metals, and pollutants to the Coastal Ocean. Treatise Estuar. Coast. Sci 4, 205–234.

Kwon, E.Y., Kim, G., Primeau, F., Moore, W.S., Cho, H.M., DeVries, T., Cho, Y.K., 2014. Global estimate of submarine groundwater discharge based on an observationally constrained radium isotope model. Geophys. Res. Lett. 41 (23), 8438–8444.

Mahanty, M.M., Mohanty, P.K., Panda, U.S., Pradhan, S., Samal, R.N., Rao, V.R., 2015. Characterization of tidal and non-tidal variations in the Chilika lagoon on the east coast of India. Int. J. Sci. Eng. Res. 6, 564–571.

Mahanty, M.M., Mohanty, P.K., Pattnaik, A.K., Panda, U.S., Pradhan, S., Samal, R.N., 2016. Hydrodynamics, temperature/salinity variability and residence time in the Chilika lagoon during dry and wet period: measurement and modeling. Cont. Shelf Res. 125, 28–43.

Moore, W.S., 1996. Large groundwater inputs to coastal waters revealed by ^{226}Ra enrichments. Nature 380 (6575), 612.

Moore, W.S., 1997. High fluxes of radium and barium from the mouth of the Ganges-Brahmaputra River during low river discharge suggest a large groundwater source. Earth Planet. Sci. Lett. 150 (1–2), 141–150.

Moore, W.S., 1999. The subterranean estuary: a reaction zone of ground water and sea water. Mar. Chem. 65 (1–2), 111–125.

Moore, W.S., 2010. The effect of submarine groundwater discharge on the ocean. Annu. Rev. Mar. Sci. 2, 59–88.

Muduli, P, Kanuri, V, Robin, R, Kumar, B, Patra, S, Raman, A, Rao, G, Suubramanian, B, 2012. Spatio-temporal variation of CO_2 emission from Chilika Lake, a tropical coastal lagoon, on the east coast of India. Estuarine coastal and shelf science 113, 305–313. https://doi.org/10.1016/j.ecss.2012.08.020. In this issue.

Muduli, P.R., Kanuri, V.V., Robin, R.S., Kumar, B.C., Patra, S., Raman, A.V., Subramanian, B.R., 2013. Distribution of dissolved inorganic carbon and net ecosystem production in a tropical brackish water lagoon, India. Cont. Shelf Res. 64, 75–87.

Négrel, P., Allègre, C.J., Dupré, B., Lewin, E., 1993. Erosion sources determined by inversion of major and trace element ratios and strontium isotopic ratios in river water: the Congo Basin case. Earth Planet. Sci. Lett. 120 (1–2), 59–76.

Nuruzzama, M., Rahaman, W., Tripathy, G.R., Mohan, R., Patil, S., 2020. Dissolved major ions, Sr and $^{87}Sr/^{86}Sr$ of coastal lakes from Larsemann hills, East Antarctica: solute sources and chemical weathering in a polar environment. Hydrol. Process (in press, DOI: 10:1002/hyp.13734).

Peucker-Ehrenbrink, B., Fiske, G.J., 2019. A continental perspective of the seawater $^{87}Sr/^{86}Sr$ record: a review. Chem. Geol. 510, 140–165.

Rahaman, W., Singh, S.K., 2012. Sr and $^{87}Sr/^{86}Sr$ in estuaries of western India: impact of submarine groundwater discharge. Geochim. Cosmochim. Acta 85, 275–288.

Rahaman, W., Singh, S.K., Raghav, S., 2011. Dissolved Mo and U in rivers and estuaries of India: implication to geochemistry of redox sensitive elements and their marine budgets. Chem. Geol. 278, 160–172.

Rengarajan, R., Sarma, V.V.S.S., 2015. Submarine groundwater discharge and nutrient addition to the coastal zone of the Godavari estuary. Mar. Chem. 172, 57–69.

Rodellas, V., Garcia-Orellana, J., Masque, P., Feldman, M., Weinstein, Y., 2015. Submarine groundwater discharge as a major source of nutrients to the Mediterranean Sea. Proc. Natl. Acad. Sci. 112, 3926–3930.

Samanta, S., Dalai, T.K., 2016. Dissolved and particulate barium in the ganga (Hooghly) river estuary, India: Solute-particle interactions and the enhanced dissolved flux to the oceans. Geochim. Cosmochim. Acta 195, 1–28.

Sarkar, S., Bhattacharya, A., Bhattacharya, A., Satapathy, K., Mohanty, A., Panigrahi, S., 2012. Chilika Lake. In: Encylopedia of Lakes and Reservoirs. Springer publications, Dordrecht, pp. 148–156.

Sharma, M., Balakrishna, K., Hofmann, A.W., Shankar, R., 2007. The transport of osmium and strontium isotopes through a tropical estuary. Geochim. Cosmochim. Acta 71 (20), 4856–4867.

Singh, S.K., Rai, S.K., Krishnaswami, S., 2008. Sr and Nd isotopes in river sediments from the Ganga Basin: sediment provenance and spatial variability in physical erosion. J. Geophys. Res. 113 (F3), 1–18.

Street, J., Knee, K., Grossman, E., Paytan, A., 2008. Submarine groundwater discharge and nutrient addition to the coastal zone and coral reefs of leeward Hawi'i. Mar. Chem. 109, 355–376.

Taniguchi, M., Burnett, W.C., Cable, J.E., Turner, J.V., 2002. Investigation of submarine groundwater discharge. Hydrol. Process. 16 (11), 2115–2129.

Tarantola, A., 2005. Inverse Problem Theory and Methods for Model Parameter Estimation. 89 SIAM Publishers.
Trezzi, G., Garcia-Orellana, J., Rodellas, V., Masqué, P., Garcia-Solsona, E., Andersson, P.S., 2017. Assessing the role of submarine groundwater discharge as a source of Sr to the Mediterranean Sea. Geochim. Cosmochim. Acta 200, 42–54.
Tripathy, G.R., Das, A., 2014. Modeling geochemical datasets for source apportionment: comparison of least square regression and inversion approaches. J. Geochem. Explor. 144, 144–153.
Tripathy, G.R., Singh, S.K., 2010. Chemical erosion rates of river basins of the ganga system in the Himalaya: reanalysis based on inversion of dissolved major ions, Sr, and $^{87}Sr/^{86}Sr$. Geochem. Geophys. Geosyst. 11 (3), 1–20.
Tripathy, G.R., Singh, S.K., Krishnaswami, S., 2012. Sr and Nd isotopes as tracers of chemical and physical erosion. In: Handbook of Environmental Isotope Geochemistry. Springer, Berlin, Heidelberg, pp. 521–552.
Vance, D., Teagle, D.A., Foster, G.L., 2009. Variable quaternary chemical weathering fluxes and imbalances in marine geochemical budgets. Nature 458 (7237), 493.
Vengosh, A., Spivack, A.J., Artzi, Y., Ayalon, A., 1999. Geochemical and boron, strontium, and oxygen isotopic constraints on the origin of the salinity in groundwater from the Mediterranean coast of Israel. Water Resour. Res. 35, 1877–1894.
Wang, R., You, C., 2013. Uranium and strontium isotopic evidence for strong submarine groundwater discharge in an estuary of a mountainous island: a case study in the Gaoping River Estuary, Southwestern Taiwan. Mar. Chem. 157, 106–116.
Wang, Z., Liu, C., Han, G., Xu, Z., 2001. Strontium isotopic geochemistry of the Changjiang estuarine waters: implications for water–sediment interaction. Sci. China Ser. E Eng. Mater. Sci. 44, 129–133.
Weis, D., Kieffer, B., Maerschalk, C., Barling, J., De Jong, J., Williams, G.A., Hanano, D., Pretorius, W., Mattielli, N., Scoates, J., Goolaerts, A., Friedman, R., Mahoney, J., 2006. High-precision isotopic characterization of USGS reference materials by TIMS and MC-ICP MS. Geochem. Geophys. Geosyst. 7 (8), 1–30.
Xu, Y., Marcantonio, F., 2007. Strontium isotope variations in the lower Mississippi River and its estuarine mixing zone. Mar. Chem. 105 (1–2), 118–128.